2020

LPS from subgingival plaque and the periodontal pathogen Porphyromonas gingivalis, its effect on M1 and M2 macrophage responses and potential as a biomarker

Strachan, Alexander

UNIVERSITY OF PLYMOUTH

LPS from subgingival plaque and the periodontal pathogen *Porphyromonas gingivalis*, its effect on M1 and M2 macrophage responses and potential as a biomarker

by

Alexander Strachan

A thesis submitted to the University of Plymouth

in partial fulfilment for the degree of

DOCTOR OF PHILOSOPHY

Peninsula

School of Dentistry

September 2020

Acknowledgments

This thesis could not have been completed without the support of colleagues, friends and family. I would like to take this opportunity to thank all of those who have contributed and to apologise for any omissions from the following.

First and foremost, thanks must go to Dr Svetislav Zaric and Dr Andrew Foey, for your guidance, knowledge, encouragement and especially your patience and friendship.

Thanks should also go to those at South Devon College and in particular Luke Peakman, who started out on this journey with me.

There are a number of people who have helped and given advice throughout this process, Dr Barbara Durante, life was always more eventful when you were around. The many technicians, including Dr Will Vevers, Dr Lee Hutt and Dr Paul Waines, I thank you for your help and advice on every occasion I have needed it.

Professor Simon Jackson and his research group and in particular Dr Wondwossen Abate and Dr Anas Sattar all a fountain of knowledge within the field in which we work.

All those at the electron microscopy centre past and present, Dr Roy Moate, Mr Peter Bond and Mr Glenn Harper for your help and letting me stay later than I should looking at macrophages and bacteria. And to everyone there now who has had to put up with me writing up whilst I should be making little things look big. A particular thanks to Dr Natasha Stephen, who probably didn't realise how much I had left to write when she employed me.

Great thanks must go to Dr Vikram Sharma, his assistance and advice with the proteomics aspect of this work was invaluable.

Thank you also to the dental school, particularly the administrators, Bernice, Francesca and Amber who have had to put up with me for quite some time and Dr Vehid Salih who has helped me progress through some difficult times.

To my family, my children, Ethan, Meghan and Charlie, you can have me back now. To my mum Barbara, your support at many times throughout has got us through.

And finally to my wife, Liz, this was always a joint effort and *we* did it.

Author's Declaration

At no time during the registration for the degree of Doctor of Philosophy has the author been registered for any other University award without prior agreement of the Doctoral College Quality Sub-Committee.

Work submitted for this research degree at the University of Plymouth has not formed part of any other degree either at the University of Plymouth or at another establishment.

Publications:

STRACHAN, A., HARRINGTON, Z., MCILWAINE, C., JERREAT, M., BELFIELD, L. A., KILAR, A., JACKSON, S. K., FOEY, A. & ZARIC, S. 2019. Subgingival lipid A profile and endotoxin activity in periodontal health and disease. *Clin Oral Investig,* 23**,** 3527-3534.

DOI: 10.1007/s00784-018-2771-9.

PEARL: http://hdl.handle.net/10026.1/13033

Multiple national and international conferences were attended, at which 7 poster and 5 oral presentations were presented, as such, a full list is given in appendix C.

Word count of main body of thesis: 47,671

Signed .....

Date…02/09/2020……

LPS from subgingival plaque and the periodontal pathogen *Porphyromonas gingivalis*, its effect on M1 and M2 macrophage responses and potential as a biomarker

Alex Strachan

Abstract

Chronic periodontitis is an inflammatory disease which, in response to a dysbiotic biofilm results in tissue destruction and ultimately tooth loss. The mechanisms which initiate the disease are poorly understood, as are the effectors which cause periods of exacerbation and remission experienced by sufferers of the disease. Lipopolysaccharide (LPS) is an archetypal microbial molecular pattern that instigates an immune response from macrophages (MΦ), key orchestrators of host immune response. Repetitive exposure Is also demonstrated to induce a quiescent state known as endotoxin tolerance, thought to be a protective mechanism but which may also confer protective benefits to potential pathogens. Several bacteria, including keystone periopathogen *Porphyromonas gingivalis* (PG) is able to modify the bio-reactive lipid-A portion of LPS which in turn modifies immune response. The aims of this study were to characterise lipid-A profiles from subgingival plaque and PG LPS and determine their effects on MΦ biology. Lipid-A isolated from patient samples revealed distinct profiles which demonstrated a correlation with inflammatory potential when used to stimulate polarised MΦs. The rFC assay demonstrated sufficient sensitivity to detect these lipid-A profiles and represents a potential diagnostic test. Patient derived and PG LPS induced diverse and opposing reactions in MΦ subsets, with M2 MΦs producing higher levels of TNF-α and Th_{17} associated IL-23 compared to M1 MΦs. Proteomic and subsequent gene ontology analysis indicated opposing mechanisms of activation in MΦ subsets. The unfolded protein response was identified to be induced in M1 MΦs challenged with PG LPS combined with an increased susceptibility towards internalisation of bacteria. M2 MΦs however identified a potential bacterial evasion mechanism through the manipulation of antigen processing and presentation. Proteomic analysis following secondary stimulation (endotoxin tolerisation) suggests that mechanisms which are associated with tolerisation of M1 MΦs and both stimulation and tolerisation of M2 MΦs is due to reprogramming events conferred by a combination of TNF-α, type-I interferons and epigenetic regulation.

List of Contents

List of Figures

List of Tables

AA	Aggregatibacter actinomycetemcomitans
AKT	AKT serine/threonine Kinase
AMP	Antimicrobial peptide
AOAH	Acyloxyacyl hydrolase
ATF	Activating transcription Factor
AUC	Area under curve
BACH	BTB Domain And CNC Homolog
BI	Bleeding index
BOP	Bleeding in probing
BP	Biological process
BSA	Bovine serum albumin
CAL	Clinical attachment loss
CBP	CREB binding protein
CC	Cellular component
CD	Crohns disease
CD14	Cluster of differentiation 14
CEBPB	CCAAT Enhancer Binding Protein Beta
CHOP	CCAAT-enhancer-binding protein homologous protein
COMP1	Cooperates with Myogenic Proteins 1
COX	Cyclooxygenase
CP	Chronic periodontitis
CPG	5'—C—phosphate—G—3
CREB	cAMP-response element binding protein
CRF	Corticotropin releasing factors
CT	Cross tolerance
CYLD	CYLD Lysine 63 Deubiquitinase
DAVID	Database for Annotation, Visualization and Integrated Discovery
DC	Dendritic cells
DNA	Deoxyribose nucleic acid
ds	Double stranded
E. coli	*Escherichia coli*
ELISA	Enzyme linked immunosorbent assay
ELK1	ETS Transcription Factor ELK1
EN1	Engrailed Homeobox 1
ER	Endoplasmic reticulum
ERK	Extracellular signal-regulated kinases
ESI	Electrospray ionization
ET	Endotoxin tolerance
EU	Endotoxin units
FASP	Filter aided separation
FDR	False discovery rate
FEG	Field emission generating
FN	*Fusobacterium nucleatum*
GAP	Generalised aggressive periodontitis
GATA3	GATA Binding Protein 3

GCF	Gingival crevicular fluid
GCSF	Granulocyte-colony stimulating facto
GH	GeneHancer
GIT	Gastrointestinal tract
GMCSF	Granulocyte-macrophage colony-stimulating factor
GO	Gene ontology
GRE	Glucocorticoid response element
HDAC	Histone deacetylase
HIF-1α	Hypoxia-inducible factor 1-alpha
HRP	horseradish peroxidase
HTF	HER2 transcription factor
IBD	Inflammatory bowel disease
ICAM1	Intracellular adhesion molecule
IE	Intestinal epithelium
IFN	Interferon
IL	Interleukin
iNOS	Inducible nitric oxide synthase
IP10	Interferon-Inducible Protein 10 Receptor
IRAK	Interleukin 1 Receptor Associated Kinase
IRF	Interferon Regulatory Factor
IRG1	Immune-responsive Gene
ISG	Interferon associated genes
IκBKE	Inhibitor Of Nuclear Factor Kappa B Kinase Subunit Epsilon
JAK	Janus Kinase
JE	Junctional epithelium
JNK	JUN N-Terminal Kinase
JUN	Jun Proto-Oncogene, AP-1 Transcription Factor Subunit
KDO	Keto-deoxy-d-manno-8-octanoic acid
LAL	*Limulus* amebocyte lysate
LAP	Localised aggressive periodontitis
LBP	LPS binding protein
LC-MS	Liquid chromatography–mass spectrometry
LFQ	Label free quantification
LL	Lower left
LPS	Lipopolysaccharide
MAL	MyD88-adapter-like
MAMP	Microbial associated molecular pattern
MAPK	Mitogen-activated protein kinase
MAX	MYC Associated Factor X
MCP2	Monocyte Chemotactic Protein 2
MD2	Myeloid Differentiation Protein-2
MF	Molecular function
MIF	Macrophage Migration Inhibitory Factor
MIP	Macrophage Inflammatory Protein
miR	Micro RNA
MKK	Map kinase kinase
MMP	Matrix metalloproteinase
MR	Mannose receptor

MyD88	Myeloid Differentiation Primary Response 88
MYOGNF1	Myogenin/Neurofibromin
MΦ	Macrophage
NFY	Nuclear Transcription Factor
NFκB	Nuclear factor kappa B
NLR	Nod-like receptor
NO	Nitric oxide
NXK22	NK2 Homeobox 2
OC	Oral cavity
PAMP	Pathogen associated molecular pattern
PAX	Paired Box
PBMC	Peripheral blood mononuclear cell
PD	Probe depth
PERK	Protein kinase R
PG	*Porphyromonas gingivalis*
PGE_2	Prostaglandin E_2
PI3K	Phosphatidylinositol-4,5-Bisphosphate 3-Kinase
PKA	Protein kinase A
PMA	phorbol-12-myristate-13-acetate
PMNs	Polymorphonuclear cells
PTPB1	Polypyrimidine Tract Binding Protein 1
Q-TOF	Quad-Time of flight
RANTES	Regulated Upon Activation, Normally T-Expressed, And Presumably Secreted (CCL5)
REL	REL Proto-Oncogene, NF-KB Subunit
rFC	Recombinant factor C
RFX1	Regulatory Factor X1
RIP	Receptor-Interacting Protein
RIPA	Radioimmunoprecipitation assay
RNA	Ribonucleic acid
RNS	Reactive nitrogen species
ROC	Receiver operating characteristic
ROS	Reactive oxygen species
RP58	Zinc Finger Protein 513
RSV	Respiratory syncytial virus
SARM	Sterile alpha and armadillo-motif-containing protein
SCFA	Short chain fatty acid
SDS-PAGE	Sodium dodecyl sulphate polyacrylamide gel electrophoresis
SE	Sulcular epithelium
SEM	Scanning electron microscopy
SHIP	Src homology 2 (SH2) domain-containing inositol 5'phosphatase
SHP	Small heterodimer partner
SIGIRR	Single Ig IL-1-related receptor
SIKE	Suppressor of IκB kinase-ε
SOCS	Suppressor of cytokine signalling
SOD2	Superoxide dismutase 2
SREBP	Sterol regulatory element-binding protein

SRF	Serum Response Factor
ss	single stranded
ST	Stimulated
ST2	Suppression Of tumorigenicity 2
STAT	Signal transducer and activator of transcription
TAB	TAK1-binding protein
TAG	TRAM-adaptor with a GOLD domain
TAK	TGF-β-activated kinase
TAM	Tumour associated macrophage
TANK	TRAF family member associated NFκB activator
TAX	Transient Axonal Glycoprotein
TBK	Tank binding Kinase
TCF11MAFG	Transcription Factor 11 MAF BZIP Transcription Factor G
TF	Transcription factor
TGF-β	Transforming growth factor beta
Th	T helper
TIMP	Tissue inhibitor of metalloproteinases
TIR	Toll/IL-1R
TL	Tolerised
TLR	Toll like receptor
TMB	3,3,5,5-tetramethyl benzidine
TNF-α	Tumour necrosis factor alpha
TOLLIP	Toll-interacting protein
TPA	Tetradecanoylphorbol-13-acetate
TRAF	TNFR-associated factor
TRAM	TRIF-related adaptor molecule
Treg	regulatory T cells
TRIF	Toll/interleukin-1 receptor (TIR)-domain-containing adaptor protein inducing interferon-β
TYK	tyrosine kinase
UPR	Unfolded protein response
UC	Ulcerative colitis
US	Unstimulated
USCS_TFBS	University of California, Santa Cruz transcription factor binding site
VD_3	1α, 25-dihydroxyvitamin D3
VEGF	Vascular endothelial growth factor
YY	Yin And Yang 1
ZID	Zinc Finger And BTB Domain Containing 6

Chapter 1

Introduction

1.1 Introduction

Diseases that affect the oral mucosa represent some of the most prevalent pathologies and for many of which satisfactory methods of treatment and resolution remain elusive. Chronic periodontitis (CP) is not only regarded as the most prevalent of the oral mucosal pathologies but the most prevalent inflammatory disease worldwide and despite efforts to the contrary, prevalence rates in the UK has remained at approximately 45% of the population (White et al., 2012).

CP is a multifactorial disease, for which the precise triggers of pathogenesis are unknown, but multiple studies implicate an inappropriate immune response to the resident microbiota (Hajishengallis and Lamont, 2012; Ebersole et al., 2013; Jain et al., 2013).

Innate immune cells, the first line of defence against infection, are equipped with a number of receptors which recognise highly conserved molecules expressed by potential pathogens. Endotoxins expressed on the bacterial outer membrane, once bound to the corresponding receptor, instigate a response intended to resolve the bacterial infection. The nature of the response elicited being dependent upon a multitude of factors; location, structure of the invading microbe, the responding immune cell phenotype and the surrounding local environment (Chen et al., 2018).

Toll like receptors (TLRs) recognise a range of conserved pathogen associated molecular patterns (PAMPs). TLR-ligand binding may activate several downstream signalling mechanisms which can result in the production of several inflammatory mediators including; cytokines, proteolytic enzymes, antimicrobial peptides and lead to the recruitment of other immune cells via chemokines.

Following successful clearance of infection, these inflammatory mediators require the instigation of regulatory mechanisms to suppress the induced inflammatory response preventing unwarranted inflammation, returning to homeostatic, anti-inflammatory environment (Chen et al., 2018).

Endotoxin tolerance (ET) is one such regulatory mechanism, defined in the middle of the twentieth century (Beeson, 1946) following observations of a reduced endotoxin induced fever as a result of multiple exposure to a typhoid vaccine. Latterly, ET has been referred to as: *"The reduced capacity of a cell to respond to gram negative bacterial LPS after an initial exposure to this stimulus"* (Vergadi, Vaporidi and Tsatsanis, 2018) and has been recognised as a host safety mechanism, instigated in the face of prolonged bacterial challenge (Biswas et al., 2007). This regulatory response can be thought of in two pathologically relevant scenarios; as a homeostatic mechanism to prevent an inflammatory response in areas extensively colonised by commensal microbiota (i.e. the large intestine and oral cavity) or as a preventative mechanism to restrict tissue damage at sites of prolonged pathogenic infection. In the case of the latter, exposure to endotoxins such as lipopolysaccharide (LPS) initiates an inflammatory response to affect a resolution of the infection. Inefficient clearance can lead to a prolonged, repetitive exposure and as such, a prolonged inflammatory response. As a result, instigation of ET is thought to prevent damage resulting from prolonged periods of inflammation, whereby repetitive exposure to LPS fails to induce an optimal immune response; and therefore, further tissue damage, via the down-regulation of host inflammatory mediators (Lopez-Collazo and del Fresno, 2013). Recent studies however, have begun to dispute the pretence that ET is a mechanism of retreat and protection and that it

may represent reprogramming resulting in a change of tactics in the ongoing battle (Butcher et al., 2018).

Whilst ET, in the event of either hypothesis being true, is intended to shift to a more beneficial state for the host, systemic tolerisation is recognised as a major contributing cause of mortality in the case of bacteraemia and sepsis, potentially facilitating further systemic infection (Biswas and Lopez-Collazo, 2009; Pena et al., 2014). The role of ET in sepsis has been widely studied but ET has also been identified in the circulating monocytes of cystic fibrosis patients who suffer from recurrent respiratory infection, yet little has been done to highlight the potential role of ET in the pathologies associated with the oral mucosae (del Fresno et al., 2008; del Fresno et al., 2009; del Campo et al., 2011). Both the loss and instigation of tolerance in this environment has profound effects on both the host and microbial community, which can constitute a number of pathogenic and auto-immune associated diseases. This suggests that the immune-suppressive nature of ET is not always beneficial to the host and presents a mechanism which is open to manipulation by pathogenic bacteria.

A further consideration when regarding disease progression is that CP does not adhere to a linear model, whereby patients suffering from these conditions experience periods of inflammatory exacerbation followed by periods of remission and *vice versa* (Schappi and Zappa, 1990; Silva et al., 2008; Taylor, 2014). The cause of this fluctuation in progression is unknown, but the instigation and/or loss of ET may act as a potential player in the aetiology of the disease and further understanding may represent a useful tool to aid detection, progression, treatment and prognosis.

The oral mucosa is a dynamic environment which has evolved to exist in a homeostatic state whilst colonised by a multitude of bacteria having co-evolved to induce optimal conditions in the mucosa for both host and microflora (Fung et al., 2014). Colonisation of the mucosal surfaces by commensals contributes to homeostasis in a number of ways: absorption of nutrients and competition with potential pathogens for space and nutrients (Kamada et al., 2013). To allow this commensal occupation, the residing "healthy" microbiota must be allowed to flourish and survive both in the presence of, and unperturbed by, the host immune system. Several mechanisms are responsible for tolerance to these symbiotic residents, many of which are still not fully understood but compartmentalisation to their relevant niche and the balance between microbiota vs immune response both play a pivotal role (Kamada et al., 2013; Hajishengallis, 2014a).

The onset of disease is deemed to be as a result of the loss of balance between the resident microbiota and the reciprocating host immune response. This imbalance can result due to a number of factors, including genetics, diet, mechanical injury, and shift in microbiota or immune response. To date, no single factor has been identified to instigate the onset of disease or the transitional phases from inflammation to quiescence and back. It is likely that a combination of these factors present lead to a cascade of events skewing host immune response from health to disease.

1.2 Risk factors for periodontal disease

Due to the multifactorial nature of periodontal disease, several risk factors have been identified which increase susceptibility. As a consequence of similar environmental and tissue organisation, other mucosal diseases, such as those of the gut, may share similar molecular mechanisms to CP. Inflammatory bowel diseases (IBD), are multifactorial diseases, which, like CP, also result from an inappropriate host immune response to the resident microbiota and demonstrate a non-linear model of progression (Schappi and Zappa, 1990; Silva et al., 2008; Taylor, 2014). The IBD pathologies, ulcerative colitis (UC) and Crohn's disease (CD) however, are described in many studies as an ongoing inflammatory response to the resident microbiota and environmental factors in a *susceptible host* and it is this genetic susceptibility which differs from CP (Abraham & Cho, 2009; Matricon, Barnich & Ardid, 2010; Zaric et al., 2010; Khor, Gardet and Xavier, 2011). Risk factors have been identified for CP and IBD and have been extensively reviewed and compared here: AlJehani, 2014 and Ananthakrishnan, 2015, risk factors for periodontal disease (PD) are summarised in table 1.1.

Risk factors for periodontal disease		
Modifiable risk factors	**Nonmodifiable risk factors**	**Other Risk characteristics**
Pathogenic species of bacteria	Osteoporosis	Age
Smoking	Hematological disorders	Sex
Diabetes mellitus	Host response	Socioeconomic status
Cardiovascular disease	Female hormone alterations	Education and race
Drug induced disorders	Pregnancy	Genetics
Stress		C-reactive protein
Obesity		

Table 1.1 Risk factors for periodontal disease. Modifiable and nonmodifiable risk factors recognised as significant risk factors which may contribute to periodontal disease. Other risk factors are also indicated which have been considered and may be implicated. (Summarised from Aljehani, 2014).

1.2.1 Genetic factors in chronic periodontitis

Whilst not recognised as the predominant factor in susceptibility as it is in CD and UC, genetic susceptibility has long been suspected to play a role in periodontal diseases, as some individuals appear to exhibit differential responses to a similar microbiota. Some develop an inappropriate immune response leading to disease progression whilst for others, homeostasis remains. Familial studies have also contributed to the data supporting a genetic susceptibility playing a role in localised aggressive periodontitis (LAP) (Laine, Crielaard & Loos, 2012). Many initial studies examined polymorphisms in genes associated with proteins which play a key role in the pathogenesis of the disease; cytokines, IL-1β, TNF-α, IL-4, IL-6 and IL-10 as well as Fcγ receptors and pattern recognition receptors, Toll like receptor 2 (TLR2), TLR4 and cluster of differentiation 14 (CD14). An extensive review of these studies referred to the limitations of studies utilising small cohorts (Laine, Crielaard & Loos, 2012). This review highlights the importance of considering ethnicity when comparing cohorts and thus surmised that limited evidence existed for an association with these genes and periodontitis. Studies since have struggled to find any significant association, although possible suggestive evidence for six loci, albeit at a reduced confidence level, have been identified; ninein, neuropeptide Y, Wnt family member 5A, ELKS/RAB6-interacting/CAST family member 2, natural cytotoxicity triggering receptor 2 and EGF-like module containing, mucin-like, hormone receptor-like 1 (Divaris et al., 2013). Interestingly this study indicates a possible role for neurogenic inflammatory mechanisms in periodontitis, however the study requires further investigation to provide significant data. A more recent review demonstrates that despite progression in methodological approaches, significant correlations still remains elusive. Existing data does, however, suggest that

polymorphisms within key signalling molecules may influence disease severity (Dosseva-Panova, Mlachkova & Popova, 2015).

1.2.1.1 Genetic associations with periodontal disease

In recent years, genome wide association studies (GWAS) and subsequent meta-analysis, have allowed for the study of polymorphisms across an entire genome, to date they have struggled to consistently prove direct associations between genetic modifications and CP (Nibali et al., 2017; Shungin et al., 2019; Loos and Van Dyke, 2020). Due to the number of polymorphisms which occur in any individual, identifying a statistically proven association with disease compared to the control is difficult and the limitations of using GWAS studies are highlighted in a review by Arne Schaefer (2018). This review does go on however to highlight a number of genes which have been suggested to demonstrate associations with PD. Glycosyltransferase 6 domain containing 1 (GLT6D1) was one of the first genes to be identified in a GWAS study, associated with aggressive periodontitis. Whilst little is known about the encoded protein, it is known to be expressed in selective tissues, including leukocytes and the gingivae (Schaefer et al., 2010; Schaefer, 2018,). Subsequently this study was expanded, and two additional positive associations were identified both of which are plausible candidates to affect host immune response (Munz et al., 2017a; Schaefer, 2018). Two single nucleotide polymorphisms (SNPs) were found at the genes which code for the antimicrobial defensin alpha 1 (DEFA1) and 3 (DEFA3) genes. These two genes are highly copy variable and arise from a 19 kb region and only differ by a single base pair. As such this locus was designated the antimicrobial peptide genes defensin alpha 1 and alpha 3 variable copy locus DEF1A3 (Munz et al., 2017a; Schaefer, 2018). Human alpha defensins are small cationic peptides shown to

be produced by a number of immune cells, including monocytes and neutrophils, which can act against bacteria, fungi and viruses (Klotman and Chang, 2006; Lopez-Bermejo et al, 2007; Rodriguez-Garcia et al, 2007; Escribese et al 2011). This same study also identified an association with SIGLEC5 (Munz et al., 2017a; Munz et al., 2018a; Schaefer, 2018). Sialic acid-binding immunoglobulin-type lectins (SIGLECS) are a group of transmembrane pattern recognition receptors (PRRs) which recognise sialic acids, molecules expressed by the majority of mammalian cells yet rarely in microbes (Angata, 2018). As such these have been shown to demonstrate regulatory functions as a recognition of self (as opposed to PPRs which recognise potential pathogenic epitopes). SIGLEC5 in particular has been associated with PD and tooth loss, in both European and Chinese Han populations (Munz et al.,2017a; Schaefer, 2018; Shungin et al., 2019; Tong et al., 2019). SIGLEC5 is expressed prominently by neutrophils and macrophages and has correspondingly been shown to regulate the activation of cells with a myeloid lineage (Shungin et al, 2019). It should also be noted that, as these receptors have coevolved with a microbial community, some have developed mechanisms to utilise these receptors for their own protection such as Neisseria menegitidis, which expresses a sialyated form of lipopolysaccharide on its outer leaflet (Jones, Virji and Crocker, 2003; Shugin et al, 2019). The study by Tong et al, within the Chinese Han population also found an association between ninein (NIN) and CP, an observation previously made within a study of white American Europeans (Divaris et al., 2013; Tong et al., 2019). NIN, an alias of which is Glycogen Synthase Kinase 3 Beta-Interacting Protein, may therefore be associated with regulating a number of pro-inflammatory signalling pathways. Munz et al however, have gone on to identify several other candidate genes including some also associated with coronary artery disease (CAD); vesicle

associated membrane proteins 3 and 8 (Vamp3 and Vamp8), snare proteins involved in vesicle trafficking and TNF-α release (Murray et al., 2005; Munz et al., 2018a; Schaefer, 2018; Loos and Van Dyke, 2020). Antisense coding RNA in the ink4 locus (ANRIL) was also identified as a result of the potential association between PD and CAD, whilst its role in PD is unknown it Is thought to be associated with VAMP3 (Schaefer et al., 2009; Ernst et al., 2010; Munz et al., 2018a; Schaefer, 2018; Loos and Van Dyke, 2019). Similarly, an SNP in plasminogen (PLG) was shown to demonstrate genome wide significance with CAD and was subsequently corroborated using the data generated by Munz et al in their 2017(a) study (Schaefer et al, 2015; Munz et al, 2017a, Munz et al, 2017b; Schaefer, 2018; Loos and Van Dyke, 2020). Latterly, Munz et al (2018b) have gone on to identify novel risk loci which may implicate the acute phase protein; Orosomucoid 1 (ORM1).

By utilising a different approach, a study examining the genome wide transcriptome in peripheral blood monocytes, stimulated with LPS from the keystone periopathogen *Porphyromonas gingivalis,* identified 902 genes which were significantly induced following six hours of stimulation (Gölz et al., 2016). Prominent transcripts included a number of chemokines associated with periodontitis: CCL3 (MIP-1α), and CCL4 (MIP-1β) act as a chemoattractant for a number of cells, including macrophages (MΦs) as well as activating PMNs and MΦs, CCL5 (RANTES), a pleiotropic biomolecule, acting as a chemoattractant for monocytes and $CD4^+$ T-cells and inducing histamine release from eosinophils and basophils. CCL8 (MCP2) also acts as a chemoattractant for monocytes and T-cells as well as eosinophils and basophils. CCL23 (MIP3) is immunoregulatory, acting upon monocytes and resting T-cells, as well as attracting dendritic cells

(DCs), neutrophils and osteoclast precursors. In addition, IL-8 a key molecule in periodontitis, due to its properties as a chemoattractant for neutrophils, was elevated, both transcriptionally and in secreted protein. Pro-inflammatory tumour necrosis factor alpha (TNF-α) and regulatory IL-10 were elevated, whereas transforming growth factor beta (TGF-β) was significantly reduced. Nacht domain leucine-rich repeat and PYD-containing protein 3 (NLRP3) inflammasome formation also increased thus affecting IL-1β production. This, also combined with increased surface expression of the T-cell co-stimulatory molecule CD-86 and the major histocompatibility complex (MHC) class II surface molecule; HLA-DR. This study goes on to implicate a number of proteins including immune-responsive gene 1 (IRG1), tissue inhibitor of metalloproteinases 2 (TIMP2), superoxide dismutase 2 (SOD2) and hypoxia-inducible factor 1-alpha (HIF-1α), which whilst in this study, is associated with PD, are also known to be associated and therefore may contribute towards the progression of additional pathologies.

1.3 The oral microbiota in health and disease

The importance of both oral and gut microbiota has become increasingly apparent in recent years. Variations in microbiome heterogeneity and composition have been associated with several diseases including IBD and PD (Ley et al., 2006; Sartor, 2008; Sartor, 2010; Costalonga and Herzberg, 2014; Deng et al., 2017). In the gut and oral cavity, the microbiome is an integral dynamic part of the environment.

In the periodontal diseases, the abundance or scarcity of various bacterial species have been shown to correlate with an increased risk of disease (Tables 1.2 and 1.3), many of which are also associated with other medical conditions (Vrakas et al, 2017). Notably two of the most heavily associated periodontal pathogens, *Aggrebacter antinomycetemcomitans* and *Porphyromonas gingivalis are the only species associated with CP,* generalised aggressive periodontitis (GAP), gingivitis and LAP (Table 1.3).

1.3.1 Bacterial species associated with periodontal disease

As previously mentioned, variation in the relative abundance of various bacterial species has been shown to correlate with an increased risk of periodontal disease, many of which are also associated with other medical conditions. *Streptococcus mutans* has been implicated in the formation of dental caries (Misaki et al., 2016). *Aggregatibacter actinomycetemcomitans* (AA) has been associated with the rarer form of periodontitis, LAP (Henderson et al., 2002; Malik, 2015). AA shares the ability to citrullinate host proteins with another synonymous oral pathogen *Porphyromonas gingivalis* (PG) (Lundberg et al., 2010; Wegner et al., 2010; Konig et al., 2016). Citrullination by PG has been presented as a potential mechanism of instigating autoimmunity in rheumatoid

Phyla		**Genera**		
Health	**Periodontal Disease**	**Health**	**Periodontal Disease**	*References*
Actinobacteria[1,3]	↑Bacteriodetes[1,4]	*Acinetobacter*[4]	↓*Acinetobacter*[4]	1 (Wang et al., 2013)
Firmicutes[1,2]	↓Firmicutes[2]	*Actinomyces*[1,2,3]	*Actinomyces*[1,2,3]	2 (Shi M et al., 2018)
Fusobacteria[3]	↑Fusobacteria[2,3]	*Capnocytophaga*[1,2]	*Capnocytophaga*[1,2]	3 (Abusleme et al., 2013)
Proteobacteria[1,2,4]	↑Saccharibacteria[2]	*Corynebacterium*[1,2]	↓*Corynebacterium*[1]	4 (Griffen et al., 2012)
	↑Spirochaetae[2,3,4]	*Fusobacterium*[2,4]	↑[3]*Fusobacterium*[2]	
	↑Synergistetes[3,4]	*Haemophilius*[1,2,4]	↓*Haemophilius*[2,4]	
		Leptotrichia[2]	↑*Leptotrichia*[1,2]	
		Mobiluncus[2]	↑[3,4]*Neisseria*[2]	
		Neisseria[1,2]	↑*Porphyromonas*[1,4]	
		Prevotella[4]	↑*Prevotella*[1,2,4]	
		Rothia[1,2]	↓*Rothia*[2]	
		Streptococcus[1,2,3,4]	↓*Streptococcus*[1,2,3,4]	
		Veillonella[2]	↑*Treponema*[1,2,3,4]	
			↑*Veillonella*[1,3]	

Table 1.2 Predominant bacteria in health and disease by phyla and genera. Changes in the abundance of bacteria associated with health and periodontal disease, are indicated at the phylum and genera level. ↑↓ demonstrates abundance relative to a healthy microbiome.

Disease associated species	CP	GAP	GVTS	LAP	References
Actinomyces viscous[5]	☐	☒	☒	☐	5 (Popova et al., 2014)
Aggrebacter antinomycetemcomitans [6,5,7,8,9]	☒	☒	☒	☒	6 (Kakuta et al., 2017)
Campylobacter gracilis[10,11]	☒	☐	☐	☒	7 (Fine et al., 2007)
Campylobacter rectus[6,10,12]	☒	☒	☒	☐	8 (Cirelli et al., 2018)
Campylobacter showae[10,12]	☒	☐	☐	☐	9 (Morinushi et al., 2000)
Eikenella corrodens[6,13]	☐	☒	☐	☒	10 (Socransky et al., 1998)
Eubacterium nodatum[10,14,16]	☒	☒	☐	☒	11 (Faveri et al., 2009)
Fusobacterium nucleatum[6,10,17]	☒	☒	☐	☐	12 (Macuch and Tanner, 2000)
Fusobacterium periodonticum[10,14]	☒	☐	☐	☐	13 (Fujise et al., 2004)
Peptostreptococcus micros[6,10,21]	☒	☐	☐	☐	14 (Chiranjeevi et al., 2014)
Porphyromonas gingivalis[6,9,10,11, 16,17,18,19,20]	☒	☒	☒	☒	15 (Heller et al., 2012)
Prevotella intermedia[6,10,11,14]	☒	☒	☐	☒	16 (Haffajee et al., 2006)
Prevotella nigrescens[10,22]	☒	☐	☒	☐	17 (Taxman et al., 2012)
Streptococcus constellatus[10,23]	☒	☐	☐	☐	18 (Kazi & Bharadwaj, 2017)
Streptococcus mitis[5]	☐	☐	☒	☐	19 (Kumawat et al., 2016)
Streptococcus sanguis[17]	☐	☐	☒	☐	20 (Hajishengallis et al., 2012)
Tannerella forsythia[6,10,11,14,16]	☒	☐	☐	☒	21 (Kazi & Bharadwaj, 2017)
Treponema denticola[6,10,11,14,16,19]	☒	☒	☐	☒	22 (Lie et al., 2001)
Veillonella parvula[14,17,18]	☐	☐	☒	☐	23 (Rams et al., 2014)

Table 1.3 Bacteria associated with periodontal disease. Increased abundance of individual species associated with periodontal disease are indicated, demonstrating associations with specific periodontal diseases.

CP = Chronic Periodontitis, GAP = Generalised Aggressive Periodontitis, GVTS = Gingivitis, LAP = Localised Aggressive Periodontitis.

arthritis, but more prevalently, PG has been heavily associated with CP (Lundberg et al., 2010). In the context of CP, PG is a member of the "red complex" bacteria in conjunction with *Treponema denticola* and *Tannarella forsythia* (Ximenez-Fyvie et al., 2000; Holt and Ebersole, 2005; da Silva-Boghossian et al., 2011). For some time, the finger was pointed at this trio as the primary instigators of CP pathogenesis, due to their high prevalence in patients suffering with the disease and their array of virulence factors (Lamont and Jenkinson, 1998; Socransky et al., 1998). More recently the scope has widened to implicate the biofilm as a whole, whereby subversion of the biofilm towards a pathogenic phenotype creates a dysbiosis in the local environment (Berezow et al., 2009). Whilst this is unlikely to be sufficient to instigate disease progression, it is likely to tip the balance for those in which other factors increase susceptibility and reduce the amount of microbial shift which is tolerable to maintain homeostatic conditions (Hajishengallis et al., 2012).

Having recognised the importance of the polymicrobial community in disease progression, it has been suggested that it may be open to manipulation and subversion. The "keystone hypothesis" suggests that even in relatively low numbers, PG is able to subvert structure and diversity within the biofilm, shifting it towards a pathogenic disposition (Hajishengallis et al., 2012). To achieve; this PG forms synergistic relationships with other bacterial colonies such as *Fusobacterium nucleatum* (FN) (Signat et al 2011). This relationship reciprocates within the complex biofilm, favouring bacteria that contribute to an environment complimentary to the keystone pathogen. Formation of periodontal pockets due to the subgingivally migrating biofilm, creates an optimal anaerobic environment for survival and proliferation. Interestingly, prevalence of FN is also heavily

associated with IBD, particularly CD (Dharmani et al., 2011; Strauss et al., 2011; Gevers et al., 2014; Bashir et al 2016).

Despite studies identifying bacteria associated with disease, many of these, including PG are commonly found in healthy individuals and are not effective indicators of future disease (Griffen et al., 1998; Suchett-Kaye et al., 1999). In addition, poor oral hygiene and build-up of plaque in the oral cavity may induce inflammation in the form of gingivitis and increase risk but does not inevitably lead to alveolar bone loss which is the key identifier of periodontitis (Lertpimonchai et al., 2017). This potentially supports the implication of potential pivotal players affecting the poly-microbial nature of these diseases and that the action of the microbiome as a whole may be greater than the individual sum of its parts (Papa et al., 2012). In future studies, the move towards poly-cellular and particularly poly-microbial models would aid to elucidate the potentially as yet unknown mechanisms of pathogenicity presented by a cooperative microbiome.

1.4 Mucosae: barriers to infection

The mucosa of the oral cavity (OC) serves to defend against continuous exposure to potential foreign non-self-antigens, the oral microbiota and other potentially parasitic organisms. As such there are several factors which are pivotal in the way these potential immune activators are processed so as to limit unwarranted host immune response. Preservation of the commensal microbiota within this environment is essential to maintain homeostasis. Inappropriate recognition of commensal bacteria and/or dietary products leading to the subsequent activation of the host immune system has been associated with autoimmunity and chronic inflammatory diseases (Garside et al., 1999; Thompson-Chagoyan et al., 2005).

The oral environment is one of unique composition, comprising both hard and soft tissues and subject to rapid fluctuations in environmental conditions; pH, temperature, introduction of foreign, non-self-objects as well as nutrients and oxygen availability. It has been stated that up to 1000 species reside in the oral cavity, both commensal and pathogenic, including bacteria, viruses, fungi, protozoa, yeast and archaea (Aas et al., 2005; Dewhirst et al., 2010; Wade, 2013). The hard surfaces of the teeth allow certain bacteria, including *Actinomyces, Capnocytophaga, Haemophilus, Neisseria, Streptococcus and Veillonella* species to preferentially and vigorously adhere, facilitating the formation of complex biofilms (dental plaque) (Huang et al., 2011). Additionally, and importantly, in contrast to the gut mucosa, the oral cavity is subject to oral hygiene regimens.

A number of mechanisms are employed to combat pathogenic behaviour in the mouth; secretory IgA produced by plasma cells in the salivary gland, lysozymes which cleave N terminal linkages in the peptidoglycan layer disrupting cellular

integrity of gram positive bacteria (Nash et al., 2006; Brandtzaeg, 2013;). Peroxidases, mucins and defensins are all secreted into the saliva and gingival crevicular fluid (GCF), as well as lactoferrin, which restricts iron availability to haem auxotrophic bacteria (Grover and Grover, 2014; Tsai et al., 2017).

1.4.1 The junctional and sulcular epithelium

Chronic periodontitis involves inflammation of the junctional epithelium (JE) and sulcular epithelium (SE) in response to bacterial stimulation. This specific oral epithelium differs from its IE counterpart in that structurally it is much less complex with no muscularis mucosae, goblet, Paneth or M-cells etc. In contrast to IE, the JE consists of stratified squamous cells and remains a permeable barrier as a primary function (Yajima-Himuro et al 2014). The SE is found above the JE and lines the gingival sulcus, a margin around the tooth, within which is the gingival crevicular fluid (GCF). As such, the SE forms the apical surface which is in constant contact with the oral microflora and open to mechanical damage due to mastication and brushing (Moutsopoulos and Konkel, 2018). The JE sits adjacent to the tooth surface and forms a tight ring around the tooth surface, thus protecting deeper tissues from bacterial challenge. Where the tightly regulated IE restricts transportation through the epithelial barrier to small molecules, the JE and SE allows the transition of host immune cells, antimicrobial peptides and other immune secretory factors to pass into the GCF (Fig. 1.1). As a result, the primary method of defence in the GIT, i.e. compartmentalisation via an epithelial mechanical barrier, is not able to prevent microbial stimulation of host immune cells in periodontal tissues. The JE and particularly SE, is therefore a site of perpetual low-level inflammation where the subgingival microbiota constantly

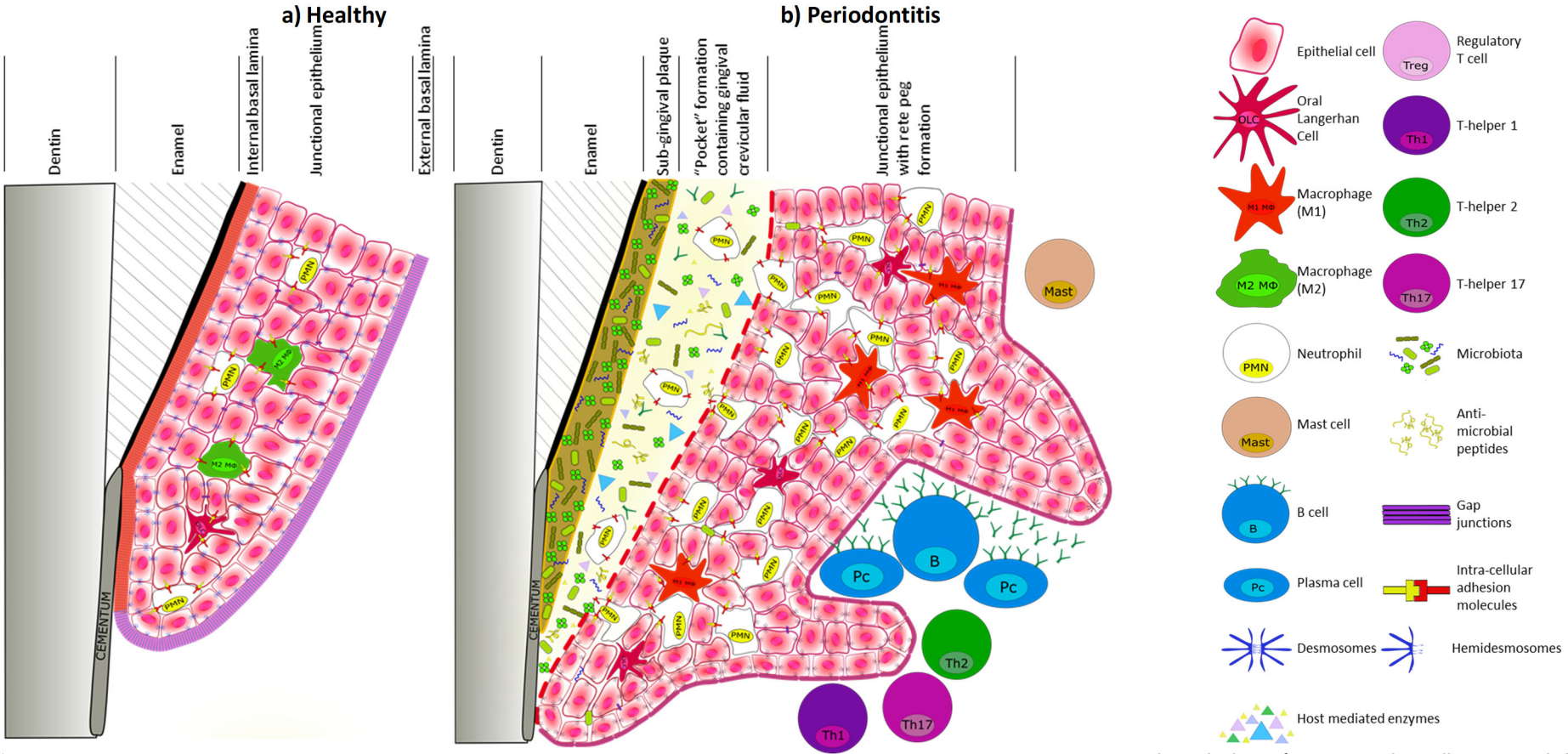

Figure 1.1. The junctional epithelium in health and periodontal disease. In healthy mucosa (a), the junctional epithelium forms a tight collar around the tooth. This epithelium is permeable to allow molecules and immune cells to traverse into the sulcular epithelium and gingival crevice above. Desmosomes and gap junctions enable permeability, whilst M2 MΦs and neutrophils reside in the epithelium, ready to respond. In disease (b), plaque migrates apically down the tooth surface, the internal lamina becomes ulcerated and hemisdesmosomes are degraded, allowing further apical migration and infiltration into the epithelium. As a result, epithelial cells secrete IL-1β and IL-8 causing extensive neutrophil infiltration and inflammation, driving an M1 MΦ phenotype. These cells activate and recruit B-cells and mast cells, increasing mucosal permeability and influence the differentiation of T-helper cells to drive inflammation.

challenge host innate immune cells (Yajima-Himuro et al., 2014). Even patients who present with good oral health may exhibit observable levels of cellular infiltrate within the SE and JE and supporting lamina propria when tissue biopsies are studied under a microscope (Lorenzi et al., 2014). As with the IE, MΦs and DCs (oral langerhan cells) are present, but the majority of the cellular infiltrate consists of neutrophils, particularly in disease. In health, to maintain a homeostatic environment, the balance between the predominantly symbiotic microbiota and host immune response must remain intact, as reviewed by Zaric et al (2010).

1.4.2 Mechanisms of epithelial degradation

A number of mechanisms exist which may affect epithelial integrity, thus potentially contributing towards an imbalanced immune response. Stress has long been attributed to contribute to IBD, and both psychological and physical stress is able to physically alter intestinal permeability via the hypothalamic-pituitary-adrenal axis (Fasano, 2012; de Punder et al., 2015). This same mechanism has also been suggested to be associated with PD, with higher levels of cortisol identified in saliva obtained from those with periodontal disease (Mannem and Chava, 2012; Gunepin et al., 2017). As part of the 'fight or flight' response initiated by the sympathetic nervous system, mechanisms are activated which remodel the availability of water, nutrients and minerals to primary organs in preparation for the required physiological reaction (Yu et al., 2013; de Punder et al., 2015). Under stress conditions, corticotropin releasing factors (CRF) are key in regulating the availability of these essential molecules and have been shown to affect homeostatic tolerance (Overman et al., 2012; Yu et al., 2013). Furthermore, CRF has been shown to breach induced endotoxin tolerance by

upregulating both TLR4 expression and claudin-2 expression in intestinal epithelial cells (Yu et al., 2013).

Several gut (and disease) associated bacteria exhibit machinery with which a similar loss in barrier integrity can be achieved. Species of *Bacteroides, Bifidobacterium, Propionibacterium, Lactobacillus, Clostridium*, amongst others, produce SCFAs which have been shown to have anti-inflammatory properties. Butyrate, shown to limit LPS induced inflammation via downregulation of TNF-α, intracellular adhesion molecule 1 (ICAM1), cyclooxygenase 2 (COX2), IL-1β and modulation of IL-10, and acetate and propionate which reduces TNF-α and IL-6 (but not IL-8) (Tedelind et al 2007; Foey, 2011; Macfarlane and Macfarlane, 2012; Russo et al., 2012;). Somewhat paradoxically, butyrate has been shown to influence barrier permeability and in particular regulation of claudin-2 expression (Peng et al., 2007; Ploger et al., 2012). The effect of SCFAs has particular relevance to CP as both PG and FN have been shown to produce SCFAs as by products (Yu et al., 2014; Cueno and Ochiai, 2018).

Studies which have examined this process, indicate that five SCFAs are produced by PG and FN alone as metabolic by-products (Yu et al., 2014). Butyric acid is retained within the gingival tissues for prolonged periods and reaches significant levels of 14.4 – 20 mM, leading to oxidative stress (Botta et al., 1995; Cueno et al., 2013; Cueno, Saito and Ochiai, 2016). Butyric acid is also recognised to inhibit histone deacetylases (HDACs), leading to epigenetic and chromosomal modifications which affect gene expression (Ochiai et al., 2011). In addition, the red complex bacteria, *Treponema denticola* and PG have been demonstrated to degrade cellular junctions such as E-cadherin and occludins via secretory proteases (Ji, Choi and Choi, 2015).

Other common enteric pathogens can also affect IE permeability; *H. pylori* can also modify claudin-2 expression, *B. fragalis* and *C. dificile* both produce enterotoxins which lead to the degradation of cadherins and actin filaments respectively and *V. cholera* produces proteases which act on occludins within tight junctions and similar bacterial mechanisms may prove relevant to the progression of CP (Arbeloa et al., 2010; Simovitch et al., 2010; Thanabalasuriar et al., 2010; Chow et al., 2011; Bischoff et al., 2014).

1.5 Endotoxins, triggers of inflammation.

Endotoxins are archetypal PAMPs expressed on the bacterial outer membrane, once bound to the corresponding receptor, instigate a response intended to resolve the bacterial infection. The recognition of LPS by innate immune cells, such as MΦs instigates a number of antimicrobial responses, including inflammatory cytokine and chemokine secretion, production of reactive oxygen species (ROS) and reactive nitrogen species (RNS) as well as matrix metalloproteinases (MMPs) and AMPs, all promoting the pro-inflammatory response to resolve potentially detrimental bacterial activity (Molinaro et al., 2015).

1.5.1 Lipopolysaccharides

Lipopolysaccharide, the most intensely studied of all the microbial endotoxins confers structural rigidity to gram negative bacteria and interacts directly with the surrounding environment. The canonical form of LPS is recognised as that isolated from *E. coli*, however LPS structure has been shown to vary, not only between species but within species, dependent upon environmental cues (Fukuoka et al., 2001; Novem et al., 2009; Zenobia et al., 2014; Molinaro et al., 2015) . Variation in LPS composition occurs in two biologically active regions; the absence or existence of an O-antigen polysaccharide and variation in acylation and phosphorylation of the lipid-A anchor (Rietschel et al., 1994; Alexander and Rietschel., 2001). Structurally, the O-antigen region binds to the oligosaccharide core, which in turn links to Lipid-A via the 3-deoxy-D-manno-octulosonic acid (KDO) region (Fig. 1.2). LPS which lacks the O-antigen is termed rough LPS whereas LPS exhibiting the full structure is termed smooth LPS due to its microscopic appearance whereby, the edges of colonies are rough and

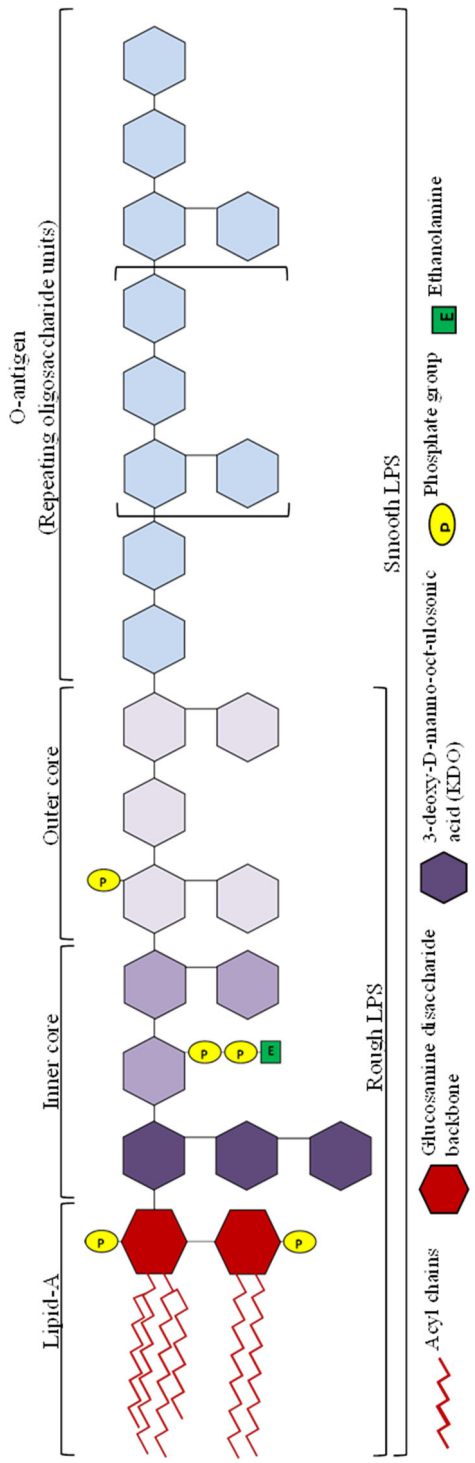

Figure 1.2. Typical lipopolysaccharide structure. Consisting of the Lipid-A anchor bound to KDO region which forms part of the core region, LPS which terminates at this point is termed rough LPS, whereas the addition of the O-antigen (repeating oligosaccharide units which can varying length) is termed smooth LPS.
(Maeshima and Fernandez, 2013; Steimle and Autenrieth, 2016).

agglutinate in saline (Alexander & Rietschel, 2001). Polysaccharide length (or ablation of) has been shown to affect the formation of micelles due to the variation if the hydrophobic lipid-A and hydrophilic polysaccharide regions (Molinaro et al., 2015). This may have particular relevance to inflammatory potential as the formation of micelles masks the bio-reactive lipid-A region. Once released from the bacterial cell wall, LPS with sufficient chain length, due to the hydrophilic nature of the core/O-antigen regions compared with the hydrophobic lipid-A, can lead to micelle formation, concealing the more immune-activatory, hydrophobic, lipid-A region. With regards to *Porphyromonas gingivalis*, this has been further elaborated with the discovery of species-specific A-LPS and O-LPS profiles, which is shown to affect hemin binding, which in turn affects LPS Lipid-A structure (P aramonov et al., 2001; Al-Qutub et al 2006; Rangarajan et al 2008; Rangarajan et al 2017).

1.5.2 Lipid-A modification

Variation in lipid-A structure influences bacterial survival; reduction in the number of negatively charged phosphate groups reduces the overall charge, affecting structural integrity and rigidity as well as the ability to interact with available ions including cationic AMPs, whereby a reduction in anionic groups within Lipid-A may limit AMP interaction (Alexander and Rietschel, 2001; Molinaro et al., 2015). Modification of lipid-A structure also influences innate immune response, thus also contributing to bacterial survival. For example, *Yersinia pestis,* when cultured at 27°C, the body temperature of a flea, the hexaacylated Lipid-A structure prevails, whereas at 37°C, the modified (and therefore resource and energy depleting) less immune-stimulatory tetraacylated formation predominates, reducing inflammatory potential in the human host aiding bacterial survival (Kawahara et al., 2002). In recent years the variation in LPS structure has become more widely recognised to include a number of bacterial species and the potential role that this may play in disease (Steimle and Autenrieth, 2016). Several gut associated pathogens have also been shown to express modified lipid-A (including *H. pylori)* (Fig. 1.3) (Molinaro et al 2015; Steimle and Autenrieth 2016). Modulation of environmental temperature is an additional mechanism which has been suggested to influence lipid-A structure expressed by the periopathogen; PG (Curtis et al 2011).

Hemin availability has also been suggested to trigger the switch in the lipid-A structure of PG (Al-Qutub et al., 2006; Coats et al., 2009). As a haem auxotroph, PG may be able to influence haem availability through lipid-A modification (Olczak et al., 2015). Low levels of haem (<1 μg/ml), result in a comparatively immunogenic penta-acylated/mono-phosphorylated lipid-A structure (termed

LPS_{1690} due to its mass/charge ratio), whilst at higher (>10 μg/ml) concentrations the weaker tetra-acylated/mono-phosphorylated ($LPS_{1435/1449}$) predominates (Jain & Darveau, 2010). To date, five different forms of LPS have been isolated from PG, all of which display varying levels of immunogenicity (Fig. 1.4) (Jain and Darveau 2010).

1.5.3 Immune recognition of modified lipid-A

Differences in structure between the canonical *E. coli* LPS and PG LPS have been known for some time to instigate differential immune responses, for which it is likely that modification of lipid-A is at least partially responsible (Coats et al., 2011).

The mechanisms through which these modified structures signal has been widely debated ranging from TLR4 in isolation, TLR2 at the expense of TLR4 and TLRs 2 and 4 in combination as well as cooperation with TLR9 (Burns et al., 2006; Papadopoulos et al., 2013; Muthukuru and Darveau, 2014; Kim et al., 2015; Nativel et al., 2017).

Reduction in acylation is thought to affect binding to the TLR4/MD2 complex. In the case of *E. coli* LPS, five of the acylated chains bind to the hydrophobic cavity of MD2, with the remaining sixth chain binding TLR4 (Park et al., 2009; Maeshima and Fernandez, 2013). In many cases it has been suggested that the tetra-acylated isoforms instead bind TLR2, and in addition act as an antagonist for TLR4 (Coats et al., 2003; Coats et al., 2009; Jain and Darveau, 2010; Li et al., 2013; Holden et al., 2014; Muthukuru and Darveau, 2014). Manipulation of conventional TLR signalling may contribute to the ability of PG to influence overall biofilm composition by allowing gram negative pathogenic bacteria to proliferate which would normally instigate a robust immune response, mechanisms which

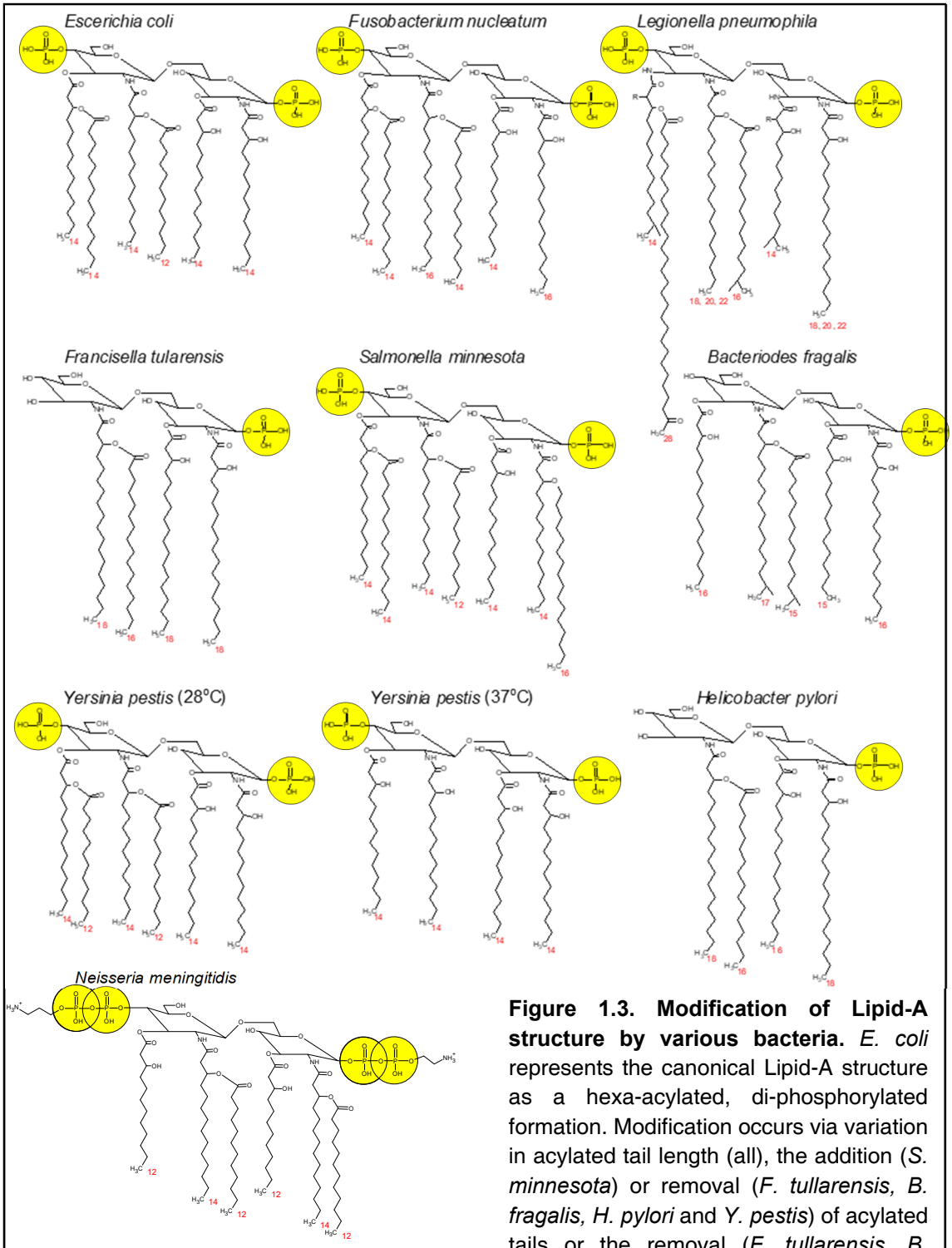

Figure 1.3. Modification of Lipid-A structure by various bacteria. *E. coli* represents the canonical Lipid-A structure as a hexa-acylated, di-phosphorylated formation. Modification occurs via variation in acylated tail length (all), the addition (*S. minnesota*) or removal (*F. tullarensis, B. fragalis, H. pylori* and *Y. pestis*) of acylated tails or the removal (*F. tullarensis, B. fragalis* and *H. pylori*) or modification (*N. meningitidies*) of phosphate groups (indicated in yellow) due to environmental cues.

Compiled from Weintraub et al., 1989, Asai et al., 2007, Maeshima & Fernandez, 2013, Molinaro et al., 2015, Steimle & Autenrieth, 2016.

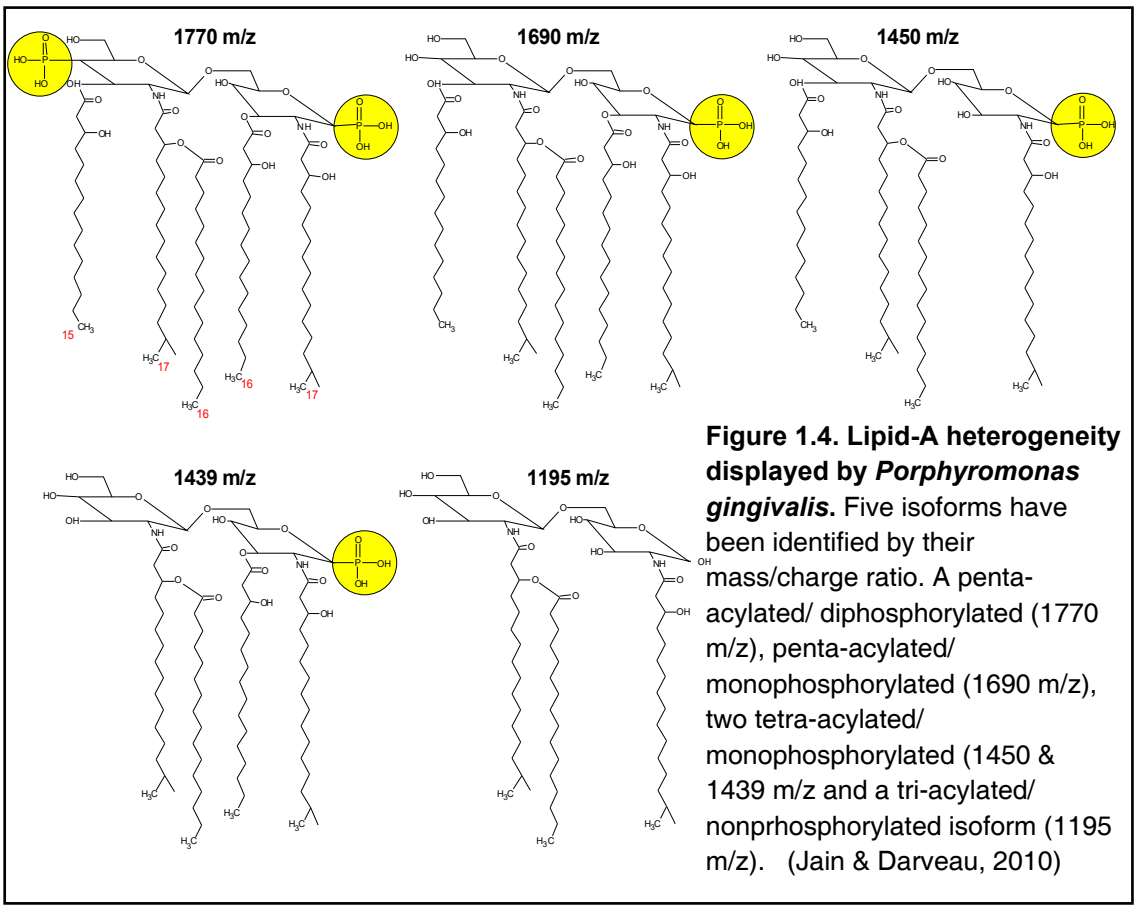

Figure 1.4. Lipid-A heterogeneity displayed by *Porphyromonas gingivalis*. Five isoforms have been identified by their mass/charge ratio. A penta-acylated/ diphosphorylated (1770 m/z), penta-acylated/ monophosphorylated (1690 m/z), two tetra-acylated/ monophosphorylated (1450 & 1439 m/z and a tri-acylated/ nonprhosphorylated isoform (1195 m/z). (Jain & Darveau, 2010)

have also been identified in periodontal disease (To et al., 2015). The case for PG LPS mediated TLR2 signalling is not unanimously supported and some studies suggest that this is primarily due to impurities such as lipoproteins being evident in LPS isolates (Jain & Darveau, 2010; Jain et al., 2013).

In addition to variation in acylation, position and number of phosphate groups also dictates lipid-A immunogenicity variation of which has been associated with periodontal disease (Coats et al., 2009; Zenobia et al., 2014). Even with structurally similar (penta-acylated/mono-phosphorylated) LPS isolated from *Bacteroides fragalis,* also suggested to signal via TLR2 and *Porphyromonas gingivalis* still managed to elicit differential immune responses due to location of the mono-phosphate group and potentially, minor variations in fatty acid structure (Alhawi et al., 2009; Berezow et al., 2009).

Additional mucosal defences have been shown to be modified by variation of LPS structure or species of origin. Small cationic peptides, defensins, can disrupt and penetrate bacterial membranes leading to cell death. PG LPS_{1690} has been shown to significantly upregulate human beta defensin-1, 2 and 3 mRNAs, whilst conversely PG $LPS_{1435/1449}$ resulted in a down-regulation. Modulation of human beta defensin by these LPS isoforms may therefore be associated with the subtleties of TLR2 and 4 signalling (Lu et al., 2009).

Of the bacteria known to modify lipid-A structure, PG is the most studied and may serve to indicate the potential effects of lipid-A modification in other pathologies. The signalling mechanisms associated with its LPS in relation to TLR4 have recently been thoroughly reviewed, in which they highlight the importance of two regulatory peptides found in saliva: leptin and ghrelin (Slomiany & Slomiany, 2018). The former was also found to affect both *E. coli* and *H. pylori* infection in the gut mucosae, in addition to limiting the negative impact of PG on salivary mucin production by suppressing PG LPS induced endothelin-1 expression (Slomiany and Slomiany, 2004). Whereas ghrelin, a regulatory hormone is implicated in a number of downstream functions including nitric oxide (NO) and prostaglandin E2 (PGE_2) production, and phosphatidylinositol 3-kinase (PI3K)/AKT signalling. A pleiotropic eicosanoid, PGE_2 demonstrates both pro-and anti-inflammatory properties but with particular relevance to CP is a known strong inducer of IL-8 expression, a chemoattractant for neutrophils (Yu and Chadee, 1998).

Several mucosal pathologies have, in recent years been discussed as diseases driven by a shift from Treg to the Th_1/Th_{17} axes, with the role of Th_{17} cells becoming more prominent as drivers of chronic inflammation (Moutsopoulos et

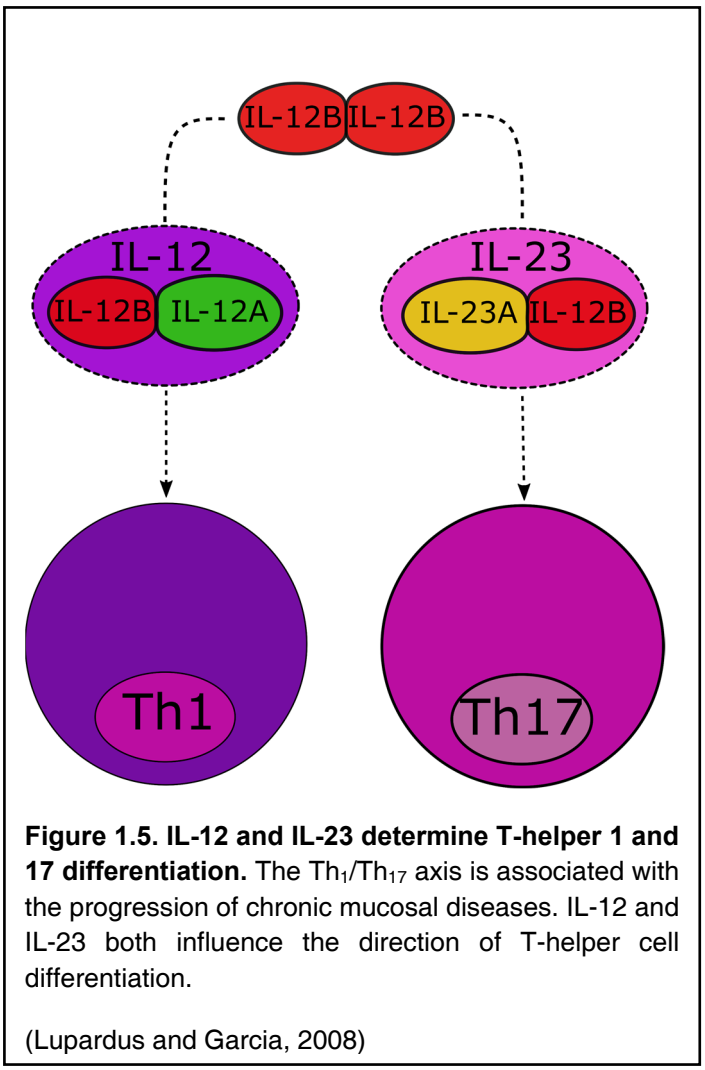

Figure 1.5. IL-12 and IL-23 determine T-helper 1 and 17 differentiation. The Th_1/Th_{17} axis is associated with the progression of chronic mucosal diseases. IL-12 and IL-23 both influence the direction of T-helper cell differentiation.

(Lupardus and Garcia, 2008)

al., 2012; Harbour et al., 2015). Key to the Th_1/Th_{17} axis is the balance between IL-12 and IL-23 respectively (Fig.1.5). IL-23 has been shown to be produced by macrophages in response to PG LPS stimulation and it has been suggested that lipid-A structure may influence the induction of the Il-12/IL23 responses (Allam et al., 2011; Arnold et al., 2016; Butcher et al., 2018). The production and ratio of the IL-12 and IL-23 subunits are critical in directing the route of disease progression and therefore minor alterations may be sufficient in modifying disease state. PGE_2 has been shown to induce IL-12a production in DCs whereas PGE_2 downregulates the IL12b subunit in monocytes (Kocieda et al., 2012; Kalim and Groettrup, 2013; Shi et al., 2015). IL-12b also exists as a homodimer which is proposed to antagonise IL-12 receptors, differential selective expression of IL-12b in its functional form induced by PGE_2 may go some way to explain the role of PGE_2 as a fine tuner of functional IL-12 and IL-23 heterodimers, potentially skewing towards a Th_{17} driven response (Kalinski et al., 2001; Khayrullina et al., 2008). PGE_2 is a pleiotropic lipid mediator that is found in increased levels in the gingival and periodontal tissues of those with CP (Bage et al., 2010). Prostaglandins are synthesised via the conversion

of membrane lipids to arachidonic acid, which is then converted to prostaglandin H_2 via COX1 and/or COX2. The final group of prostaglandin E synthases convert the unstable prostaglandin H_2 into the main prostaglandins, including PGE_2 (Bage et al., 2010; Bergqvist et al., 2019). Expression of COX2 is associated with key mechanisms associated with inflammation and have been successfully targeted with nonsteroidal anti-inflammatory drugs as a method of pain relief. The effects of PGE_2 are however, not confined to the pro-inflammatory status and have been shown to induce IL-10 production and limit TNF-α production as well as influencing MΦ polarisation towards an M2 MΦ phenotype (Bergqvist et al., 2019). In addition, exogenous levels of PGE_2 have been demonstrated to supress TNF-α production in bone marrow derived MΦs of a murine origin (Bergqvist et al., 2019). This narrative is further complicated by the correlation between iNOS induction, a function associated with M1 MΦs, and the formation of PGE_2 (Slomiany and Slomiany, 2018).

1.5.4 Host lipid-A modification

It is not only the microbial communities which utilise de-acetylation as a mechanism of reducing immune activation. Acyloxyacyl hydrolase (AOAH) is an endogenous host lipase produced by primary antigen presenting cells; MΦs and DCs, which effectively deactivates LPS by removing acyl chains, preventing binding to the TLR4/MD2 binding complex (Lu et al., 2008; Ojogun et al 2009). However, rather than acting as a component of ET, AOAH is shown in murine models to hasten recovery from ET, perhaps by limiting repetitive LPS binding (Lu et al., 2008). The expression of AOAH has been associated with Th_{17} driven immunity through the influence of colonic DCs and susceptibility and maintenance of ET in MΦs (Janelsins et al., 2014; Lu et al., 2013).

1.6 Macrophages

Macrophages (MΦs) have been extensively studied since their identification by Elie Metchnikoff in 1882, due to their role as the first line of defence against infection and maintaining homeostasis. The importance of MΦs as regulators of inflammation and therefore homeostasis should not be underestimated and indeed, they have been described as “a dispersed homeostatic organ” and conversely, MΦs are found in significant levels in the tissues of those suffering from CP (Foey, 2015a; Gordon and Pluddermann, 2017). Distributed throughout the body, distinct populations demonstrate substantial heterogeneity, enabling a level of specialisation dependent upon location.

Tissue resident MΦs are deployed during embryonic development and are replenished and reinforced by blood monocytes which differentiate to MΦs following diapedesis into the specified tissue as well as localised proliferation (Foey, 2015a; Gordon and Pluddermann, 2017). As a result, tissue MΦs consist of a dynamic population of embryonic and blood derived monocytic origin, each demonstrating variable differences in preprograming (Foey 2015a). MΦ functions are numerous and extensive, in addition to their phagocytic and anti-microbial/viral capabilities. They act as antigen presenting cells and express both activatory and suppressive molecules which in combination orchestrate the innate and adaptive immune response. Equipped with a number of receptors which recognise highly conserved molecules expressed by potential pathogens including Toll like receptors (TLRs), NOD like receptors (NLRs) and scavenger receptors, MΦs are the first to respond, limiting deleterious effects of infection. Ligation of PAMPs to their corresponding receptor initiates a multitude of responses aimed at resolving the infection and where this is unachievable,

limiting progression until specialised adaptive responses are raised. The dichotomy between homeostatic and inflammatory responses has been addressed through the identification of MΦ subsets which presents phenotypes disposed towards opposing functions.

1.6.1 Macrophage polarisation.

At present, MΦs are categorised by their activation status into two distinct subsets: M1 (classical) and M2 (alternative). Traditionally this was done with the intention of aligning MΦ subsets with the Th_1 and Th_2 paradigm identified in T-helper cells (Gordon and Martinez, 2010). This was not without validity as classically activated MΦs were stimulated with IFNγ and bacterial LPS and in this activated state, stimulate Th_1 cells to produce IFNγ, inducing a positive feedback mechanism. Likewise, alternatively activated MΦs are achieved using IL-4 and IL-13, with IL-4 being typically associated with Th_2 cells (Martinez and Gordon, 2014). Subsequently as with the identification of additional T-helper phenotypes, $Th_{9/17/22}$ etc., MΦ subset characterisation has proven more complex than the traditional polarised system. Whilst classically activated M1 MΦs remain diametrically opposed to alternatively activated M2 MΦs in their primary functionality, the characterisation of multiple M2 sub-profiles has somewhat blurred the boundaries between M1 and M2 subsets (Fig. 1.6). Functions such as $CD8^+$ T-cell activation (CD86), Th_1 cell differentiation (IL-12), antigen presentation (MHCII) and inflammatory cytokine secretion (TNFα) have been shown to be functions attributed to both the M1 and certain M2 subsets. Remarkably, inducible nitric oxide synthase (iNOS) and thus nitric oxide production, regarded as a key anti-microbial function of M1 MΦs has been identified in M2b MΦs (Foey, 2015a).

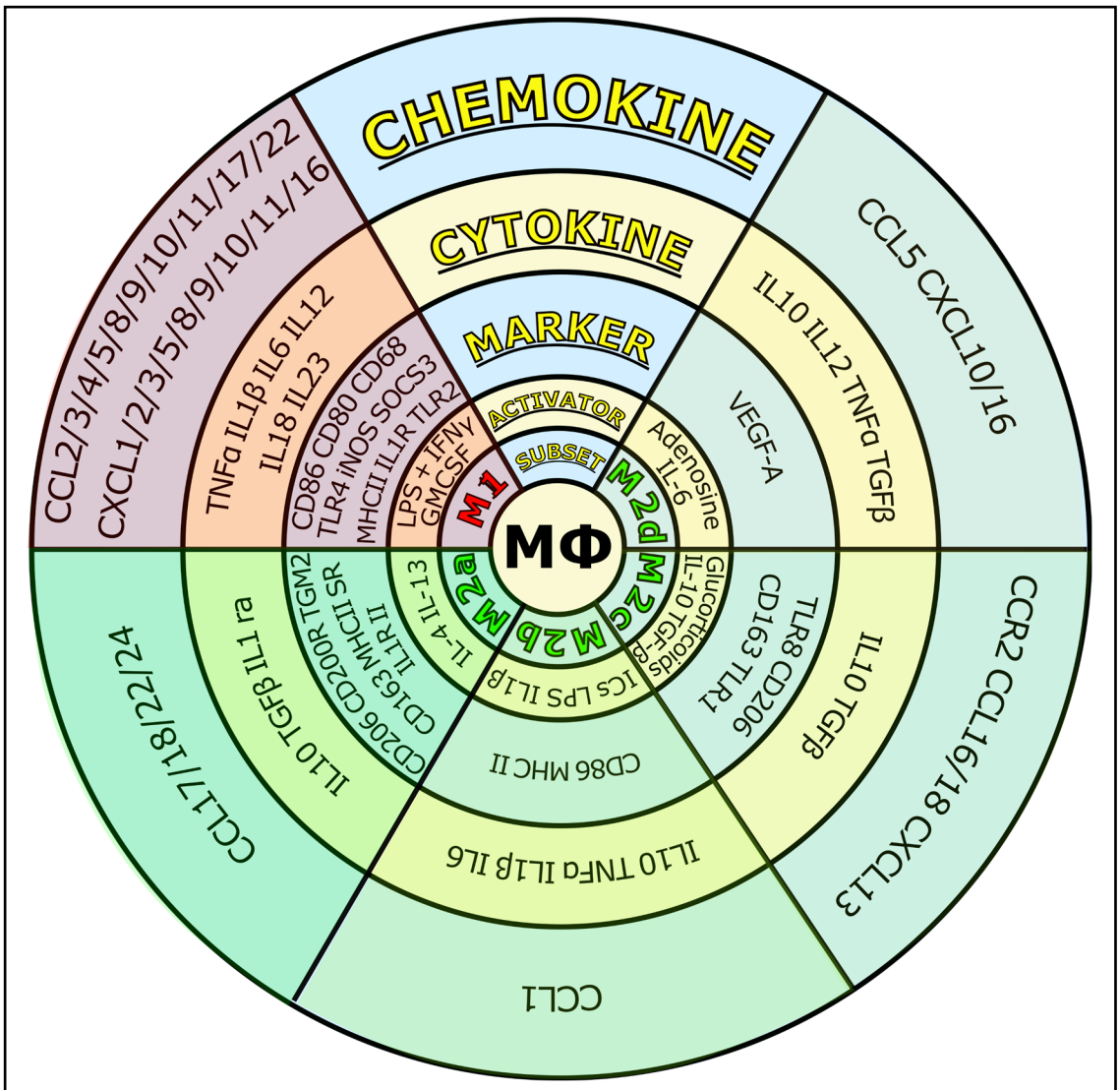

Figure 1.6. Human macrophage polarisation. MΦs have been suggested to polarise into specific subsets, M1 and multiple M2 phenotypes: a-d. No specific marker has been identified for each subset, with each displaying individual phenotypes which respond to specific activator molecules, display specific surface marker proteins and produce a particular cytokine and chemokine profile, indicated above for each subset.
This figure is adapted from Duluc et al (2007), Foey (2015a) and Röszer et al (2015).

This is in stark contrast to traditionally associated M2 MΦ arginine metabolism, resulting in ornithine and ultimately polyamine production, which promotes growth and proliferation, or proline, inducing collagen production (Rath et al., 2014).

The characterisation of MΦs associated with specific disease states further complicates the matter and supports the notion of plasticity dependent upon environmental cues.

Whilst similar to M2d MΦs, tumour associated MΦs (TAMS) have been identified to be a distinct phenotype separate from those of M1 and M2 (Duluc et al., 2007). In atherosclerosis, additional phenotypes have been identified, directly associated with the localised microenvironment linked to the disease; M4 and Mox subsets are activated by platelet factor 4 and oxidised phospholipids. Interestingly the trio of HA-mac, M(Hb) and Mhem MΦs all respond to either haem or haemoglobin, a trait that may be shown to influence the behaviour of haem auxotrophic bacteria (Foey, 2015a). The concept of MΦ plasticity has been mooted for some time, suggesting that M1 and M2 MΦs are opposing ends of a sliding scale, with M2a, b, c & d being points along that scale (Mantovani et al., 2004; Gordon and Martinez, 2010; Foey, 2015a; Röszer et al., 2015). As the array of identified subsets and groups is as of yet a lab-based paradigm, not seen *in-vivo*, the characterisation of disease-associated profiles adds to the suggestion that MΦs display a high degree of plasticity and adaptability. These subgroups likely represent a snapshot of the status of a tissue resident MΦ at a particular moment in time, dependent upon their origin and local environment.

1.6.2 Macrophage recognition of LPS

A number of conserved microbial elements instigate an immune response via a multitude of receptors. Charles Janeway first presented the framework which would describe pattern recognition receptors (Murdock and Nunez, 2016). Subsequently the identification of the highly conserved TOLL receptor in drosophila lead to the discovery of the LPS receptor – TLR4 (Anderson, Bokla and Nüsslein-Volhard, 1985; Hoshino et al., 1999). To date 10 TLRs have been identified in humans, all recognising conserved bacterial, viral, fungal elements

Toll like receptor	Exogenous ligand	*Reference*
TLR1	Lipoproteins	(Takeuchi et al., 2002)
	Lipopeptides	(Takeuchi et al., 2002)
TLR2	Lipoglycans	(Quesniaux et al., 2004)
	Modified Lipopolysaccharide	(Darveau et al., 2004)
	Lipoteichocic Acid	(Schroder et al., 2003)
	Peptidoglycan	(Takeuchi et al., 1999)
	Zymosan	(Ozinsky et al., 2000)
	Phospholipomannan	(Li et al., 2009)
	Protozoan GPI anchor	(Campos et al., 2001)
	Viral envelope proteins	(Boehme et al., 2006)
TLR3	dsRNA	(Alexopoulou et al., 2001)
TLR4	Lipopolysaccharide	(Shimazu et al., 1999)
	Lipid-A	(Qureshi et al., 1985)
	Glycoinositolphospholipids	(Medeiros et al., 2007)
	Mannan	(Tada et al., 2002)
	Viral envelope proteins	(Madeira et al., 2016)
	RSV F-protein	(Rallabhandi et al., 2012)
TLR5	Flagellin	(Hayashi et al., 2001)
TLR6	Multiple diacyl lipopeptides	(Takeuchi et al., 2001)
TLR7	ssRNA	(Heil et al., 2004)
TLR8	ssRNA	(Heil et al., 2004)
TLR9	CpG DNA	(Hemmi et al., 2000)
	dsDNA	(Zannetti et al., 2014)

Table 1.4 Known exogenous ligands to human toll like receptors. TLRs recognise conserved molecular patterns derived from potentially pathogenic sources i.e. of bacterial, viral, protozoan and fungal origin. TLRs 2 and 1 or 6 dimerize to recognise increase specificity and to date, no specific ligand has been identified for TLR10.

as well those associated with helminth worm infection and protozoa (Table 1.4) thus providing a method of non-specific recognition at the first instance of potential infection. To date, no ligand has been identified for TLR10 (Beutler and Rehli, 2002).

1.6.2.1 TLR complex formation

Binding of bacterial LPS to TLR4 requires the cooperation of a number of accessory proteins; firstly, serum LPS binding protein (LBP) attaches, allowing the additional binding of CD14, a molecule involved in both TLR2 and 4 signalling. CD14 may either be in a soluble form or membrane bound and it optimises LPS

detection in conjunction with LBP by accessing and monomerising aggregated LPS (Ulevitch and Tobias, 1995; Park and Lee, 2013;).

In the case of TLR4, it homodimerizes and forms a complex with myeloid differentiation factor 2 (MD-2) whereas TLR2 heterodimerizes with either TLR1 or TLR6. MD-2 binds TLR4 via hydrophilic interactions with the primary binding site of LPS, the lipid-A anchor region (Fig1.2). The acyl chains and phosphate groups of lipid-A are critical for MD-2 binding. For optimal binding five of the six lipid chains are bound inside the MD-2 pocket and the remaining chain is exposed to the hydrophobic surface regions of MD-2 where it forms a hydrophobic interaction. Typical, phosphorylated lipid-A further stabilises the receptor complex by interacting directly with the dimerised TLRs due to their charge affecting hydrogen bonds (Park and Lee, 2013).

Dimerization of the extracellular TLR4 domains complete with the conformational changes induced by MD-2/CD14/LPS binding leads to repositioning of the intracellular Toll/IL-1R (TIR) TLR4 domains. Following optimal LPS binding, changes to the TIR domains enable interaction with the TIR domains of adaptor proteins such as myeloid differentiation factor 88 (MyD88) and MyD88 adaptor-like (MAL), beginning the sequence of initiating signal transduction, leading to distinct innate immune responses (Kenny and O'Neill, 2008).

1.6.2.2 TLR signal transduction

Signalling via TLR4 has been extensively studied due to its association with bacterial infection and its early identification relative to other TLRs. Signalling transduction occurs via two primary pathways; MyD88-dependant and MyD88-independent, while intensely studied, the complexity of these signalling

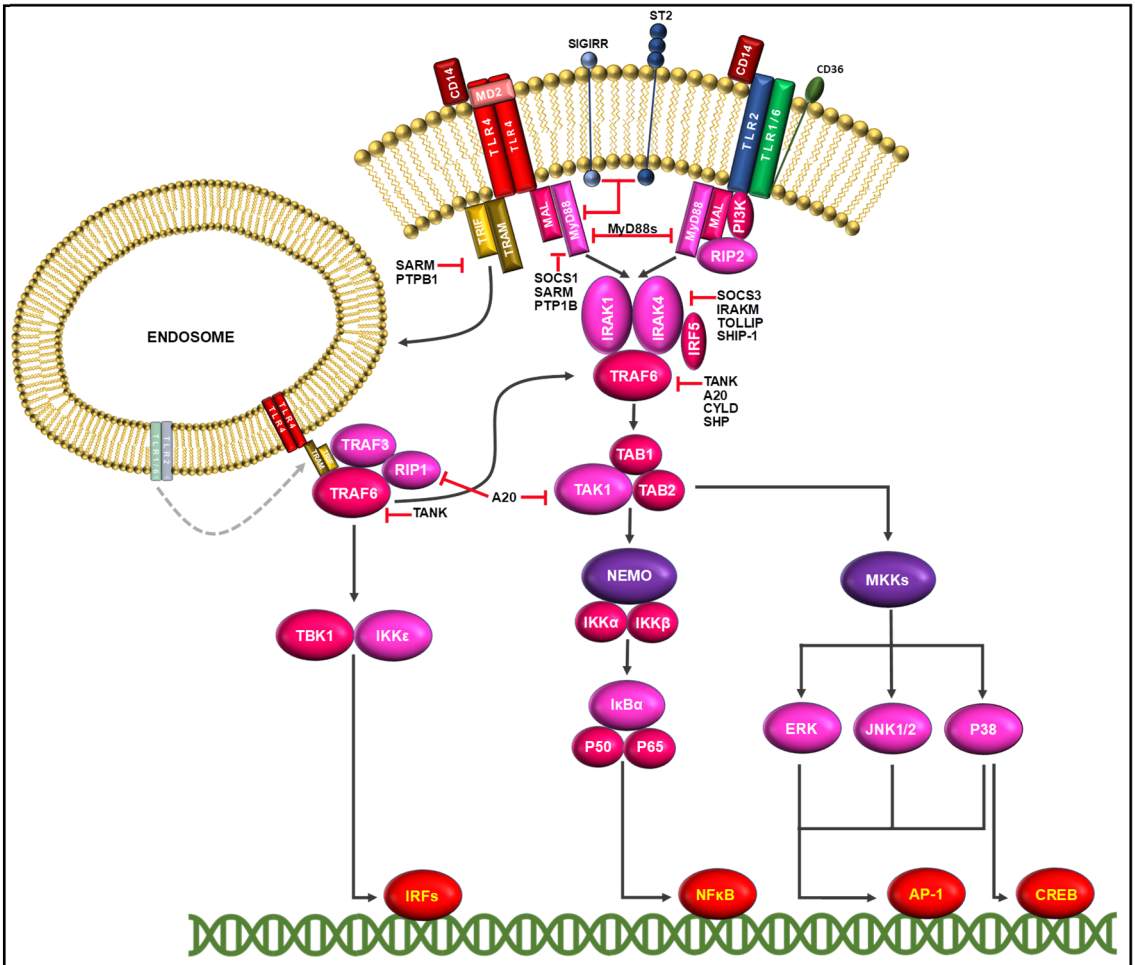

Figure 1.7. Human TLR2/4 signalling mechanisms. *Two primary signalling mechanisms* have been identified in TLR4 signalling; MyD88-dependant which is shared with TLR2 signalling and MyD88-independent which whilst there is emerging evidence for TLR2 mediated signalling, is still yet to be defined. MyD88 mediated signalling is associated with the production of pro-inflammatory cytokines and chemokines through the NF□B transcription factor or via MAP kinases leading to AP-1 and CREB activation. The MyD88-independent signalling pathway recruits the adaptors, TRIF and TRAM (indicated in brown), which upon LPS binding relocate the LPS/TLR/TRIF/TRAM complex to internal endosomes and is associated with type-1 interferon responses. Both signalling mechanisms are tightly regulated at phases throughout the signalling cascade to prevent unwarranted or excessive inflammation. Diagram is compiled from Hoeffler and Habener (1990), Ollivier et al (1996), Houslay and Kolch (2000), Souza et al (2001), Jin and Conti (2002), Foey and Brennan (2004), Zhang et al (2007), Mogensen (2009), Wen, Sakamoto and Miller (2010), Yamamoto and Takeda (2010) Kondo, Kawai and Akira (2012) and Newton and Dixit (2012).

mechanisms are constantly being updated but the fundamental signalling pathways are indicated in Fig 1.7.

1.6.2.2.1 MyD88-dependant signalling

The MyD88-dependant pathway is instigated by conformational changes to the dimerised TLR, leading to the recruitment of adaptor proteins MyD88 and MAL to

the cytoplasmic TLR/TIR domain, leading to a signalling cascade indicated in figure 1.7 (Newton and Dixit, 2012). Regulatory mechanisms (section 1.6.2.3) affect the signalling pathway so as to enable or restrict the activation of multiple transcription factors. Ultimately, the p50/p65 sub-units (NFκB) translocate into the nucleus and activate expression of a range of pro-inflammatory genes such as TNF-α and IL-8 (Newton and Dixit, 2012). The TRAF6 complex, when activated and translocated to the cytosol is also capable of phosphorylating a group of MAP kinases which results in the phosphorylation and activation of p38, ERK and the c-Jun N-terminal kinase (JNK) leading to the activation of the transcription factors AP-1 and cyclic adenosine monophosphate response element binding protein (CREB) (Mogensen, 2009, Newton and Dixit, 2012, Yamamoto and Takeda, 2010). CREB is also a transcription factor with numerous targets including COX2, macrophage inhibitory factor (MIF), IL-6, IL-10 and TNF-α (Mayr and Montminy, 2001; Brenner et al., 2003).

1.6.2.2.2 MyD88-independant signalling

This alternative signalling pathway has been identified to be utilised by the endosomal TLRs, TLR3,7,8 and 9, as well as TLR4 which also undergoes receptor mediated endocytosis, complete with bound LPS. Internalisation is controlled by the GTPase dynamin, facilitating endosomal translocation, and enabling MyD88-independent associated adaptor protein recruitment (Kagan et al., 2008). These signalling events predominantly lead to the phosphorylation of interferon regulatory factors (IRFs) such as IRF3 enabling its translocation to the nucleus, and the production of type-I IFNs and promotion of IFN inducible genes (Takeuchi and Akira, 2010). Recently TLR2 has been indicated to utilise this

alternative pathway but the mechanisms of which are still under investigation (Nilsen et al., 2015).

1.6.2.3 Negative regulation of TLR signalling.

The induction of pro-inflammatory molecules has potentially detrimental effects on host tissue and therefore a robust system of negative regulation exists which controls the induction of such genes and their activating functionality. Negative regulation of TLR signalling has been extensively reviewed by Kondo, Kawai and Akira (2012) and a summary of relevant negative regulators is indicated in figure 1.7.

The sterile alpha and armadillo-motif-containing protein (SARM) is one such regulator which affects both the MyD88-dependant and -independent pathway (Peng et al., 2010). It is suggested that this is mediated through a modified glycine residue, located in the BB-loop of the SARM TIR domain which is able to bind and inhibit progression of both TRIF and MyD88 complex signalling when initiated by ligand binding to either TLR4 or TLR2 in an HEK cell model (Carlsson, Ding and Byrne, 2016).

The TRAF family member associated NFκB activator (TANK) is another example of a modulator of both the MyD88-dependant and -independent pathway due to its ability to inhibit ubiquitination of TRAF6 (Kondo, Kawai and Akira, 2012). Two members of the Src homology 2 (SH2) domain-containing inositol 5'phosphatase (SHIP) family also modulate both pathways – SHIP-1 affecting the MyD88-dependant pathway via IRAK1/2 whilst SHIP-2 modulates the MyD88-independent pathway via TRIF and TBK1 (Kondo, Kawai and Akira, 2012).

The TRAM-adaptor with a GOLD domain (TAG) was identified as a negative regulator of MyD88-independent signalling which was found to dissociate TRIF from TRAM and localise to late endosomes where TAG restricts IRF3 activation (Palsson-McDermott et al., 2009). It is suggested that endosomal internalisation of receptors may form part of a protective mechanism to as to prevent tissue damage caused by prolonged inflammation.

The small heterodimer partner (SHP) has also been suggested to limit TRAF6 ubiquitination as well as acting directly on specific NFκB subunits, the mechanisms of which require further study (Zhang and Shen, 2011).

Eight suppressor of cytokine signalling (SOCS) proteins have been identified, of which all possess an SH2 domain and a short, C-terminal domain, the SOCS box (Hilton et al., 1998). SOCS proteins recruit Cullin5 to form an E3 ubiquitin ligase complex (Kamizono et al., 2001). A recent study however, has extended the functional profile of SOCS1 (Liau et al., 2018). Additional functionality is mediated through the kinase inhibitory region of SOCS1 which blocks the substrate binding groove of JAK1, JAK2 and TYK2 (Liau et al., 2018). SOCS1 and SOCS3 are unique in the ability to interact directly with Janus kinases (JAKs) which in turn activate STAT mediated signalling (Yasukawa et al., 1999). SOCS1, the most potent of the SOCS group, has been shown to inhibit the production of IFNα/β/γ, IL-12/23, IL-4/13 in murine models (Liau et al., 2018).

The thioesterase enzyme cylindramtosis (CYLD) has been associated with the de-ubiquitination of TRAF6 and ultimately TLR2 signal transduction (Yoshida et al., 2005). Additionally, it can interact with IκKγ, preventing phosphorylation of IκB (Mathis et al., 2016). The specific link to TLR2 mediated signalling may arise from its association with JNK2 activation in a cAMP/PKA dependant manner, inducing

IL-10 production and the upregulation of SOCS3 (Aronoff et al., 2006; Gasperini et al., 2002; Komatsu et al., 2013). The activation of JNK being identified as the primary pathway when TLR2 is activated via specific pathogenic bacteria (Diya et al., 2008).

Toll-interacting protein (TOLLIP) has been implicated in the suppression of inflammatory responses yet also the promotion of low-grade inflammation (Kowalski and Li, 2017). Suppressive actions are thought to be due to its affinity with phosphoinositide through its C2 domain which facilitates binding to intracellular membrane functions, interfering with endosomes, lysosomes and phagosomes etc. In addition, TOLLIP has been shown to directly interact with the IRAK complex preventing autophosphrylation (Bulut et al., 2001; Zhang and Ghosh 2002). A recent study has found that *E. coli* K12 mediated, ET induced, TOLLIP expression was preferentially induced in M1 MΦs whereas IRAK-M was favoured in M2 MΦs (Al-Shaghdali et al., 2019).

Unique to monocytes and macrophages, IRAK-M lacks both kinase activity and displays a minimal ability to be phosphorylated. However, it is able to limit downstream signalling by binding IRAK4 during its initial TLR binding event, preventing the conformational changes induced by phosphorylation, which allows its dissociation from the receptor to form the IRAK/TRAF6 complex (Kobayashi et al., 2002).

1.7 Endotoxin tolerance

Despite having been recognised for some time, the exact mechanisms which drive this phenomenon are as yet, unknown (Liu et al., 2019). This is likely due to the complexity of a multitude of signalling parameters, each influencing each other and additionally each being susceptible to influence by environmental factors in combination with pre-existing cellular programming. A number of mechanisms have been studied and suggested to contribute towards ET including reduction in receptor expression, plasticity between MΦ subsets, instigation of intracellular suppressive molecules and epigenetic modification restricting transcription of pro-inflammatory genes. Furthermore, it is suggested that ET is not a standardised response to multiple exposures of LPS and that modification of LPS structure may influence the induction and magnitude of ET (Martin et al., 2001; Butcher et al., 2018).

Given the differential capabilities of *E. coli* and PG LPS to induce an inflammatory response, it is reasonable to consider their potential to differentially induce ET. Indeed, this has been shown to be the case; *E. coli* LPS induced ET suppresses IL-1β, IL-6 and TNF-α whereas PG LPS induced ET suppresses IL-1β but not IL-6 and TNF-α in human MΦs (Martin et al., 2001). Additionally, *E. coli* LPS was shown to reduce TLR4 expression whilst PG LPS enhances TLR2/CD14 expression. This somewhat conflicts with a study utilising the same THP-1 derived macrophages (Foey and Crean, 2013). Whilst this agrees with the inability of PG LPS to suppress IL-6 and TNF-α, they also conclude that IL1-β secretion is not affected (Foey & Crean, 2013). This study utilises a model whereby THP-1 pro-monocytes are driven towards differential polarisation utilising PMA to drive towards an M1 profile, but alternatively, vitamin D_3 is used

to push towards an M2 profile. It is this M2 type MΦ which is demonstrated to be more susceptible to PG LPS induced tolerisation of the cytokine profile measured (Foey & Crean, 2013).

MΦ subsets therefore exhibit differential sensitivity to ET using PG LPS, with the M1 subset more resistant to tolerisation in comparison with the M2 subset and M2 MΦs showing an increase in the regulatory cytokine, IL-10 due to a differential sensitivity to STAT3 activation which is suggested to influence plasticity between MΦ subsets (Foey & Crean, 2013; Foey et al., 2017). Many studies have examined the phenotypic properties of tolerised MΦs which led to suggestions that these cells resembled a less inflammatory M2 type MΦ though this was somewhat disputed (Pena et al., 2011; Rajaiah et al., 2013). The matter is complicated by the lack of identification specific markers of classically, M1 and alternatively activated M2 MΦs particularly compared to the comparative ease of T-helper subset identification, although several attempts have been made (Martinez and Gordon, 2014; Murray et al., 2014).

Transcriptomic analysis using bone marrow derived MΦs using a murine model, has revealed that tolerised MΦs adopt a hybrid state with features of both subsets, suggesting that a level of plasticity exists (O'Carroll et al., 2014). A later study, which assessed the transcriptomic profile resulting from tolerance induced through several distinct TLRs found that each induced its own distinct profile, with TLR4 inducing the most comprehensive level of tolerisation, primarily via NFκB signalling (Butcher et al., 2018). This same study found that IFNβ was tolerised via both TLR2 and TLR4, whereas IL-6 and IL-10 were tolerised via TLR4 but not TLR2. IFNβ specifically plays a role in regulating MyD88-independent signalling, but pre-treatment with LPS suppresses STAT1 phosphorylation due to SOCS3

suppressive mechanisms, independent of STAT3, TNF-α, IL-6 and IL-10 (Ando et al., 2015; Zaric et al., 2011). In addition, IFNβ is also shown to be upregulated in MΦs tolerised through TLR4 and not TLR2 in a murine model, implicating a potential role for the MyD88-independent TRIF/IRF3 pathway in TLR4 mediated tolerance (Biswas et al., 2007). A later study utilising human monocytes shows diminished levels of IFNβ in tolerised cells and may highlight differential responses between murine and human immune responses. This disagreement may also be due the transition from translation through to secretion as different time points were utilised to measure both message and protein (Piao et al., 2009). The study focused the induction of negative regulators to disrupt MyD88-dependent and-independent pathways and their observations included a reduction in IFNβ expression, concomitantly with increases in suppressor of IκB kinase-ε (SIKE), SARM, TOLLIP, IRAK-M, SHIP-1 and SOCS1. This resulted in a decrease in p38 phosphorylation, IκBα degradation and ultimately a reduction in TNF-α, IL-6 and IL-8. The study identified potential dysregulation of the MyD88-independent pathway via disruption to tank binding kinase 1 (TBK1) and TRIF activation (Piao et al., 2009).

Ubiquitin Ligase has been investigated as a potential regulator of TBK1 and IL-1R associated kinase 1 (IRAK1), in particular Pellino-1 a mediator of K48 ubiquitin ligase has been shown to positively regulate TLR4 and TLR2 mediated pro-inflammatory mechanisms and furthermore be down-regulated during ET (Murphy et al., 2015). The TRAF3 complex has also proved to be a target for Pellino-1 mediated ubiquitination and K63 ubiquitination was suppressed by ET impairing ubiquitination of IRAK1, TRAF6 and TGF-β activated kinase 1 (TAK1), accompanied by increased expression of the de-ubiquitination enzyme A20,

suggesting a role in both MyD88-dependent and-independent signalling (Li et al., 2016; Xiong et al., 2011). Ubiquitin ligases, in particular E3 ligases, due to their increased specificity have been proposed as a target for pharmacological therapies with a potential to modify TNF-α, IL-6 and PGE_2 production (Zeng et al., 2015).

Following the induction of ET TNF-α is regularly measured as an indicator of inflammation. This canonical inflammatory cytokine can be both affected and the effector in cross tolerance (CT) i.e. the suppression of pro-inflammatory responses due to pre-exposure to TNF-α. A less effective method of suppression than ET, type-I interferons have been shown to further modulate CT via chromatin remodelling, regulating access to transcription factor binding events (Park et al., 2017). This study finds significant differences between ET and IFN assisted CT, particularly in the ability of IFNα to prevent TNF-α suppression. In addition, this study found that using this method of tolerisation, the JAK/STAT pathway, leading to antiviral responses, remains functional, a mechanism recognised as suppressed via traditional ET. This study highlights the importance of considering the dynamicity of the intra- and extra-cellular events which together may fine tune MΦ responses.

The study of micro-RNAs which interfere with signalling mechanisms has brought attention to AKT signalling pathways. AKT is involved in numerous functions including cell survival and metabolism but is also recognised as a modulator of MΦ polarisation (Arranz et al., 2012). This serine/threonine specific protein kinase is found in three forms, AKT1, AKT2 and AKT3, both AKT1 and AKT2 have been shown to affect the induction of the microRNAs miR-155 and miR-146a with the latter also shown to be highly expressed in endotoxin tolerised THP-1, cells the

former however is a negative regulator of SOCS1 and SHIP1 (Androulidaki et al., 2009; Nahid et al., 2009; Mann et al 2017; Vergadi et al., 2017). MΦ's that are SHIP-1$^{-/-}$ have been shown to be refractory to endotoxin tolerisation whilst AKT2$^{-/-}$ MΦs exhibit a higher level of IL-10 production (Sly et al., 2004; Arranz et al., 2012). Additionally, the balance of these two micro-RNAs are suggested to represent a diametrically opposed positive and negative feedback loop in the regulation of NFκB via both TLR2 and TLR4 activation in both homeostasis/tolerance and disease (Mann et al., 2017). In conjunction, degradation of IRAK1 and reduction of TRAF6, correlate with increased expression of miR-146a (Chassin et al., 2010; Liu et al., 2014). Cyclooxygenase 2 (COX-2) and its enzymatic product, PGE_2 both correlate with increased levels of miR-155 in both cancer and asthma whilst a decrease in miR146a instigates an up-regulation of COX-2 (Cornett and Lutz, 2014; Comer et al., 2015).

1.8 Biomarkers for periodontal disease.

Given the understanding of periodontal diseases that has been demonstrated throughout this chapter, it would seem logical that some of the measurable parameters may serve as indicators of periodontal disease diagnosis and severity. This is indeed the case, but the identification of a single measurable analyte has so far proven difficult.

The national institute of health defines biomarkers as:

"a characteristic that is objectively measured and evaluated as an indicator of normal biological processes, pathogenic processes, or pharmacological responses to therapeutic intervention"

(Biomarkers Definitions Working Group, 2001).

Multiple efforts have been made to identify biomarkers which can aid in the detection and diagnosis of periodontal disease (Taylor, 2014). To date, a number of candidates have been identified but due to the complex nature of periodontal disease pathogenesis, their application thus far has been limited and no satisfactory candidate has been identified to aid early detection (González-Ramírez et al., 2019). The complexity of the disease presents a wide array of potential biomarkers which may positively associate with disease state, incorporating both host response and bacterial composition, which may encompass a number of processes including metabolic, genetic and molecular changes (Taylor, 2014; Stathopoulou, Buduneli and Kinane, 2015; Arias-Bujanda et al., 2020; Lundmark et al., 2019). An additional consideration is the location from which the analyte is obtained. Previous studies have examined blood, serum and plasma levels of molecules associated with systemic changes (Stathopoulou,

Marker	Serum	Saliva	GCF	References
Albumin	☐	☒	☐	Verhulst et al., 2019
Alkaline phosphatase	☐	☒	☒	Dabra and Singh, 2012; Khongkhunthian et al., 2014; Patel et al., 2016
Chitinase	☐	☒	☐	Verhulst et al., 2019
Cortisol	☒	☐	☐	Ishisaka et al., 2008
C-reactive protein	☒	☐	☐	Nakajima et al., 2010; Lobão et al., 2019
Haemoglobin	☐	☒	☐	Arias-Bujanda et al., 2020
HDL	☒	☐	☐	Nibali et al., 2007
HGF	☐	☒	☐	Taylor, 2014
IFN-γ	☐	☒	☐	Dede, Özden and Avci, 2013
IL-1β	☐	☒	☒	Barksby et al., 2007; Buduneli and Kinane, 2011; Yue et al., 2013; Taylor, 2014; Ebersole et al., 2015; Liukkonen et al., 2016; Arias-Bujanda et al., 2020
IL-6	☒	☒	☐	Nakajima et al., 2010; Taylor, 2014; Ebersole et al., 2015; Arias-Bujanda et al., 2020; Lobão et al., 2019
LDL	☒	☐	☐	Nibali et al., 2007
MCP-1	☐	☒	☐	Gupta, Chaturvedi and Jain, 2013; Nishka et al., 2018
MIP-1α	☐	☒	☐	Taylor, 2014; Ebersole et al., 2015
MMP-8	☐	☒	☒	Gursoy et al., 2010; Gursoy et al., 2013; Kinney at el., 2014; Miricescu et al., 2014; Morelli et al., 2014; Taylor, 2014; Ebersole et al., 2015; Heinz, Paliwal and Ivanovski, 2015; Mauramo et al., 2018; Arias-Bujanda et al., 2020
MMP-9	☐	☐	☒	Kinney et al., 2014; Taylor, 2014; Arias-Bujanda et al., 2020
PGE2	☐	☒	☐	Yue et al., 2013

Table 1.5 Protein biomarkers which demonstrate sensitivity in periodontal disease testing. Multiple proteins have been identified which are shown to be associated with periodontal disease, isolated from either serum, saliva or gingival crevicular fluid. Those listed have demonstrated a significant sensitivity to differentiate between disease states. Currently the matrix metalloproteinase MMP-8 demonstrates the best sensitivity and specificity to act as a diagnostic biomarker.

Buduneli and Kinane, 2015; Lobão et al., 2019). Subgingival plaque and GCF however give a much more localised, site specific view of disease status, whereas saliva resides somewhere in between containing both local and systemic components which are more representative of overall oral health (Taylor, 2014; Stathopoulou, Buduneli and Kinane, 2015).

Any potential biomarker must exhibit both specificity and sensitivity, being able to identify not only those with periodontal disease but also distinguishing them from those that suffer with gingivitis and recognising healthy individuals. Recent advances in analytical techniques such as microarray gene expression and proteomics have allowed for the evaluation of multiple potential biomarkers based upon relative expression when comparing samples from patients with PD to controls (Azuki, Tetsuro and Numabe, 2019; Suzuki, Horie and Numabe, 2019; Tsuchida et al., 2019). It should be noted however, that association with disease state does not necessarily translate through to sensitivity and specificity. Those proteins which have demonstrated a level of specificity have been indicated in table 1.5. Of the proteins listed in table 1.5, MMP-8 currently represents the most consistent and promising target as a single molecule biomarker, with point of care tests currently in development (Räisänen et al., 2019; Taylor et al., 2019).

One of the main problems with looking at a single analyte as a biomarker to aid diagnosis and particularly prediction, is that these markers are most often a product of immune reactions. Several studies have tried to increase sensitivity of detection by measuring multiple analytes such as multiple markers or combining protein markers with patient health parameters but these still rely on a heightened immune response to generate the analytes (Ebersole et al., 2015; Verhulst et al., 2019). A recent study by Lundmark et al (2019) have combined inflammatory mediators with 16S rRNA sequencing of the oral microbiota. Positive correlations were observed between *Treponema* and *Selenomas* species and Chitinase 30like 1, SIL-6Rα and gp130/sIL-6Rβ, as well as a negative correlation between *Filifactor alocis* and IL-10. This serves to highlight the multifactorial nature of PD and reaffirms the importance of the balance between immune response and microbiota in the development of PD. Given the role that the microbiota plays in

the pathogenesis of the disease, a potential future predictive and prognostic test would track the oral microbial profile. Yet as prominent disease associated bacteria have been shown to modify their virulence factor, simply determining microbial composition may not suffice, as these species may be evident in health and disease but express a virulence factor with a higher inflammatory potential. A potential target biomarker may therefore be the profile of virulence factors such as lipid-A/LPS as they are modified between health and disease.

1.9 Hypothesis and aims

Modification of lipid-A is becoming widely recognised as a modulator of host immune responses. *Porphyromonas gingivalis* is considered a keystone pathogen in the progression of CP and one of its key virulence factors and potential survival mechanisms is its ability to modify its expressed lipid-A structure. Whilst the onset of CP is known to be due to the imbalance between host immune response and the resident microbiota, lipid-A modification may represent a mechanism of instigating and/or regulating that imbalance contributing to both the onset of the disease and the transitions from periods of quiescence and exacerbation experienced by CP sufferers.

Understanding the association between lipid-A modification and disease will help to refine further research models in this area as well as aid diagnosis and personalised treatment plans, which at present are not viable due to a lack of understanding. Building on this understanding, the role that lipid-A modification has on the phenomenon of endotoxin tolerance will elucidate mechanisms which are potentially detrimental and/or beneficial to both the host and pathogen and which may influence disease progression. Furthermore, the identification of an LPS detection assay which is sensitive to lipid-A modification would potentially track changes to lipid-A/LPS profiles, thus acting as a biomarker, whereby the assay may prove a diagnostic tool for the clinician.

The specific aims of this study are as follows:

- To analyse the lipid-A profile obtained from subgingival plaque samples obtained from patients with CP and compare it to healthy individuals and those same patients following standardised periodontal therapy.
- To determine the endotoxin activity and inflammatory potential of LPS isolated from these patient groups and determine the level of correlation compared to measured clinical parameters.
- To ascertain how patient derived LPS compares with canonical *E. coli* K12 LPS, PG LPS and specific PG LPS isoforms in instigating key cytokine production associated with inflammation, PMN recruitment, regulation and the instigation of the adaptive immune response.
- To evaluate the potential of these sources of LPS to supress cytokine production via endotoxin tolerance.
- To investigate whole cell protein responses in M1 and M2 MΦs to endotoxin tolerisation using characterised PG LPS, allowing for gene enrichment to identify mechanisms affected by stimulation and tolerisation with PG LPS which may shed new light on potential disease associated mechanisms.

Chapter 2
Structure-function implications of lipid-A modification

2.1 Introduction

Whilst detection of LPS is most commonly associated with TLR4 signalling in humans (as referred to in section 1.6.2), a comparatively more rudimentary and prehistoric recognition mechanism has been identified in the Atlantic horseshoe crab (*Limulus polyphemus*). Blood cells within the crab, amoebocytes, recognise LPS initiating an endotoxin-triggered enzyme cascade which reacts to form a clot, preventing further interaction (Iwanaga, 2007). Due to its inflammatory potential, detection of LPS is fundamental in numerous industries and the *Limulus* amoebocyte lysate (LAL) assay, based upon this reaction, is the most widely used assay for endotoxin measurement within the pharmaceutical industry (Steimle et al., 2016). This colorimetric assay is highly sensitive but is susceptible to false positive indication due to interaction with fungal (1→3)-β-D-glucans (Asai et al., 2007 Steimle et al., 2016). The clotting cascade can proceed through the activation of a number of clotting factors, B and C are associated with endotoxin recognition whereas Factor G is associated with the recognition of fungal products. To increase specificity and reduce the ecological burden related to harvesting of amoebocytes, a recombinant factor C (rFC) assay has recently been developed (Bolden and Smith, 2017). This modified assay removes the additional enzymatic steps, leaving just factor C, which when activated directly cleaves a fluorogenic substrate (Fig 2.1).

As TLR signalling has been shown to be affected by lipid composition, it is plausible that the increased specificity and sensitivity of the rFC assay may also demonstrate a level of susceptibility and as such may represent a method of detection relevant to periodontal disease. To date, the identification of a marker which specifically indicates the current status of the disease, as opposed to the

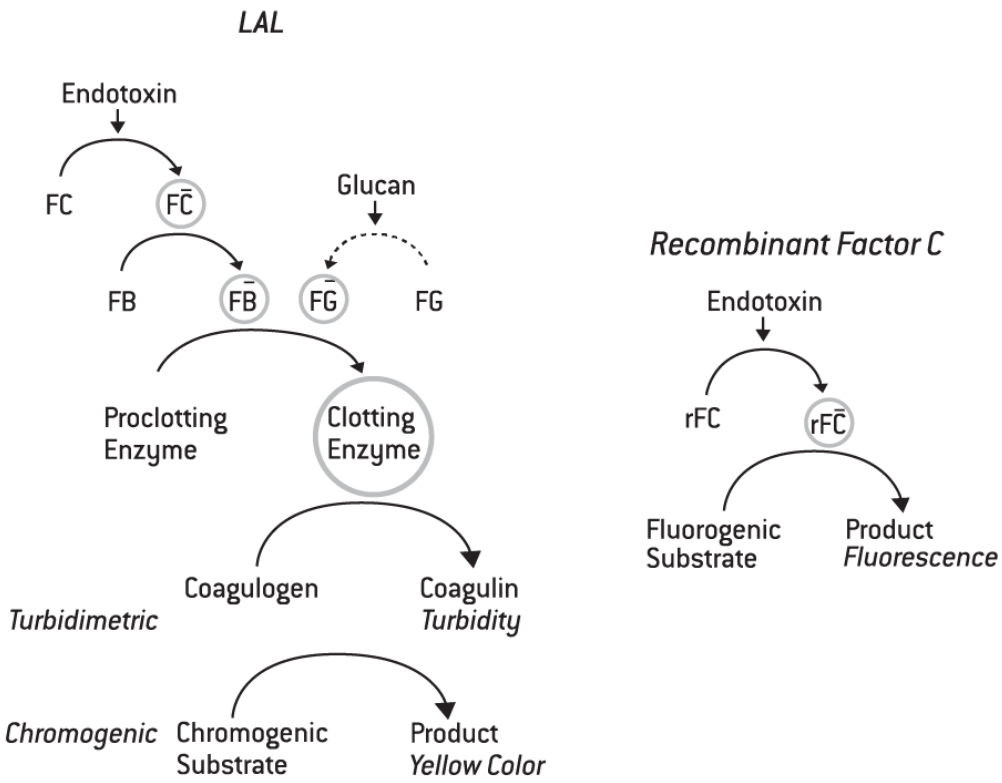

Figure 2.1 Comparison of traditional LAL assay and rFC assay cascades. The traditional LAL assay (left) incorporates 3 clotting factors, B, C and G, B and C recognising endotoxins whilst factor G is activated by β-glucans and thus as an analytical assay, may return false positives due to fungal contamination. The rFC assay (right) isolates the factor C component and activation results in a direct cleavage of the fluorogenic substrate.

(Lonza, 2020)

clinical observations which give an indication of damage caused historically by the disease, remain elusive. The elucidation of this pathogenic mechanism in relation to lipid-A structure-function-clinical implications is central to the understanding of host-microbial interaction at periodontally healthy and CP sites. Therefore, in this chapter, this study set out to examine structural diversity of subgingival lipid-A isoforms in healthy individuals and those presenting with CP (before and after periodontal therapy). The factor C based assay was used to assess endotoxin activity of subgingival LPS to ascertain sensitivity to lipid-A modification this was subsequently compared to clinical observations and inflammatory cytokine production by M1 and M2 MΦs.

2.1.1 Rationale for THP-1 cell model

It has been demonstrated for some time that as key orchestrators and regulators of immune responses, both M1 and M2 macrophages are pathologically important in periodontal health and disease (Charon, Toto and Gargiulo, 1981). More recently, the relevance of MΦ subset polarisation to periodontal health and disease has been examined (Zhou et al., 2019). As such, it was necessary to identify a macrophage model which would allow the incorporation of these subsets. Whilst considering this and the volume of cells required to perform the various experiments throughout this study it was not viable to utilise peripheral blood, monocyte derived macrophages. In addition, due to the variation in key immune responses such as IL-8, a murine model was not deemed suitable for this study (Hol, Wilhelmsen and Haraldsen, 2009). This study therefore utilises an established MΦ model based in the human THP-1 cell line.

A number of studies have utilised the pro-monocytic human THP-1 macrophage model whereby the cells are differentiated into M1 and M2 like macrophages. These cells are derived from the peripheral blood of a 1 year old male with acute monocytic leukaemia and in the past decade has been demonstrated to be an accurate model to study the differentiation or maturation as well as the immune response of monocytes and macrophages in different pathologies (Tsuchiya et al., 1982; Daigneault et al., 2010; Qin, 2012).

THP-1 cells were initially described as single rounded cells that grow in suspension, and that do not adhere to a culture plate, with the ability to be continuously cultured over extended periods (Tsuchiya et al., 1982). This study also finds that the monocyte-like THP-1 cells can be matured using 12-O-

tetradecanoylphorbol-13-acetate (TPA), also known as phorbol-12-myristate-13-acetate (PMA).

Differentiation of THP-1 cells towards M1-like macrophages has been demonstrated to occur via the protein kinase C (PKC) signalling pathway. PMA, analogous to diacylglycerol (DAG), a prolific second messenger binds directly to the PKC C1 domains and increases the affinity for phospholipids and Ca^{2+} (Castagna et al., 1982).

In addition to maturation to an M1-like phenotype, THP-1 cells have been pushed towards an M2-like phenotype using 1α, 25-dihydroxyvitamin D_3 (VD_3) (Schwende et al., 1996; Daigneault et al., 2010; Foey and Crean, 2013). Whilst less well defined than the phorbol ester induced differentiation of M1 like THP-1 cells, there is mounting evidence to support this hypothesis (Table 2.1) and VD_3 has been shown to induce an M2-like state in other cell lines (Foey and Crean, 2013).

Microglial cells have been demonstrated to exhibit an anti-inflammatory phenotype following VD_3 exposure in line with that of an M2 profile (Verma and Kim, 2016). It has also been demonstrated (in a murine model utilising the RAW264.7 cell line) that VD_3 may be able to push M1-like MΦs towards an M2 phenotype, recognised by the upregulation of the mannose receptor (MR), Arg-1 and IL-10 (Zhang et al 2015).

A number of matrix metalloproteinases (MMPs) have also been shown to be affected by VD_3-exposed peripheral blood mononuclear cells (PBMCs); MMP9, of particular relevance to CP, was shown to be reduced in expression, secretion and activity whilst MMP7 and 10 responses induced by *Mycobacterium*

Supporting evidence for THP-1 cell model		
	PMA/M1 Subset	VD3/M2 Subset
Gene Expression	Arginase$^{neg/lo}$ CR3 CR4 ICAM1 ICAM2 IL-8^{hi} IL-10^{lo} IL-12p40^{hi} iNOS^{hi} TNF-α^{hi}	Arginase^{hi} CD14^{hi} CD206^{hi} DC-SIGN^{hi} IL-8^{lo} IL-10^{hi} iNOS$^{neg/lo}$ TNF-α^{lo}
Functional Responses to LPS stimulation	IL-10^{lo} IL-12^{hi} Phagocytosis^{lo} Superoxide^{hi} TNF-α^{hi}	IL-10$^{hi/med}$ IL-12$^{neg/lo}$ Phagocytosis^{hi} Superoxide^{lo} TNF-α^{lo}
Surface Markers	CCR1^{+} CCR2^{lo} CD206^{lo} TLR4^{hi}	CD206^{hi}
Proteomic Profiling	CCL20 isoform 2 ICAM-1 IL-1β SOD isoform 4 TLR2 TNF-α induced protein 8	CD68 C-type mannose receptor 2 TGF-β_1 Integrin αM Macrophage capping protein, Myeloid cell nuclear differentiation antigen
Reproduced Observations	THP-1 + IFNγ/LPS treatment	THP-1 + IL-4 treatment

Table 2.1. Supporting evidence for the THP-1 derived macrophage subset cell model that corresponds with primary cell studies.
Derived from: Fleit and Kobasiuk, 1991; Prieto et al., 1994; Schwende et al., 1996; Baqui et al., 1998; Baqui et al., 1999; Foey, 2004; Gordon and Taylor, 2005; Traore et al., 2005; Chanput et al., 2010; Daigneault et al., 2010; Matilainen et al., 2010; Foey, 2011; Gynther et al., 2011; Habil, 2011; Habil 2012; Belfield, 2013; Chanput et al., 2013; Habil, 2013; Verma, Jung and Kim, 2014; Foey et al., 2015a; Waring et al., 2016 (unpublished).

tuberculosis infection were attenuated, despite limited action on the regulatory tissue inhibitor of metalloproteinases (TIMPs). Again, VD_3 was shown to induce IL-10 secretion (associated with the M2 phenotype) as well as prostaglandin E_2 (PGE_2) in *Mycobacterium tuberculosis*-infected PBMCs (Coussens et al, 2009). Given the substantial amount of studies which support this model and the importance of M subsets in the study of CP, combined with the established data surrounding gene expression, cytokine and chemokine as well as functional

responses to LPS stimulation, this model best supports our methods of investigation.

2.2 Experimental design

This part of the study aims to identify and compare LPS profiles obtained from periodontally healthy and CP patients and determine the potential application of the rFC LAL assay as a biosensor to indicate the activity of periodontal disease and inflammatory potential of subgingival microbiota. To do this, patients were recruited to the study and subgingival plaque samples obtained from either CP or healthy sites as applicable (verified by scanning electron microscopy). LPS was isolated from these samples, prior to three phases of analysis;

Phase 1

Identification of Lipid A profile in samples of healthy and individuals with CP via electrospray ion source mass spectrometry.

Phase 2

Determination of the endotoxin activity in LPS isolated from subgingival plaque samples via rFC LAL assay.

Phase 3

Evaluation of the inflammatory potential of extracted LPS on human macrophages.

2.3 Materials and methods

A comprehensive list of reagents and suppliers are listed in appendix A.

2.3.1 Patient study population.

Approval of the study protocol was obtained from the Health Research Authority, UK (NRES Committee South West—Cornwall and Plymouth 14/SW/0020), and the study was conducted in accordance with the Helsinki Declaration of 1975, as revised in 2013. All participants provided written consent.

Thirty-two individuals (11 female, 21 male, mean age 46) with chronic periodontitis (CP) and 33 systemically and periodontally healthy (H) persons (18 female, 15 male, mean age 31) were recruited from patients presenting to the Peninsula Dental School, University of Plymouth, UK (Table 2.2).

	Healthy n = 33	CP n = 32	
		Baseline	Post-treatment
Age (Years)	31 ± 9	46 ± 9	46.9 ± 9
O'Leary plaque index (%)	14.68 ± 5.02	56.65 ± 21.53	33.92 ± 14.20
Bleeding index (%)	2.22 ±2.76	41.47 ± 18.49	23.06 ± 13.31
Probing depth (mm)	1.45 ± 0.45	5.78 ± 0.61	4.47 ± 0.58

Table 2.2 Summary of the clinical characteristics of the study population (means ± SD).

CP patients were diagnosed in accordance with the accepted clinical criteria: a minimum of four teeth in each jaw with a probing depth (PD) of ≥ 5mm, bleeding on probing and clinical attachment level (CAL) of ≥4 mm, with ≥ 50% alveolar bone loss in at least two quadrants (assessed radiographically). Periodontal health was defined as ≥ 90% of the measured sites with PD < 3 mm and no bleeding on probing (BOP). Clinical parameters (six-point pocket chart, plaque index (PI), and bleeding index (BI) and demographic characteristics of the study population were recorded as well as their smoking status (three smokers in the

healthy group and 14 in the CP group). Patients with medical disorders unrelated to periodontal disease, but likely to influence study outcomes, or with antibiotic or periodontal treatment in the previous 6 months were excluded from the study.

2.3.2 Subgingival biofilm collection

Subgingival biofilm samples were collected using a standardised protocol by clinicians inserting sterile, dental paper points for 30 seconds in three deepest bleeding pockets in CP patients and in healthy patients from three non-bleeding sites (mid-labial of UR1, mesio-buccal of UR6, and mesio-buccal of LL6) and were pooled for each individual patient. Patients with CP underwent conventional, non-surgical periodontal therapy and subgingival biofilm samples were collected from the same sites, 3 months after the completion of the therapy.

2.3.3 Scanning electron microscopy (SEM) of subgingival plaque

To verify the subgingival plaque collection technique, samples were collected from four patients exhibiting periodontal disease and one healthy individual by inserting sterile paper point as above. The samples were immediately fixed for 1 hr in 2.5% (v/v) glutaraldehyde in 0.1 M sodium cacodylate buffer. The samples were rinsed in 0.1 M sodium cacodylate three times for 15 minutes each. All samples underwent alcohol dehydration through a series of 30%/50%/70% and 90% immersions for 15 minutes each, followed by two immersions in absolute alcohol. Samples were then dried using a critical point dryer (Emitech K550, Quorum, UK). Initial sputter coating with chromium did not produce sufficient coverage so as to reduce charging effects due to the porous nature of the samples and therefore gold-palladium was used so as to minimise charging artefacts but maximise resolution (Q150T coating system, Quorum, U.K.). Scanning electron microscopy was performed using a Jeol 7001 field emission

generating scanning electron microscope (FEG-SEM) utilising the secondary electron detector for optimum surface resolution (JEOL, Tokyo, Japan).

2.3.4 LPS extraction

A number of methods have been identified to isolate LPS from bacterial biofilms, which display a varying propensity for isolating the various LPS isoforms required. Al-Qutub et al (2006) studied three methods for LPS extraction on bacterial cultures of. Their findings suggested that $MgCl_2$-EtOH LPS extraction procedure influences isolated lipid-A composition, whereas the Tri-reagent and phenol extraction methods produce a representative lipid-A profile. LPS isolated using the phenol method was demonstrated to show a reduction in the high mass/charge isoforms around m/z 1770. Curtis et al, (2011) have since however, successfully used a cold-water phenol extraction kit to isolate LPS form PG and it is this kit that was used throughout.

LPS from subgingival samples was extracted using a proprietary LPS extraction kit (iNtRON Biotechnology, South Korea) following the manufacturer's instructions. Briefly: Samples were immersed in 0.5 ml of LPS-free water and incubated for 10 minutes, following which 0.5 ml of lysis buffer was added and incubated for 5 minutes. Subsequently 200 µl of chloroform was added prior to incubation for a further 5 minutes. Samples were centrifuged at 13,000 rpm for 10 minutes at 4°C, the top layer of the resulting supernatant was then drawn off and combined with 400 µl of purification buffer, this was incubated at -20°C for 10 minutes. Following centrifugation at 13,000 rpm for 15 minutes at 4°C, the resulting pellet was resuspended in 70% ethanol. Following further centrifugation at 13,000 rpm for 10 minutes at 4°C, the ethanol was drawn off and the pellet

dried in a centrifugal evaporator/speedvac (Thermofisher, Loughborough, UK). Extracted LPS was resuspended in 500 µl of LPS-free water and stored at 4°C.

2.3.5 Identification of LPS through SDS-page and silver staining.

Pooled LPS samples (Healthy, CP and post-treatment) were analysed via silver staining for the presence of LPS. Pre-cast mini-protean TGX 8-16% gels were utilised using the Bio-Rad mini-PROTEAN tetra vertical electrophoresis system Bio-Rad, Watford, UK). 16 µl of sample were added to 4 µl of Laemmli buffer (see appendix A), this was held at 100 ^{o}C for 5 minutes prior to loading and gels were run at 120 V. To silver stain a kit was used in accordance with the manufacturer's recommendations (Thermofisher, Loughborough, UK), the gels were washed in ultrapure water before fixing twice in a 30% ethanol, 10% acetic acid solution for 15 minutes x 2. Subsequently, gels were washed in 10% ethanol for 5 minutes x 2, before being again washed in ultrapure water twice. Gels were submersed in sensitizer solution for 1 minute and washed twice in ultrapure water before incubation for 30 minutes in stain working solution. Gels were washed briefly, twice before adding developer solution. Development was stopped with 5% acetic acid.

2.3.6 Lipid-A isolation

Due to the amount of sample required versus the amount of LPS isolated in a subgingival plaque sample, for lipid-A isolation LPS from each group was pooled so as to create 3 LPS profiles representing healthy individuals, those with CP and the post treatment group. Lipid-A was then isolated by mild hydrolysis as described by Coats et al (2009). Briefly: pooled LPS samples were lyophilised and resuspended in 10 mM sodium acetate [pH 4.5] containing 1% (w/v) sodium dodecyl sulphate. This was frozen at -20^{o}C and subsequently lyophilized

overnight. The resulting lipid-A pellets were washed once in ice-cold 95% acidified ethanol and a further three times in 95% ethanol. Following centrifugation at 13,000 rpm for 10 minutes, the majority of supernatants were withdrawn, and the remaining pellet transferred to centrifugal evaporator/speedvac (Thermofisher, Loughborough, UK). The final resulting pellet was dissolved in 90% Ethanol and stored at 4^{o}C prior to analysis via mass spectrometry.

2.3.7 Mass spectrometry of lipid-A isolates

Mass spectrometry was performed by Dr Aniko Kilar at the Institute of Bioanalysis, University of Pécs, Pécs, Hungary, using the following protocol: Lipid-A was desalted with 0.1 M ammonium citrate and dissolved in methanol/dichloromethane (3:1, v/v). Mass spectrometric analysis of lipid A was performed on a 6530 Accurate Mass Quadrupole Time-Of-Flight (Q-TOF) MS system (Agilent Technologies, Singapore). Positive and negative ion mass spectra were recorded over the range of 1000–2100 m/z. The electrospray ion source (ESI) was operated using the following conditions: pressure of nebulizing gas (N_2) was 30 psi; temperature and flow rate of drying gas (N_2) was 300 °C and 7 l/min, respectively; temperature and flow rate of sheath gas was 300 °C and 11 l/min, respectively. The capillary voltage was set to 3.5 kV, the nozzle voltage to 2 kV, the fragmentor potential to 100 V, and the skimmer potential to 65 V.

2.3.8 Determination of endotoxin activity of LPS extracts by rFC LAL assay

Endotoxin activity was measured according to the manufacturer's instructions (EndoZyme, Hyglos, Germany). Subgingival LPS extracts were diluted 1/10 in endotoxin free water and 100 µl of samples or standards was added to the 96 well plate. This was followed by 100 µl of assay reagent which for each 96 well

plate comprised of 9.6 ml assay buffer, 1.2 ml of enzyme solution and 1.2 ml of fluorogenic substrate). The plate was then read at intervals of 1 minute and 90 minutes at a constant temperature of 37°C on a fluorescence plate reader with an excitation filter at 380/20 and emission filter at 440/40 (BIOTek, Swindon, UK). (Standard curve is indicated in supplemental figure S1)

2.3.9 Determination of inflammatory potential of subgingival LPS isolates

2.3.9.1 Cell line maintenance and culture

The human monocytic leukaemia cell line THP-1 (ECACC, Salisbury, Wiltshire, UK), was grown in suspension and sub-cultured 3-4 days subsequently. Cultured cells were used routinely between passages 5 and 32. Cells were maintained at 37°C, in 5% CO_2, cultured in RPMI 1640 medium supplemented with 10% (v/v) heat inactivated foetal bovine serum, 2 mM L-glutamine (referred to as “R10”).

2.3.9.2 THP-1 cell differentiation

To induce differentiation into M1-like MΦs, cells were plated at a density of 1 x 10^6 cells/ ml in R10 in tissue culture plates and incubated with PMA (25 ng/ ml) three days plus one rest/wash day during which the PMA was removed and replaced with fresh R10.

M2-like macrophages were generated by culturing cells in 10 nM 1α, 25-dihydroxyvitamin D_3 in R10, for seven days in suspension, the R10/VD_3 being refreshed after a period of 4 days (Daigneault et al., 2010). Cells were then plated at a density of 1 x 10^6 cells/ml and both subsets were washed in fresh media prior to experimental procedures.

2.3.10 Stimulation of M1 and M2 MΦs with extracted LPS

Differentiated THP-1 cells were stimulated with 50 µl of subgingival LPS extracts per million cells, for 18 hours, to allow for capture of multiple cytokine targets of interest. Cell free supernatants were collected and stored at -20°C for further analysis.

2.3.10.1 Differential sensitivity of LPS to polymyxin B mediated inhibition.

THP-1 cells were differentiated in to M1-like MΦs as these are the most responsive to LPS stimulation when evaluating TNFα. Polymyxin B was used at a final concentration of 100 µg ml^{-1} as this was found to be the highest concentration which did not affect cell mortality – determined via MTT assay. Polymyxin B was combined with either; PG LPS or *E. coli* LPS at a final concentration of 1 µg ml^{-1}, or 50 µl ml^{-1} of LPS pooled from that isolated from patients with CP. The Polymyxin B/LPS was incubated for 1 hour at room temperature prior to stimulation of M1 like macrophages. Cells were incubated for a period of 18 hours and the subsequent supernatants were removed and stored at -20C prior to analysis by ELISA.

2.3.10.1.1 Analysis of cell mortality by MTT assay.

For a 24 well plate, 500 µl of Methylthiazolyldiphenyl-tetrazolium bromide (MTT) (Thermofisher, Loughborough, UK) at a concentration of 0.5 mg/ml, diluted in PBS, was added to each well. The plate was incubated for a period up to 4 hours at 37° C and 5% CO_2 to enable the reaction to proceed. The resulting formazan derivative was then dissolved by adding 500 µl of 0.04M hydrochloric acid in DMSO and repeatedly pipetting. Absorbance was measured at 562 nm using a

POLARstar omega spectrophotometer (BMG Labtech GmbH, Ortenberg, Germany).

2.3.11 Analysis of cytokine Secretion

To quantify TNF-α and IL-8 release, supernatants were analysed using a sandwich enzyme-linked immunosorbent assay (ELISA). Cells and experimental growth media were centrifuged at 125g for 5 minutes to ensure cell-free supernatants, which were drawn and stored at -20°C prior to analysis.

In-house developed protocols, previously optimised (not shown) were utilised throughout: 96-well ELISA plates (Nunc, Fisher Scientific, UK) were coated with either 4 μg/ml of mouse anti-human TNFα or 2 μg/ml of mouse anti-human IL-8 (BD Pharmingen, Oxford, UK) in PBS and incubated overnight at 4°C. Subsequently, washed three times with wash buffer (Tween 20, diluted 1/2000 in PBS) and the plate was blocked with 2% BSA (w/v) in PBS for 4 hours. The plate was then washed three times before the application of standards and samples. Fifty microliters of samples or standard were added to the plate and again incubated overnight at 4°C. Supernatants were diluted prior to IL-8 application; M1-derived supernatants by 1/50 and M2 derived by 1/10 to ensure results fell within the upper and lower limits of detection of the assay. Prior experiments, comparing the effect of dilution factors, demonstrated no significant variation due to the level of dilution.

The plates were washed three times before biotinylated mouse anti-TNF-α or mouse anti-Human IL-8 at 0.5 μg/ml in 2% BSA (w/v in PBS) was applied and incubated at room temperature for 4 hours.

The plates were again, washed three times prior to the addition of horseradish peroxidase streptavidin conjugate (HRP) was diluted 1/250 in 2% BSA (w/v) in PBS, this was added and incubated at room temperature for 1 hour before further washing and the addition of the substrate, 3,3,5,5-tetramethyl benzidine (TMB) (Insight Biotechnology, Middlesex, UK). The reaction was stopped by addition of 1.17 mM sulphuric acid. Colour development was assayed spectrophotometrically using an OPTI Max microplate reader at 450 nm and the results analysed by Soft max Pro version 2.4.1 software (Versa Max, Molecular Devices, Sunny Vale, CA, USA). (Standard curves are indicated in supplemental figures S5-9).

2.3.12 Statistical analyses

All samples, participants, and clinical data were anonymized and locked before the codes were revealed. Sample group analysis was analysed using a student T test to compare ages between patient groups and a Fisher's exact test (preferential to a chi square test due to the relatively small sample number) was performed to compare gender and smoking status. Correlations between clinical parameters and LPS endotoxin activity and inflammatory potential were analysed using the Pearson correlation coefficient. Statistical difference was determined using a one-way ANOVA and Tukey post hoc analysis. A *p*-value below 0.05 was considered significant (* < 0.05, < 0.01, * < 0.001). To determine the performance of the rFC LAL assay as a test for detecting endotoxin as a biomarker, a ROC curve was calculated as this is a common method for comparing the diagnostic performance of multiple experimental factors (Griner et al., 1981). Statistical tests were performed using GraphPad Software version 7, sample data analysis was performed using version 8, San Diego, CA.

2.4 Results

2.4.1 Statistical analysis of sample group

Statistical analysis was performed to compare sample data for those that fall within the healthy group and those that suffer from CP (Figure 2.2).

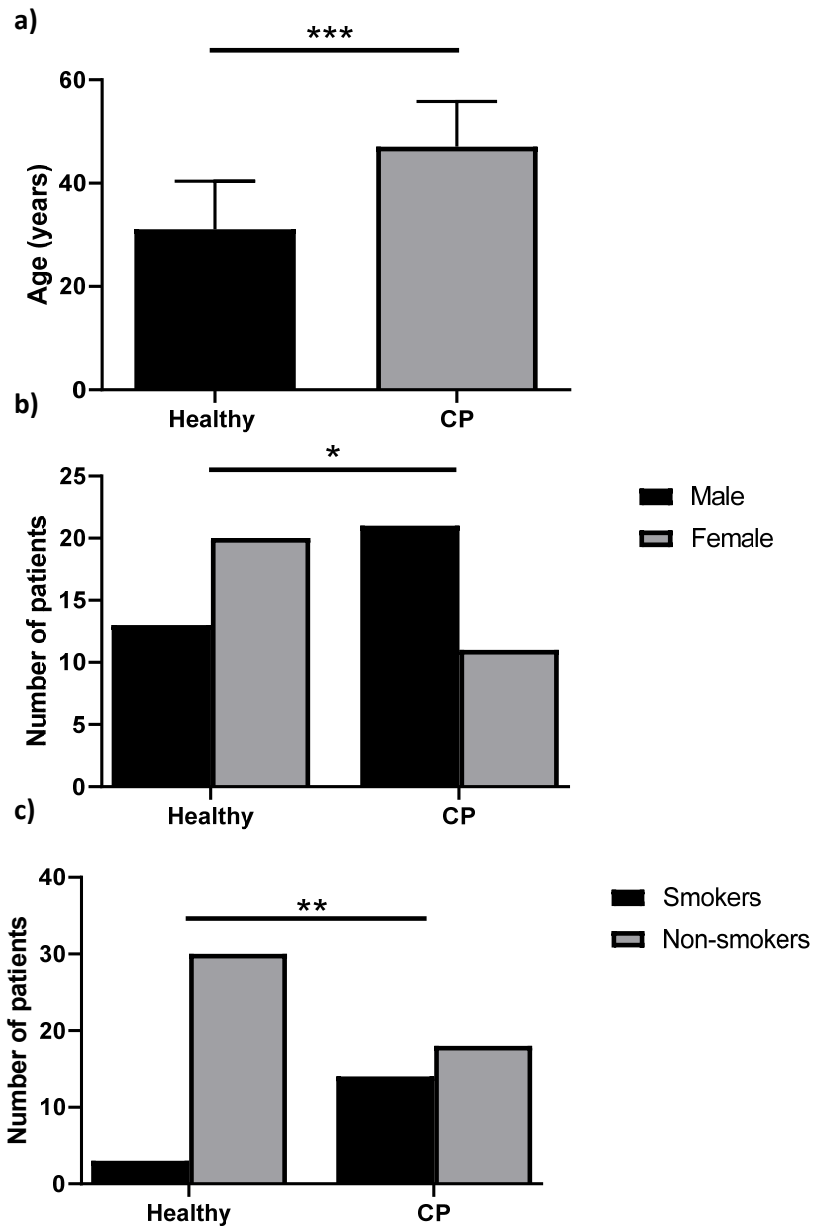

Figure 2.2 Statistical analysis comparing healthy patients and those suffering from CP. Statistical analysis of sample group reveals significant differences between patient groups, whereby the healthy group was comprised of younger individuals (a) with a higher female population (b) and fewer smokers (c) than the CP group. (***$p < 0.001$, **$p < 0.01$), *$p<0.05$).

Statistical analysis revealed significant differences between the two (healthy and CP) patient groups, where the CP population was older (Fig. 2.2a), comprised of

a higher number of males (Fig. 2.2b) and contained a higher occurrence of smokers (Fig.2.2c), compared to the healthy group of patients.

2.4.2 Scanning electron microscopy of patient plaque samples.

Samples were obtained from four patients with varying levels of chronic periodontal disease as indicated by their clinical observations (table 2.3). Scanning electron microscopy was utilised to verify sufficient collection of subgingival plaque using sterile dental paper points. Concurrently, samples were obtained from a periodontally healthy individual for comparison.

	O'Leary plaque index (%)	Bleeding index (%)	Probing depth (mm)
CP1	27.8	32.4	5.33
CP2	32.5	21.9	8.00
CP3	70.4	60.2	7.00
CP4	78.7	61.1	6.66

Table 2.3 Clinical observations of patients chosen for analysis by scanning electron microscopy of subgingival plaques collected using sterile dental paper points.

Scanning electron microscopy revealed substantial amounts of subgingival plaque collected on the sterile dental paper points (Fig. 2.3). In addition, a number of qualitative observations were made regarding the composition of the subgingival biofilm; i) plaque obtained from a periodontally healthy individual presented a reduction in the variation of bacterial morphology, with the majority of bacteria being either cocci or bacilli in shape. ii) additionally, in the healthy sample, there was an absence of erythrocyte or leukocytes within the biofilm. iii) Samples from patients with CP displayed a number of corncob structures, indicating a prolonged period of plaque accumulation (Zijnge et al., 2010). iv) plaque samples obtained from all patients with chronic periodontal disease exhibited clear increases in morphological variation with spirilla and spirochete formations evident in all samples.

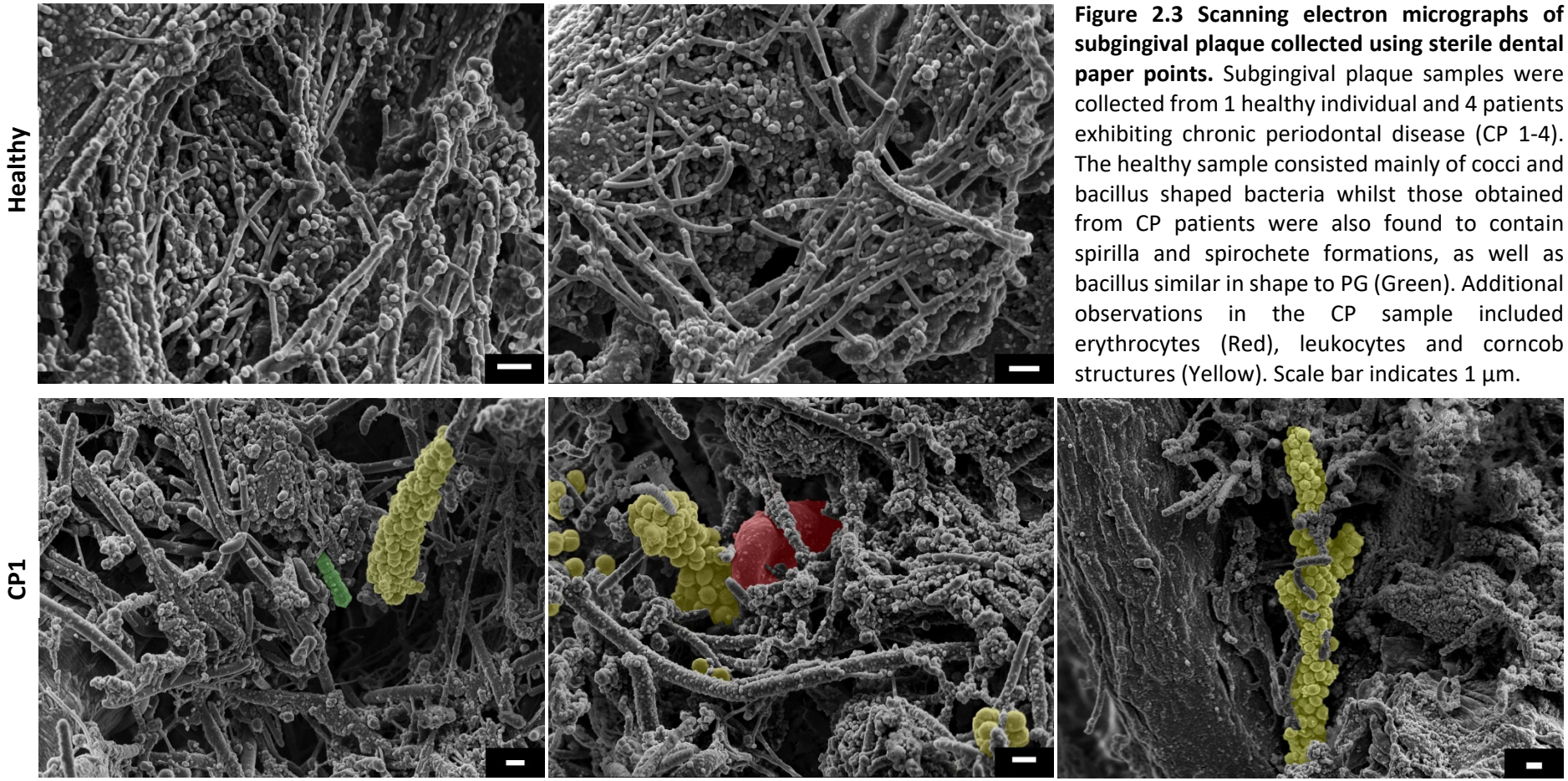

Figure 2.3 Scanning electron micrographs of subgingival plaque collected using sterile dental paper points. Subgingival plaque samples were collected from 1 healthy individual and 4 patients exhibiting chronic periodontal disease (CP 1-4). The healthy sample consisted mainly of cocci and bacillus shaped bacteria whilst those obtained from CP patients were also found to contain spirilla and spirochete formations, as well as bacillus similar in shape to PG (Green). Additional observations in the CP sample included erythrocytes (Red), leukocytes and corncob structures (Yellow). Scale bar indicates 1 µm.

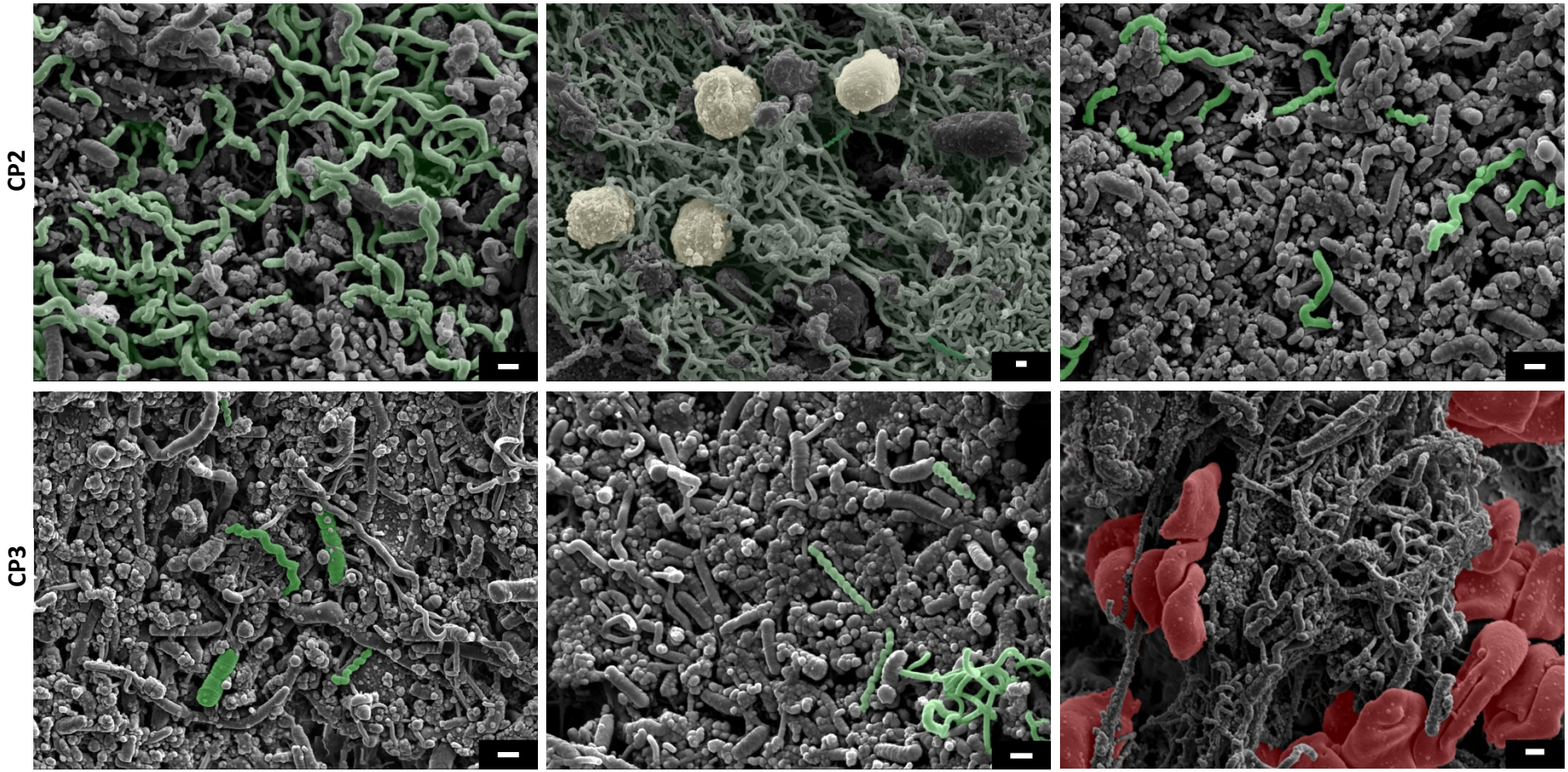
CP2
CP3

CP4

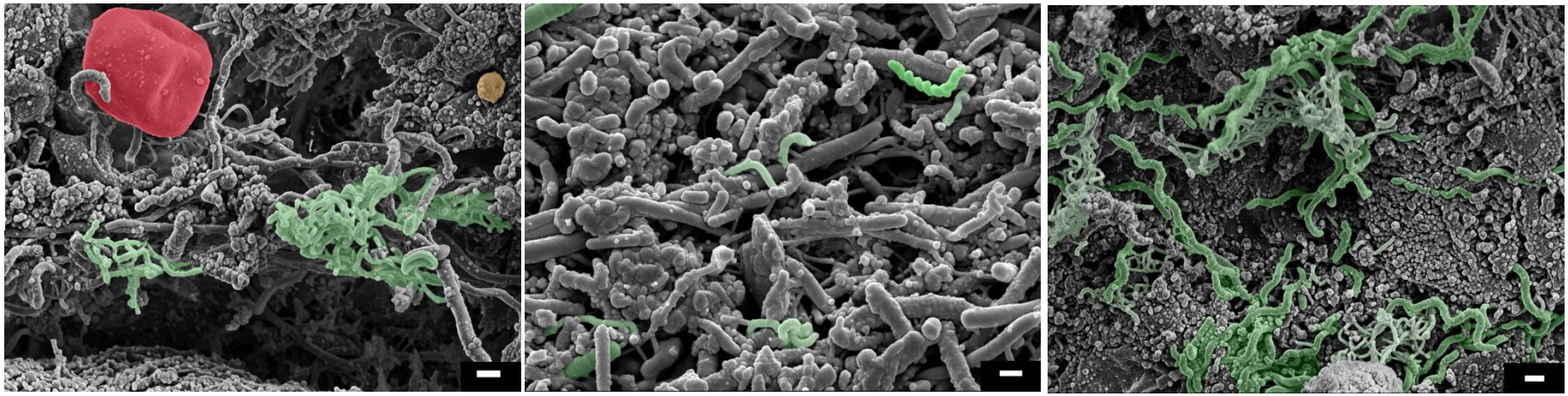

2.4.3 Identification of LPS via SDS-page and silver staining

Attempts were made to visualise LPS isolated from each patient group using silver staining techniques. Samples were pooled to create a representative profile for each patient group and the resulting samples were separated using SDS-page and subsequently silver stained (Fig 2.4).

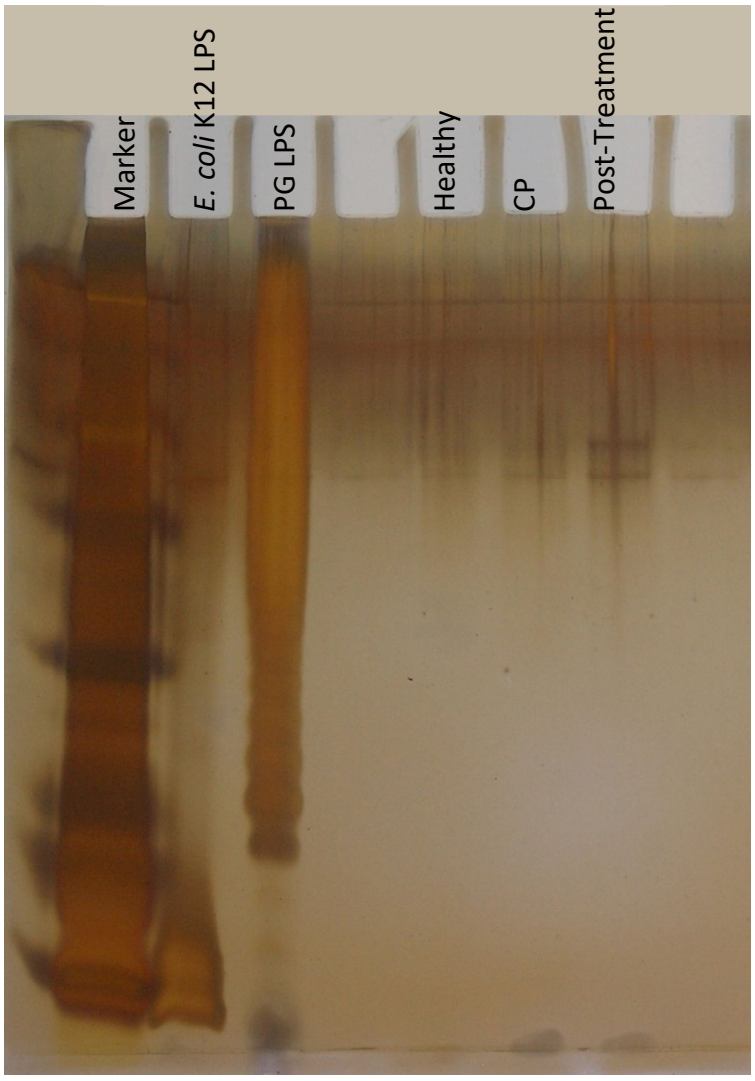

Figure 2.4 Identification of LPS via silver staning. Pooled samples were separated by SDS-page and subsequently silver stained to visualise isolated LPS. This process was repeated with similarly inconclusive results observed.

Repeated results from silver staining proved inconclusive, with minimal bands observed for all three samples. To further assess the presence of LPS, samples were used to stimulate M1 and M2 M□s in the presence of polymyxin B.

2.4.4 Differential susceptibility of LPS to polymyxin B inhibition.

Polymyxin B is an antibiotic which electrostatically binds to the negatively charged lipid-A portion of LPS via the cationic charges in the polypeptide portion of polymyxin. This cationic peptide interacts with both the acylated tails and phosphate groups, but when it binds to phosphate residues of lipid-A, polymyxin displaces magnesium and calcium ions destabilising the outer membrane of gram-negative bacteria (Trimble et al., 2016). It has been suggested that modification of lipid-A structure confers resistance to polymyxin due to a limited binding of LPS as a result of the reduction in charge caused by the under - acylation and phosphorylation (Coats et al., 2009).

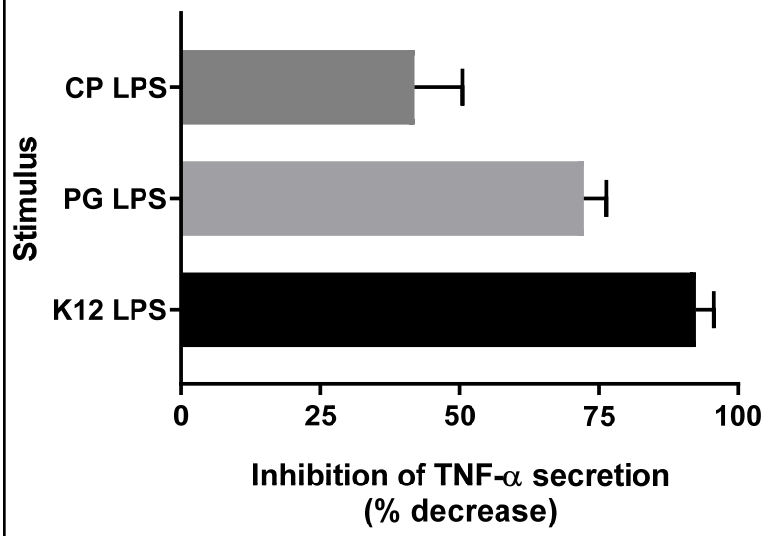

Figure 2.5 Differential susceptibility of LPS to polymyxin B inhibition. M1 MΦs were stimulated with either *E. coli* K12, PG LPS or LPS isolated from patients with CP, following 1 hour of pre-incubation with polymyxin B. Subsequently, TNF-α production was measured and compared to positive controls. Experiments were performed in technical triplicates and biological duplicates. Figures indicate results of 1 representative experiment.

Polymyxin B at a final concentration of 100 μg/ml, was incubated with either PG LPS (as analysed for mass spectrometry (Fig. 2.3 a & e)), *E. coli* K12 LPS at 1 μg/ml or LPS pooled from CP patients, at 50 μl/ml for 1 hour prior to stimulation of M1 MΦs (as the optimal producers of TNF-α), subsequent supernatants were analysed following 8 hours of stimulation (to coincide with peak production of TNF-α), and compared to positive controls (Fig 2.5).

2.4.5 Structural characterisation of subgingival lipid-A isoforms

To determine the lipid-A profiles potentially associated with health and disease, lipid-A was isolated from 4 groups of LPS samples. Firstly, a commercially available and widely used LPS obtained from the perio-pathogen *Porphyromonas gingivalis* (Invivogen, California, US). Secondly, 3 samples containing LPS obtained and pooled from patients recruited to the study who were identified as either periodontally healthy, those with CP and also those CP patients who underwent conventional forms of therapy from which samples were obtained again from the same sites after three months. The isolated lipid-A was then analysed by mass spectrometry, where each sample was analysed a minimum of three times during the optimisation process and similar results observed on each occasion.

Characteristic lipid-A molecular signatures were observed in the spectra of LPS extracts from the three groups of patients. Mass spectrometry analyses of lipid-A isolated from pooled healthy and CP subgingival plaque samples revealed the presence of prominent, high m/z peaks (which were between 1600 and 1900 m/z) in CP samples (Indicated in red), which were not present in the healthy group (green) (Fig. 2.6(b) and 2.6(c)). These high m/z values are consistent with more phosphorylated and over-acylated lipid-A isoforms as it is the case with reported PG LPS (Fig. 2.6 (a) and 2.7 (a)). Interestingly, in subgingival samples taken from the same sites, 3 months after the completion of periodontal therapy, these ions were not detectable (Indicated in blue) (Fig. 2.6 (d)). The lipid-A mass spectrum of the pooled post-treatment samples resembled the spectrum of healthy individuals (predominantly in the positive-ion mode) (Fig. 2.6 (b) and (d)), consistent with less-acylated, hypo-phosphorylated lipid-A isoforms. Of additional

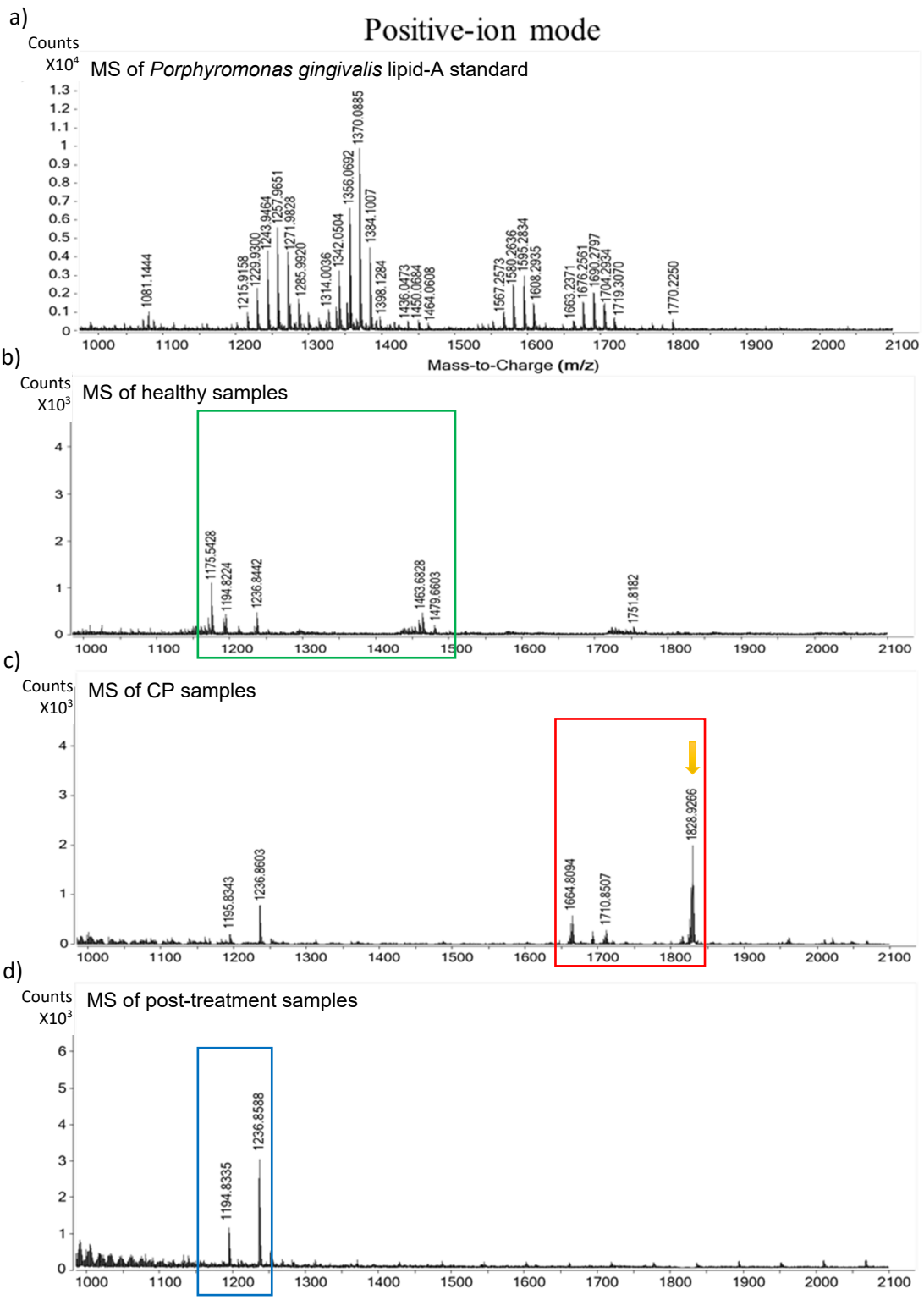

Figure 2.6 Illustrative electrospray ionization mass spectra of lipid-A profiles in positive ion mode. Mass spectra of lipid-A profiles isolated from *P. gingivalis* LPS (InvivoGen) (a) and pooled subgingival plaque samples obtained from healthy individuals (b), chronic periodontitis patients (c), and chronic periodontitis patients 3 months after periodontal therapy (d). Lipid-A obtained from patients with CP was shown to be of a higher mass/charge ratio indicating a higher level of acylation and phosphorylation compared to both the healthy and post-treatment samples. Analysis of samples was performed a minimum of 3 times as part of the optimisation process, with similar results observed throughout, prior to final optimised spectra indicated above.

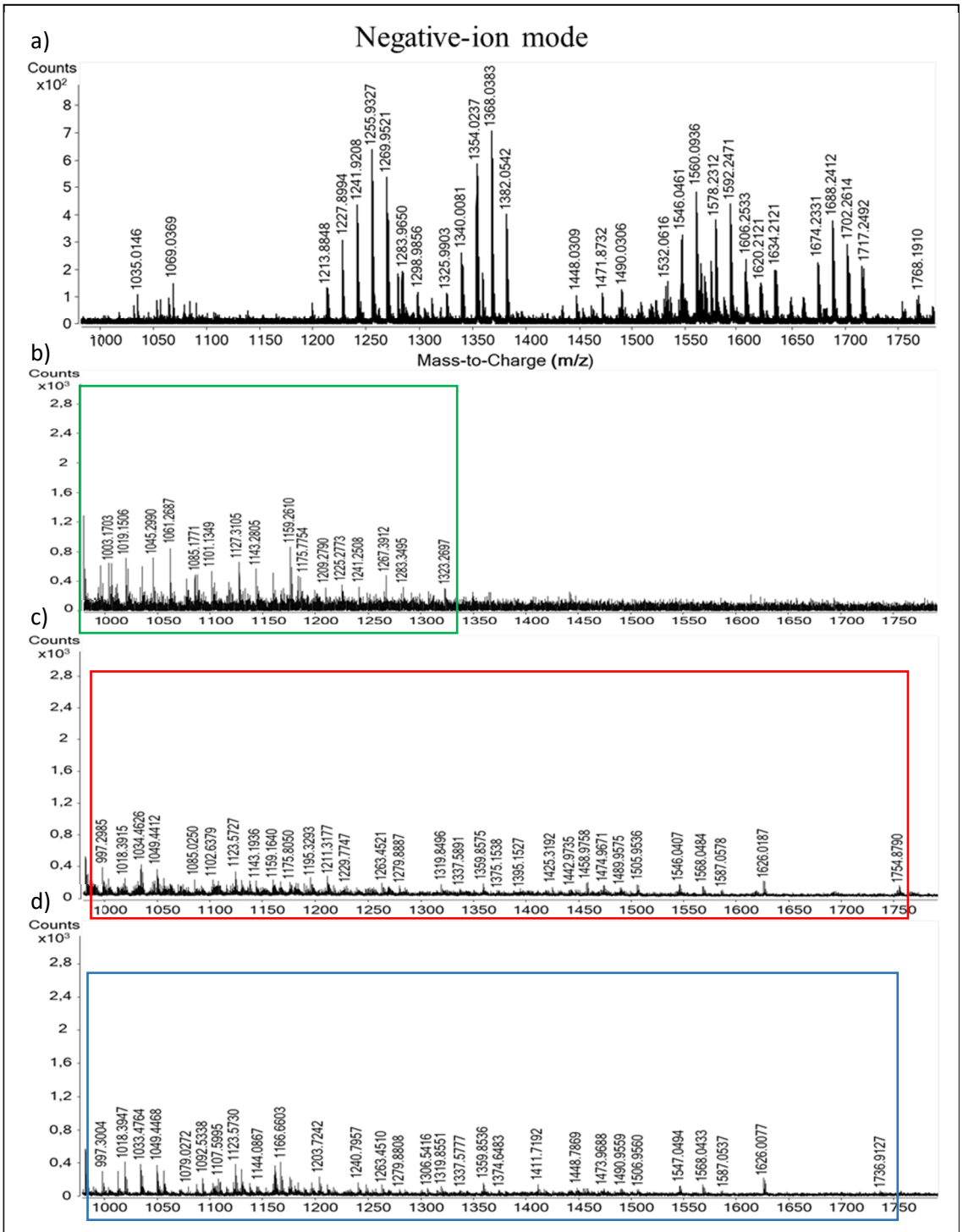

Figure 2.7 Illustrative electrospray ionization mass spectra of lipid-A profiles in negative ion mode. Mass spectra of lipid-A profiles isolated from *P. gingivalis* LPS (InvivoGen) (a) and pooled subgingival plaque samples obtained from healthy individuals (b), chronic periodontitis patients (c), and chronic periodontitis patients 3 months after periodontal therapy (d). In negative ion mode, Lipid-A obtained from patients with CP and those that underwent post treatment were shown to be of a higher mass/charge ratio compared to the healthy sample. Analysis of samples was performed a minimum of 3 times as part of the optimisation process, with similar results observed throughout, prior to final optimised spectra indicated above.

note is the identification of a significant peak at a mass to charge ratio of 1828 m/z in the CP profile which correlates with the lipid-A of *F. nucleatum* (yellow arrow), a key facilitator of PG pathogenesis (Saito et al., 2008).

2.4.6 Endotoxin activity of subgingival biofilm samples

Endotoxin activity of subgingival LPS extracts was measured for each individual patient using the recombinant factor C assay. LPS extracts from chronic periodontitis patients showed significantly higher levels of endotoxin activity compared to healthy individuals (Fig. 2.8). Most healthy patients' endotoxin activity was below the level of 10 EU/ml while in a significant number of patients with CP (19), this value exceeded 20 EU/ml. Smoking status did not significantly influence the level of subgingival endotoxin activity (see supplemental figure S2). Endotoxin activity of samples taken after periodontal treatment was significantly lower compared to the corresponding CP samples, with values at a similar range as for healthy individuals (Fig. 2.10). Interestingly, in all three groups of samples, there were two distinct sub-groups: one in the lower range of EU/ml where most of the healthy and post-treatment samples are found and one within a higher range of endotoxin activity where most of the CP samples occur. These two sub-groups may represent differences in disease activity and progression, two of the disease signatures currently unmeasurable at point-of-care. A further notable point of interest is the ability of these subgroups to induce TNF-α secretion (Fig. 2.9). The four healthy individuals identifiable in figure 2.8, demonstrating an endotoxin activity level above that of the rest of the group did not significantly induce TNF-α, above the level of the remainder of the healthy group. The 8 individuals which demonstrate an increased level of endotoxin activity in the post treatment group however correspond with the highest inducers of TNF-α within that group (Fig. 2.9).

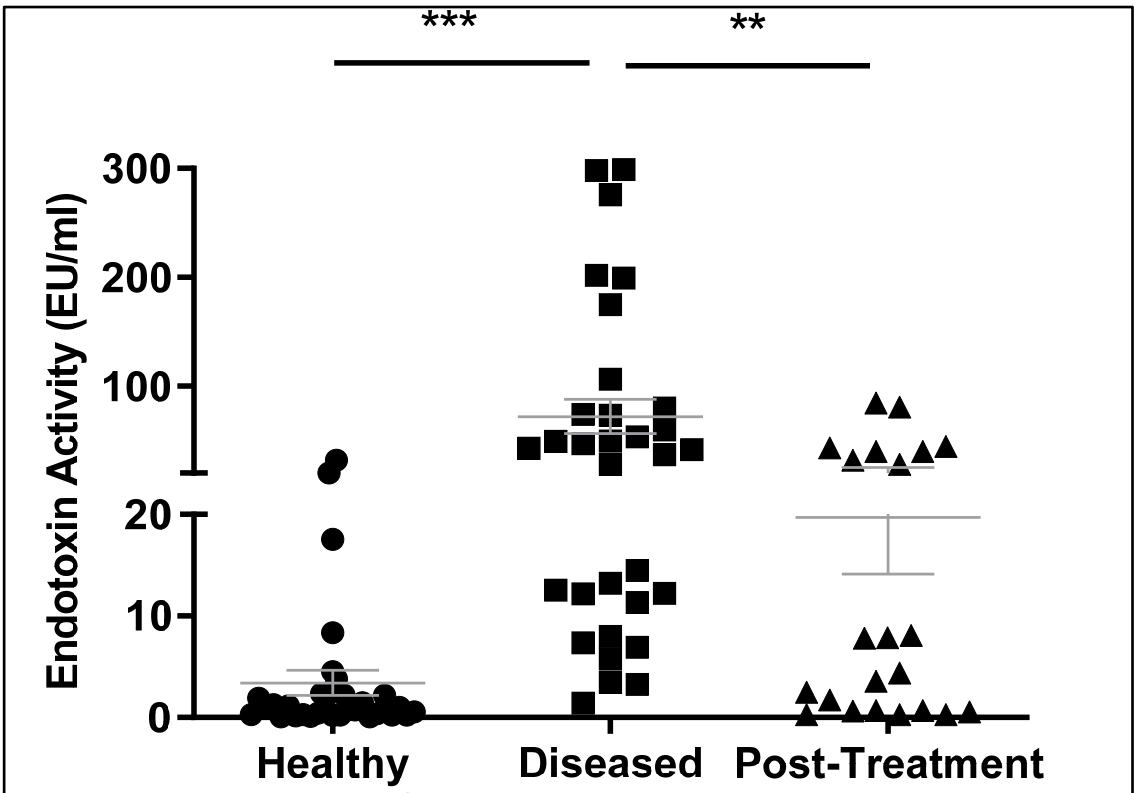

Figure 2.8. Endotoxin activity of subgingival LPS extracts
Endotoxin activity of subgingival LPS extracts from individuals with healthy periodontium and chronic periodontitis patients before and after periodontal treatment. Lines represent mean values with SEM (***p < 0.001, **p < 0.01). (Samples were run in technical triplicates and biological duplicates, figures are of 1 representative experiment)

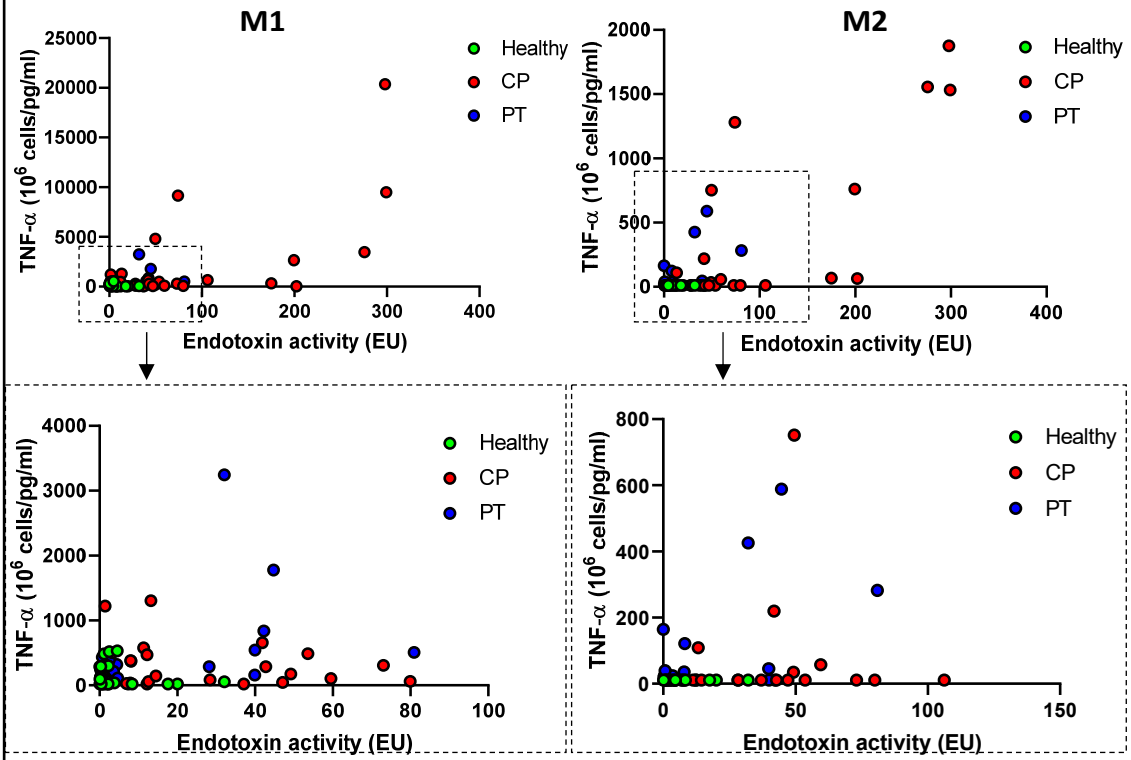

Figure 2.9. Differential inflammatory potential responses between patient groups.
Endotoxin activity predominantly corresponds with an increased inflammatory potential (the induction of TNF-α secretion in M1 and M12 MΦs) in the CP (red) and post-treatment (PT) (blue) groups, whereas samples from healthy individuals (green) did not demonstrate an increased inflammatory potential with an increase in endotoxin activity.

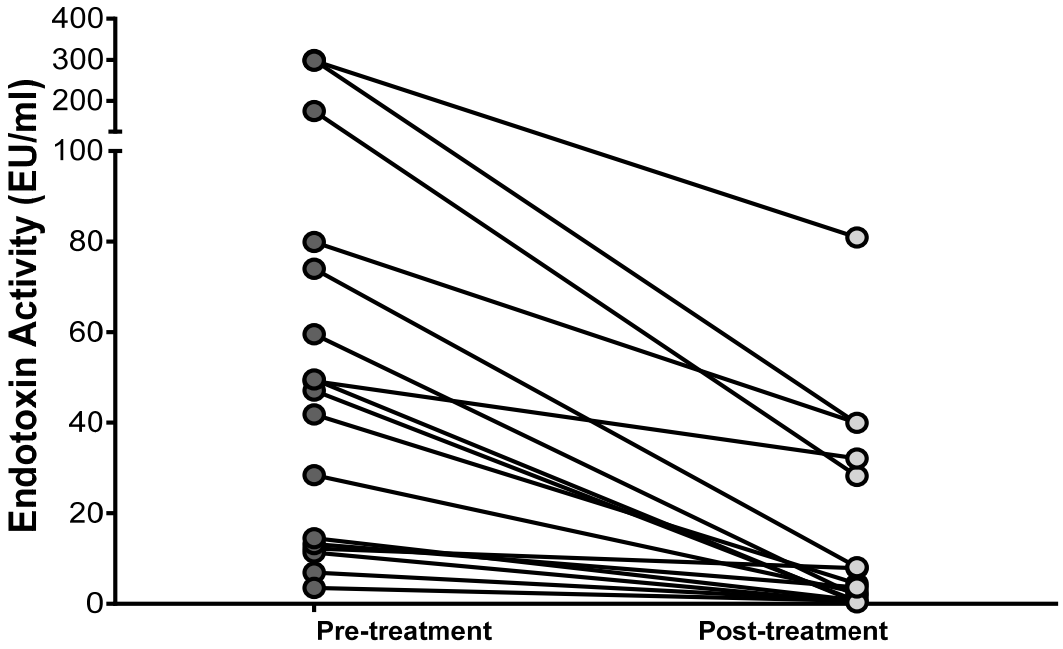

Figure 2.10. Endotoxin activity of subgingival LPS extracts indicating pre-and post-treatment levels.

Endotoxin activity of subgingival LPS extracts isolated from chronic periodontitis patients before and after periodontal treatment. Lines connect individual patients, prior and following treatment.

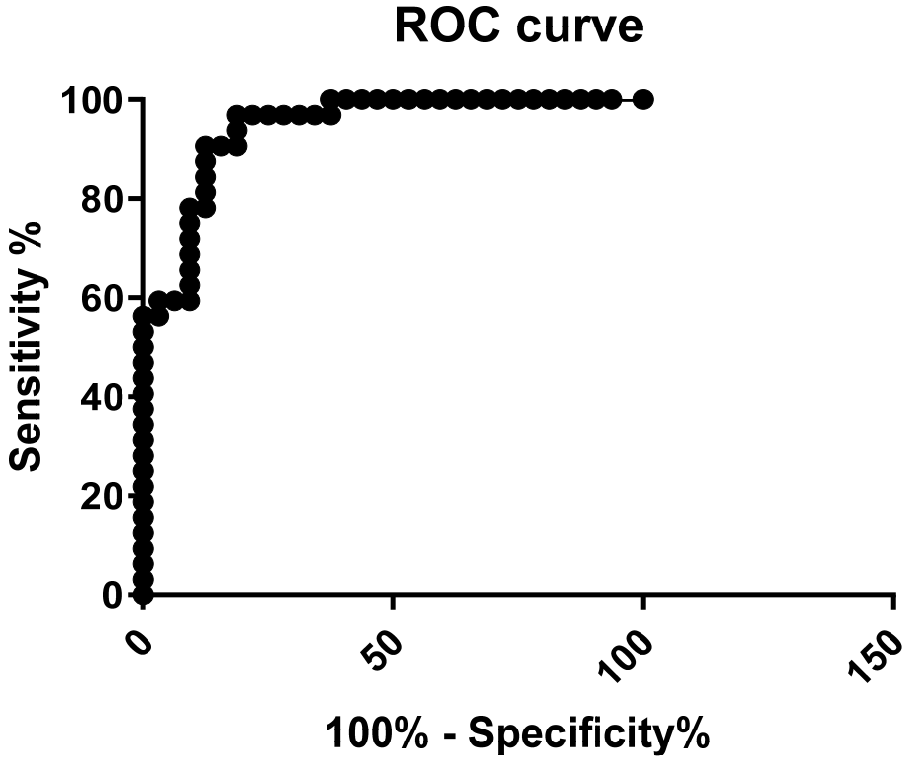

Figure 2.11. The ROC curve for endotoxin activity (EU) in healthy and CP patients as a biomarker for the disease status

The receiver operating curve (ROC) demonstrates a good predictable value of endotoxin activity levels (area under the curve (AUC) of 0.94) and the optimal cut-off point of 5.2 EU (sensitivity 90.63% and specificity 87.50%).

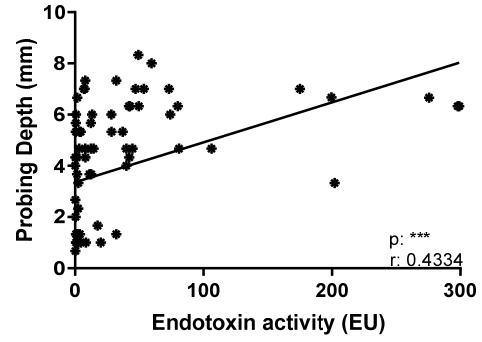

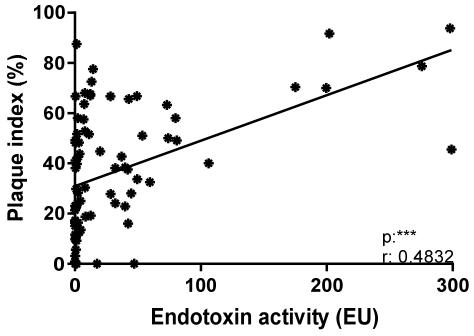

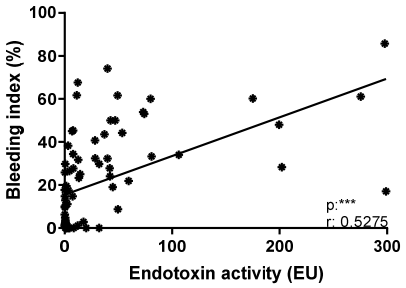

Figure 2.12 Correlation between endotoxin activity and clinical measurements. Clinical measurements; probing depth (mm), plaque index (%) and bleeding index (%) plotted against endotoxin activity (EU) measured by rFC LAL assay, correlate to a low/moderate level when analysed using the Pearson correlation coefficient (r). (***p < 0.001)

The diagnostic performance of subgingival endotoxin activity as a biomarker for disease status was evaluated using the receiver operating curve (ROC) which demonstrated a good predictable value of endotoxin activity levels (area under the curve (AUC) of 0.94) and the optimal cut-off point of 5.2 EU (sensitivity 90.63% and specificity 87.50%) (Fig. 2.11).

Clinically measured parameters demonstrated a low to moderate level of correlation with endotoxin activity when determined via the Pearson correlation coefficient (Fig 2.12). Probing depth and plaque index indicated a low level of correlation with r values of 0.4334 and 0.4832 respectively and bleeding index resulting in a moderate correlation with an r value of 0.5275 (classification of r-value as used by Mukaka, 2012). The low to moderate correlation observed between clinically measured characteristics and endotoxin activity may further indicate that clinical parameters alone may not represent current disease state and maybe susceptible to influence by historical damage.

2.4.7 Inflammatory potential of subgingival LPS extracts

Inflammatory potential of subgingival LPS extracts from each patient was assessed in M1 and M2 like MΦs, by measuring the production of TNF-α and IL-8. TNF-α production by M1 and M2 like MΦs challenged with LPS extracts from most of the healthy individuals was undetectable while LPS extracts from

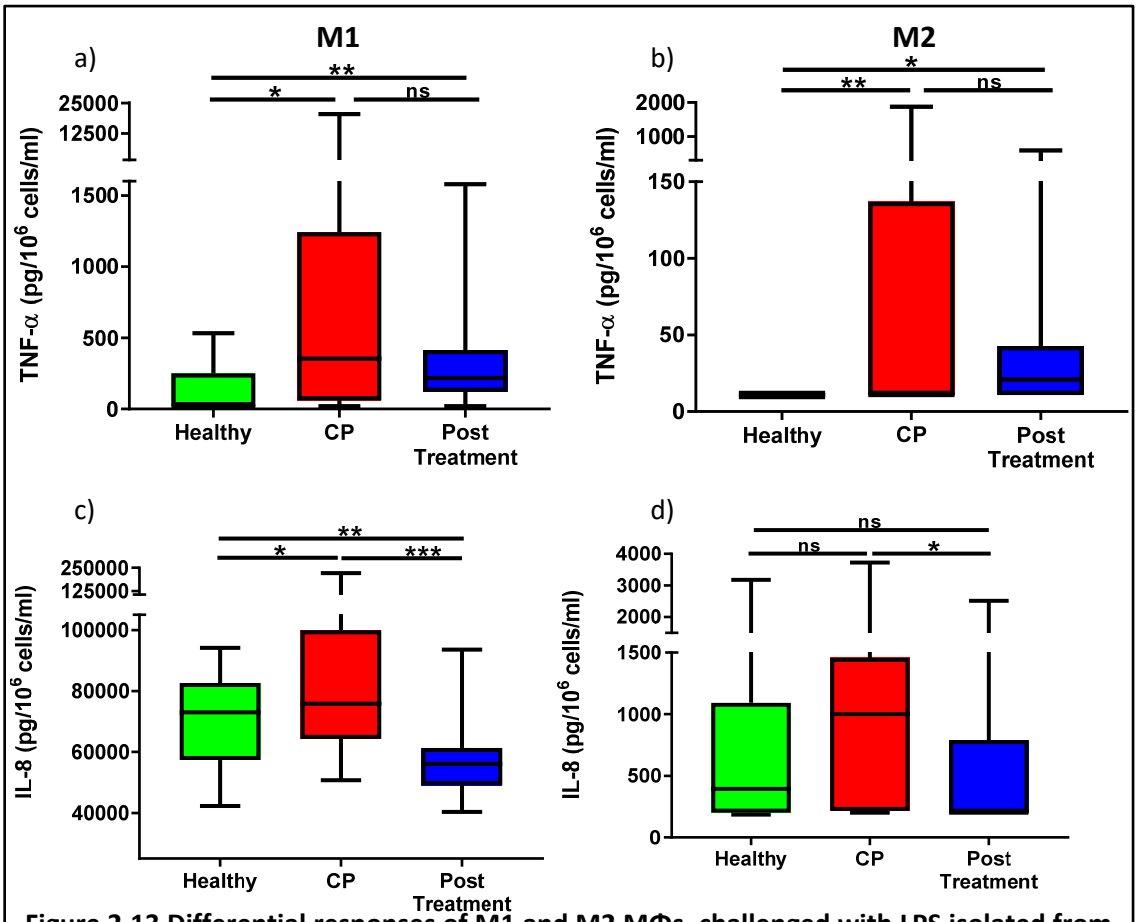

Figure 2.13 Differential responses of M1 and M2 MΦs, challenged with LPS isolated from healthy, CP and post treatment plaque samples.
M1 and M2 macrophages were challenged with LPS extracts from healthy, CP and post-treatment subgingival plaque samples for 18 h and the production of TNF-α (a & b) and IL-8 (c & d) measured by ELISA. (*p<0.05, **p<0.01, ***p<0.001). Technical triplicate experiments with biological duplicates were performed, figures are of 1 representative experiment).

CP patients triggered significantly higher production of TNF-α (Fig. 2.13 (a) & (b)). There was a trend of decreased TNF-α production by macrophages challenged with post-treatment LPS extracts whilst still significantly higher than that induced by LPS from healthy patients.

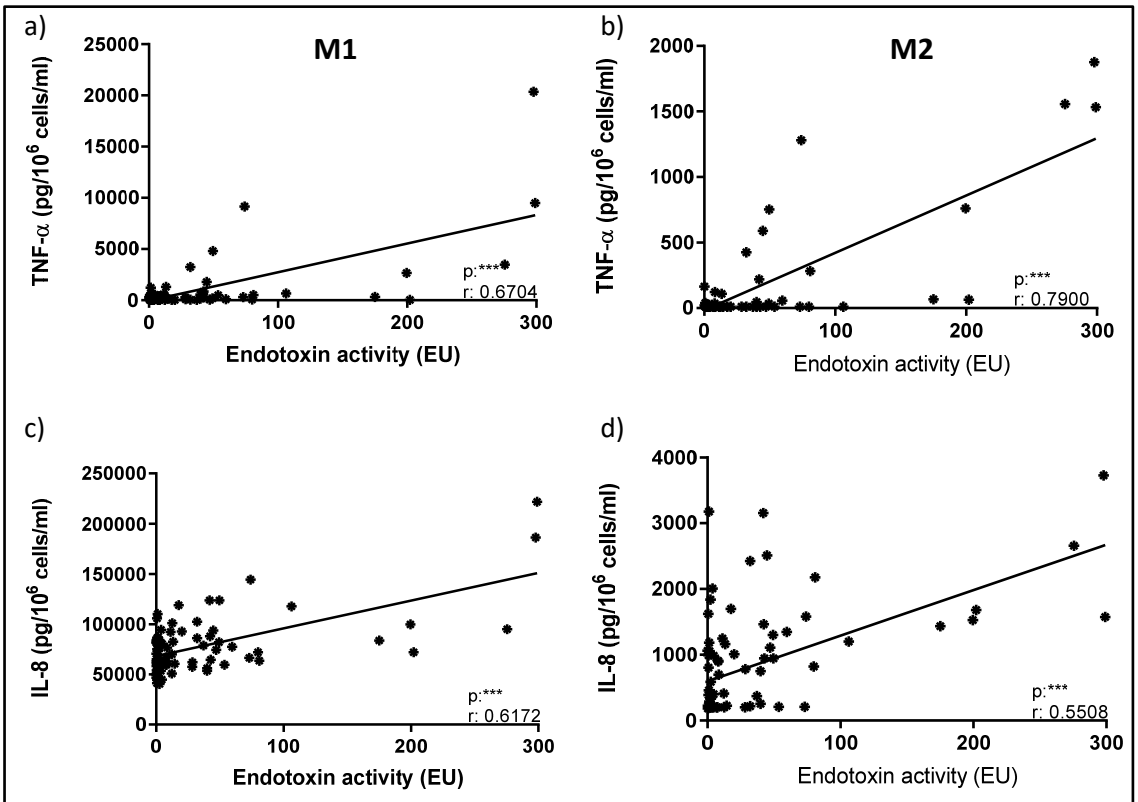

Figure 2.14 Correlation between inflammatory potential and endotoxin activity.
Cytokine production demonstrates an increased correlation with endotoxin activity compared to clinical parameters. TNF-α (a & b) and IL-8 (c & d) produced by M1 and M2 macrophages challenged with patient derived LPS and endotoxin activity are assessed for correlative association using the Pearson correlation coefficient (r). (***p<0.001).

Similarly, IL-8 production was significantly greater in M1 macrophages treated with CP LPS extracts compared to both healthy and post-treatment samples (Fig. 2.13 (c) & (d)). In addition, CP samples triggered a wider range of TNF-α and IL-8 levels compared to healthy and post-treatment samples. Moreover, significantly higher levels of IL-8 than TNF-α were observed in the healthy group in both M1 and M2 macrophages. Additionally, the homeostatic/anti-inflammatory M2 macrophage, demonstrates no significant modulation of IL-8 production when treated with LPS isolated from either healthy or CP patients. This robustness of IL-8 response may serve to depict the importance of neutrophil transmigration for periodontal homeostasis. There was a strong positive correlation between endotoxin activity levels of subgingival LPS extracts and their inflammatory potential measured by the production of TNF-α and IL-8 ($p < 0.001$) (Fig. 2.14).

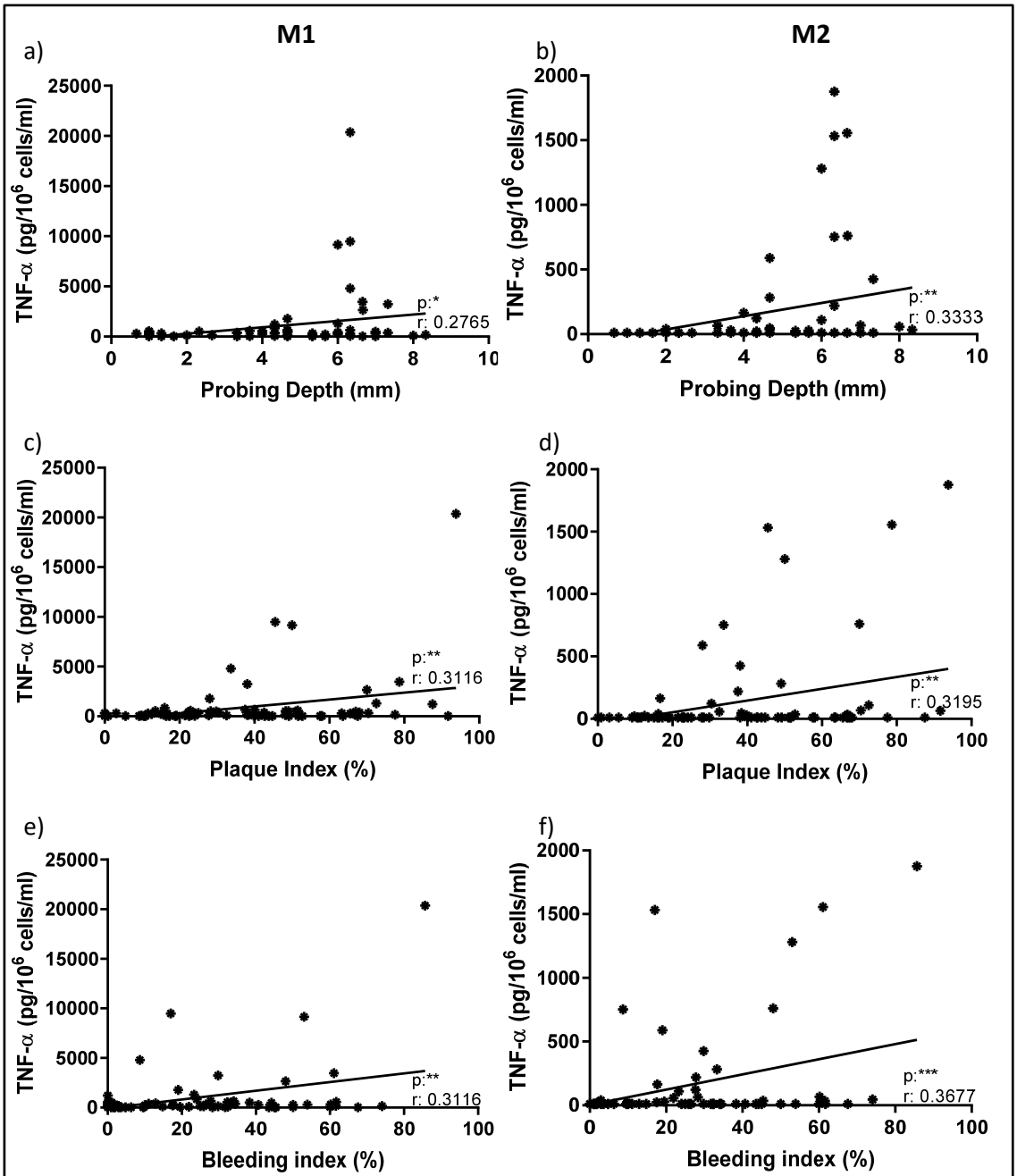

Figure 2.15 Correlation between TNF-α production and clinical characteristics.
The level of correlation between clinical parameters and TNF-α production is substantially lower than when compared with endotoxin activity. M1 ((a), (c), & (e)) or M2 ((b), (d) & (f)) macrophages are evaluated against clinical characteristics; probing depth ((a) & (b)), plaque index ((c) & (d)) or bleeding index ((e) & (f)) using the Pearson correlation coefficient (r). (*p<0.05, **p<0.01, ***p<0.001).

In contrast, the correlation between cytokines used to measure inflammatory potential and clinical parameters were low when compared to the production of TNF-□ in M1 M□s and M2 M□s (Fig. 2.15) and negligible in comparison to IL-8 production (Fig. 2.16).

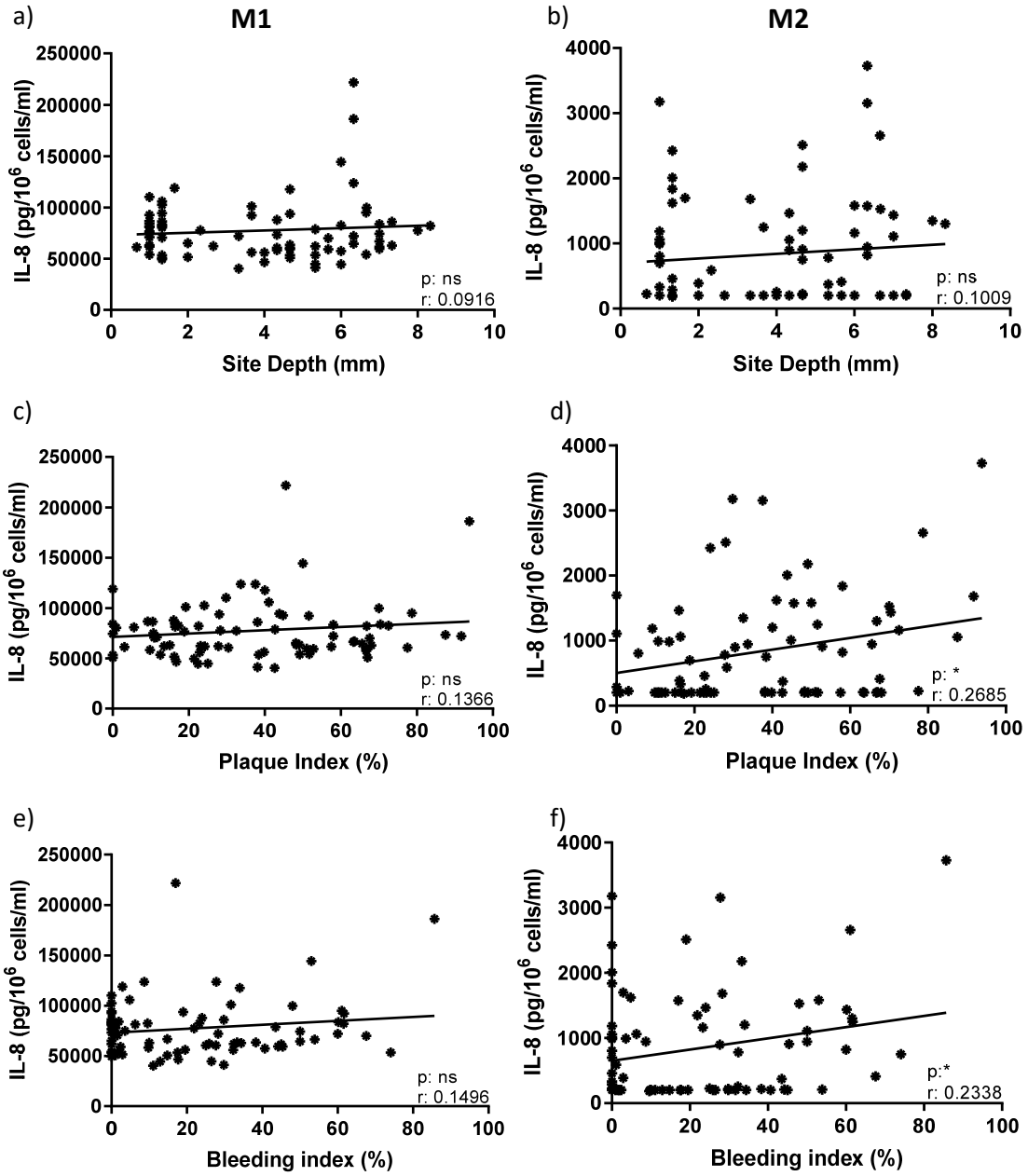

Figure 2.16 Correlation between IL-8 production and clinical characteristics.

The correlation between clinical parameters and IL-8 production was the lowest level of correlation observed. M1 ((a), (c), & (e)) or M2 ((b), (d) & (f)) macrophages are evaluated against clinical characteristics; probing depth ((a) & (b)), plaque index ((c) & (d)) or bleeding index ((e) & (f)) using the Pearson correlation coefficient (r). (*p<0.05, **p<0.01, ***p<0.001).

2.5 Discussion

This study is the first to examine lipid-A compositions of LPS isolated directly from subgingival biofilm samples and not from cultured bacteria. The methods used to isolate and extract LPS from the subgingival biofilms are not without limitations. Reproducibility of these LPS profiles is likely to vary, this however is to be expected within such a dynamic environment associated with a fluctuating disease state. In addition, the cold-water phenol extraction method may influence the LPS profile to exclude those isoforms with a higher mass charge ratio (Al-Qutub et al., 2006). Should this be the case, it is likely that the results in this study are conservative and the LPS profile associated with CP is even more skewed towards the LPS isoforms with a higher level of phosphorylation and acylation. Silver staining to identify isolated LPS proved inconclusive, bringing into question the extraction methods. This may be due to the limitations of the assay and the lower limit of detection (250 pg), given the relatively small amount of LPS isolated on each dental paper point. Whilst this staining technique was not sufficient to confirm the presence of LPS, both the mass spectrometry results and the reduction in inflammatory response observed when MΦs were exposed in conjunction with polymyxin B, support the assumption that LPS is present in these samples.

This study does show however, that there are significant structural differences between lipid-A isoforms isolated from subgingival plaque samples from healthy individuals and patients with chronic periodontitis. Mass spectrometry analysis revealed the presence of peaks at a higher mass to charge ratio in CP patients that correspond to more phosphorylated and over-acylated lipid-A isoforms. These peaks were not observed in healthy patients or in CP patients after

periodontal treatment. There is strong evidence that the expression of highly phosphorylated and acylated lipid-A isoforms is an important virulence factor of many prominent human pathogens. John *et al*. have shown that the lipid-A of all *N. meningitis* invasive isolates are hexa-acylated whereas the lipid-A of significant number of carrier strains are penta-acylated (John et al., 2016). *Pseudomonas aeruginosa* from cystic fibrosis patients is able to synthesize a unique hepta-acylated lipid-A moiety, not normally present in environmental isolates, that significantly contributes to the overall inflammatory burden of the airways of these patients (SenGupta et al., 2016). In contrast*, H. pylori* modifies its lipid-A by removal of phosphate groups from the 1- and 4′-positions of the lipid-A backbone producing under-acylated and under-phosphorylated lipid-A isoforms which are characterised by strikingly low endotoxicity. These modifications decrease the recognition of this bacterium by TLR4 and are key to its ability to colonise a mammalian host (Cullen et al., 2011). Previous studies have shown that periodontal therapy leads to a rapid reduction in periodontal pathogens and a slower reduction in other species that can be sustained for at least 2 years (Socransky et al., 2013). These results complement these findings with the fact that not only is the composition of subgingival microflora different between healthy and CP patients but also that there are significant differences in microbial structural components at a subspecies level. Further studies are needed to determine the dynamics and stability of these changes in longer terms.

A number of limitations should be considered within this study. The unmatched nature of the patient's ages within the healthy patients and those with CP present a possible contributing factor to the differences in LPS proles observed. The influence of aging on the lipid-A structure is not known but the long-term stability of the oral microbiome and the similarity of subgingival microbiota composition

between older adults and youngsters with periodontal health and periodontitis have been documented (Feres et al., 2016) Their study concludes that, the composition of the subgingival biofilms is very similar in older adults to that of youngsters and adults in both health and disease. In addition, the nature of the subgingival biofilm bacterial composition is likely affected more so by the formation of the periodontal pocket and the anaerobic environment within, than the age of the overall oral biofilm. Gender is another factor which which was demonstrated to significantly differ between patient groups, although, only just at the 95% confidence level ($p = 0.477$). Periodontitis has been shown to demonstrate a higher prevalence in males (57%) compared to females (39%) and as the CP group consists of a greater number of males than the healthy group, as such this should be considered as an influencing factor within the data (Ioannidou, 2017). Smoking status was also demonstrated to be significantly different within the patient groups with a higher number of smokers in the CP group compared to the healthy patient group. This however is not surprising given the increased risk associated with smoking and CP. Furthermore, smoking status was not shown to influence inflammatory potential within each patient group (Fig. S2, appendix E).

The recombinant factor C assay (rFC) is widely used for the screening of lipopolysaccharide in pharmaceutical products and can detect a wide range of divergent LPS structural species (Ding and Ho, 2010). The minimal lipid-A structural prerequisites for the activation of factor C are the presence of the 4′-phosphatediglucosamine backbone. However, full expression of factor C activity is also dependent on the presence of fatty acids attached to this backbone, and interestingly does not depend on the type of LPS aggregate structure (Gutsmann et al., 2010). The ratio of high and low endotoxic LPS is crucial for the regulation

of the intestinal immune balance, where high endotoxic LPS isoforms support intestinal inflammation while low endotoxic LPS promotes intestinal homeostasis (Gronbach et al., 2014). These results show significantly increased endotoxin activity of subgingival plaque samples from CP patients compared to healthy individuals and treated CP patients. The differences in endotoxin activity are in agreement with different lipid-A profiles observed in these three groups of samples via mass spectrometry. Subgingival endotoxin activity levels exhibited a high level of sensitivity, specificity, and accuracy in confirming the clinical classification of chronic periodontitis status.

The destruction of alveolar bone and periodontal ligament is caused by the ability of subgingival microbial community to induce a dysregulated inflammatory response in periodontal tissues (Camelo-Castilo et al., 2015). Subgingival plaque samples from CP sites have been shown to strongly activate TLR4, whereas matched samples obtained from healthy sites have been more variable with some of them displaying strong TLR4 antagonism (To et al., 2015).

In this study, inflammatory potential of subgingival LPS extracts, measured by the production of TNF-α in M1 and M2 like MΦs, was significantly higher in CP patients compared to healthy individuals. Whereas IL-8 production was upregulated in CP patients compared to healthy in M1 like MΦs and IL-8 production was at a significantly higher level of amplitude when compared to M2 MΦs. This lower level of production combined with the resistance to modulation may represent the low level of IL-8 requirement necessary to maintain homeostatic conditions.

In addition, a strong, positive correlation between subgingival endotoxin activity levels and inflammatory potentials of subgingival LPS extracts supports a

potential use of subgingival endotoxin activity measurements as a biomarker for the development of inflammatory periodontal conditions. The rFC assay may therefore present the basis of a chairside assay to aid the clinician. These were in stark contrast to the correlative values obtained by comparison of either endotoxin activity or inflammatory potential to clinical characteristics, affirming that individual clinical characteristics are only representative of historical damage due to disease, whereas both inflammatory potential and endotoxin activity may be more representative of current disease state.

This study has also shown that the correlation between inflammatory potential and endotoxin activity is an indicator of disease state but the MΦ subset which predominates within the periodontal tissue may heavily influence both disease progression and instigation, with differential responsiveness to lipid-A modification as well as a potential plasticity dependent upon structure of the corresponding stimulant.

Chapter 3

Cytokine response to stimulation and tolerisation using different LPS moieties.

3.1 Introduction

In chapter 2, pro-inflammatory TNF-α and chemotactic IL-8 were measured and TNF-α was demonstrated to be significantly increased in MΦs stimulated with LPS isolated from CP patients compared to those that were periodontally healthy, yet somewhat surprisingly IL-8 was less affected by lipid-A profile. Mass spectrometry revealed lipid-A profiles that were markedly different between cohorts. In addition, proprietary PG LPS was demonstrated to contain a variety of lipid-A moieties.

In this chapter, proprietary PG LPS (of the same batch used to produce the mass spec profile in figure 2.6/7) was compared in responsiveness to LPS pooled from each patient group i.e. CP, healthy and post treatment. The same PG LPS was also compared to *E. coli K12* LPS as the archetypal for of LPS which demonstrates minimal variation and a higher level of endotoxin activity due to increased phosphorylation and acylation. This will indicate which cytokines, and therefore which mechanisms are predominantly affected by changes in lipid-A structure. Furthermore, preliminary investigations into responses to individual PG LPS isoforms were also examined, to compare exposure to singular and multiple lipid-A moieties. As such, this phase of the study sets out to investigate how these indicators of inflammation (IL-8 and TNF-α), as well as anti-inflammatory IL-10 and key cytokines associated with T-helper differentiation (IL-12 and IL-23) are affected by single and repetitive stimulation.

Repetitive exposure to LPS (ET) results in a diminished inflammatory response compared to naïve stimulation. This diminished response however, is not a total state of anergy as some responses remain unaffected (Al-Shaghdali *et al.*, 2019; Foey & Crean, 2013; Zaric *et al.*, 2011). As such the ET, may supress some

responses, whilst maintaining or even amplifying others and comparing responses to LPSs may help elucidate additional mechanisms which may drive the pathology.

3.2 Materials and methods

3.2.1 THP-1 cell line maintenance, culture and differentiation.

THP-1 cell line maintenance, culture and differentiation was performed as indicated in sections 2.3.9.1 and 2.3.9.2.

3.2.2 Stimulation protocols

3.2.2.1 M1 and M2 MΦs stimulated with PG and *E. coli* LPS

Differentiated cells were stimulated with proprietary LPS derived from either PG or *E. coli* (K12) (Invitrogen, Renfrewshire, UK) at a concentration of 1 μg/ml for a period of 18 hours. Resulting supernatants were stored at -20^{o}C prior to analysis by ELISA.

3.2.2.2 M1 and M2 MΦs stimulated with PG LPS isoforms

Commercially available PG LPS with specific Lipid-A Structure; LPS_{1690} (penta-acylated and mono-phosphorylated) and $LPS_{1449/1435}$ (referred to as PG LPS_{1435}) (tetra-acylated and mono-phosphorylated) were purchased from Astarte Biological (See Fig. 3.1 for mass spectrometry analysis). Due to the limited quantity of available LPS, the optimal concentration was determined using standard PG LPS (Invitrogen, Renfrewshire UK) by analysing measurement of TNF-α in response to titrated concentrations of LPS ranging from 10 ng/ml to 10 μg/ml by ELISA (see supplemental figure S3). Differentiated THP-1 cells were stimulated with 700 ng/ml of either LPS_{1690} or $LPS_{1449/1435}$ for a period of 24 hours with supernatants collected over this period and stored at -20°C for further analysis.

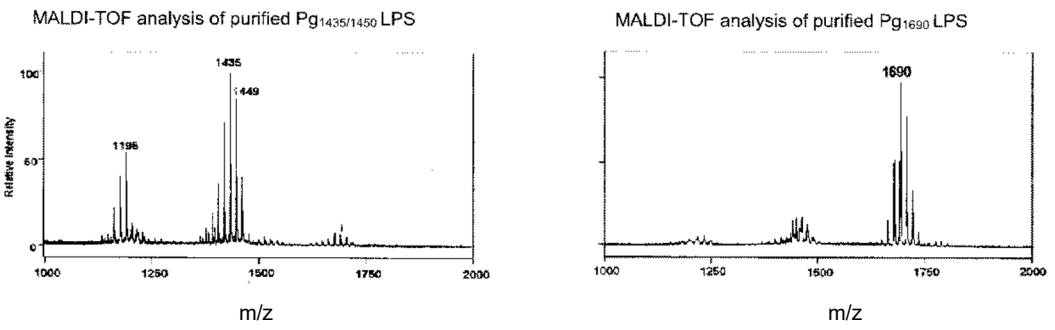

Figure 3.1 The deduced structure of the Lipid-A moiety of PG LPS$_{1690}$ and PG LPS$_{1449/1435}$, As analysed by matrix assisted laser desorption ionization time of flight (MALDI-TOF). PG LPS$_{1690}$ contains a negative mass ion charge of 1690 which represents a penta-acyl Lipid-A. PG LPS$_{1449/1435}$ contains two species of Lipid-A with mass ions of 1449 and 1435, representing tetra-acyl isoforms. A minor species of tri-acyl lipid-A is also present with a negative mass of 1195. (Data provided by Astarte Biologics, Bothwell, USA)

3.2.2.3 M1 and M2 MΦs stimulated with LPS isolated from subgingival plaque samples

Due to the limited quantity of LPS available which was isolated from subgingival plaque, these were pooled to create three samples of LPS, representative of the healthy, diseased and post treatment groups. This was used to stimulate M1 and M2 MΦs for a period of 18 hours to allow for capture of multiple cytokine targets of interest, using 50 µl of LPS isolate per millilitre of cells. Supernatants were collected and stored at -20°C for further analysis.

3.2.3 Scanning electron microscopy (SEM) to determine morphological changes induced in M1 and M2 MΦs by PG LPS isoforms

To visualise morphological changes induced by stimulation with either PG LPS$_{1690}$ or PG LPS$_{1435}$, stimulated cells were examined using SEM. Cells were grown on Aclar film (Agar scientific, Essex, UK) as this preferentially adheres macrophages. Undifferentiated THP-1 cells, unstimulated and stimulated M1 and M2 MΦ cells were cultured on the growth substrate, where stimulated cells were treated with either PG LPS$_{1690}$ or PG LPS$_{1435}$ at 700 µg/ml for 8 hours to coincide

with the optimal period or response to stimulation (for supporting data see supplemental figures S4). Substrate bound cells were washed in PBS prior to fixation for 1 hr in 2.5% glutaraldehyde in 0.1 M sodium cacodylate buffer overnight. Subsequently, the samples were rinsed in 0.1 M sodium cacodylate three times for 15 minutes each. All samples underwent alcohol dehydration through a series of 30%/50%/70% and 90% immersions for 15 minutes each, followed by two immersions in absolute alcohol. Samples were then dried using a critical point dryer (Emitech K550, Quorum, Lewes, UK). Samples were sputter coated with gold/palladium using the Q150T coating system (Quorum, Lewes, UK) Scanning electron microscope analysis was performed using a Jeol 7001 field emission generating scanning electron microscope (FEG-SEM) utilising the secondary electron detector for increased surface resolution (JEOL, Tokyo, Japan).

3.2.4 Induction of tolerisation in M1 and M2 MΦs

To induce a tolerised state, differentiated cells were exposed to LPS for a period of 24 hours before being washed twice in fresh media and stimulated for a second time, for a period of 18 hours (Foey & Crean, 2013). Resulting supernatants were removed and stored at -20^{o}C prior to analysis by ELISA.

3.2.4.1 Tolerisation of M1 and M2 MΦs with PG and *E. coli* LPS

Tolerisation with PG and *E. coli* (K12) LPS was carried out using repeat exposures at 1 μg/ml, as indicated in section 3.2.4.

3.2.4.2 Tolerisation in M1 and M2 MΦs with patient derived LPS

Patient derived LPS was used to induce tolerisation using repeat exposures to 50 μl of pooled LPS per ml of cells as indicated in section 3.2.4. Cross exposure

was utilised by sensitising with derived LPS derived from the healthy group followed by stimulation with LPS from the CP group, and *vice versa*.

3.2.4.3 Tolerisation in M1 and M2 MΦs with PG LPS isoforms

An initial investigation was performed using commercially available PG LPS with specific Lipid-A Structures (LPS_{1690} and $LPS_{1449/1435}$). MΦs were sensitised using each isoform using a range of concentrations – 0.01, 0.1 and 1.0 μg/ml. To minimise usage of reagents, a stimulatory concentration of 0.5 μg/ml was used, as previous titration experiments have shown this as sufficient to induce a significant inflammatory response (this is demonstrated to induce significant responses as per supplementary figures S3). Cross exposure was also achieved by sensitising with one isoform and stimulating with the other.

3.2.5 Analysis of cytokine Secretion

Cytokine production was measured by ELISA, with the protocol referred to in section 2.3.11 of chapter 1, modified to incorporate the appropriate detection and capture antibodies as listed in table 3.1.

Target Cytokine	Capture Antibody (μg/ml)	Detection Antibody (μg/ml)	Lower limit of detection. (pg/ml)
IL-8	2	0.5	13
IL-10	1	1	7
IL-12	1	1	7
IL-23	2	1	13
TNF-α	4	0.5	7

Table 3.1 Concentrations used for in-house optimised ELISAs and LLODs

3.2.6 Statistical analyses

All samples, participants, and clinical data were anonymized and blocked before the codes were revealed. In order to analyse differences between examined groups of patients, one-way analysis of variance with Tukey post-hoc test was performed, using GraphPad Software version 7, San Diego, CA. A *p-value* below 0.05 was considered significant (* < 0.05, < 0.01, * < 0.001).

3.3 Results

3.3.1 LPS induced cytokine profile in response to *E. coli* and PG LPS.

Secretion of a cytokine profile associated with inflammation (TNF-α and IL-8), neutrophil chemotaxis (IL-8), regulation of inflammation (IL-10) and the differentiation of naïve $CD4^+$ T cells (IL-12 and IL-23), relevant to CP was measured in M1 and M2 MΦs exposed to commercially available *E. coli* K12 and PG LPS.

E. coli LPS was shown to Induce a substantially higher inflammatory response in M1 MΦs, demonstrating a 824% increase in TNF-α secretion in comparison to M2 MΦs. *E. coli* LPS was also shown to induce a significantly higher level of TNF-α secretion in M1 MΦs ($p<0.001$) compared to that induced by PG LPS. Conversely PG LPS induced a significantly higher level of TNF-α secretion in M2 MΦs compared to M1Φs ($p< 0.001$) (Fig. 3.2a).

In contrast to TNF-α, IL-8 is secreted in significantly higher levels in both M1 and M2 MΦs stimulated with PG LPS compared to those exposed to *E. coli* LPS ($p< 0.001$). M1 MΦs were shown to be the primary producers of IL-8 once normalised to basal levels of IL-8 production, with significantly increased production induced by both PG and *E. coli* in M1 MΦs compared to M2 MΦs ($p<0.001$) (Fig. 3.2b).

IL-23 secretion demonstrated the most markedly differential result observed across the measured profile. The Th17 associated cytokine was only significantly induced M2 MΦs in response to stimulation with PG LPS (Fig. 3.2c).

IL-10 and IL-12 were not consistently measurable above the lower limit of detection (see table 3.1) across multiple experiments and were therefore not deemed to be significant results.

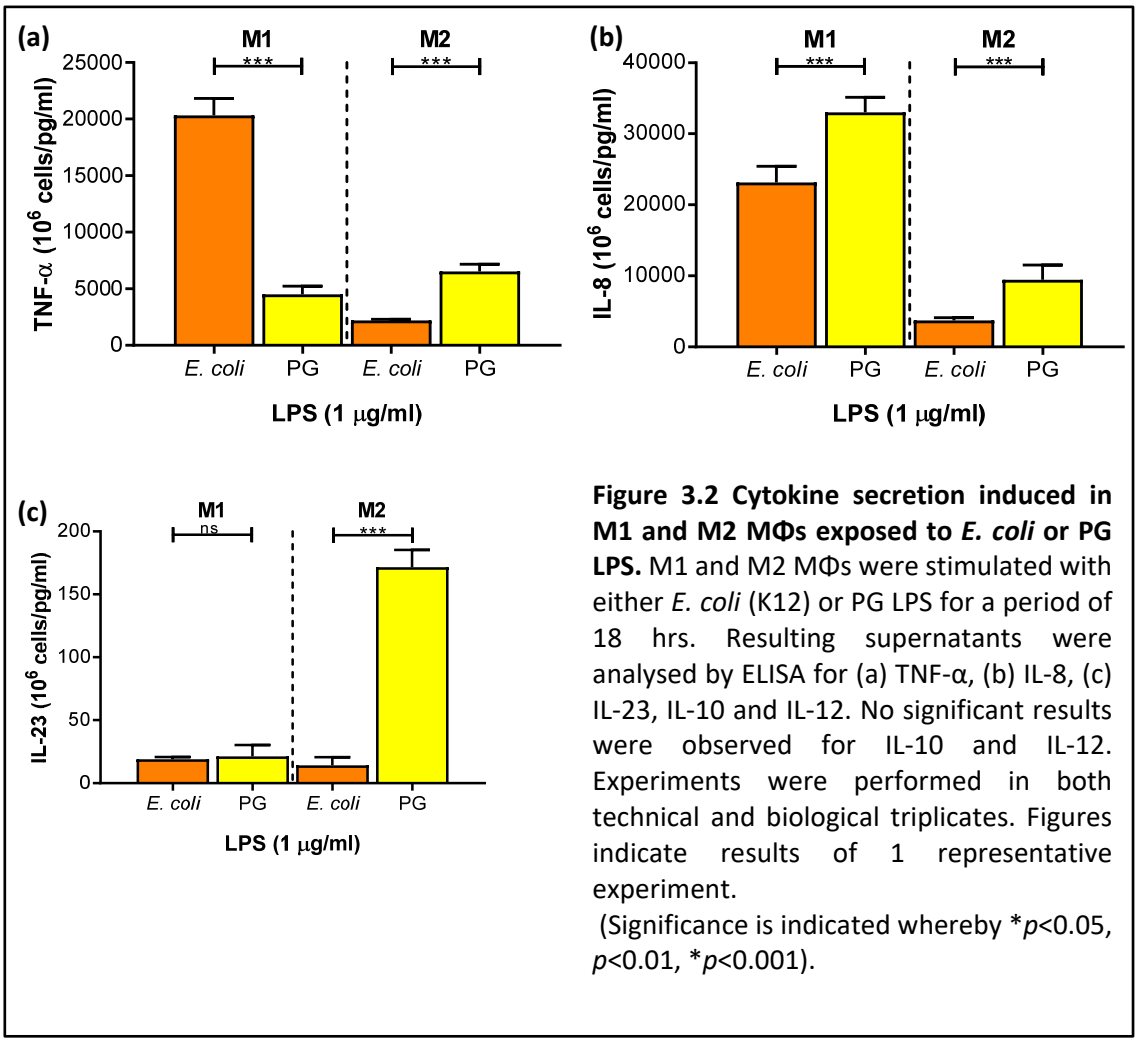

Figure 3.2 Cytokine secretion induced in M1 and M2 MΦs exposed to *E. coli* or PG LPS. M1 and M2 MΦs were stimulated with either *E. coli* (K12) or PG LPS for a period of 18 hrs. Resulting supernatants were analysed by ELISA for (a) TNF-α, (b) IL-8, (c) IL-23, IL-10 and IL-12. No significant results were observed for IL-10 and IL-12. Experiments were performed in both technical and biological triplicates. Figures indicate results of 1 representative experiment.

(Significance is indicated whereby **p*<0.05, *p*<0.01, **p*<0.001).

3.3.2 Differential stimulatory potential of PG LPS isoforms

Having determined differential responses to patient derived LPS and contrasting responses between PG LPS and *E. coli* LPS and the existing data which demonstrates variation between PG LPS isoforms (summarised in chapter 1), this study sought to determine the effect of lipid-A modification on cytokine production in macrophage subsets. Commercially available PG LPS isoforms were obtained (Astarte Biologics, Bothell, WA, USA) with mass to charge ratios of 1690 or 1435/1449, representing penta-acylated/mono-phosphorylated and tetra-acylated/mono-phosphorylated structures, respectively. TNF-α and IL-8 production by M1 and M2 MΦs was measured over a 24-hour period by ELISA.

TNF-α production was shown to be significantly affected by both PG LPS isoform and MΦ subset. In M1 MΦs, TNF-α production remained significantly higher in amplitude over a period of 24-hours when stimulated with PG LPS_{1690} in comparison to PG LPS_{1435} (Fig. 3.3a). The initial response to PG LPS_{1690} stimulation, over the first 2 hours is significantly ($p<0.05$ consistently over a 24 hour period) higher than that of PG LPS_{1435} in M2 MΦs. TNF-α production continues to increase to a higher amplitude at 4 hours than that of PG LPS_{1690} and remains so throughout the remaining 20 hours (Fig. 3.3b). Differential responses in IL-8 production are less conclusive and appear to be less affected by PG LPS isoform and MΦ subset (Fig. 3.3 c & d). An interesting observation, however, is the apparent continuation of the rise in IL-8 production in M2 MΦs stimulated with the PG LPS_{1435} at 24 hours whereas IL-8 production induced by PG LPS_{1690} appears to have plateaued after 12 hours (Fig. 3.3 d).

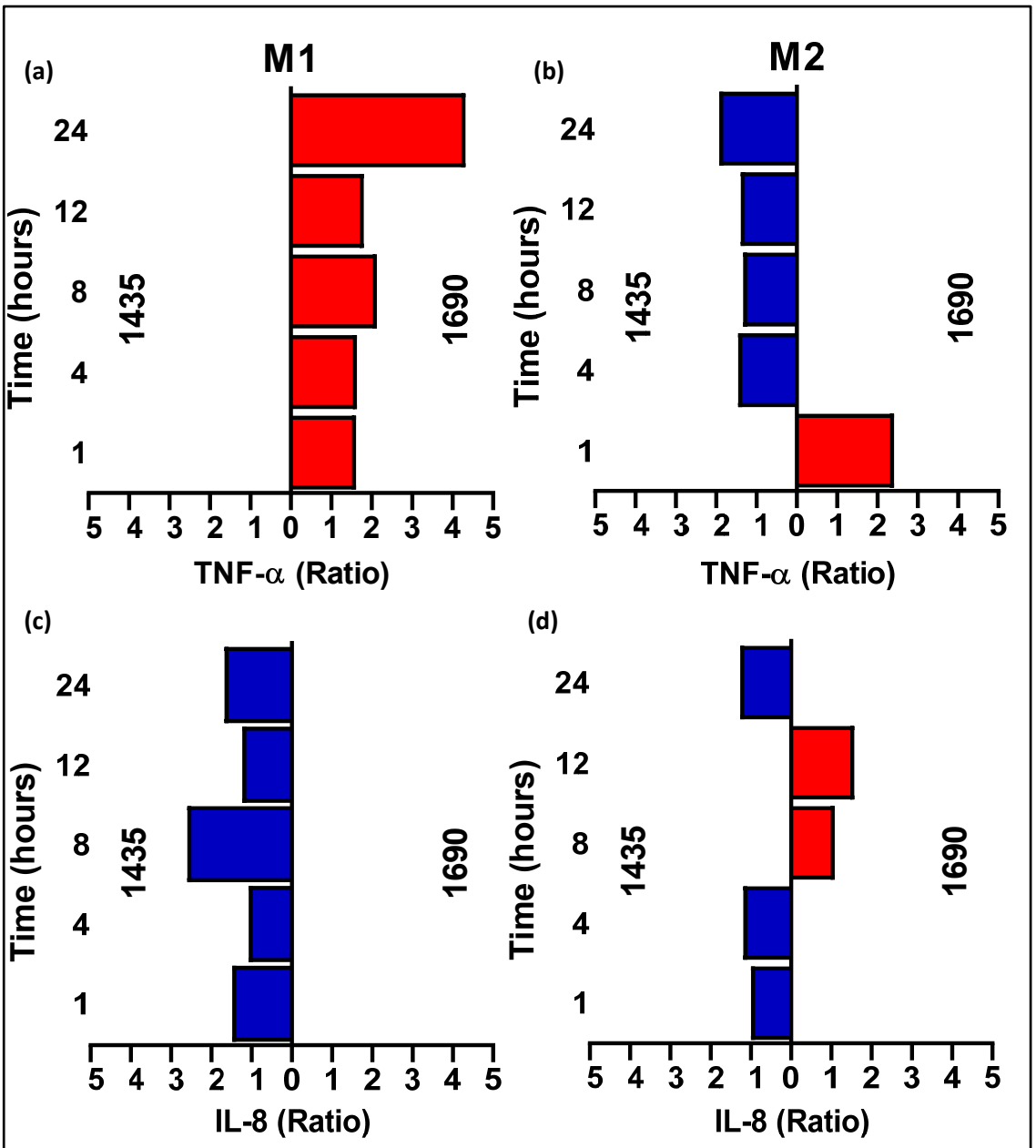

Figure 3.3 Differential susceptibility of MΦ subsets to stimulation by PG LPS Isoforms
The production of TNF-α (a & b) and IL-8 (c & d) by M1 (a & c) and M2 (b & d) macrophages stimulated with PG LPS_{1690} (red) or PG LPS_{1435} (blue) over a period of 24 hours. Results are indicated as a ratio of production, where a positive value was observed by either 1435/1690 (blue) or 1690/1435 (red). M1 MΦs produced a higher level of TNF-α when stimulated with PG LPS_{1690}, whereas M2 MΦs production was highest in response to PG LPS_{1435}. IL-8 secretion was less susceptible to influence bit M1`MΦs responded with increased IL-8 production to PG LPS_{1435} Experiments were performed in technical duplicates and biological triplicates. Figures indicate results of 1 representative experiment.
(Significance is indicated whereby *p<0.05, p<0.01, *p<0.001).

3.3.3 Scanning electron microscopy of THP-1 cells and MΦ morphologies.

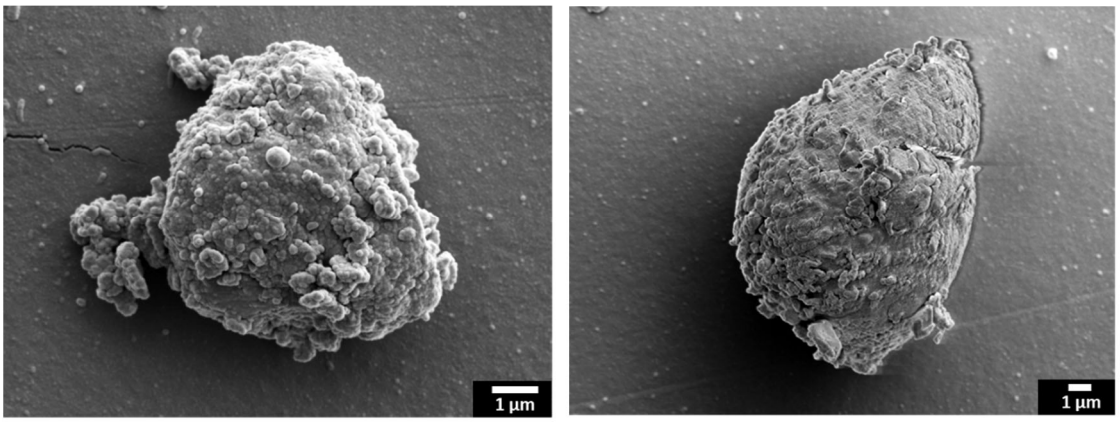

Figure 3.4 Scanning electron micrographs of undifferentiated THP-1 cells.
Undifferentiated THP-1 cells were cultured on sections of Aclar film prior to fixation, alcohol dehydration and critical point drying. Samples were sputter coated and imaged using a Jeol JSM 7001F FEG-SEM at 8 kV using the secondary electron detector.

Given the differential ability to induce a TNF-α secretion in M1 and M2 MΦs, analysis was carried out to determine if morphological changes were induced in either subset by each PG LPS isoform. To analyse morphological changes which may indicate plasticity between M1 and M2 MΦs which exhibit visibly identifiable phenotypes, cells were cultured on Aclar film prior to stimulation with PG LPS isoforms. Cells were stimulated for a period of 8 hours prior to fixation, preparation and analysis by scanning electron microscopy (SEM).

Due to the varying levels of adherence between samples, it was not possible to prove statistical significance. However, a number of observations were made which may support the hypothesis of plasticity. M1 MΦs (Fig. 3.5 a-d) demonstrate a phenotypic morphology undifferentiated THP-1 cells (Fig. 3.4) and M2 MΦs (Fig. 3.6 a-d). M1 MΦs appear larger in size and with an elongated form and whilst being highly adherent, have the ability to stretch and extend to contact other cells. Conversely M2 MΦs tend to retain the spherical appearance and contact with other cells appears to occur via extended tendril like protrusions.

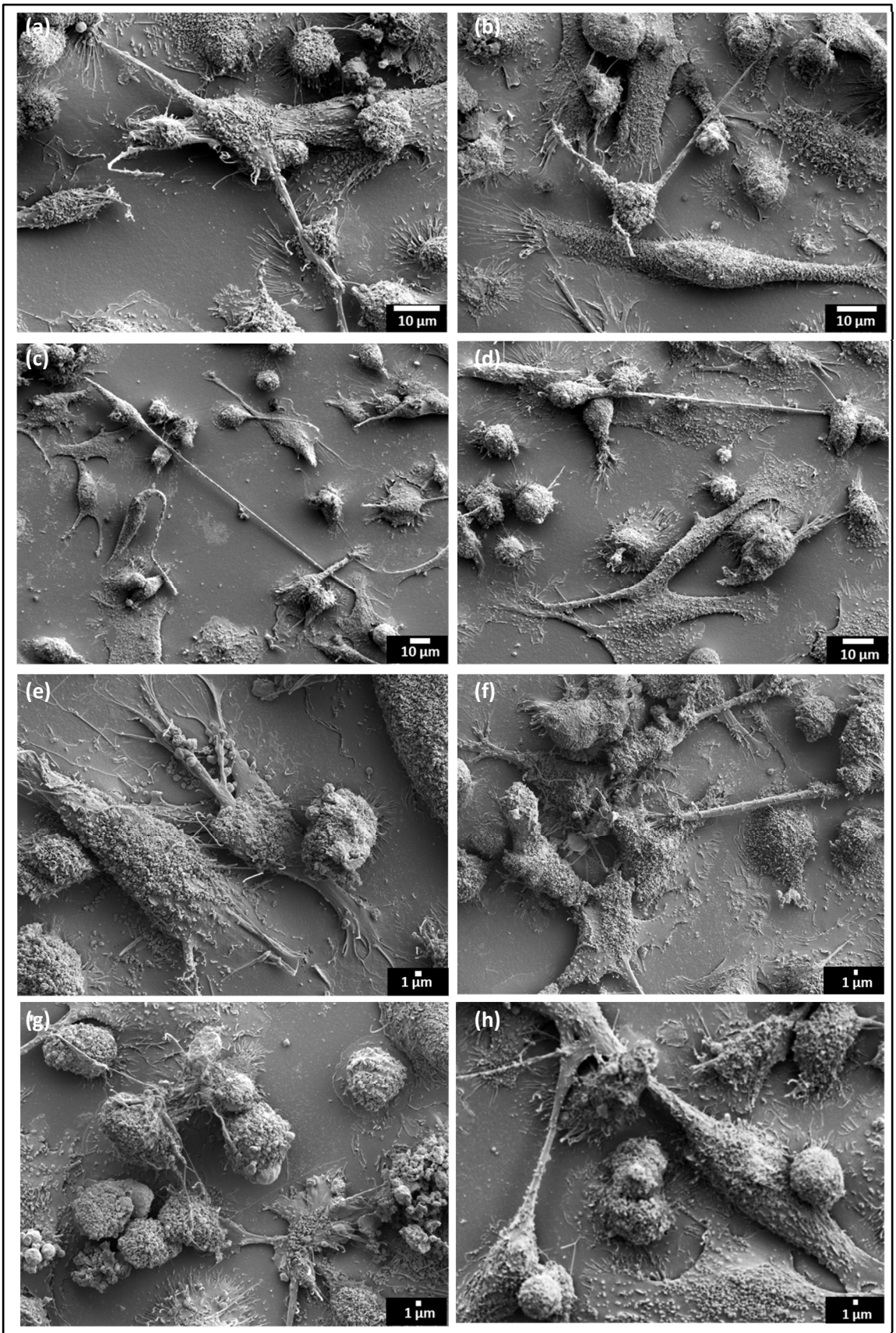

Figure 3.5 Scanning electron micrographs of stimulated and unstimulated M1 MΦs.
M1 MΦs cultured on Aclar film were either unstimulated (a-d) or stimulated with PG LPS_{1690} (e & f) or PG LPS_{1435} (g & h) for a period of 8 hours, prior to fixation. Samples were sputter coated and imaged using a Jeol JSM 7001F FEG-SEM at 8 kV, using the secondary electron detector.

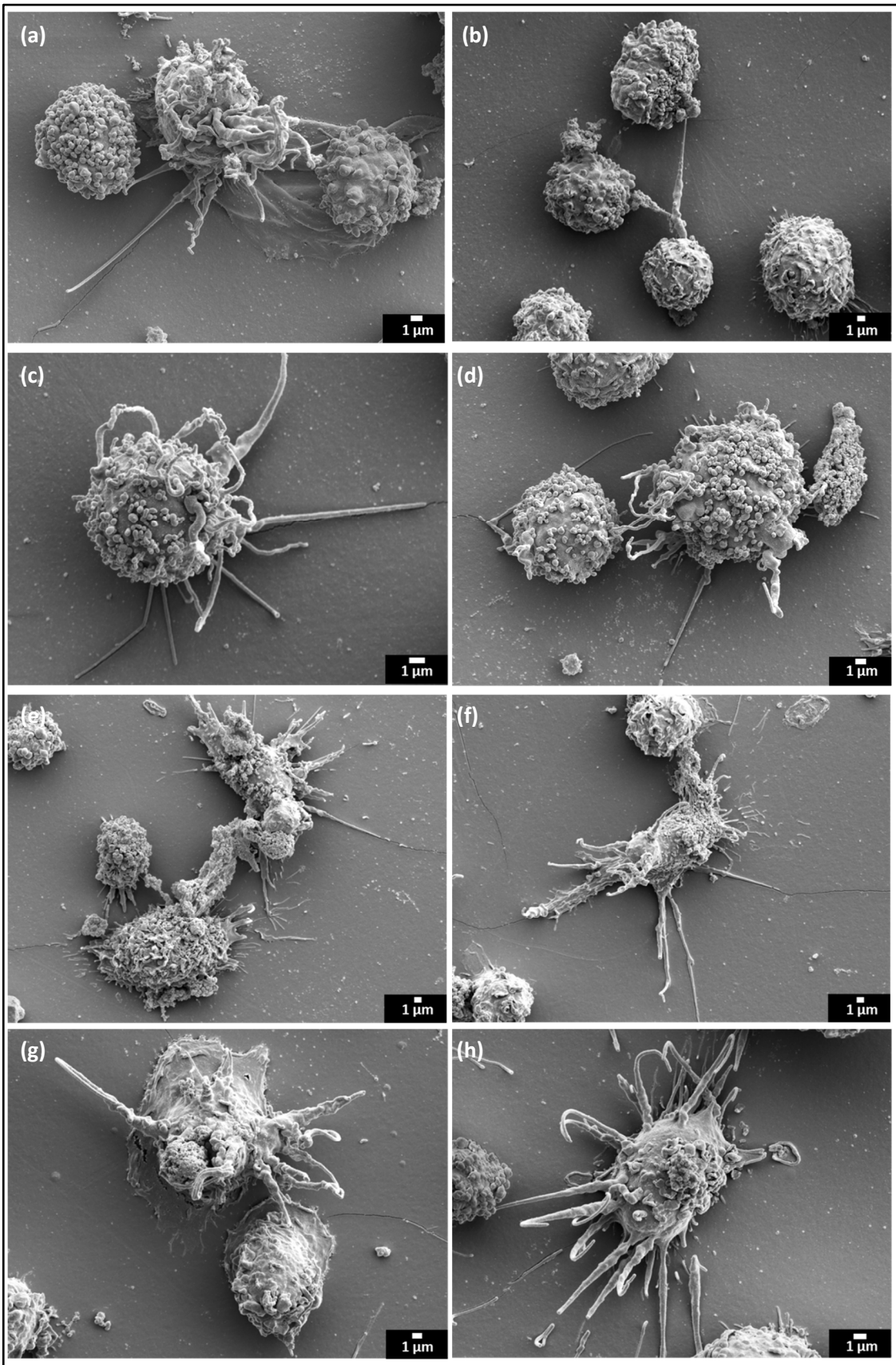

Figure 3.6 Scanning electron micrographs of stimulated and unstimulated M2 MΦs.
M2 MΦs cultured on Aclar film were either unstimulated (a-d) or stimulated with PG LPS_{1690} (e & f) or PG LPS_{1435} (g & h) for a period of 8 hours, prior to fixation. Samples were sputter coated and imaged using a Jeol JSM 7001F FEG-SEM at 8 kV, using the secondary electron detector.

Whilst not conclusive, PG LPS_{1690} appears to maintain, if not exaggerate the M1 phenotype (Fig. 3.5 e & f), with increased spreading and cellular interaction. A notable observation, in addition to the typical M1 morphology was the appearance of vesicular like bodies at the cell surface (Fig. 3.5e). M2 MΦs, though not uniform, PG LPS_{1690} does appear to reduce the number of cells which retain the typical M2 associated spherical appearance and increase cellular adhesion, normally associated with M1 MΦs (Fig. 3.6 e & f). Similar observations are made when considering the PG LPS_{1435} isoform, but this time inducing an exaggerated M2 phenotype in M2 MΦs, with increases in cellular protrusions but also higher levels of adherence (Fig. 3.6 g & h). In M1 MΦs however, PG LPS_{1435} appears to induce an increase in spherical cells with protruding tendrils, traits associated with M2 MΦ morphology (Fig. 3.5 g & h).

3.3.4 Differential sensitivity to endotoxin tolerisation of M1 and M2 MΦs repeatedly exposed to *E. coli* or PG LPS.

Following the identification of significant variation in the ability of PG LPS to induce inflammatory cytokines in comparison to *E. coli* LPS, this study set out to determine the ability of these endotoxins to supress inflammatory cytokine secretion through ET. M1 and M2 MΦs were exposed to a either PG or *E. coli* LPS for a period of 24 hours to sensitise the cells to tolerisation. Following successive washes in fresh R10, the cells were once again exposed to the same stimulus for a period of 18 hours. Resulting cell-free supernatants were stored at -20^{o}C prior to analysis by ELISA.

M1 and M2 MΦs showed a differential sensitivity to tolerisation. As this study has already shown, *E. coli* K12 LPS induces a significantly higher level of TNF-α in response to *E. coli* LPS compared to PG LPS in M1 MΦs (Fig. 3.2a). Whilst the induction of ET reduced the overall secretion of TNF-α, M1 MΦs proved somewhat resistant to tolerisation with *E. coli* LPS, equating to a 47% reduction compared to 65% in M2 MΦs (Fig 3.7a), PG LPS, despite the lower level of TNF-α induced by a single exposure, achieved 70% reduction in M1 MΦs, greater than that of *E. coli* LPS. M2 MΦs, however, which displayed an opposing sensitivity to a single stimulation in comparison to M1 MΦs achieved a 94% reduction in TNF-α (Fig. 3.7a).

IL-8 presented diametrically opposed results when tolerisation was induced with *E. coli* LPS between M1 and M2 subsets. Interestingly, *E. coli* LPS displayed a contrastingly different response in its ability to induce IL-8 secretion, with IL-8 production 84% lower in M2 MΦs than M1 MΦs (Fig. 3.2b). The ability of *E. coli*

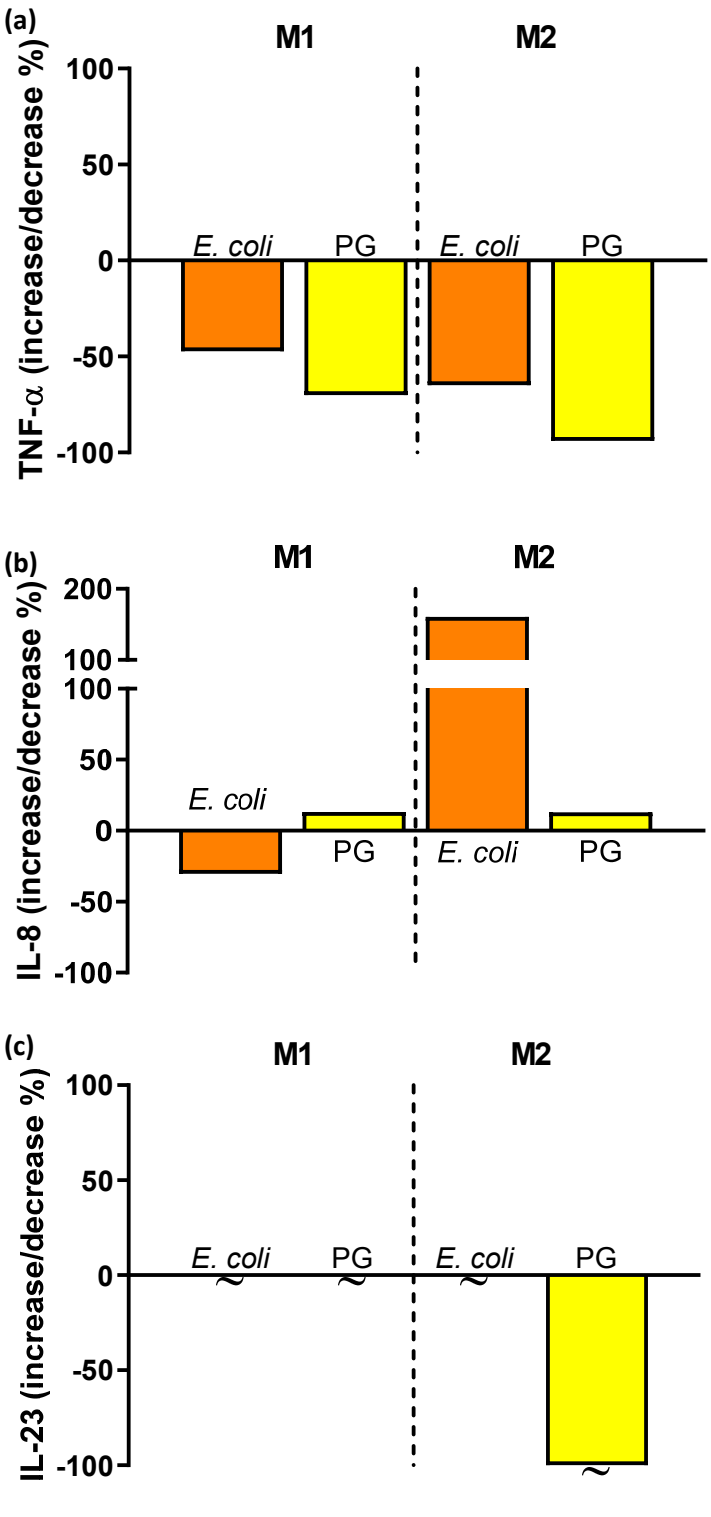

Figure 3.7 Tolerisation of inflammatory cytokine secretion induced by PG and *E. coli* LPS. Tolerisation was induced in M1 and M2 MΦs by exposing MΦs to either PG or *E. coli* LPS for 24 hrs prior to a secondary stimulation of 18 hrs. Results are indicated as a percentage increase or decrease compared to the positive control (stimulated). Experiments were performed in both technical and biological triplicates. Figures indicate results of 1 representative experiment.

~ – below the lower limit of detection of the assay (if no bar is present, cytokine was not significantly measured following initial stimulation measured).

LPS to tolerise IL-8 secretion, was markedly different between M1 and M2 MΦs, inducing a 30% reduction and 160% increase respectively. PG LPS, similarly, demonstrated a contrasting ability to induce IL-8 secretion – a 249% increase in M1 MΦs compared to M2Φs (Fig. 3.2b), yet the ability to induce tolerisation of IL-

8 (or lack thereof), was found to be insignificant with both M1 and M2 MΦs demonstrating a 13% increase in both subsets (Fig. 3.7b).

Induction of IL-23 secretion was notable as it was only observed in M2 MΦs in response to PG LPS (Fig. 3.2c). Equally notable was the ability repeated exposure to PG LPS to totally supress IL-23 secretion to a level below the lower limit of detection of the assay (Fig. 3.7c).

3.3.5 Differential sensitivity to endotoxin tolerisation of inflammatory cytokines in M1 and M2 MΦs by specific LPS isoforms.

The commercially available PG LPS isoforms used which demonstrated a differential ability to stimulate MΦ subsets in section 3.3.2 were used in a preliminary investigation to assess responses to repeated exposure. As a preliminary, exploratory investigation, a reduced concentration was used for the secondary stimulation. However, subsequent mass spectrometry of following batches of PG LPS isoforms indicated peaks below the 1000m/z level, as such it was deemed that the production and isolation method was no longer reliable and further experiments were not possible. As biological repeats were not performed, these results should be treated with caution but are included notably contrasting results are observed. Differentiated M1 and M2 MΦs were each sensitised by exposure to titrated concentrations of either PG LPS_{1690} or PG LPS_{1435} for 24 hours prior to two changes of R10 and subsequent re-stimulation for 18 hours. Cross exposure was also performed with the aim of analysing the effect of switching isoform from one to another. The resulting cell-free supernatants were drawn and stored at -20^{o}C prior to analysis by ELISA.

MΦs both sensitised and subsequently stimulated with PG LPS_{1435} (Fig. 3.8a) displayed remarkably opposing results. In M1 MΦs, sensitising at a concentration of 0.01 μg/ml, TNF-α secretion reduced below the level of detection, whereas concentrations at 0.1 and 1.0 μg/ml resulted in a 64.8% and 73.6% reduction respectively. In M2 MΦs this trend was reversed - 0.1 and 1.0 μg/ml sensitising concentrations ablated TNF-α secretion, whereas 0.01 μg/ml only achieved a 55.6% reduction.

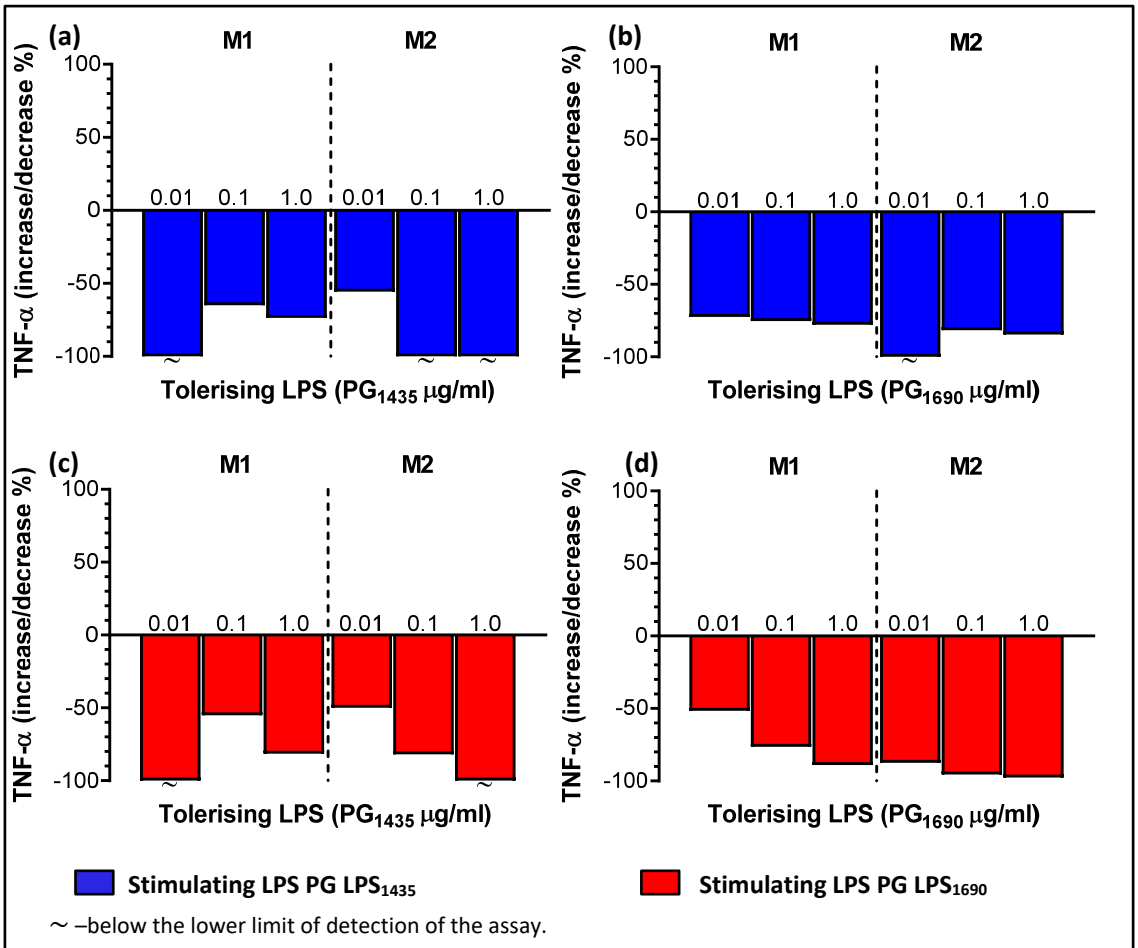

Figure 3.8 Preliminary investigation into the ability of PG LPS isoforms to tolerise TNF-α secretion. M1 and M2 MΦs were sensitized with either PG LPS_{1435} or PG LPS_{1690} for 24 hours at concentrations of 0.01, 0.1 and 1.0 μg/ml, then subsequently stimulated with either PG LPS_{1435} or PG LPS_{1690} for 18 hours. Results are indicated as a percentage increase or decrease compared to the positive control (stimulated). Data is preliminary where experiments where performed in technical duplicates but were not biologically repeated.

When M1 and M2 MΦs where both sensitised and subsequently stimulated with PG LPS_{1690} (Fig. 3.8d) a typical titrated response as one might have expected previously was observed, with M1 MΦs appearing more resistant to tolerisation of TNF-α secretion with 51.5% (0.01), 76.5% (0.1) and 99% (1.0 μg/ml) reductions and 87.5% (0.01), 95.5% (0.1) and 97.5% (1.0 μg/ml) reductions by M2 MΦs.

When the protocol was modified to assess the effect of switching isoforms, again the results were remarkably contrasting. When sensitised with PG LPS_{1690} and stimulated with PG LPS_{1435} (Fig. 3.8b), M1 MΦs demonstrated a relatively uniform and resistant response to tolerisation compared to M2 MΦs. All three

sensitising stimulations produced a similar level of suppression 72.3% (0.01) 75.2% (0.1) and 77.7% (1.0 μg/ml). M2 MΦs display a profile similar to that of M1 MΦs tolerised with PG LPS_{1435}. A sensitising concentration at 0.01 μg/ml ablates TNF-α secretion and the concentrations of 0.1 and 1.0 μg/ml reduce TNF-α secretion albeit by an 81.6% and 84.6% reduction, respectively.

When sensitised with PG LPS_{1435} and stimulated with PG LPS_{1690} (Fig. 3.8c) the response observed in M1 and M2 MΦs was again, noticeably contrasting. In M1 MΦs, a sensitising concentration of 0.01 μg/ml reduced TNF-α secretion below the lower limit of detection whilst conversely this was observed in M2 MΦs sensitised at 1.0 μg/ml.

IL-8 measured in the response to tolerisation protocols produced data which whilst interesting, somewhat conflicts the resistance to tolerisation observed earlier in MΦs exposed to the same protocol using PG and *E. coli* LPS. MΦs both sensitized and subsequently stimulated with PG LPS_{1435} (Fig. 3.9a), again performs differently in its ability to induce tolerisation, dependent upon subset. M1 MΦs demonstrated the least variation in response to a sensitising exposure, at with an increase of 10.1% observed at 0.01 μg/ml and reductions of 16.3% at 0.1 μg/ml and 44% at 1.0 μg/ml. M2 MΦs, however, reduced IL-8 secretion in response to both 0.1 and 1.0 μg/ml sensitisations (74.5% and 71.8% respectively), whilst a concentration at 0.01 μg/ml proved ineffective at inducing a tolerised state.

When M1 and M2 MΦs where both sensitised and subsequently stimulated with PG LPS_{1690} (Fig. 3.9d) the most effective tolerisation of IL-8 secretion was

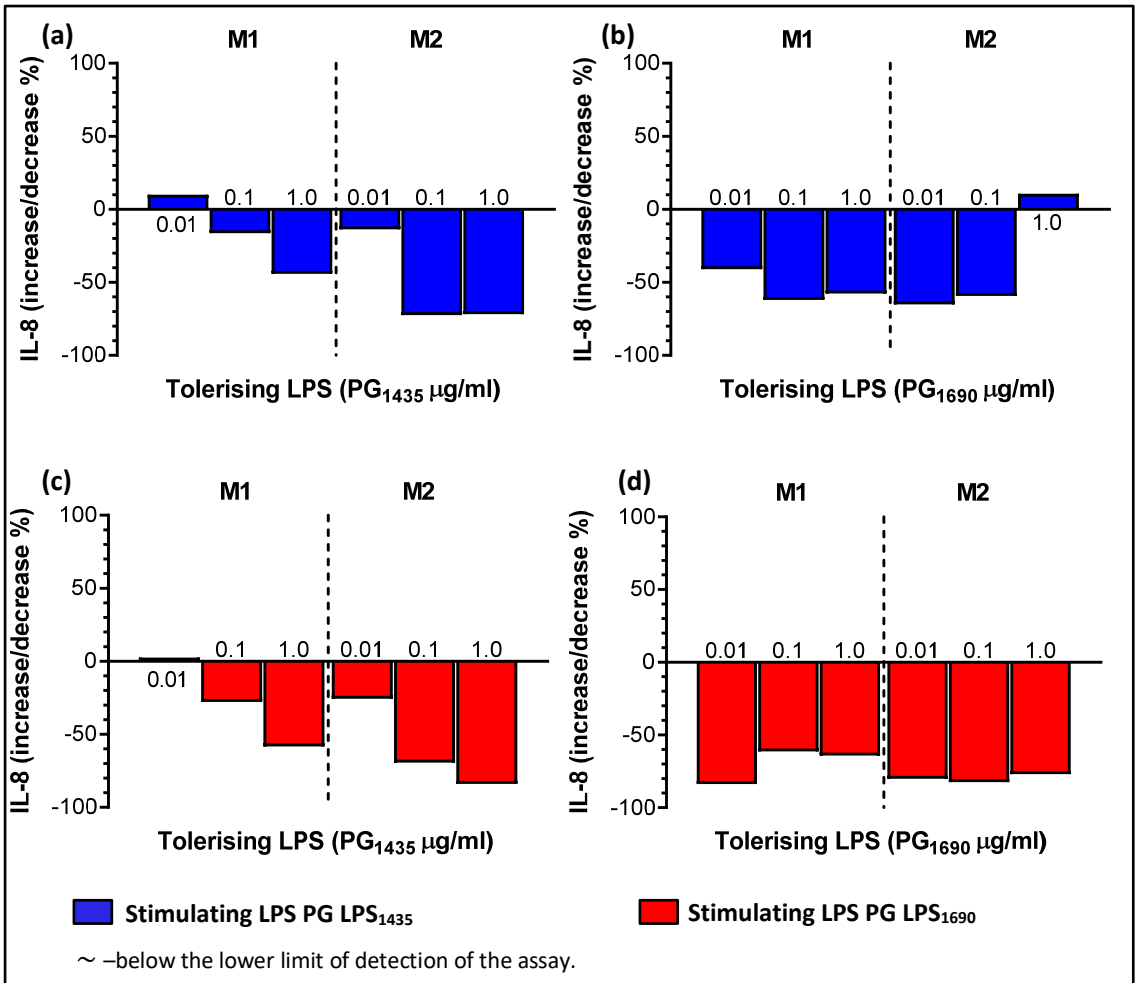

~ –below the lower limit of detection of the assay.

Figure 3.9 Preliminary investigation into the ability of PG LPS isoforms to tolerise IL-8 secretion. M1 and M2 MΦs were sensitized with either PG LPS_{1435} or PG LPS_{1690} for 24 hours at concentrations of 0.01, 0.1 and 1.0 μg/ml, then subsequently stimulated with either PG LPS_{1435} or PG LPS_{1690} for 18 hours. Supernatants were collected and IL-8 was measured by ELISA. Data is preliminary where experiments where performed in technical duplicates but were not biologically repeated.

observed, affecting both MΦ subsets. In M1 MΦs tolerisation was most effective at a concentration of 0.01 μg/ml, corresponding to an 83.7% reduction whereas 0.1 and 1.0 μg/ml concentrations achieved a 61.3% and 64.1% reduction respectively. Less variation was observed in M2 MΦs demonstrating, 80.1% (0.01), 82.4% (0.1) and 77% (1.0 μg/ml) reductions.

When sensitised with PG LPS_{1690} and stimulated with PG LPS_{1435} (Fig. 3.9b) M1 MΦs behave in a similar way to that previously observed in M1 MΦs tolerised using *E. coli* LPS (Fig. 3.7). Moderate levels of reduction were induced by all sensitising concentrations, with 0.1 and 1.0 μg/ml, resulting in 62% and 57.7%

respectively and 41% for 0.01 μg/ml. M2 MΦs demonstrated a similar response when sensitised at 0.01 (65.2%) and 0.1 μg/ml (59.2), yet when the sensitising concentration was increased to 1.0 μg/ml, a small 10.8% increase was observed.

When sensitised with PG LPS_{1435} and stimulated with PG LPS_{1690}, (Fig. 3.9c) a remarkably similar response is observed to that induced in M1 and M2 MΦs when TNF-α secretion was measured, albeit at a lower amplitude. Tolerisation was shown to increase with sensitising concentration with 1.0 μg/ml achieving a 58.3% reduction in M1 MΦs and an 83.9% reduction in M2 MΦs.

3.3.6 Inflammatory cytokine response to pooled LPS isolated from subgingival plaque.

LPS isolated from patients recruited to the study and characterised in chapter 2 was pooled to represent the three classifications from which they were recruited; Healthy (H), those with chronic periodontal disease (CP) and those who had received standard forms of dental therapeutic treatment (T). M1 and M2 MΦs were stimulated for a period of 18 hours with these pooled LPS samples at a concentration of 50 µl/ml. Cell-free supernatants were collected and stored at -20^{o}C prior to analysis by ELISA.

In MΦs stimulated with LPS pooled from either healthy patients or those with periodontal disease, the secretion of TNF-α was shown to be induced significantly higher in M2 MΦs than M1 MΦs (healthy – $p<0.05$, diseased – $p<0.005$). As seen previously, when observing individual patient derived LPS, the LPS from diseased patients was significantly higher than the other two groups (Fig. 3.10a).

M1 MΦs remained the optimum producers in IL-8 for both, and in particular those treated with LPS isolated from the diseased group, whereby IL-8 secretion was 2.4-fold higher in M1 MΦs compared to M2 MΦs (Fig. 3.10b).

As observed when stimulated with proprietary PG LPS, M2 MΦs were the only consistently significant producers of IL-23. LPS from both the healthy and diseased groups significantly stimulated production of IL-23 in M2 MΦs (Fig. 3.10c).

The measurement of IL-10 and IL-12 did not indicate consistent significant production above the lower limit of detection (refer to table 3.1).

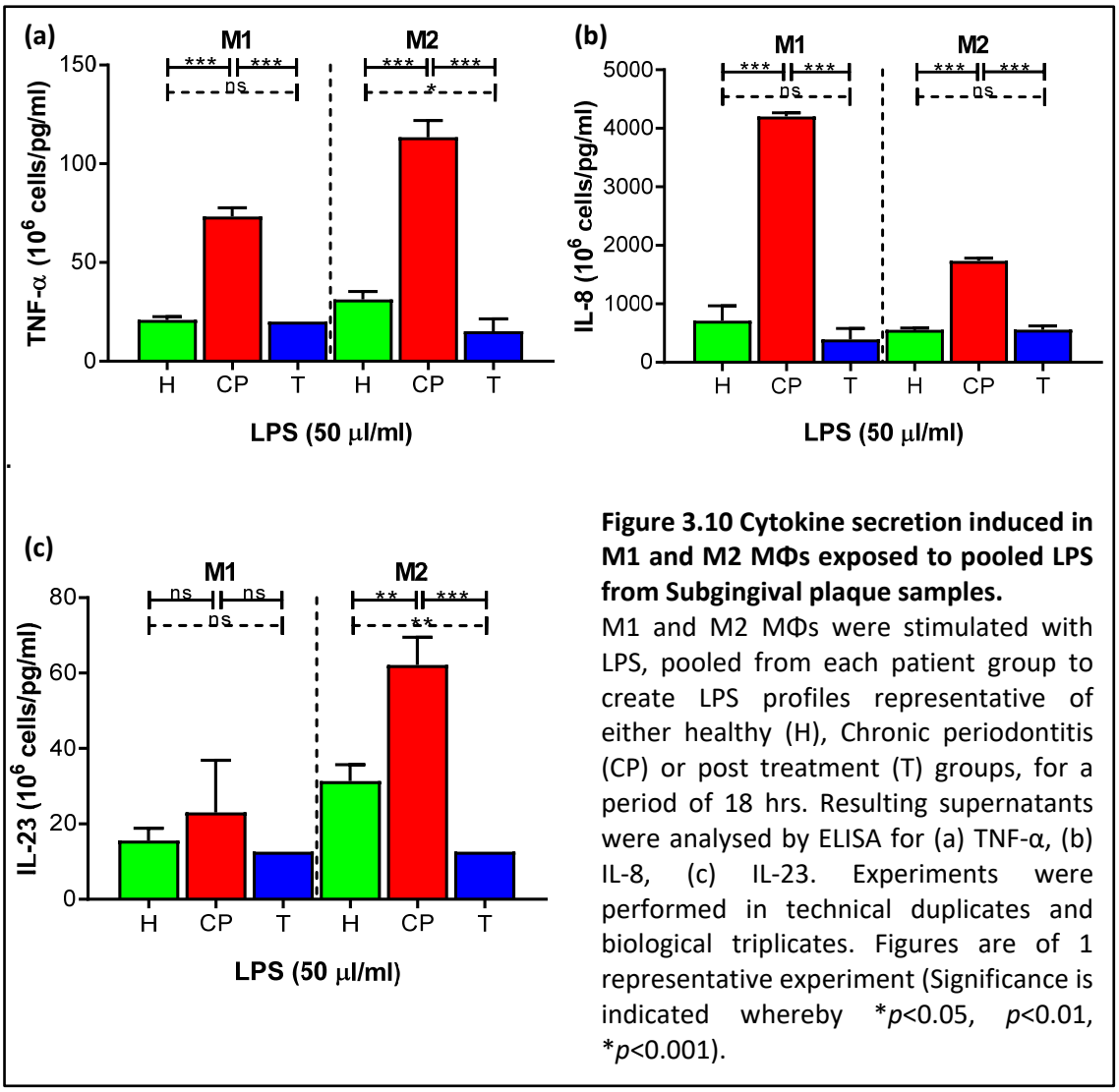

Figure 3.10 Cytokine secretion induced in M1 and M2 MΦs exposed to pooled LPS from Subgingival plaque samples.

M1 and M2 MΦs were stimulated with LPS, pooled from each patient group to create LPS profiles representative of either healthy (H), Chronic periodontitis (CP) or post treatment (T) groups, for a period of 18 hrs. Resulting supernatants were analysed by ELISA for (a) TNF-α, (b) IL-8, (c) IL-23. Experiments were performed in technical duplicates and biological triplicates. Figures are of 1 representative experiment (Significance is indicated whereby *p<0.05, p<0.01, *p<0.001).

3.3.7 Induction of endotoxin tolerance in response to pooled LPS isolated from subgingival plaque.

Pooled LPS was used to induce tolerisation in M1 and M2 MΦs to assess the effect of repeat exposures to clinically derived LPS isolates. To examine the potential effect on disease state homo- and hetero-tolerisation was performed by sensitising with one isolate and tolerising with another.

Although suppression of TNF-α is observed, M1 MΦs once again demonstrated a resistance to tolerisation, in comparison with M2 MΦs. The M1 MΦ response to repeated exposure to LPS from the healthy group instigated a 61.7% reduction in TNF-α secretion and a 69.8% reduction in those exposed twice to LPS from the CP group. Hetero-tolerisation exerted minimal variation on M1 MΦs stimulated with LPS from the diseased when alternatively, sensitised with LPS from the healthy group, a similar reduction of 73.4%. In M1 MΦs stimulated with LPS from the healthy group, whilst sensitised by that from the CP group, this cross exposure extended to a 79.7% reduction in TNF-a secretion (Fig. 3.11a).

M2 MΦs again indicated a contrasting tendency to tolerisation whereby the largest reduction in TNF-a secretion below the lower limit of detection of the assay in each of the H, CP and T groups. Hetero-tolerisation however, resulted in reductions in the range of those observed in M1 MΦs, with M2 MΦs stimulated with LPS from the diseased group (and sensitized with LPS from the healthy group developing a 71.6% reduction and the reverse, a 70.5% reduction (Fig. 3.11a).

IL-8 demonstrated a considerable resistance to tolerisation and in a number of cases, demonstrated a substantial increase in IL-8 secretion in response to the

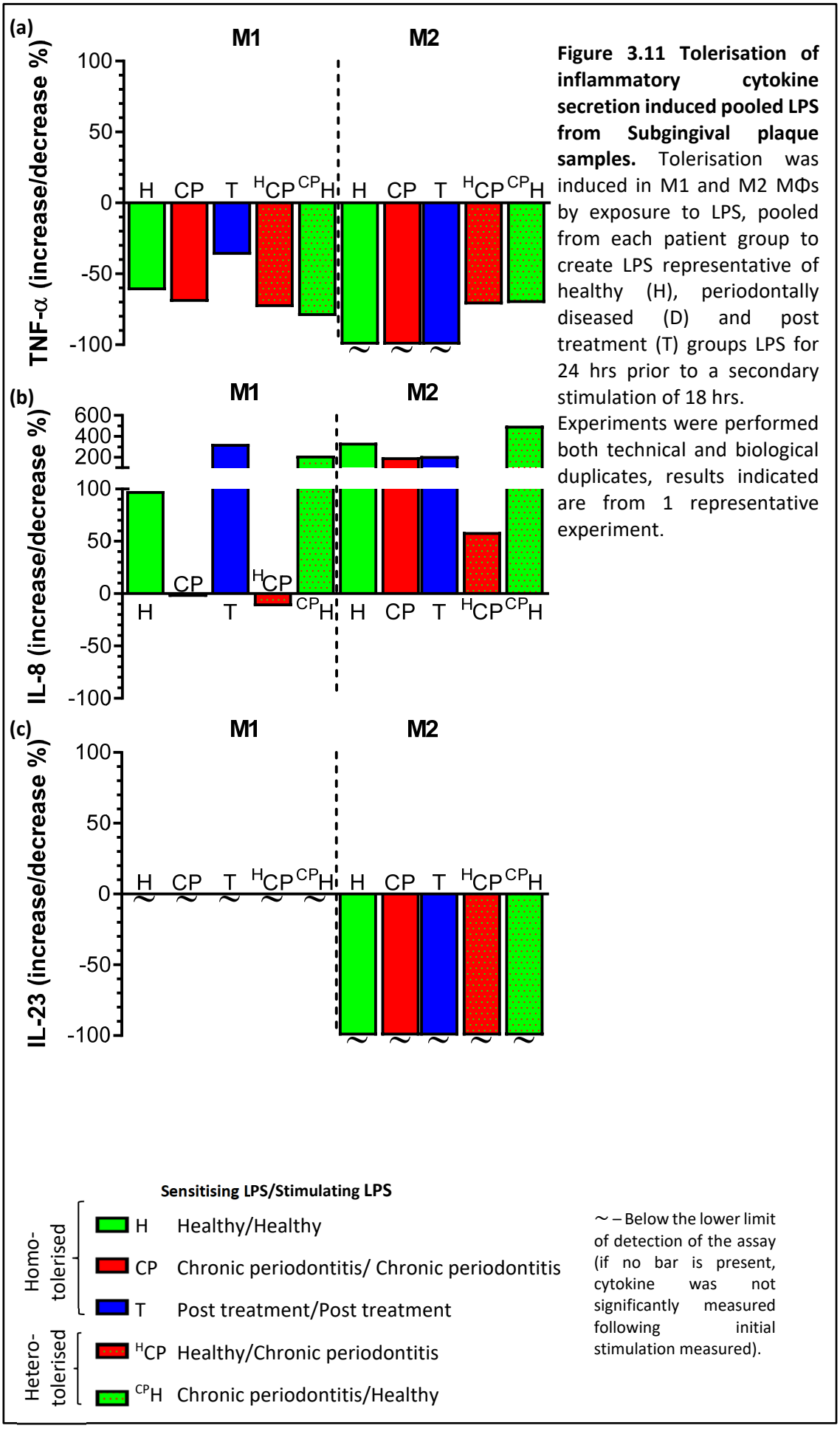

Figure 3.11 Tolerisation of inflammatory cytokine secretion induced pooled LPS from Subgingival plaque samples. Tolerisation was induced in M1 and M2 MΦs by exposure to LPS, pooled from each patient group to create LPS representative of healthy (H), periodontally diseased (D) and post treatment (T) groups LPS for 24 hrs prior to a secondary stimulation of 18 hrs. Experiments were performed both technical and biological duplicates, results indicated are from 1 representative experiment.

secondary stimulus (Fig. 3.11b). No form of sensitisation was effective at reducing IL-8 secretion significantly in either M1 or M2 MΦs. Sensitisation and stimulation with LPS pooled from the healthy group induced a 98% increase in M1 MΦs and a 340.9% increase in M2 MΦs. When performed with LPS from the diseased group, M1 MΦs remained largely unchanged compared to the stimulated level (3% decrease). M2 MΦs however, saw 201.3% increase in IL-8 secretion when exposed twice to LPS from the CP group. Of particular interest was the induction of IL-8 in response to sensitising and stimulating with LPS from patients who had undergone therapeutic treatment. Having demonstrated to have a relatively low inflammatory potential when assessing TNF-α, IL-8 and IL-23, following a single naïve stimulation, IL-8 secretion was augmented in response to a secondary stimulation – 328.6% in M1 MΦs and 210.5% M2 MΦs. Also, of additional interest was the observations made when hetero-tolerisation was performed. Both subsets of MΦ demonstrated a low to moderate response to sensitisation with LPS from the healthy group when stimulated with LPS from the CP group, with M2 MΦs 58.8% increase. When this stimulation protocol was reversed to incorporate sensitisation with LPS from the CP group and stimulation from the healthy group, considerable increases were observed in both subsets. M1 MΦs demonstrated a 215.7% increase in IL-8 pro production, whilst M2 MΦs demonstrated 501% increase.

IL-23 demonstrated to be the cytokine tested which presented the highest sensitivity to tolerisation (Fig. 3.11c). Having been shown to be induced in response to LPS from both the healthy and CP group, this production was ablated, below the lower limit of detection, regardless of the origin of LPS.

3.4 Discussion

As indicated in chapter 1 there has been a number of studies which present data regarding the ability of LPS isolated from PG to both induce and tolerise inflammatory mediators produced by MΦs, some of which conflict with the results indicated within this chapter (Martin et al., 2001; Diya et al., 2008; Pena et al., 2011; Foey & Crean 2013; Rajaiah et al., 2013 Al-shaghdali et al., 2019). Studies examining *E. coli* derived LPS are, in general more stable in the scope of their findings, which likely reflects the stability of lipid-A composition homogeneity (Steimle et al., 2016). That said, even *E. coli* is suggested to modify its lipid-A structure under certain conditions and minor modifications affecting phosphorylation are indicated to occur in one-third of wild-type *E. coli* K12 populations (Zhou et al., 1999; Lamarche et al., 2008; Larrouy-Maumus et al., 2016). Discrepancies between studies utilising proprietary PG LPS may of course be attributed to the ability of PG to modify its lipid-A structure, meaning that commercially available LPS (often used in such studies) may contain a variation of lipid-A structures. This study has demonstrated this in figure 2.6/7 of chapter 2, whereby mass spectrometry of lipid-A isolated from proprietary LPS produced a number of peaks, indicating various lipid-A moieties with varying levels of acylation and phosphorylation. The LPS from which lipid-A was isolated for analysis by ESI mass spectrometry was the same as that which was used to throughout this chapter. Examining these peaks further indicate a predominance of under acylated and under phosphorylated moieties with the majority of *m/z* ratios falling between 1215 and 1464 with two other clusters at 1567 – 1608 and 1663 – 1719 and a further single peak at 1770 *m/z* (Fig. 2.6).

When the ability of PG LPS to induce TNF-α secretion on M1 and M2 MΦs was assessed, it was found that PG demonstrated a significantly diminished ability to induce secretion in M1 MΦs compared to that of *E. coli*. Whereas M2 MΦs were stimulated to secrete TNF-α significantly higher than that induced by *E. coli* LPS or PG LPS in M1 MΦs (Fig. 3.2). When this is considered in conjunction with the nature of PG LPS isoforms; PG LPS_{1690} and PG LPS_{1435}, to induce TNF-α in MΦ subsets (Fig. 3.3), the observation can be made that supports the suggestion that M2 MΦs are more susceptible to stimulation by lipid-A moieties with lower *m/z* ratios. This, when considered along with the relevance of haem concentration affecting lipid-A modification (refer to section 1.5.2, chapter 1), and an increase in inflammation leading to an increase in haem availability, implicates the local MΦ subset population in affecting PG survival and immunogenicity. Furthermore, whilst M1 MΦs remained the prominent producers of IL-8, PG LPS again was able to significantly stimulate IL-8 secretion above that induced by *E. coli* in M2 MΦs. (Fig. 3.2). LPS pooled from patient groups behaved in a remarkably similar manor; both the healthy and diseased derived LPS induced higher levels of TNF-α when compared to their corresponding M1 MΦs (Fig. 3.10). This somewhat conflicts with the results obtained from LPS derived isolated from individual patients (Fig. 2.9, chapter 2). The preliminary investigation which analysed the ability of PG LPS isoforms to induce ET may serve to elucidate the reason for this. Again, the proprietary PG LPS behaved in a generally similar fashion to that of the patient groups when ET was induced in M1 and M2 MΦs, whereby TNF-α was able to be suppressed to a degree in M1, and more so in M2 MΦs, whereas IL-8 was not. When ET was induced using specific PG LPS isoforms, notable differences were observed compared to the results obtained when using either

PG or patient derived LPS. M1 MΦs tended do display a resistance to tolerisation of TNF-α secretion regardless of the isoform used to instigate ET, a result observed by Foey and Crean (2013). A notable anomaly to this was the ability of the PG LPS_{1435} isoform to induce tolerisation when a low concentration of sensitising stimulus was used, leading to total ablation of TNF-α secretion. M2 MΦs however, were considerably more sensitive to suppressing TNF-α secretion when ET was induced, although, again, the amplitude of reduction varied dependent upon sensitising concentration (Fig. 3.8). The most marked result observed when inducing ET using specific LPS isoforms was that of the ability to suppress IL-8 secretion (Fig. 3.9). Both isoforms were able to supress IL-8 secretion in both subsets at most concentrations, a function noticeably absent when ET is induced using PG or patient derived LPS. Whilst this experiment should be viewed with caution due to the lack of repeat experiments it may indicate the importance of considering the overall lipid-A profile in its entirety. As this study has demonstrated in chapter 2, LPS obtained from subgingival biofilms contains a number of lipid-A structures, as does commercially available PG LPS. It is possible, therefore that the contrasting results observed when using PG or patient derived LPS compared to specific LPS isoforms may be due to the cumulative effect of a combination of LPS structures in concert to elicit an effect which differs from that obtained when using a single, specific isoform. The contrasting variations observed when sensitising concentration is altered, may also highlight the importance of relative quantities of LPS structures within an LPS profile. This may also serve to explain the reduction in TNF-α amplitude observed when stimulated with pooled patient samples, in that by pooling these samples, the relative composition within these samples may have been shifted to alter the overall immunogenic effect on M1 MΦs. This finding serves to highlight

the importance of analysing patient specific profiles to determine potential disease susceptibility and aid diagnosis and treatment.

In addition to the above was the contrasting data provided which shows secretion of IL-23 induced by PG LPS but not *E. coli* LPS in M2 MΦs (Fig. 3.2c). This subset dependent response was also observed in M2 MΦs stimulated with LPS from either the healthy or disease group (Fig. 3.10c). Most commonly associated with Th_{17} differentiation, IL-23 appears to work in concert with a number of additional signals, including IL-6, TGF-β and IL-1β to drive T-helper cells towards a Th_{17} subset (Revu *et al.*, 2018; Stritesky, Yeh & Kaplan, 2008; Tristao *et al.*, 2017). Whilst the specific mechanisms and requirement for components signalling molecules remains unclear, the requirement for the IL-23 complex to derive the specific Th_{17} subset, rather than the IL-12 driven Th_1 subset is consistently accepted (Aggarwal *et al.*, 2003; Girolomoni *et al.*, 2017; Oppmann *et al.*, 2000). Furthermore, since the identification of the Th_{17} phenotype, a number of pathologies, particularly auto-immune diseases have been attributed to abnormalities in the Th_{17} driven response (Girolomoni *et al.*, 2017; Harbour *et al.*, 2015; Moutsopoulos *et al.*, 2012). Regulated Th_{17} immune associated response, instigates the production of antimicrobial peptides and pro-inflammatory cytokines by other immune and tissue resident cells to combat bacterial infection (Revu et al., 2018). Conversely, dysregulation of the Th_{17} associated immune response has been proposed as one of the driving mechanisms of CP (Hajishengallis, 2014). IL-23 also demonstrated that it was susceptible to tolerisation due to repetitive exposure to PG LPS or patient derived LPS. This may also be expected as tolerisation is generally regarded as a suppression of pro-inflammatory molecules in response to repeated exposure to endotoxin.

As previously discussed, IL-8 however, is resistant to tolerisation by repeated exposure to PG LPS and demonstrates a response which increases with secondary stimulation. Neutrophils, the front line of the innate immune defence form the majority of leukocyte populations and as such they have been associated with the formation of CP for a number of years (Zaric et al., 2010). Tissue isolated from individuals exhibiting CP, demonstrates significantly increased levels of neutrophil infiltration into the gingival tissues. IL-8, as a primary neutrophil chemoattractant and activator is therefore suspected to play a significant role in disease instigation and progression (Schutyser *et al.*, 2002; Van Damme *et al.*, 1990). Granulocyte-colony stimulating factor (G-CSF) is considered to be the primary regulator of neutrophil and progenitor proliferation, maturation and release within bone marrow (Bajrami et al., 2016). Of particular significance to this study, is the ability of IL-17 to up-regulate G-CSF production in fibroblasts, structural cells, abundant in periodontal tissues and pivotal in tissue repair. The role that this mechanism may play in chronic periodontal diseases has been proposed by Cortés-Vieyra, Rosales and Uribe-Querol (2016). They propose a feedback loop mechanism which leads to the constant proliferation and mobilisation of neutrophils at sites of chronic inflammation. They have also highlighted the role played by MΦs in the production of IL-23, a function which is supressed by the phagocytosis of apoptotic neutrophils. What is imminently noticeable about this model is the MΦ as the source of IL-23 and the potential effect that disruption to this regulation of MΦ derived IL-23 may have on chronic inflammation, both in its instigation and progression.

Chapter 4

Proteomic analysis of MΦ responses to PG LPS stimulation and tolerisation.

4.1 Introduction

The findings presented within this study have demonstrated that the induction of inflammatory responses and subsequent tolerisation of those responses in macrophages utilising LPS as a stimulus is open to substantial variation. PG LPS was shown to significantly differ in its ability to both induce and tolerise key cytokines when compared with canonical *E. coli* LPS. A number of questions arise when analysing the data observed in MΦs exposed to either PG LPS or patient derived LPS. Firstly, why are M2 MΦs more responsive to stimulation with PG LPS than *E. coli* LPS? TNF-α, IL-8 and in particular, IL-23 were all secreted at significantly higher levels when stimulated with PG LPS compared to *E. coli* LPS. Secondly, as the origin of the stimulus remain the same, at what point do the signalling mechanisms which result in TNF-α and IL-8 production diverge, resulting in the suppression of TNF-α when tolerisation is induced, but not IL-8? Thirdly, what is the potential role that the production of IL-23 may play in the instigation and progression of periodontal disease given that it was observed to be produced by M2 MΦs, regarded as the generally homeostatic/regulatory subset? Finally, to what degree is the element of plasticity relevant to interpreting ET? MΦs stimulated with pure PG LPS isoforms seem to support the possibility that there is an element of plasticity, both morphologically and characteristically.

It should not be underestimated how difficult these questions would be to answer using traditional molecular biological techniques. Identifying the signalling mechanisms which determine tolerisation of TNF-α but not IL-8 would require analysing a number of signalling cascades, negative regulators, knock-on effects due to levels of redundancy as well as numerous transcription factors. Using traditional methods, such as Western blot, PCR and ELISA would allow for the

analysis of specific signalling molecules, but are all susceptible to variation in the interpretation of linkage between message, transcription and secretion, due to the kinetics of each process and the time points chosen for each methodology. Furthermore, these methods (in the traditional sense) examine one analyte at a time and are therefore both time consuming and expensive and more importantly, not representative of an overall biological systemic state.

Liquid chromatography–mass spectrometry (LC-MS) has been successfully used to characterize complex matrices such as human blood, serum and tissue (Adkins et al., 2002. Khatib-Shahidi et al., 2006. Such-Sammartin et al., 2015.). In this process, proteins are isolated, refined and analysed to determine the mass/charge ratio to reveal protein-peptide characteristics. Subsequent bioinformatics analysis allows for the identification and quantification of proteins from the initial peptides, allowing for the determination of relative protein production/expression. A significant addition to the interpretation of this data is due to the data mining now possible due to the abundance of online databases which cross reference a number of resources to determine linkage and associations. Databases such as KEGG, Reactome and BioCarta are pathway orientated and assess lists of proteins for metabolism and signalling interactions. Furthermore, the Database for Annotation, Visualization and Integrated Discovery (DAVID) bioinformatics resources incorporate these databases to allow for multiple analyses and combine it with statistical analysis and functionality for gene ontology and protein interaction.

To determine the status of M1 and M2 MΦs in the stimulated and tolerised state, compared to that of a basal level, it was decided that a whole cell proteomic approach would be adopted. Whilst not an endpoint to define specific molecular

signalling events, proteomic analysis would provide a “snapshot” of the overall proteome status following stimulation and tolerisation. When compared to specific isoforms of PG LPS, the commercially available PG LPS was shown to more closely resemble the inflammatory potential demonstrated by LPS isolated form patients recruited to the study reported on in chapter 2. This may be due to the heterogenic composition of commercial PG LPS, something which has been demonstrated in LPS isolated from subgingival biofilms. As such, to evaluate the status of the cellular system in the basal, stimulated and tolerised state, whole cell proteomic analysis was carried out on M1 and M2 MΦs stimulated and/or tolerised using PG LPS with the compositional profile identified in figure 2.6/7a.

4.2 Materials and methods

A full list of buffers and reagents is provided in appendix A.

A list of Protein abbreviations is provided in appendix B.

For supplemental figures see appendix D

4.2.1 Differentiation of THP-1 derived M1 and M2 MΦs.

THP1 cell maintenance and culture was adhered to as indicated in section 2.3.9.1. Cells were cultured in T75 flasks, duplicate flasks were used and combined to generate a single sample for proteomic analysis, for each stimulatory state; unstimulated (US), stimulated (ST) and tolerised (TL). These experiments were repeated to create technical triplicates.

4.2.2 Stimulation and tolerisation of M1 and M2 MΦs

Cells undergoing tolerisation were incubated for a period of 24 hours in media containing PG LPS at a concentration of 1 μg/ml. Stimulated cells were cultured for 24 hours in R10. All cells were washed in fresh media twice prior to stimulation. Both sets of cells, those to be tolerised and stimulated were incubated in R10 containing PG LPS at a concentration of 1 μg/ml for a period of 18 hours. Supernatants were drawn off and stored at -20^{o}C prior to analysis by ELISA.

4.2.3 Analysis of cytokine secretion

To verify the induction of endotoxin tolerance and cellular responses as observed previously, TNF-α and IL-8 release was quantified. For ELISA protocol, refer to section 2.3.11. Results were consistent with previous observations indicated in figures 3.2 and 3.7 (Fig. 4.1).

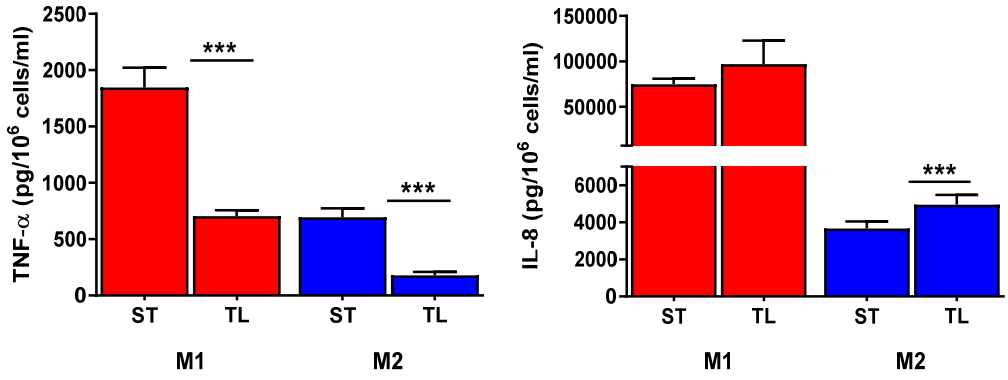

Figure 4.1. Verification of induction of endotoxin tolerance by ELISA. TNF-α and IL-8 production was measured for each replicate to ensure the both the induction of endotoxin tolerance (TNF-α) and similar cellular responses to previous experiments (IL-8). Figure demonstrates results from one experiment where technical triplicate and biological duplicates were performed. Statistical significance indicated where $p > 0.001$***.

4.2.4 Isolation of cellular proteins

Cells were washed twice in ice cold DPBS and spun in a centrifuge for 5 minutes at 2500g, the resulting pellet was resuspended in 250 µl of RIPA buffer (Thermofisher, Loughborough, UK) containing protease Cocktail Inhibitor (Roche, Sigma Aldrich, Dorset, UK) and a pipettor was used to thoroughly mix the samples. A sonic probe was used to disrupt cell membranes, twice for 20 seconds, at 50% pulse, on ice. Samples were then mixed for 15 minutes on ice prior to centrifugation at 15000g for 15 minutes. Supernatants were drawn and stored at -80^{o}C.

4.2.5 Protein yield quantification

Total protein concentration for each sample was calculated by BCA Assay (see supplementary figure S10 for standard curve). A proprietary BCA kit was used (Pierce, Thermofisher, Loughborough, UK) and was used in line with the manufacturer's recommendations, however this was optimised to reduce the amount of sample usage and adapted for the likely amount of yield. Briefly; Standards were created by creating dilutions of provided BSA in RIPA buffer from

2.5 μg/ml to 200 μg/ml. Samples were diluted 1/50 (previously optimised to bring within range of detection of assay, not shown) and added in conjunction with the standards to a 96 well microplate in 100 μl aliquots. Working reagents were prepared as per the manufacturers recommended protocol and added to each well in 100 μl aliquots. The plate was incubated for 2 hours at 37°C prior to being cooled and read at 562 nm using a POLARstar omega spectrophotometer (BMG Labtech GmbH, Ortenberg, Germany). Subsequent statistical analysis was performed using GraphPad Software version 7, San Diego, CA.

4.2.6 Verification of uniform protein extraction

Following quantification, verification of uniform protein extraction was performed by SDS-polyacrylamide gel electrophoresis. Acrylamide gels (10% w/v) were poured into a Bio-Rad Mini-PROTEAN Tetra casting system (Bio-Rad, Watford, UK). Sample proteins were diluted in Laemmli and loading buffer so as to achieve 10 μg of protein per well. Samples were boiled for 5 minutes at 100 °C prior to loading alongside a 10 – 250 kD Precision Plus All Blue protein ladder (Bio-Rad, Watford, UK) and running in a Bio-Rad Mini-PROTEAN Tetra Vertical Electrophoresis Cell at 120 V. Gels were subsequently stained in Coomassie Brilliant Blue G-250 (Pierce, Thermofisher, Loughborough, UK) for 45 minutes before de-staining overnight in methanol (Fisher Scientific, Loughborough, UK). This was performed twice to assess variations between lanes.

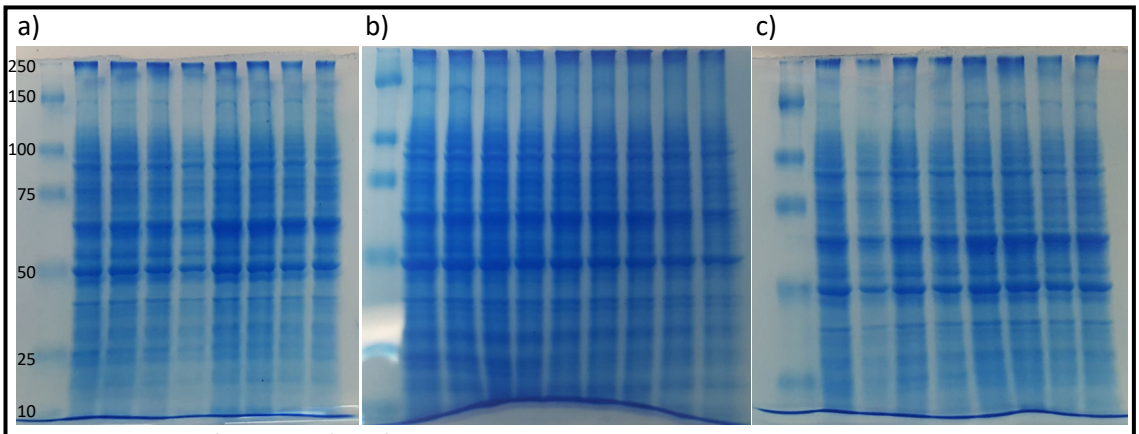

Figure 4.2. Verification of uniform protein isolation.
Confirmation of uniform protein extraction and protein yield quantification was performed by SDS-PAGE. One 10% acrylamide gel was run per technical replicate (a-c).

4.2.7 Protein purification, mass spectrometry and data handling

Purification was carried out under the guidance of Dr Vikram Sharma at the Proteomics Core Laboratory at the Derriford Research Facility, University of Plymouth. 50 μg of sample protein was digested using the filter aided sample preparation (FASP) method (Wisniewski et al., 2009). The resulting tryptic peptides underwent further purification by stage tip filtration (Rappsilber et al., 2003).

Liquid chromatography tandem mass spectrometry analysis was performed on the Orbitrap Velos Pro mass spectrometer (Thermo Fisher, Bremen, Germany) equipped with the Ultimate 3000 UPLC system (Thermo Fisher, Germany) by Dr Vikram Sharma using the method described by Zhou et al (2015). Protein identification at 1% false discovery rate (FDR) and label free quantification (LFQ) were performed using MaxQuant also by Dr Sharma.

4.2.8 Gene ontology (GO) and transcription factor binding site analysis

GO enrichment analyses proteins which demonstrated a 2-fold change in expression relative to MΦ subset and/or stimulation status were analysed using

the Database for Annotation Visualization and Integrated Discovery (DAVID, version 6.8. (http://david.abcc.ncifcrf.gov/). Enrichment of GO FAT terms were analysed with parameters set using an ease score of 0.1 and the Benjamini method. Results were deemed statistically significant where p-value <0.05 and a maximum of 50 terms were recorded for each data set. Transcription factor binding sites for inflammatory cytokines were determined using GeneHancer – the human database of regulatory elements and their target genes, part of the GeneCards Human Gene Database (http://genecards.org).

4.2.9 Graphical presentation

GO terms and transcription factor matrices were plotted using GraphPad version 7 (GraphPad, Dan Diego, USA). Protein heatmaps were compiled and produced using Heatmapper online Software (http://Heatmapper.ca) and all supplemental figures are found in appendix D.

4.2.10 Nomenclature

To standardise references to stimulatory status the following nomenclature will be used throughout:

	Unstimulated	Stimulated	Tolerized
Sensitizing Stimulus (LPS)	-	-	+
Primary Stimulus (LPS)	-	+	+
Nomenclature	US	ST	TL

4.2.11. Data analysis workflow

Label free quantification (LFQ) values were used to determine relative expression ratios of proteins. Relative expression was determined for the whole proteome (PS. Fig. PS1.1), response following stimulation (ST) (compared to the unstimulated response) (PS. Fig. PS1.3) and response following tolerisation (TL)

(compared to the stimulated response) (PS. Fig. PS1.11). For proteins which demonstrated a 2-fold change, gene ontology (GO) enrichment analysis of the responsive proteins were analysed using the Database for Annotation, Visualization and Integrated Discovery (DAVID) v6.8. Go terms were ranked by statistical significance with a threshold for significance set at a *p-value* of 0.05 to include a maximum of 50 terms. GO term enrichment was performed to analyse for biological process (BP), cellular component (CC) and molecular function (MF) (PS. Fig. PS1.2).

For the two stimulatory states, ST and TL, proteins were subsequently separated depending upon their direction of response i.e. increase (**M1**$^{\mathbf{ST}\uparrow}$ and **M2**$^{\mathbf{ST}\uparrow}$) or decrease (**M1**$^{\mathbf{ST}\downarrow}$ and **M2**$^{\mathbf{ST}\downarrow}$) and GO analysis was performed on each of these profiles.

It was apparent that within enrichment analysis for a set of proteins, multiple terms can be identified which carry similar functionality i.e. “Entry into host” and “Entry into host cell”, and to a wider degree, “interaction with host” as cumulative host/virus/pathogen interactions. Furthermore, the same term maybe identified in multiple analyses across different subsets and responses. To determine which genes are involved in each process and to examine the complex interaction. involved in each process, terms were grouped into associations and the data mapped into matrices demonstrating relative protein expression.

To attempt to investigate the potential impact that protein responses identified in this proteomic study may have on the production and secretion of these inflammtory mediators (such as those studied in chapter 3), the University of California, Santa Cruz Genomics Institute Transcription factor binding site database (UCSC_TFBS) function was utilised using the protein interaction

function within the DAVID Bioinformatic datatbase. Each of these was then cross-referenced with the transcription binding sites for each cytokine of interest using the Genehancer functionality of the Gene-cards suite. In addition, the EMBL-EBI IntAct database for molecular interaction was used to search for potential intracellular signalling molecules which may influence these transcription factor/binding site events as well as additional transcription factors.

Finally, relative expression of proteins was compared to examine the potential demonstration of plasticity between subsets, in that at a protein level, one subset may be manipulated to express that protein at a similar level to the other. To achieve this, original LFQs were compared for each stimulatory status of each subset. Then for each status, the three states of the opposing subsets were compared to determine which proteins were expressed within 95% of any state of the opposing subset.

Analytical workflow

PS refers to proteomic supplemental figures in appendix D which indicates full supporting data to support condensed figures which are indicated in this chapter.

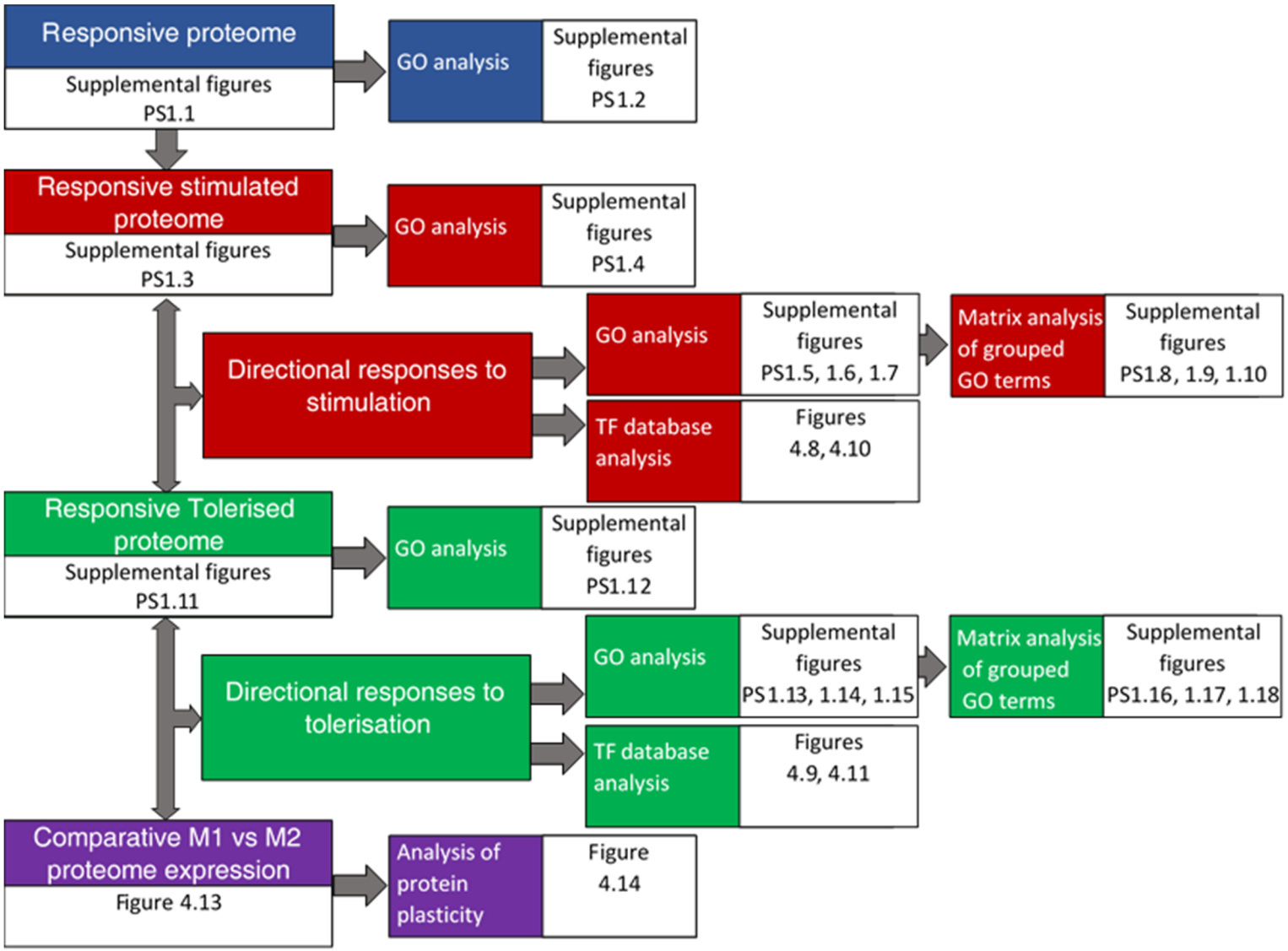

4.3 Results

4.3.1 GO analysis reveals differential methods of response to stimulation with PG LPS between MΦ subsets.

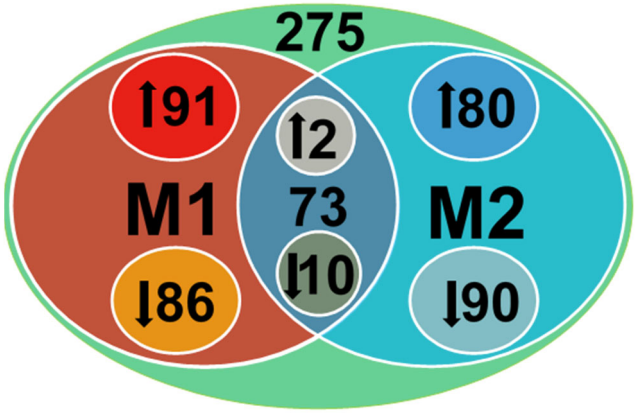

Figure 4.3. M1 and M2 MΦ proteome response to stimulation with PG LPS. 275 proteins were found to alter expression by a minimum of a 2-fold ratio compared with the unstimulated/basal level of expression, 177 in M1 MΦs and 170 in M2 MΦs. 91 proteins were shown to increase expression in M1 MΦs and 80 in M2 MΦs. 86 proteins decreased their expression in response to stimulation in M1 MΦs and 90 in M2 MΦs. 12 proteins were identified to respond in a similar nature in both subsets, 2 of these increasing in expression and 10 decreasing in expression, whilst the remainder responded differently.

A total proteome of 1039 proteins were identified from their peptides and of these 337 demonstrated a 2-fold change in expression in responsiveness to stimulation and/or tolerisation, 222 in M1 MΦs and 265 in M2 MΦs, with 115 proteins which were responsive in both subsets.

When this was analysed further dependent upon the direction of response to stimulation (in comparison to the basal, unstimulated level), only 13 proteins in both M1 and M2 MΦs responded in a similar direction (Fig. 4.3)

Following GO analysis, the resulting data was compiled to create figures 4.4 and 4.5. GO terms and transcription factors associated with each stimulatory state for each MΦ subset is illustrated where the size of each representative symbol indicates the relative numbers of terms identified within that group. For

comprehensive supporting supplemental data see appendix D for proteomic supplemental (PS) figures.

Within figures 4.4 and 4.5 a number of interesting groups appear which may indicate significant changes in MΦ biology in response to stimulation with PG LPS.

When enriched for biological process (PS. Fig. PS1.5a), terms connected to response to a stimulus where found in both subsets and in responses which both increased and decreased, although somewhat surprisingly, more so in $M1^{ST\downarrow}$ and $M2^{ST\uparrow}$. Terms associated with immune responses to stimulus (PS. Fig. PS1.8d) incorporate a wide array of proteins with varying functions. 2 terms refer to responses to cytokines and are both observed only in terms derived from the $M2^{ST\downarrow}$ dataset. Interestingly, terms referring to homeostatic process and innate/immune response are observed only in M1 MΦs but with homeostatic process enriched in proteins which increase and immune response in proteins which decrease in expression. RNS/ROS associated terms were restricted primarily to proteins which $M1^{ST\downarrow}$ only, with the only associated term in $M2^{ST\downarrow}$ being “organonitrogen compound catabolic process” (PS Fig. PS1.5b).

Processes which may be associated with epigenetic modification i.e. “DNA geometric change”, where also evident in $M1^{ST\downarrow}$ but also $M2^{ST\uparrow}$ (PS Fig. PS1.4a).There was however a subset of terms associated with the regulation of translation and transcription which were only associated with $M2^{ST\uparrow}$. When the protein profiles which contributed to each term were analysed (PS. Fig. PS1.8), within the DNA modification group (PS. Fig. PS1.8b), there is a prominent group of mini-chromosome maintenance proteins (MCM), this family of 6 proteins, MCM2-7, are all observed (an alias for MCM3 in HCC5) and are associated with

the majority of terms in this group. What is remarkable about this group of DNA helicases, is the diametrically opposing response in M1 MΦs compared to M2 MΦs when stimulated with PG LPS, whereby expression increases in M2 MΦs and reduces in M1 MΦs. Of the proteins identified to be associated with translation and transcription, a notable group is again evident. Eukaryotic initiation factors (EIF) are associated with the majority of terms due to their regulation of ribosome formation and elongation. When terms arising under cellular component were analysed, terms associated with DNA, epigenetic modification and translation (PS. Fig. PS1.9c) can be separated into 2 distinct groups, chromosomal associated and ribonucleoprotein associated terms which both occur in $M1^{ST\downarrow}$ and $M2^{ST\uparrow}$. Chromosomal associated protein profiles are dominated by MCM proteins as well as STAT1. When enriched for molecular function (PS. Fig. PS1.6), $M1^{ST\downarrow}$ and $M2^{ST\uparrow}$ profiles are dominated by terms which are associated with DNA binding and translation events (PS. Fig. PS1.10d), with terms referring to helicase activity, RNA binding, nucleoside/nucleotide binding, chromatin and DNA binding.

A potentially important set of terms which arose from the $M1^{ST\uparrow}$ data were those associated with iron transport and transferrin activity (PS Fig. PS1.5a).relevant considering the effect of haem availability on PG LPS lipid-A modification (discussed in section 1.5.2).

In addition to these observations, several groups of terms were identified which suggest mechanisms induced by stimulation which may be shown to affect host pathogen interaction.

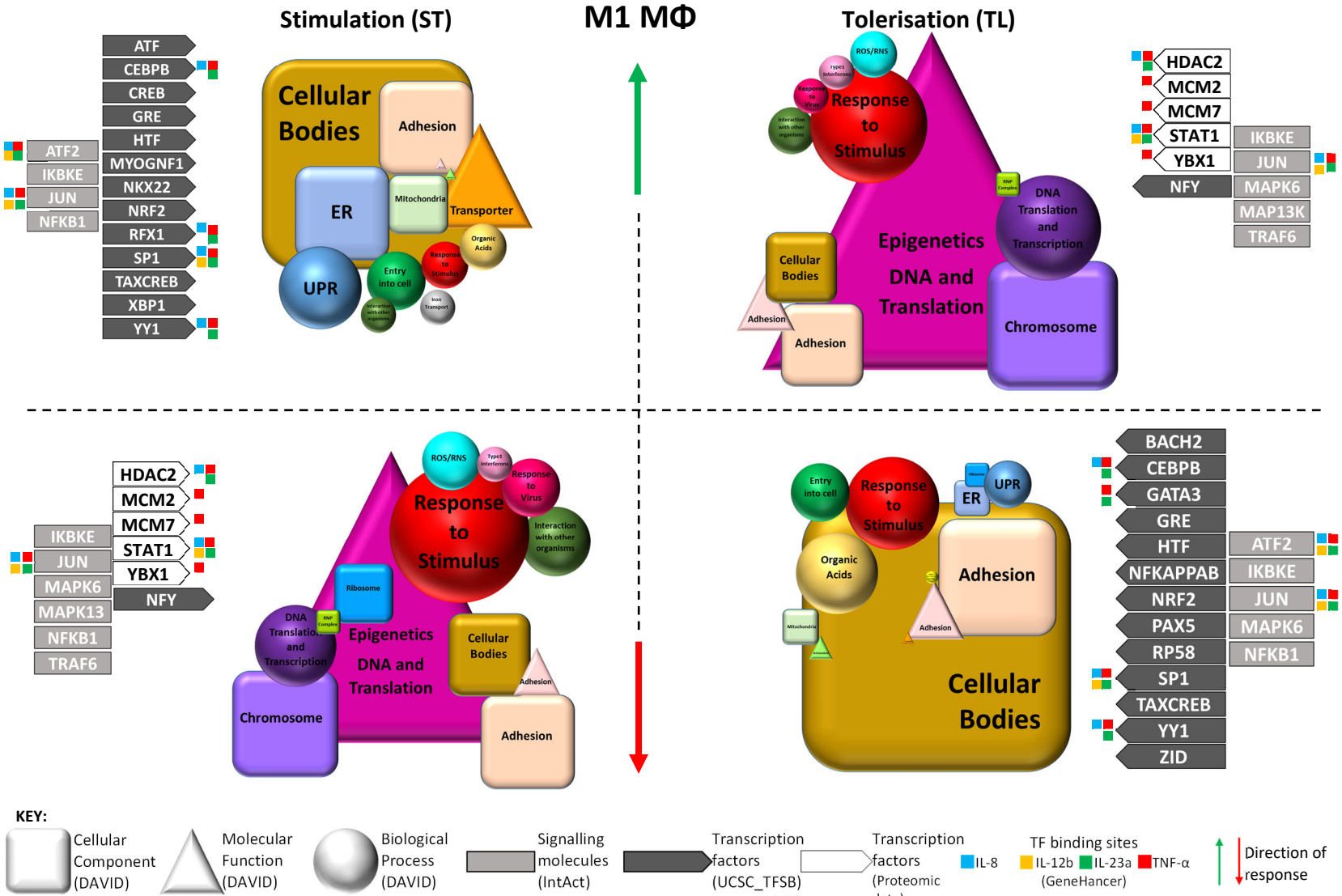

Figure 4.4 Overview of cellular responses to stimulation and tolerisation in M1 MΦs. Cellular responses were grouped following enrichment analysis. Each are represented where size is proportional to number of associated terms returned. Signalling molecules and transcription which are associated with each stimulatory status and direction of response indicated as are transcription factor binding sites.

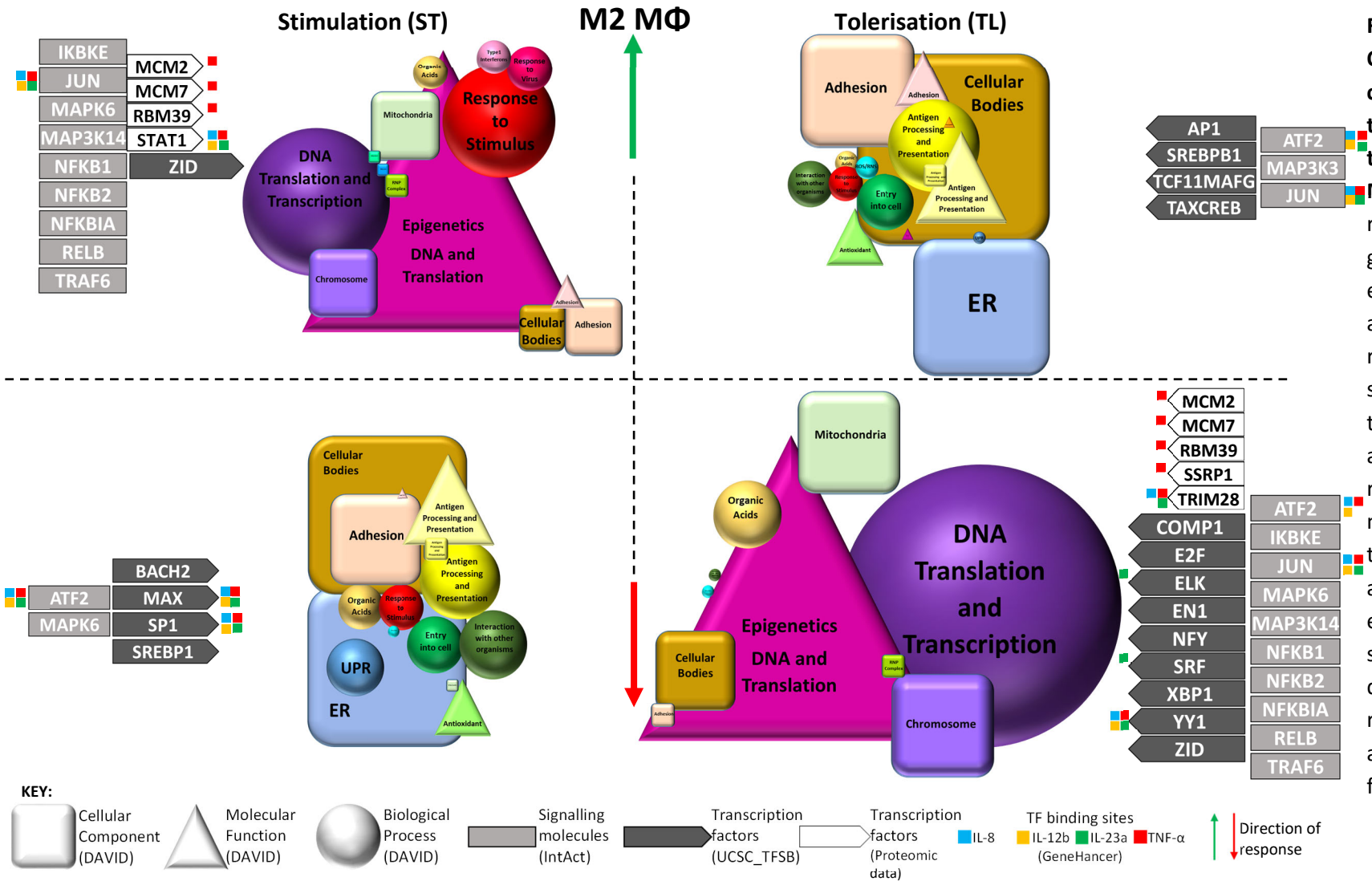

Figure 4.5 Overview of cellular responses to stimulation and tolerisation in M2 MΦs. Cellular responses were grouped following enrichment analysis. Each are represented where size is proportional to number of associated terms returned. Signalling molecules and transcription which are associated with each stimulatory status and direction of response indicated as are transcription factor binding sites.

4.3.1.1 Entry into host

GO-TERM	MΦ Subset	Response (↑↓)	-log10 p value	ANPEP	CTSB	ICAM1	ITGB1	ITGB5	ITGB6	ITGB7	LAMP1	SCARB2	TFRC
EI Cell Of OO Involved In Symbiotic Interaction	M1	↑	5.95	■	■		■	■	■	■		■	■
EI Cell Of OO Involved In Symbiotic Interaction	M2	↓	4.88	■	■	■		■		■	■	■	
Entry Into Host	M1	↑	5.95	■	■		■	■	■		■	■	■
Entry Into Host	M2	↓	4.88	■	■	■		■		■	■	■	
Entry Into Host Cell	M1	↑	5.95	■	■		■	■	■	■		■	■
Entry Into Host Cell	M2	↓	4.88	■	■	■		■		■	■	■	
EI OO Involved In Symbiotic Interaction	M1	↑	5.95	■	■		■	■	■	■		■	■
EI OO Involved In Symbiotic Interaction	M2	↓	4.88	■	■	■		■		■	■	■	
Viral Entry Into Host Cell	M1	↑	5.95	■	■		■	■	■	■		■	■
Viral Entry Into Host Cell	M2	↓	4.88	■	■	■		■		■	■	■	

Table 4.1 Grouped terms associated with entry into host which were identified under "biological process" following stimulation. Each term indicates which MΦ subset (M1 or M2) and direction of response (↓↑) the term was identified from, as well as the level of significance for each term and the proteins which are associated. (Abbreviations: EI = entry into, OO = other organism).

There several terms which directly refer to "entry into host" which are shown to be enriched from $M1^{ST\uparrow}$ and $M2^{ST\downarrow}$ (Table 4.1). Integrins are prominent within these terms, with integrins β1, β 5, β 6 and β 7 all increased in M1 MΦs but only integrins β5 and β7 reduced in M2 MΦs. In addition, the aminopeptidase (ANPEP) is identified in both subsets as is cathepsin B (CTSB) and the scavenger receptor SCARB2. The intracellular adhesion molecule, ICAM1 and the lysosomal associated membrane protein, LAMP1 both feature only in M2 MΦs whilst the transferrin receptor is only evident in M1 MΦs.

4.3.1.2 The unfolded protein response

Terms associated with ER stress and unfolded protein responses were found to be associated with $M1^{ST\uparrow}$ $M2^{ST\downarrow}$ (Tables 4.2 and 4.3) M1 MΦs demonstrated an increase in the UPR response with 11 proteins being upregulated in response to stimulation with PG LPS (Table 4.2). 3 of these proteins are involved in the degradation process of misfolded proteins, Acyl-CoA Dehydrogenase Very Long Chain (ACADVL), ATPase H+ Transporting V0 Subunit D1 (ATP6V0D1) and

GO-TERM	MΦ Subset	Response (↑↓)	-log10 p value	ACADVL	AIFM1	ATP2A2	ATP6V0D	BCAP31	DERL1	DNAJC3	HM13	PDIA3	SEC61B	SSR1	TBL2	TMEM33	TPP1	UGGT
Cellular Response To Topologically Incorrect Protein	M1	↑	6.20	■			■		■	■				■	■	■	■	■
Cellular Response To Topologically Incorrect Protein	M2	↓	2.28							■			■	■	■		■	
Cellular Response To Unfolded Protein	M1	↑	6.53	■			■		■	■				■	■	■	■	■
Cellular Response To Unfolded Protein	M2	↓	2.43							■			■	■	■		■	
Endoplasmic Reticulum Unfolded Protein Response	M1	↑	6.60	■			■		■	■				■	■	■	■	■
Endoplasmic Reticulum Unfolded Protein Response	M2	↓	2.47							■			■	■	■		■	
Ire1-Mediated Unfolded Protein Response	M1	↑	4.64	■			■			■				■		■	■	
Ire1-Mediated Unfolded Protein Response	M2	↓	2.36							■			■	■			■	
Response To Endoplasmic Reticulum Stress	M1	↑	7.15	■	■	■	■		■	■		■		■	■	■	■	■
Response To Endoplasmic Reticulum Stress	M2	↓	2.79					■		■	■		■	■	■		■	
Response To Unfolded Protein	M1	↑	5.73	■			■		■	■				■	■	■	■	■
Response To Topologically Incorrect Protein	M1	↑	5.44	■			■		■	■				■	■	■	■	■

Table 4.2 Grouped terms associated with the unfolded protein response, which were identified under "biological process" following stimulation. Each term indicates which MΦ subset (M1 or M2) and direction of response (↓↑) the term was identified from, as well as the level of significance for each term and the proteins which are associated.

Table 4.3 (below) Grouped terms associated with the Endoplasmic reticulum response, which were identified under "cellular component" following stimulation. Each term indicates which MΦ subset (M1 or M2) and direction of response (↓↑) the term was identified from, as well as the level of significance for each term and the proteins which are associated.

GO-TERM	MΦ Subset	Response (↑↓)	-log10 p value	ACSL4	ALOX5AP	ANPEP	APMAP	ASPH	ATP2A2	BCAP31	CALU	CERS2	CHI3L1	CRTAP	DAD1	DERL1	DNAJC3	DPM1	EBP	EIF2AK2	ELOVL1	ELOVL5	ERMP1	GCS1	HACD3	HLA-B	HM13	IST1	LENG4	MPDU1	NCSTN	NUCB1	OSTC	P3H1	PDIA3	PLAUR	PLD3	PLOD1	PLOD3	POR	PTGS1	RBM3	RCN1	REEP5	RPL32	RPLP1	RPS15	RPS24	RPS26	RPS27	RPS29	RSL1D1	SEC61B	SSR1	STOM	TAP1	TAPBP	TBL2	TMED2	TMED4	TMEM33	UGGT	VKORC1
Cytosolic Ribosome	M1	↓	2.24																																															|■| |■| |■|■|■|											
Cytosolic Small Ribosomal Subunit	M1	↓	2.59																																																	|■| |■|■|■|											
Endoplasmic Reticulum	M1	↑	7.69	■			■	■	■		■	■			■	■	■	■	■			■		■	■	■			■		■		■		■		■	■	■		■		■											■	■			■		■	■	■	
Endoplasmic Reticulum	M2	↓	6.60		■		■	■		■	■		■	■			■				■		■			■	■			■		■		■		■		■		■	■		■	■									■	■		■	■	■	■				■
Endoplasmic Reticulum Lumen	M1	↑	2.20					■			■						■																		■								■																				■	
Endoplasmic Reticulum Lumen	M2	↓	2.98					■			■			■			■																	■		■							■																					
Endoplasmic Reticulum Membrane	M1	↑	8.20	■				■	■		■	■			■	■	■	■	■			■		■	■	■			■				■				■	■	■		■													■				■		■	■		
Endoplasmic Reticulum Membrane	M2	↓	6.23		■			■		■	■						■				■		■			■	■			■					■		■		■	■												■	■		■	■	■	■				■
Endoplasmic Reticulum Part	M1	↑	8.94	■				■	■		■	■			■	■	■	■	■			■		■	■	■			■				■		■		■	■	■		■		■											■				■		■	■	■	
Endoplasmic Reticulum Part	M2	↓	7.66		■			■		■	■			■			■				■		■			■	■			■				■		■		■		■	■		■	■									■	■		■	■	■	■				■
Endoplasmic Reticulum Sec Complex	M2	↓	1.77														■																																				■										
ER-Golgi Intermediate Compartment	M2	↓	2.43			■				■																		■				■																											■				
Integral Component Of ER Membrane	M1	↑	3.69					■								■						■			■	■																																■			■		
Integral Component Of ER Membrane	M2	↓	4.69					■		■											■					■	■																													■	■	■					
Integral Component Of Lumenal Side Of ER Membrane	M2	↓	3.23							■																■	■																														■						
Intrinsic Component Of ER Membrane	M1	↑	3.61					■								■						■			■	■																																■			■		
Intrinsic Component Of ER Membrane	M2	↓	4.59					■		■											■					■	■																													■	■	■					
Lumenal Side Of ER Membrane	M2	↓	3.23							■																■	■																														■						
Nuclear Outer Membrane-ER Membrane Network	M1	↑	8.02	■				■	■		■	■			■	■	■	■	■			■		■	■	■			■				■				■	■	■		■													■				■		■	■		
Nuclear Outer Membrane-ER Membrane Network	M2	↓	6.08		■			■		■	■						■				■		■			■	■			■					■		■		■	■												■	■		■	■	■	■				■
Ribosomal Subunit	M1	↓	2.34																																					■			■		■		■	■	■												
Ribosome	M1	↓	2.49																	■																				■			■		■		■	■	■												
Ribosome	M2	↑	1.41																	■																				■				■		■				■											
Rough Endoplasmic Reticulum	M2	↓	4.28							■							■										■					■						■															■										
Rough Endoplasmic Reticulum Membrane	M1	↑	2.28														■																					■	■																								
Rough Endoplasmic Reticulum Membrane	M2	↓	3.79							■							■																					■															■										
Sec61 Translocon Complex	M2	↓	1.64							■																																											■										
Small Ribosomal Subunit	M1	↓	2.09																																									■		■	■	■												

DERL1, whilst Transmembrane Protein 33 (TMEM33), Protein Disulfide Isomerase Family A Member 3 (PDIA3) and UDP-Glucose Glycoprotein Glucosyltransferase 1 (UGGT) are all associated with the regulation of misfolded proteins. 3 proteins are affected by stimulation with PG LPS in both M1 and M2 MΦs; DnaJ Heat Shock Protein Family (Hsp40) Member C3 (DNAJC3), Signal Sequence Receptor Subunit 1 (SSR1), an integral ER membrane transport protein and Transducin Beta Like 2 (TBL2), a regulator of the PERK pathway in the UPR are increased in response to stimulation in M1 MΦs but decreased in M2 MΦs. A single protein, SEC61 Translocon Beta Subunit (SEC61B), a trans-membrane ER transport protein, is the only protein identified in this group which is affected solely in M2 MΦs, reducing in expression. Terms associated with the endoplasmic reticulum (Table 4.3) can be separated into 2 distinct groups, the ER itself and ribosome associated terms. ER associated terms are found in $M1^{ST\uparrow}$ and $M2^{ST\downarrow}$, conversely ribosome associated terms are primarily found in $M1^{ST\downarrow}$ although a single term occurs in $M2^{ST\uparrow}$.

4.3.1.3 Type-I interferon responses

Type-I interferon responses were associated with $M2^{ST\uparrow}$ and $M1^{ST\downarrow}$, those terms referring to type-I interferon responses (table 4.4) demonstrate a high level of significance, despite these terms being enriched from a relatively small number of proteins. String analysis (Fig. 4.6) demonstrates the high level of association of these interferon associated genes. Identical terms are observed for each subset with minor variations between M1 and M2 MΦs. Two peptides were identified for HLA-A and expression of each was dependent upon the MΦ subset. The only other variation was in the expression of MX2 and OAS3 which were modified in M1 MΦs but not M2 MΦs.

GO-TERM	MΦ Subset	Response (↑↓)	-log10 p value	HLA-A	HLA-A	IFIT1	ISG15	MX1	MX2	OAS2	OAS3	STAT1
Cellular Response To Type I Interferon	M1	↓	7.05		■	■	■	■	■	■	■	■
Cellular Response To Type I Interferon	M2	↑	4.66	■		■	■	■		■		■
Response To Type I Interferon	M1	↓	6.89		■	■	■	■	■	■	■	■
Response To Type I Interferon	M2	↑	4.55	■		■	■	■		■		■
Type I Interferon Signaling Pathway	M1	↓	7.05		■	■	■	■	■	■	■	■
Type I Interferon Signaling Pathway	M2	↑	4.66	■		■	■	■		■		■

Table 4.4 Grouped terms associated with type-I interferons host which were identified under "biological process" following stimulation. each term indicates which MΦ subset (M1 or M2) and direction of response (↓↑) the term was identified from, as well as the level of significance for each term and the proteins which are associated.

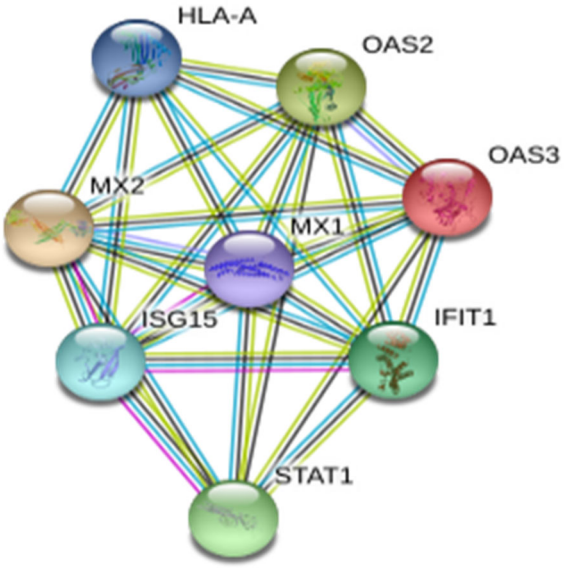

KEY:

Coloured nodes: query proteins and first shell of interactors,

Filled nodes: some 3D structure is known or predicted

Interactions;
Blue – from curated databases,
Pink – experimentally determined,
Yellow – textmining,
Black – co-expression.

Figure 4.6 String analysis of associated type-I interferon proteins. The association between type-I interferon associated proteins which in M1 MΦs decreased and in M2 MΦs increased in expression following stimulation with PG LPS, was visualised using the STRING database v11 (String-db.org).

4.3.1.4 Antigen processing and presentation

Protein profiles from which the enrichment terms associated with antigen processing and presentation, are solely enriched from $M2^{ST\downarrow}$. This was evident when enriched for both biological process (table 4.5) and molecular function (table 4.6). The majority of these terms centre around Transporter 1, ATP Binding Cassette Subfamily B Member (TAP1) and TAP Binding Protein (TAPBP) with the addition of proteins such as annexin 11 (ANXA11), B Cell Receptor Associated Protein 31 (BCAP31) and HLA-B.

GO-TERM	MΦ Subset	Response (↑↓)	-log10 p value	BCAP31	CTSD	HLA-B	ICAM1	IFI30	ITGB5	TAP1	TAPBP
Antigen Processing And Presentation (AP&P)	M2	↓	4.03	■	■	■	■	■	■	■	■
AP&P Of Endogenous Antigen	M2	↓	2.55			■				■	■
AP&P Of Endogenous Peptide Antigen	M2	↓	2.66			■				■	■
AP&P Of Endogenous Peptide Antigen Via Mhc Class I	M2	↓	2.72			■				■	■
AP&P Of Exogenous Peptide Antigen	M2	↓	2.15		■	■		■	■	■	
AP&P Of Peptide Antigen	M2	↓	3.72	■	■	■		■	■	■	■
AP&P Of Peptide Antigen Via Mhc Class I	M2	↓	4.15	■		■		■	■	■	■

Table 4.5 Grouped terms associated with antigen processing and presentation which were identified under "biological process" following stimulation. Each term indicates which MΦ subset (M1 or M2) and direction of response (↓↑) the term was identified from, as well as the level of significance for each term and the proteins which are associated.

GO-TERM	MΦ Subset	Response (↑↓)	-log10 p value	ANPEP	ANXA11	BCAP31	CRTAP	CTSB	GSTM3	HLA-B	HMGN1	HMGN2	ICAM1	IST1	ITGB2	MAP1S	P3H1	PPIF	SNX9	TAP1	TAPBP	TPP1	UQCRFS1	VDAC1	VIM
Antigen Binding	M2	↓	1.40		■					■										■	■				
Mhc Class I Protein Binding	M2	↓	2.39			■														■	■				
Mhc Protein Binding	M2	↓	1.97			■														■	■				
Peptide Antigen Binding	M2	↓	2.06							■										■	■				
Peptide Antigen-Transporting Atpase Activity	M2	↓	1.82																	■	■				
Peptide Binding	M2	↓	2.90	■					■	■								■		■	■	■			
Peptide-Transporting Atpase Activity	M2	↓	1.70																	■	■				
Protein Complex Binding	M2	↓	4.60		■	■	■	■		■	■	■	■	■	■	■	■		■				■	■	■
Tap Binding	M2	↓	3.29							■										■	■				
Tap1 Binding	M2	↓	1.70																	■	■				
Tap2 Binding	M2	↓	1.82																	■	■				

Table 4.6 Grouped terms associated with antigen processing and presentation which were identified under "Molecular function" following stimulation. Each term indicates which MΦ subset (M1 or M2) and direction of response (↓↑) the term was identified from, as well as the level of significance for each term and the proteins which are associated.

4.3.2 GO analysis indicates selective restoration of MΦ subset responses to secondary stimulation (tolerisation).

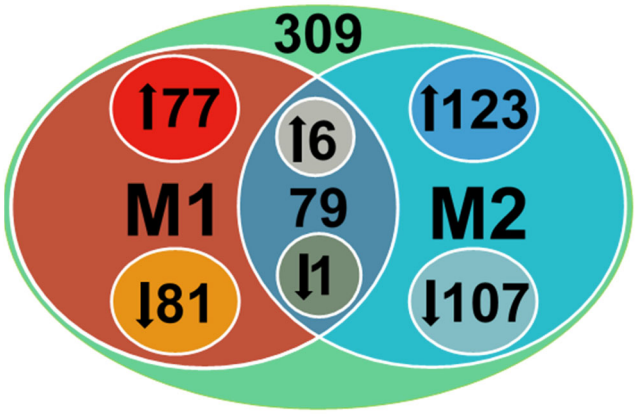

Figure 4.7. M1 and M2 MΦ proteome response to repeated stimulation with PG LPS to induce tolerisation. 309 proteins were found to alter expression by a minimum of a 2-fold change in expression, 158 in M1 MΦs and 230 in M2 MΦs when compared to the single stimulated state. 79 proteins were shown to be responsive in both M1 and M2 MΦs, with 6 of these increasing in expression and 1 decreasing in expression, whilst the remainder responded differentially between subsets. 77 proteins were shown to increase expression in M1 MΦs and 123 in M2 MΦs. 81 proteins decreased their expression in response to tolerisation in M1 MΦs and 107 in M2 MΦs.

This study has demonstrated that PG LPS can elicit multiple responses in M1 and M2 MΦs, affecting numerous mechanisms associated with biological processes, cellular components and molecular function. Subsequent analysis was repeated to examine the impact of a secondary stimulation with PG LPS on these mechanisms. 309 proteins were found to alter expression compared with the stimulated level of expression, 79 proteins were shown to be responsive in both M1 and M2 MΦs, with just 7 proteins responding in an identical manner in both subsets (Fig. 4.7).

There was evidently substantial variation in response to secondary stimulation (tolerisation), this included partial restoration of a suppressed response e.g. MX1, which in M1 MΦs was reduced 19.44-fold in response to an initial stimulation and secondary exposure increased expression 10.49-fold above the stimulated level

(PS. Fig. PS1.11). In M2 MΦs however, this was resistant to tolerisation, but initial stimulation induced an exaggerated restoration of the Lysosomal Thiol Reductase, IFI30, whereby initial stimulation induced a 26.95-fold decrease in expression, and secondary stimulation induced a 36.9-fold increase above the stimulated level. This same trend was also observed as an exaggerated suppression; CD109 expression was increased 3.18-fold in M1 MΦs above basal levels and secondary stimulation saw an 8.26-fold reduction below stimulated level, 2.6-fold lower than the basal level. It was also observed that secondary stimulation could induce an increase in expression where an in initial stimulation had failed to induce a response. HMOX1, suppressed by an initial expression in M1 MΦs, demonstrated a partial restoration of expression through tolerisation. In M2 MΦs however, initial stimulation failed to initiate a significant response (1.17-fold increase) whilst the secondary stimulation increased expression 4.56-fold above basal levels and 3.9-fold above stimulated levels.

The enrichment analysis results in remarkably similar terms but, not only identified in the opposing direction, i.e. increase in expression due to a single stimulation and a decrease in response to a secondary stimulation or *vice versa*, but also there is notably similar opposing responses between MΦ subsets as indicated in figures 4.4 and 4.5. (PS. Figs. PS1.13, 1.14 & 1.15).

Again general observations can be made with regards to MΦ functionality; and again, somewhat surprisingly, more terms associated with a response to stimulus was enriched from proteins which increase in expression in M1 MΦs following a secondary stimulation, particularly those associated with a response to virus. These were not observed in this data set in isolation, with a significant number also enriched from $M1^{TL\downarrow}$ and a small number in $M2^{TL\uparrow}$. Terms returned

associated with immune responses to stimulus are diminished in comparison to those enriched as a result of a single stimulation (PS. Fig. PS1.16d). Only 2 terms were enriched from M2 MΦs in response to a secondary stimulation compared with 13 from a single stimulation. Also, a number of immune response associated terms, such as those associated with viral responses, were enriched from $M1^{ST\downarrow}$ and $M2^{ST\uparrow}$. Interestingly, these terms are enriched in $M1^{TL\uparrow}$, but none of which are enriched from either dataset arising from M2 MΦs. The terms enriched indicate that the viral response initiated in M2 MΦs by stimulation with PG LPS remains above basal levels in M2 MΦs in response to secondary stimulation, whereas, initial stimulation suppresses the viral response in M1 MΦs but this is restored in response to a secondary stimulation.

Terms associated with DNA translation and transcription, suppressed in M1 MΦs under an initial stimulation, return to be enriched in $M1^{TL\uparrow}$. This is also reversed in M2 MΦs, being identified from $M2^{ST\uparrow}$ and subsequently $M2^{TL\downarrow}$. This reversal is also observed in proteins associated with epigenetic modification, transcription and translation (PS. Fig. PS1.16b and PS1.17c). The MCM complex indicates a restoration in expression in M1 MΦs and a suppression in M2 MΦs. Secondary stimulation reverses the expression of genes associated with regulation of gene expression, translation and initiation in M2 MΦs, with proteins such as eukaryotic translation initiation factors, supressed in response to a secondary stimulation, having been elevated in response to the initial stimulation. DNA translation and transcription analysed under molecular function (PS. Fig. PS1.18d), support the observations made under biological process and cellular component, whereby the reversal of response of the MCM complex is prominent. Additional proteins were highlighted following an initial stimulation, but the direction of response is

altered; EIF2AK2 and PTK2, following secondary stimulation are identified in $M1^{TL\uparrow}$ only. AARS, ASNS, ASS1 and CDK6 all reverse their direction of response in both subsets, following secondary stimulation, identified in the $M1^{TL\uparrow}$ and $M2^{TL\downarrow}$ profiles. An addition to this data set are the dead box helicases, DDX21, DDX48 (also known as EIF4A3) and DHX15. DDX21 and DHX15 being found in proteins which $M2^{TL\downarrow}$ and DHX15 in $M1^{TL\uparrow}$.

The four groups of term highlighted in section 4.3.1.1 – 4.3.1.4 also arise in terms generated following GO analysis of tolerised protein profile, but with notable differences;

4.3.2.1 Entry into host

GO-TERM	MΦ Subset	Response (↑↓)	-log10 p value	ANPEP	CTSB	ICAM1	ITGB5	ITGB7	LAMP1	LGALS1	SCARB2
Entry Into Cell Of OO Involved In Symbiotic Interaction	M1	↓	2.78	■	■		■	■			■
Entry Into Cell Of OO Involved In Symbiotic Interaction	M2	↑	4.96	■	■	■	■	■	■	■	■
Entry Into Host	M1	↓	2.78	■	■		■	■			■
Entry Into Host	M2	↑	4.96	■	■	■	■	■	■	■	■
Entry Into Host Cell	M1	↓	2.78	■	■		■	■			■
Entry Into Host Cell	M2	↑	4.96	■	■	■	■	■	■	■	■
Entry Into OO Involved In Symbiotic Interaction	M1	↓	2.78	■	■		■	■			■
Entry Into OO Involved In Symbiotic Interaction	M2	↑	4.96	■	■	■	■	■	■	■	■
Viral Entry Into Host Cell	M1	↓	2.78	■	■		■	■			■
Viral Entry Into Host Cell	M2	↑	4.96	■	■	■	■	■	■	■	■

Table 4.7 Grouped terms associated with entry into host, which were identified under "Biological process" following secondary stimulation. Each term indicates which MΦ subset (M1 or M2) and direction of response (↓↑) the term was identified from, as well as the level of significance for each term and the proteins which are associated. (Abbreviation: OO = other organism)

Terms associated with cellular entry (table 4.7) switch from $M1^{ST\uparrow}$ and $M2^{ST\downarrow}$, following a single stimulation, to $M1^{TL\downarrow}$ and $M2^{TL\uparrow}$, following a secondary stimulation demonstrating that cellular entry is favoured in M1 MΦs in response to a single stimulus, but that switches to the M2 subset in response to a secondary stimulus. The protein profile remains similar to that produced following a single stimulation (albeit in an opposing direction of response) with proteins associated with cellular adhesion absent from the tolerised profile, i.e. ITGB1, ITGB6 as well as the transferrin receptor but with the addition of galectin 1 (LGALS1).

GO-TERM	MΦ Subset	Response (↑↓)	-log10 p value	ACADVL	AIFM1	ATP2A2	DNAJC3	HM13	HSP70B	LMNA	PDIA3	SEC61B	SSR1	TBL2	TLN1
Cellular Response To Topologically Incorrect Protein	M1	↓	1.51	■			■						■	■	
Cellular Response To Unfolded Protein	M1	↓	1.62	■			■						■	■	
Endoplasmic Reticulum Unfolded Protein Response	M1	↓	1.65	■			■						■	■	
Response To Endoplasmic Reticulum Stress	M1	↓	3.65	■	■	■	■	■			■		■	■	
Response To Unfolded Protein	M2	↑	2.93				■		■	■		■	■	■	■

Table 4.8 Grouped terms associated with the unfolded protein response, which were identified under "Biological process" following secondary stimulation. Each term indicates which MΦ subset (M1 or M2) and direction of response (↓↑) the term was identified from, as well as the level of significance for each term and the proteins which are associated.

GO-TERM	MΦ Subset	Response (↑↓)	-log10 p value	ALOX5AP	APMAP	ARL6IP5	ASPH	ATP2A2	BCAP31	CALU	CHI3L1	DNAJC3	DPM1	EBP	ELOVL1	ERMP1	GCS1	HLA-B	HM13	HMOX1	LENG4	MPDU1	NCSTN	NUCB1	OSTC	P3H1	PDIA3	PLAUR	PLOD1	POR	PTGS1	RAB10	RBM3	RCN1	REEP5	RPLP1	RPLP2	RPS24	RSL1D1	SEC61B	SSR1	STOM	TAP1	TAP2	TAPBP	TBL2	TMED4	VKORC1
Cytosolic Ribosome	M2	↓	1.31																																■	■	■	■	■									
Endoplasmic Reticulum (ER)	M1	↓	4.58	■	■	■		■				■	■	■		■	■	■	■		■		■		■		■		■	■			■						■	■					■	■	
Endoplasmic Reticulum	M2	↑	3.59	■		■	■		■	■	■	■			■			■	■	■		■		■		■		■	■	■	■	■		■	■				■	■		■	■	■	■		■
Endoplasmic Reticulum Membrane	M1	↓	4.92	■		■		■				■	■	■		■	■	■	■		■				■		■		■	■																		
Endoplasmic Reticulum Membrane	M2	↑	4.87	■		■	■		■	■		■			■			■	■	■		■				■		■	■	■	■	■							■	■		■	■	■	■		■
Endoplasmic Reticulum Part	M1	↓	5.15	■		■		■				■	■	■		■	■	■	■		■				■		■		■	■			■						■	■					■	■	
Endoplasmic Reticulum Part	M2	↑	5.24	■		■	■		■	■		■			■			■	■	■		■		■		■		■	■	■	■	■		■	■				■	■		■	■	■	■		■
Endoplasmic Reticulum Subcompartment	M2	↑	1.91				■																								■		■	■													
Endoplasmic Reticulum Tubular Network	M2	↑	2.09				■																								■		■	■													
Integral Component Of ER Membrane	M2	↑	4.61				■		■						■			■	■																							■	■	■	■			
Integral Component Of Lumenal Side Of ER Membrane	M2	↑	2.80				■		■									■	■																									■				
Intrinsic Component Of ER Membrane	M2	↑	4.51				■		■						■			■	■																									■	■	■			
Large Ribosomal Subunit	M2	↓	1.37																																■	■		■										
Lumenal Side Of Endoplasmic Reticulum Membrane	M2	↑	2.80						■									■	■																											■			
Nuclear Outer Membrane-ER Membrane Network	M1	↓	4.80	■		■		■				■	■	■		■	■	■	■		■				■		■		■	■			■						■	■					■	■	
Nuclear Outer Membrane-ER Membrane Network	M2	↑	4.73	■		■	■		■	■		■			■			■	■	■		■				■		■	■	■	■	■							■	■		■	■	■	■		■
Ribosomal Subunit	M2	↓	1.45																														■		■	■	■	■	■									
Rough Endoplasmic Reticulum	M2	↑	3.58						■			■							■				■					■												■								
Rough Endoplasmic Reticulum Membrane	M2	↑	3.35						■			■							■				■					■												■								

Table 4.9 Grouped terms associated with the unfolded protein response, which were identified under "cellular component" following secondary stimulation. Each term indicates which MΦ subset (M1 or M2) and direction of response (↓↑) the term was identified from, as well as the level of significance for each term and the proteins which are associated.

4.3.2.2 The unfolded protein response

The unfolded protein response appears to be primarily associated with response to a single stimulation in M1 MΦs, as these terms only occur otherwise in $M1^{ST\downarrow}$ or $M2^{TL\downarrow}$. In comparison to a single stimulation, terms associated with the UPR are greatly diminished (table 4.6). In response to a single stimulation, 7 terms were enriched from proteins which increased in M1 MΦs and 5 from those that decreased in M2 MΦs. Following a secondary stimulation, a single term was returned from proteins which $M2^{TL\uparrow}$ and 4 from $M1^{TL\downarrow}$, indicating another reversal of response.

ER and ribosomal associated terms are diminished both in the number of terms enriched but also the number of relevant genes (PS. Fig. PS1.15d). 5 additional proteins are evident that were absent from the stimulated profile; ADP Ribosylation Factor Like GTPase 6 Interacting Protein 5 (ARL6IP5), HMOX1, RAB10, RPLP2 and TAP2. These proteins, with the exception of RPLP2 are all those which increase in response to a secondary stimulation in M2 MΦs whilst ARL6IP5 is also found in proteins which decrease in M1 MΦs. Those terms which do remain from the initial stimulation are observed in the opposing direction of response following a secondary stimulation.

4.3.2.3 Type-I interferon responses

Type-I IFN associated terms are all enriched from proteins which increase in M1 MΦs in response to a secondary stimulation (table 4.10). So much so that MX1, OAS2 and STAT1, which are expressed higher, relatively, in M2 MΦs in response to a single stimulation, are all expressed higher in M1 MΦs than M2 MΦs following a secondary stimulation.

GO-TERM	MΦ Subset	Response (↑↓)	-log10 p value	IFIT1	ISG15	MX1	MX2	OAS2	OAS3	STAT1
Cellular Response To Type I Interferon	M1	↑	6.00							
Response To Type I Interferon	M1	↑	5.87							
Type I Interferon Signaling Pathway	M1	↑	6.00							

Table 4.10 Grouped terms associated with type-I interferons, which were identified under "biological process" following secondary stimulation. Each term indicates which MΦ subset (M1 or M2) and direction of response (↓↑) the term was identified from, as well as the level of significance for each term and the proteins which are associated.

4.3.2.4 Antigen processing and presentation

The protein profile associated with antigen processing and presentation from terms enriched under "biological process" (table 4.11) remains similar to that identified in response to an initial stimulation in M2 MΦs, however, the direction of response in which these terms are enriched is reversed. Terms enriched for molecular function (table 4.12), reinforce these observations with terms referring to antigen processing and presentation ($M2^{ST\downarrow}$ & $M2^{TL\uparrow}$) responding in a similar manner. Following tolerisation a single term for *antigen processing and presentation* is attributed to $M1^{ST\downarrow}$. Of the protein profile associated with these terms, Fc receptor gamma chain FCERG1, PDIA3 and RAB10, Member RAS Oncogene Family (RAB10) are absent in comparison to the original profile, whereas, TAP2 is added to $M2^{TL\uparrow}$ (in addition to the previously identified TAP1 and TAPBP), as well as key binding proteins such as HLA-B, ICAM1 and ITGB5.

GO-TERM	MΦ Subset	Response (↑↓)	-log10 p value	BCAP31	CTSD	FCER1G	HLA-B	ICAM1	IFI30	ITGB5	PDIA3	RAB10	RAB8B	TAP1	TAP2	TAPBP
Antigen Processing And Presentation (AP&P)	M1	↓	1.70		■		■			■	■		■			
Antigen Processing And Presentation	M2	↑	5.00	■	■	■	■	■	■	■		■		■	■	■
AP&P Of Endogenous Antigen	M2	↑	3.70				■							■	■	■
AP&P Of Endogenous Peptide Antigen	M2	↑	3.87				■							■	■	■
AP&P Of Endogenous Peptide Antigen Via Mhc Class I	M2	↑	3.97				■							■	■	■
AP&P Of Exogenous Antigen	M2	↑	2.97		■	■	■		■	■				■	■	
AP&P Of Exogenous Peptide Antigen	M2	↑	3.06		■	■	■		■	■				■	■	
AP&P Of Peptide Antigen	M2	↑	4.50	■	■	■	■		■	■				■	■	■
AP&P Of Peptide Antigen Via Mhc Class I	M2	↑	5.50	■		■	■		■	■				■	■	■

Table 4.11 Grouped terms associated with antigen processing and presentation, which were identified under "biological process" following secondary stimulation. Each term indicates which MΦ subset (M1 or M2) and direction of response (↓↑) the term was identified from, as well as the level of significance for each term and the proteins which are associated.

GO-TERM	MΦ Subset	Response (↑↓)	-log10 p value	ANPEP	BCAP31	GSTM3	HLA-B	PPIF	TAP1	TAP2	TAPBP	TPP2
Mhc Class I Protein Binding	M2	↑	2.09		■				■		■	
Mhc Class Ib Protein Binding	M2	↑	1.54						■	■		
Mhc Protein Binding	M2	↑	2.88		■				■	■	■	
Peptide Antigen Binding	M2	↑	1.76				■		■		■	
Peptide Antigen-Transporting Atpase Activity	M2	↑	3.81						■	■	■	
Peptide Binding	M2	↑	2.11	■		■	■	■	■		■	■
Peptide-Transporting Atpase Activity	M2	↑	3.81						■	■	■	
Tap Binding	M2	↑	4.90				■		■	■	■	
Tap1 Binding	M2	↑	3.51						■	■	■	
Tap2 Binding	M2	↑	1.67						■		■	

Table 4.12 Grouped terms associated with antigen processing and presentation, which were identified under "molecular function" following secondary stimulation. Each term indicates which MΦ subset (M1 or M2) and direction of response (↓↑) the term was identified from, as well as the level of significance for each term and the proteins which are associated.

4.3.4 Transcription factor and signalling molecule analysis suggests complex mechanisms are associated with each stimulatory state.

Thus far, this study has identified numerous mechanisms which are initiated, modified or supressed by either singular or secondary stimulation with PG LPS, which bare impact upon the understanding of periodontal disease initiation and progression. That said, many of the mechanisms within this chapter are suggestive and do not relate direclty to the results observed in chapters 2 and 3, regarding the variation in secretion of key inflammatory cytokines. To atempt to investigate the potential impact that protein responses identified in this proteomic study may have on the production and secretion of these inflammtory mediators, the University of California, Santa Cruz Genomics Institute Transcription factor binding site database (UCSC_TFBS) (Figs 4.8 & 4.9). function was utilised using the protein interaction function within the DAVID Bioinformatic datatbase. Each of these was then cross-referenced with the transcription binding sites for each cytokine of interest using the Genehancer functionality of the Gene-cards suite. In addition, the EMBL-EBI IntAct database for molecular interaction (Figs 4.10 & 4.11) was used to search for potential intracellular signalling molecules which may influence these transcription factor/binding site events as well as additional transcription factors.

Results using the USCS_TFBS database indicated a stark contrast, both between MΦ subsets and stimulation and tolerisation (Figs 4.8 & 4.9). The $M1^{ST\uparrow}$ profile returned 13 individual transcription factors (TFs) (where p-value < 0.05), whereas the dataset for $M1^{ST\downarrow}$ only gave rise to 1; zinc finger and BTB Domain Containing 6 (ZID). M2 MΦs behaved in an opposing manner in, with just 1 TF, nuclear transcription factor (NFY), being returned from the $M2^{ST\uparrow}$ profile and

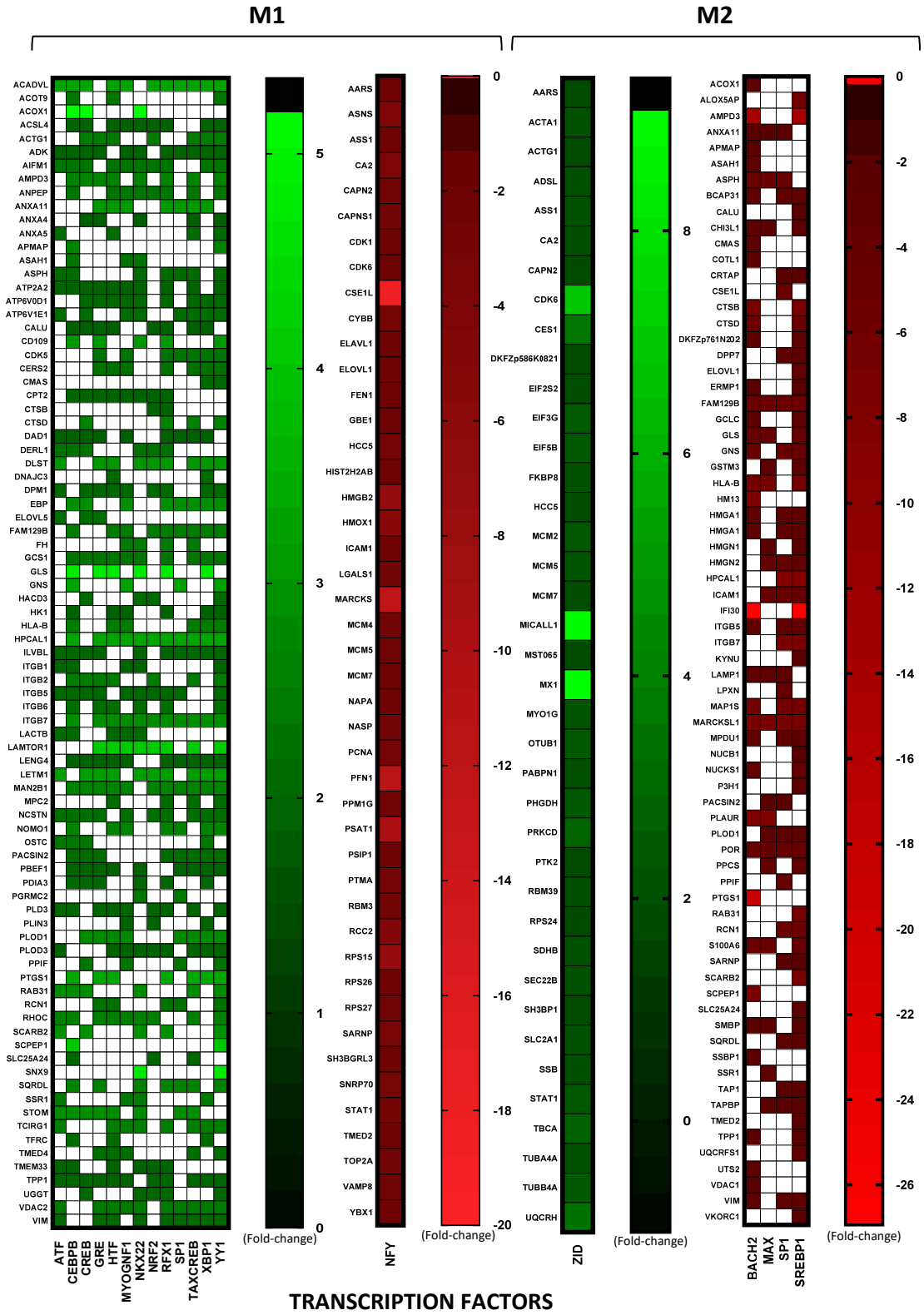

Figure 4.8 Transcription factors associated with M1 and M2 MΦ protein profiles following STIMULATION. Transcription factors associated with M1 and M2 MΦ directional responses where determined using the USCS_TFBS database within DAVID. Transcription factors are indicated for M1 and M2 MΦs which have been determined from datasets incorporating proteins which either increase (green) or decrease (red) in expression relative to the unstimulated state.

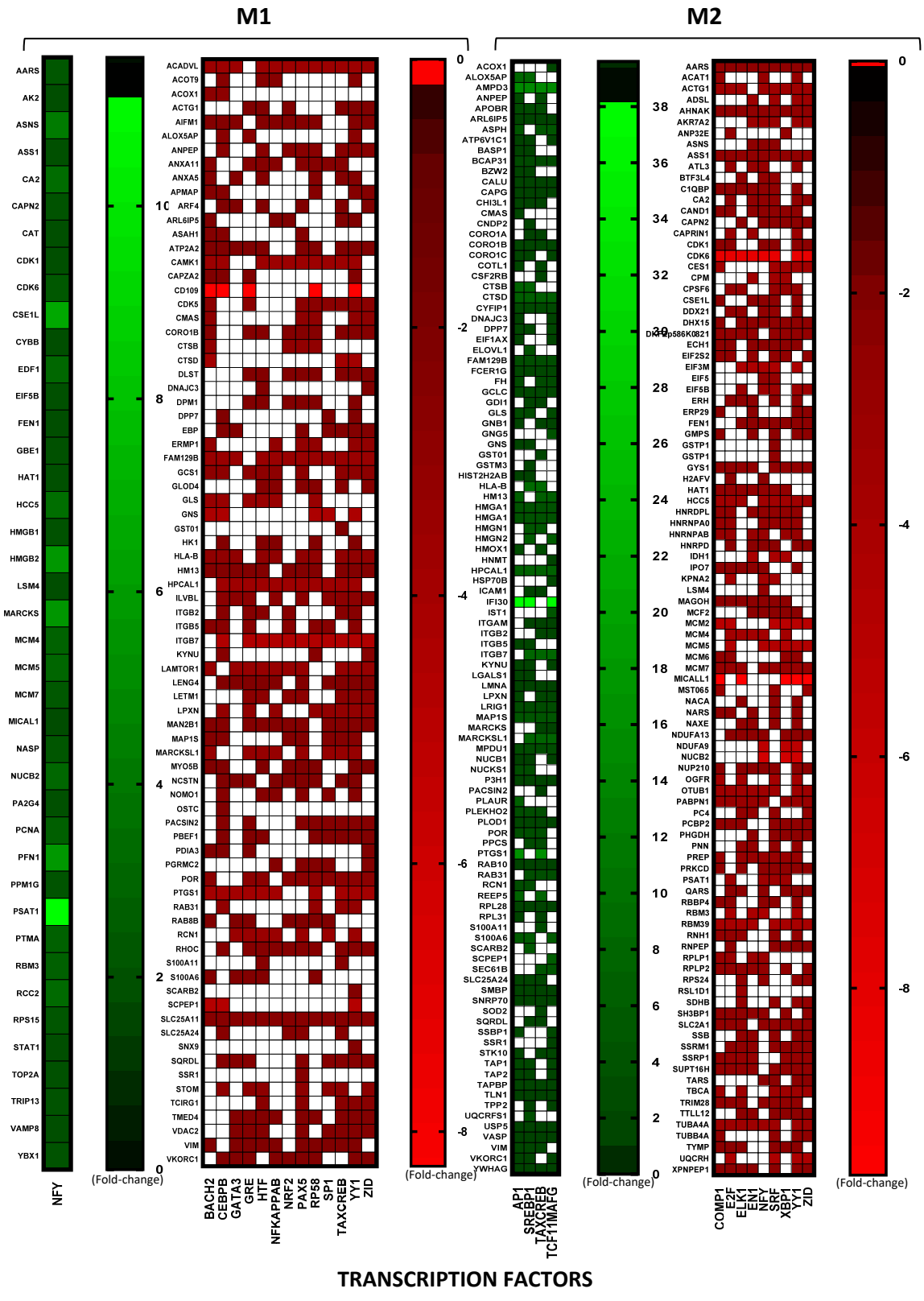

Figure 4.9 Transcription factors associated with M1 and M2 MΦ protein profiles following TOLERISATION. Transcription factors associated with M1 and M2 MΦ directional responses where determined using the USCS_TFBS database within DAVID. Transcription factors are indicated for M1 and M2 MΦs which have been determined from datasets incorporating proteins which either increase (green) or decrease (red) in expression relative to the stimulated state.

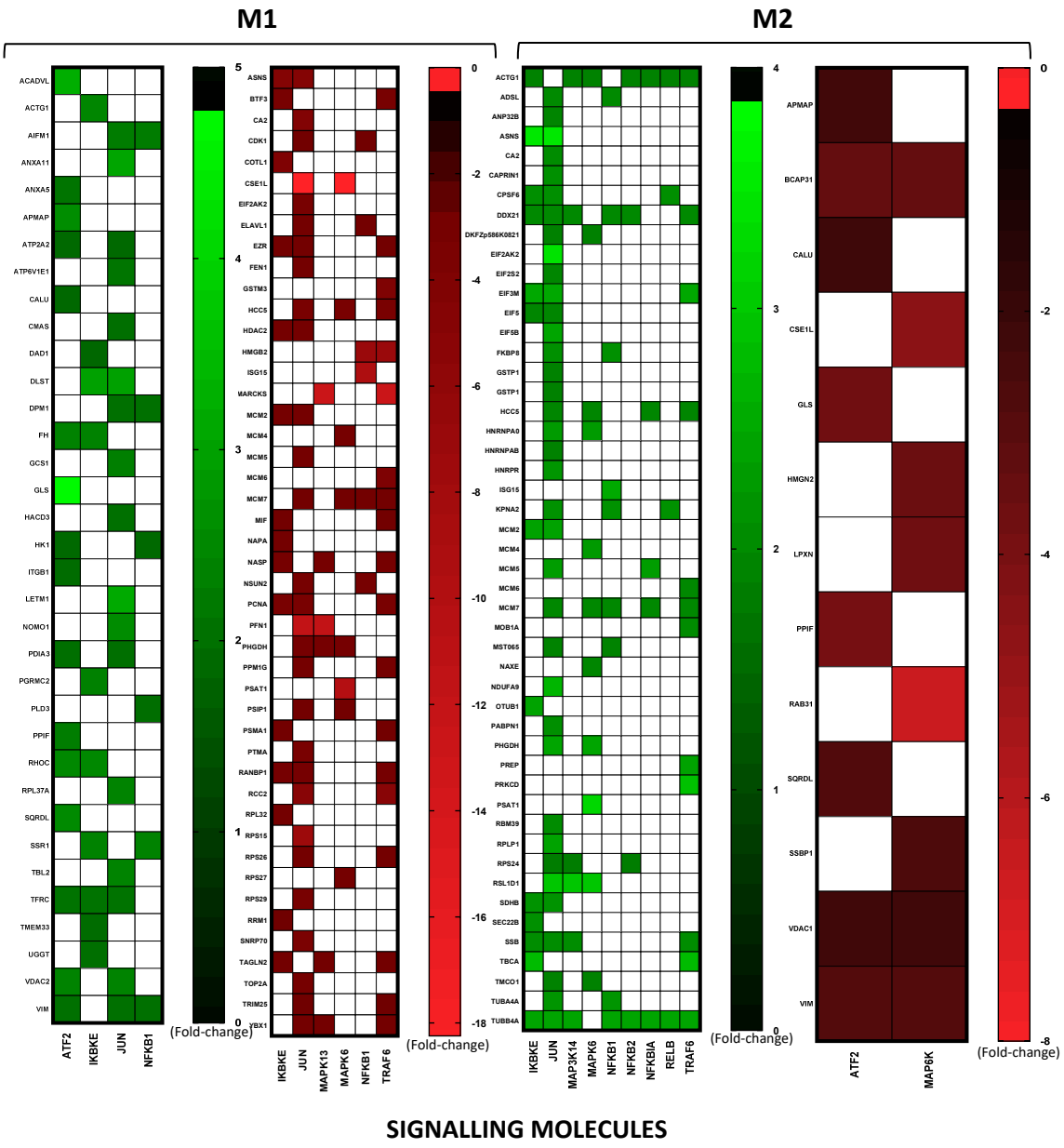

Figure 4.10 Signalling molecules associated with M1 and M2 MΦ protein profiles following STIMULATION. Signalling molecules associated with M1 and M2 MΦ directional responses where determined using the IntAct database within DAVID. Signalling molecules are indicated for M1 and M2 MΦs which have been determined from datasets incorporating proteins which either increase (green) or decrease (red) in expression relative to the unstimulated state.

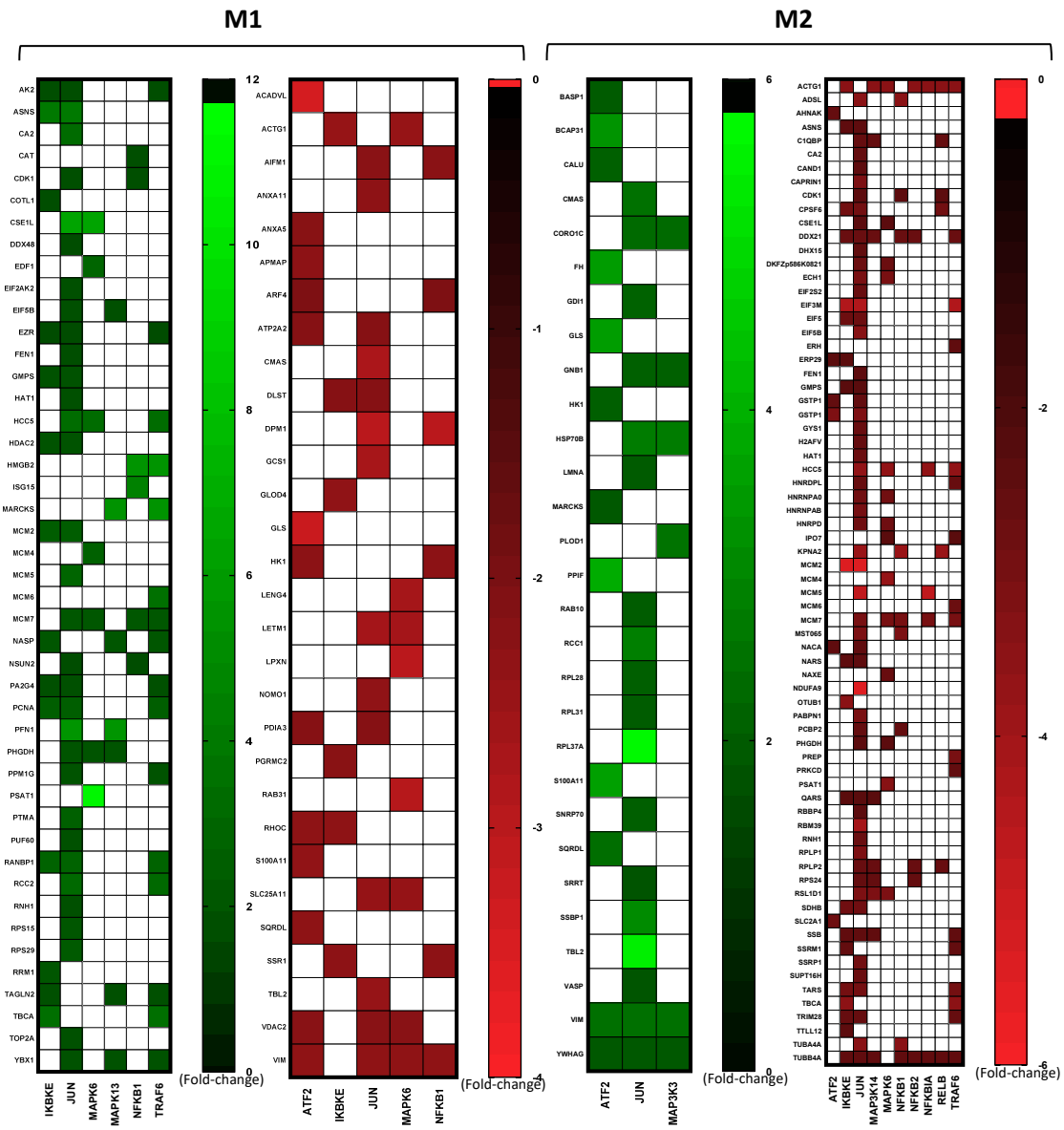

Figure 4.11 Signalling molecules associated with M1 and M2 MΦ protein profiles following TOLERISATION. Signalling molecules associated with M1 and M2 MΦ directional responses where determined using the IntAct database within DAVID. Signalling molecules are indicated for M1 and M2 MΦs which have been determined from datasets incorporating proteins which either increase (green) or decrease (red) in expression relative to the stimulated state.

4 from the $M2^{ST\downarrow}$ profile; BTB domain and CNC homolog 2 (BACH2), MYC associated factor X (MAX), sterol regulatory element-binding protein 1 (SREBP1) and Sp1 transcription factor (SP1). Following a secondary stimulation, this pattern is somewhat reversed in M1 MΦs, with a single TF, NFY arising from the $M1^{TL\uparrow}$ profile and 13 TFs now arising from the $M1^{TL\downarrow}$ profile. Of these 13 TFs, 8 are identical to those previously identified following the initial stimulation. Whereby nuclear factor kappa B (NFκB), GATA binding protein 3 (GATA3), paired box 5 (PAX5), zinc finger protein 513 (RP58) and ZID form part of the 13 transcription factors are also enriched from $M1^{TL\downarrow}$. M2 MΦs demonstrate an amount of overlap in the terms retuned following enrichment using these databases. ZID forms the only transcription factor which is enriched from the $M2^{ST\uparrow}$ profile and transfers to the $M2^{TL\downarrow}$ profile. SP1 arises from $M2^{ST\downarrow}$ and is evident in terms enriched from both the $M1^{ST\uparrow}$ and $M1^{TL\downarrow}$ datasets. NFY also appears in terms returned from the $M2^{ST\downarrow}$ profile as well as both the $M1^{ST\downarrow}$ and $M1^{TL\uparrow}$ derived terms. BACH2 is enriched from opposing profiles with differing directional responses; $M2^{ST\uparrow}$ and $M1^{TL\downarrow}$. MAX is unique to $M2^{ST\downarrow}$ whilst cooperates with myogenic proteins 1 (COMP1), E2F transcription factor (E2F), ETS transcription factor.

ELK1 (ELK1), engrailed homeobox 1 (EN1) and serum response factor (SRF) are unique to $M2^{TL\downarrow}$. Activator protein 1 (AP-1) and the nuclear factor, erythroid 2 like 1/ MAF BZIP transcription factor G (TCF11/MAFG) complex are identified only in terms from the $M2^{TL\uparrow}$ profile whereas, sterol regulatory element binding transcription factor 1 (SREBP1) switches from $M2^{ST\downarrow}$ to $M2^{TL\uparrow}$.

Analysis using the IntAct database for molecular interaction returned a number of signalling molecules of interest as well as several TFs or TF precursors (Figs.

4.10 & 4.11). Within the terms enriched from this database, jun proto-oncogene, AP-1 transcription factor subunit (JUN) is almost ubiquitous, enriched from every dataset with the exception of $M2^{ST\downarrow}$, yet it is more specific in respect to ATF, specifically referencing activating transcription factor 2 (ATF2), still from $M1^{ST\uparrow}$ but also $M2^{ST\downarrow}$ $M1^{TL\downarrow}$ and both $M2^{TL\uparrow}$ and $M2^{TL\downarrow}$, indicating a potential regulatory mechanism. In stark contrast the terms enriched from the UCSC_TFBS database, where a single term was directly associated with NFκB, several, including nuclear factor kappa B subunit 1 (NFκB1) and nuclear factor kappa B subunit 2 (NFκB2) as well as NFκ inhibitor alpha (NFκBIα), inhibitor of nuclear factor kappa B kinase subunit epsilon (IκBKε) and RELB proto-oncogene, NF-KB subunit (REL-B) were returned using the IntAct method. NFκB1 and IκBKε are both enriched from $M1^{ST\uparrow}$, $M1^{ST\downarrow}$, $M2^{ST\uparrow}$ as well as $M1^{TL\uparrow}$, $M1^{TL\downarrow}$ and $M2^{TL\downarrow}$ again suggesting that of the proteins identified in each profile, a number may act in a regulatory manner. NFκB2, NFκBIα and REL-B are all enriched in M2 MΦs only and from the same datasets $M2^{ST\uparrow}$ $M2^{TL\downarrow}$.

The signalling cascade associated TNF receptor associated factor 6 (TRAF6) is enriched from both subsets but with opposing directions of response, being; $M1^{ST\downarrow}$, $M2^{ST\uparrow}$ and $M1^{TL\uparrow}$, M2 $^{TL\downarrow}$. MAK3K3 and MAP3K14 are unique to M2 MΦ enriched terms but with MAP3K3 enriched from the $M2^{TL\uparrow}$ profile and MAPK14 from the $M2^{ST\uparrow}$ and $M2^{TL\downarrow}$ profiles. MAPK6 is also enriched from M2 MΦ datasets; $M2^{ST\uparrow}$, $M2^{ST\downarrow}$ and $M2^{TL\downarrow}$ as well as $M1^{ST\downarrow}$, $M1^{TL\uparrow}$ and $M1^{TL\downarrow}$. The remaining MAPK13 enriched only from the M1 MΦ datasets, arising from the $M1^{ST\downarrow}$ and $M1^{TL\uparrow}$ protein profiles. To determine the potential of these TFs affecting the transcriptional events resulting in inflammatory cytokine secretion, the binding TF sites for IL-8, IL-12b, IL-23a and TNF-α were obtained using the

	M1									M2								
	US vs		ST vs		TL vs		M1 vs M2			US vs		ST vs		TL vs		M2 vs M1		
	ST	TL	US	TL	US	ST	US	ST	TL	ST	TL	US	TL	US	ST	US	ST	TL
HDAC2	2.3	1.0	0.4	0.4	1.0	2.3	1.2	0.4	1.2	0.7	0.9	1.5	1.4	1.1	0.7	0.8	2.7	0.8
MCM2	2.3	0.8	0.4	0.3	1.2	2.9	1.5	0.3	3.7	0.4	2.0	2.5	5.0	0.5	0.2	0.7	3.9	0.3
MCM7	2.0	0.8	0.5	0.4	1.3	2.5	1.2	0.3	2.0	0.5	1.3	2.1	2.8	0.8	0.4	0.8	3.5	0.5
RBM39	1.0	0.8	1.0	0.8	1.3	1.2	1.2	0.6	2.8	0.5	1.8	2.2	3.9	0.6	0.3	0.8	1.7	0.4
SSRP1	1.5	0.8	0.6	0.5	1.2	1.9	1.2	0.4	2.2	0.6	1.5	1.8	2.7	0.7	0.4	0.8	2.3	0.5
STAT1	2.6	1.3	0.4	0.5	0.8	2.0	3.2	0.5	1.5	0.4	0.6	2.6	1.5	1.7	0.7	0.3	2.1	0.7
TRIM28	1.4	0.8	0.7	0.6	1.2	1.7	1.2	0.5	2.2	0.6	1.5	1.6	2.4	0.7	0.4	0.8	1.8	0.5
YBX1	2.2	1.0	0.5	0.4	1.0	2.3	1.1	0.4	1.3	0.8	1.1	1.3	1.4	0.9	0.7	0.9	2.4	0.8

Table 4.13 Relative protein expression of proteins with TF activity corresponding with inflammatory cytokine binding sites. Proteins which were cross referenced with transcription binding site data is indicated by fold-ratio change, whereby those highlighted in green, indicate a minimum 2-fold change in expression.

Genehancer (GH) function within the GeneCards suite. 5 GH identifiers were discovered for IL-8 and TNF-α and 4 for IL12-b and IL-23. The binding sites identified for each GH identifier were cross referenced with the TFs enriched above as well as the overall protein profile identified in this proteomic study. (The results are summarised in table 4.14, where it is apparent that several TFs are able to bind multiple target cytokines).

Whilst the TFs that have been identified by enrichment are inferred and may be affected by the individual interacting protein and its affect, those which are identified from proteomic data are easier to ascribe a direct level of expression. Table 4.13 Indicates fold ratio change in comparison to other stimulatory states and subsets for each protein identified in the proteomic data. Of these proteins, demonstrate a minimum 2-fold change in response to stimulation and tolerisation in M1 MΦs. Remarkably these proteins, MMC2, MMC7, HDAC2, STAT1 and YBX1 all perform in a manner which might not be expected, with expression decreased following stimulation and restored following tolerisation. Conversely, in M2 MΦs, 6 proteins demonstrate modified expression but behave in a more

	IL-8	IL-12b	IL-23a	TNF-α
GeneHancer Identifier	GH04J073739	GH05J159331	GH12J056335	GH06J031567
Transcription Factor Binding Sites	CEBPB JUN	STAT1	ATF2 CEBPB HDAC2 JUN SP1 TRIM28	ATF2 CEPBP HDAC2 MAX SP1 YBX1 YY1
GeneHancer Identifier	GH04J073702	GH05J159411	GH12J056298	GH06J031563
Transcription Factor Binding Sites	ATF2 CEBPB HDAC2 JUN MAX SP1 STAT1 TRIM28 YY1	MAX	ATF2 CEBPB GATA3 HDAC2 MAX RFX1 SP1 SRF TRIM28 YY1	HDAC2 JUN MCM2 TRIM28
GeneHancer Identifier	GH04J073716	GH05J158967	GH12J056332	GH06J031562
Transcription Factor Binding Sites	ATF2 CEBPB JUN	SP1	ELK1 HDAC2 MAX SP1 STAT1 YY1	ATF2
GeneHancer Identifier	GH04J074107	GH05J159456	GH12J056358	GH06J031733
Transcription Factor Binding Sites	CEBPB JUN MAX RFX1 SP1 STAT1 YY1	ATF2 JUN SP1	ATF2 CEBPB ELK1 MAX RFX1 SP1 STAT1 YY1	ATF2 CEBPB HDAC2 JUN MAX MCM2 MCM7 RBM39 RFX1 SP1 SSRP1 TRIM28 YBX1 YY1
GeneHancer Identifier	GH04J073735			GH06J031813
Transcription Factor Binding Sites	ATF2 JUN SP1			ATF2 CEBPB GATA3 HDAC2 JUN MAX MCM2 MCM7 RBM39 RFX1 SP1 SSRP1 TRIM28 STAT1 YY1

Table 4.14 Transcription factor binding sites for inflammatory cytokines. Transcription factor binding sites were identified for each cytokine of interest using the Genehancer functionality of the GeneCards database. These were then cross referenced with transcription factors previously identified using the UCSC_TFSB and IntAct databases (blue) and the entire responsive proteome identified in section 4.3.1 of this study (red).

conventional manner. MMC2, MMC7, RBM39 and SSRP1 Increase (although SSRP1 only shows a partial increase) following stimulation and demonstrate a significant reduction following tolerisation. In the case of MMC2, this reduction is so significant that the basal unstimulated level is 2-fold higher than the tolerised

level of expression. STAT1 and TRIM28 differ in their susceptibility to tolerisation in M2 MΦs. Stimulation causes a 2.6-fold increase in expression in STAT1 but a secondary stimulation only results in a 1.5-fold reduction, remaining 1.7-fold higher that the basal level. TRIM28, following a single stimulation initiates only a 1.6-fold increase in expression above basal levels, whereas the secondary stimulation results in a 2.4-fold reduction in expression compared to the stimulated level, dropping 1.5-fold below the unstimulated level.

4.3.5 Comparison of MΦ subsets indicates substantial plasticity on the protein level.

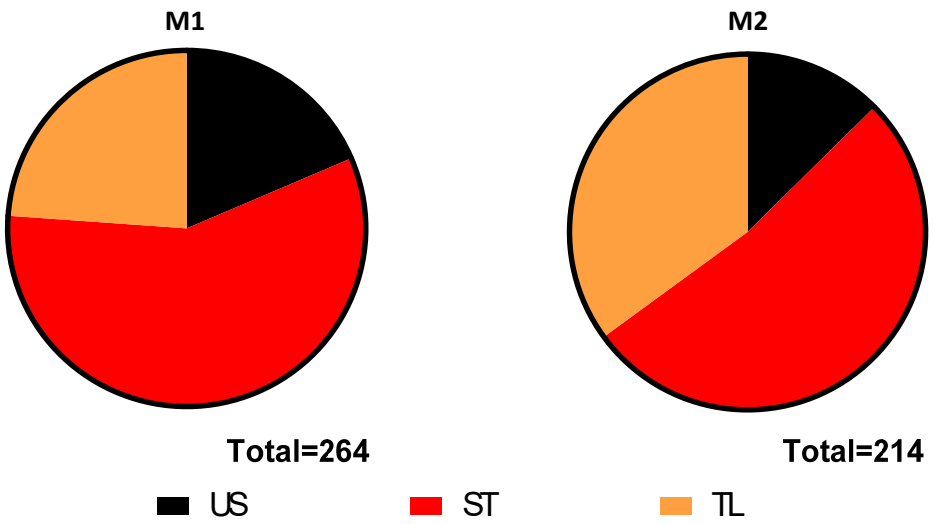

Figure 4.12 Relative protein expression between subsets per stimulatory state. Protein expression was compared between M1 and M2 subsets and those which demonstrated a 2-fold positive increase in subset vs subset were plotted. Following a single stimulation, 152 proteins were expressed higher in M1 vs M2 MΦs and 112 in M2 vs M1 MΦs. 49 proteins were higher in M1 vs M2 MΦs in the unstimulated state, with 27 higher in M2 MΦs. In the tolerised state, following a secondary stimulation, 75 proteins were higher in the M2 subset compared with M1 MΦs and 63 higher in M1 MΦs.

Relative expression of proteins was compared to examine the potential demonstration of plasticity on the individual protein level, between subsets (Fig 4.12). Previous observations, which have demonstrated opposing responses to stimulation and tolerisation and between subsets, on a single protein level as well as gene ontology terms, indicates a level of plasticity depending on stimulatory status. To examine this further, original LFQs were compared for each stimulatory status of each subset (Fig. 4.13). For each status, the three states of the opposing subsets are compared to determine which proteins were detected within 95% of any state of the opposing subset (Fig 4.14). Within these proteins are several groups which are pleiotropic in nature. These include annexins 2, 4, 5 and 11, however, the states at which these proteins are expressed at a similar level in

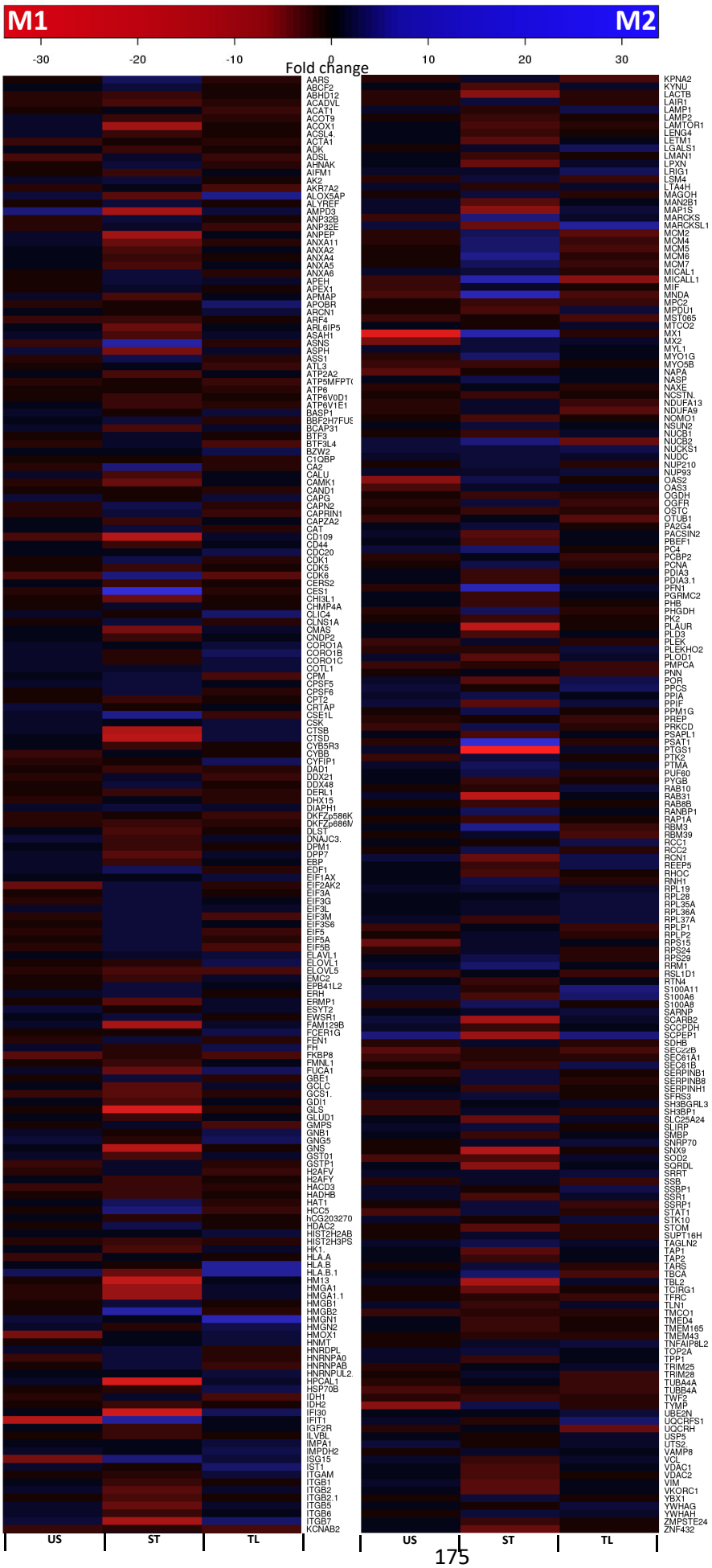

Figure 4.13 Heatmap demonstrating relative levels of expression between MΦ subsets for each stimulatory status. Protein expression was compared between subsets for each stimulatory status. Those demonstrating a 2-fold change between subsets was mapped whereby those expressed higher in M1 MΦs are shown in red and those in M2 MΦs in blue.

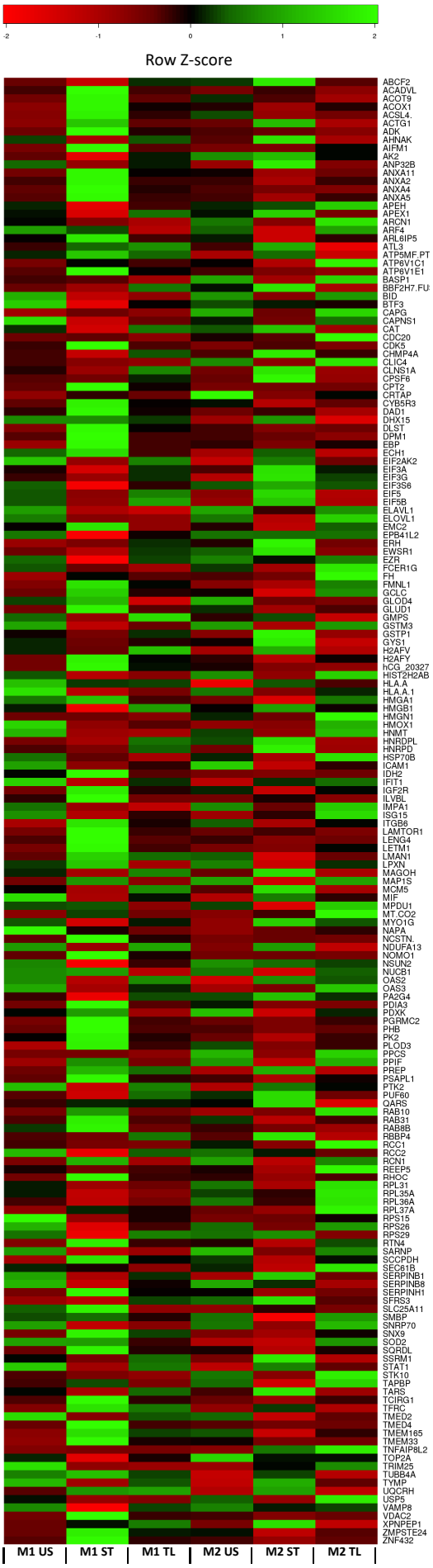

Figure 4.14 Heatmap of proteins which achieve 95% LFQ level of opposing subset, demonstrating plasticity between MΦ subsets. The LFQ value for each protein within a stimulatory status was compared with those of each status of the opposing subset to determine similarity of expression under different stimulation. Only those which achieve a similar level of expression (within 95%) are listed.

Scaling is per row due to the variation in LFQ level between proteins for visualisation purposes, as such each protein is illustrated with a representative row Z-score and protein expression is therefore not comparable between proteins.

both the unstimulated and tolerised state, indicating a similarity in response rather than plasticity. The eukaryotic initiation factors display variation in expression when analysed using this method. EIF3A, EIF3G and EIF3S6 are also expressed at similar levels when comparing unstimulated and tolerised MΦs between subsets. EIF2AK2, EIF5 and EIF5B however, differ and suggest a level of plasticity depending upon stimulatory status; EIF2AK2 sees an almost identical level of expression (99.49%) between M2 MΦs which are stimulated and M1 MΦs which are tolerised with a secondary stimulation. EIF5 and EIF5B display a similar level of expression (99.85% and 95.92% respectively) between unstimulated M2 MΦs and stimulated M1 MΦs. Several proteins already identified as being highly implicated in the type-I interferon responses, display a greatly varying level of expression between subsets. IFIT1 displays similar levels of expression between both unstimulated M2 MΦs and stimulated M1 MΦs (99.95%) and stimulated M2 MΦs and tolerised M1 MΦs (98.62%). ISG15 is also expressed similarly between stimulated M2 MΦs and tolerised M1 MΦs (96.85%). OAS2 is similar between stimulated M2 MΦs and both unstimulated (98.44%) and tolerised M1 MΦs (99.28%). OAS3 however is expressed similar to unstimulated M2 MΦs by stimulated M1 MΦs (99.11%) and STAT1 is similar in tolerised M1 MΦs to stimulated M2 MΦs (97.29%). MX1 and MX2 are not, but as can be observed in figure 4.22, levels of expression deviate substantially depending upon stimulatory status whereby both MX1 and MX2 are higher in M1 MΦs in the unstimulated state (8.25-fold and 4.74-fold respectively in comparison to M2 MΦs), yet stimulated, they are both expressed higher in M2 MΦs (8.25-fold and 2.14-fold).

4.4 Discussion.

Whilst proteomic analysis of MΦs has been carried out previously, this is the first study which analyses MΦ subset response to both stimulation and tolerisation with PG LPS (Boa et al., 2015; Court et al., 2017; Zhang et al., 2019). Furthermore, this study is novel in the use of PG LPS whereby the lipid-A structure was examined prior to its use as the stimulant.

One study that does use proteomic analysis to analyse a complex multi-cellular/ biofilm interaction model, does highlight some similarities with the results in this study (Bao et al., 2015). This host-biofilm model does identify the presence of PG within the biofilm and the incorporation of a monocytic cell line within the system (though they do not specify which cell line is utilised). The resulting supernatants underwent proteomic analysis via LC-MS, and similar to this study GO analysis was performed. Whilst this analysis is performed on all identified proteins which demonstrate a differential expression compared to controls, both responses to unfolded proteins and antigen processing and presentation feature highly in the terms enriched.

Another study which used proteomic analysis to profile polarised MΦs in response to varying oxygen levels, identified a number of proteins found within this study (Court et al., 2017). Their study compared various methods of polarisation to negative controls to assess under and over-regulated proteins which were identified for each polarisation. Two of the polarisation methods were to use IFN-γ in combination with LPS (associated with an M1 phenotype), and IL-4 + IL-13, typically associated with an M2 phenotype. These were then compared to controls. When the expression of these proteins is compared between unstimulated M1 and M2 MΦs within this study, there is a similarity, particularly

between the M1 subsets, where EIF2AK2, HLA-A, IFIT1, ISG15, MARCKS, MX1, MX2, OAS2, SOD2 and STAT1 are all associated with the IFN-γ/LPS induced cells in their study and are expressed higher in unstimulated M1 MΦs than unstimulated M2 MΦs in this study. In addition, PTGS1 was overexpressed in the IL-4/IL-13 induced MΦs which was also expressed higher in unstimulated M2 than M1 MΦs in this study.

ET has also been profiled using proteomic analysis (Zhang et al., 2018). The study uses a murine MΦ (RAW264.7) model and does not specify the origin of LPS used to induce stimulation and tolerisation. GO analysis via DAVID of differentially expressed proteins, does however return several terms which are observed in this study (see proteomic supplemental data). The murine based study observed a number of terms associated with oxidoreductase activation, DNA binding, antioxidant activity, chromatin and vesicle activity, all of which feature heavily within the terms enriched within this study. The murine study however did not go on to associate the direction of responses to each stimulatory status and the number of terms observed was relatively low compared to this study.

Proteomic analysis has also been used to attempt to identify biomarkers from saliva, GCF, blood serum etc (Bostanci et al., 2010; Nguyen et al., 2019; Qasim et al., 2019; Rizal et al, 2020). Again, several of the identified candidate proteins such as annexin-2, carbonic anhydrase-2, hexokinase-2 and members of the S100 family, have been identified within this study and demonstrate differential responses to stimulation between subsets. Annexin-2 may be of particular interest as this was shown to be upregulated in stimulated M1 MΦs and resistant to tolerisation.

Within this study, functional annotation appears to identify distinctly opposing functions and processes in M1 and M2 MΦs in response to stimulation with this specific form of PG LPS. Furthermore, functional annotation appears to suggest that not only does secondary stimulation, i.e. tolerisation, reverse the majority of these functions, but also, many are able to be performed by the opposing subset, often, in response to an opposite stimulatory status.

Whilst in-depth analysis of these findings is examined in chapter 5, due to the relevance of these functions to previous results and how this data informs our understanding of periodontal disease processes, a number of key observations can be made based upon the overall nature of functional processes.

GO analysis suggests that stimulation of M1 MΦs with PG LPS induces a number of responses which may significantly impact on both the initiation and progression of periodontal disease. Several terms were returned associated with entry to a cell, but when gene enrichment is performed, the methods used have no knowledge of the pathogen that is associated with the study from which the dataset arises and therefore could be irrelevant to periopathogens. That said, the mechanism utilised by PG to mediate cellular entry into MΦs is well understood and occurs due to interactions between the outer fimbriae of PG and the Mac-1 complex, Mac-1 is a complement receptor formed from 2 subunits, Integrin Subunit Alpha M (ITGAM or CD11b) and Integrin Subunit Beta 2 (ITGB2 or CD18) (Hajishengallis et al., 2008). Both proteins are identified in this study, with varying responses to both stimulation and tolerisation. The expression of ITGAM remains unaffected by stimulation in both M1 and M2 MΦs, ITGB2 increases in expression, 2-fold in M1 MΦs and decreases 2.6-fold in M2 MΦs, thus potentially facilitating PG internalisation of M1 MΦs and protecting M2 MΦs. Following

tolerisation, expression of ITGB2 is returned to basal level in both subsets, restoring susceptibility to pre-stimulatory levels. ITGAM however demonstrates a 2-fold increase following tolerisation in M2 MΦs only. Conversely, terms associated with cadherin binding were associated with $M1^{ST\downarrow}$ and $M2^{ST\uparrow}$, potentially enabling invasion by *F. nucleatum* which has been suggested to bind cadherins via its FAD-A adhesion in endothelial cells, although this is not fully understood (Fardini et al., 2011). Subsequent tolerisation modifies the protein profiles associated with these terms but they are still enriched from $M1^{ST\downarrow}$ and $M2^{ST\uparrow}$ in addition to $M1^{ST\uparrow}$.

Cellular entry into gingival epithelial cells has recently been suggested to result in residence of PG within autophagosomes of the ER (Lee et al., 2018). The ER is identified in numerous terms enriched across several classifications: $M1^{ST\uparrow}$, $M1^{TL\downarrow}$, $M2^{ST\downarrow}$ and $M2^{TL\uparrow}$. This suggests that the same mechanism is at work in both subsets, but in an opposing fashion. When additional terms are taken into consideration, it raises the possibility that differential mechanisms are responsible, highlighting contrasting responses between M1 and M2 MΦs which may affect disease progression.

In terms associated with the ER, returned under gene enrichment for cellular component, M1 MΦs returned several terms associated with ER stress and the UPR. The role of the UPR in inflammation has been reviewed extensively by Judith Smith (2018) and is likely to be connected to multiple groups of terms also returned from this dataset. The UPR has also been associated with periodontal disease, being induced in mice, administered orally with PG (Yamada et al., 2015). Furthermore, PMA differentiated M1 MΦs have been demonstrated to

upregulate UPR associated genes in response to stimulation with PG LPS as well as human periodontal ligament cells (Domon et al., 2008; Bai et al., 2016).

The UPR can arise due to a number of influencing factors, including hypoxia, increase in protein production demand and the accruing of misfolded proteins. Once activated, the UPR can trigger signalling pathways, initiated via either inositol requiring enzyme 1 (IRE1), activating transcription factor 6 (ATF6) and protein kinase R (PERK, also known as EIF2AK3) (Grootjans et al., 2017; Smith, 2018). IRE1 interacts with just one specific target, XBP1, identified through transcription factor databases in the $M1^{ST\uparrow}$ and $M2^{TL\downarrow}$ protein profiles only. XBP1 increases ER capacity by transcribing chaperones and increasing ER size (Hetz et al., 2011). IRE1 possesses a number of additional functions, including potentially, direct sensing of misfolded proteins and the phosphorylation of c-Jun N-terminal kinase (JNK). Via JNK, a number of mechanisms can be initialised, including autophagy and apoptosis (Nishitoh et al., 2002). IRE1 can also associate with pro-apoptotic Bcl2-agonist/killer 1 (BAK1) and Bcl-associated X protein (BAX) (Hetz et al., 2006). BAX and its agonist - BH3 Interacting Domain Death Agonist (BID) form part of the BCL-2 family of death regulators and are both found within our proteomic data from the M1 MΦ dataset. The expression of these proteins however is reduced upon stimulation; BID 2.7-fold and BAX 5.5-fold. Tolerisation fails to fully restore basal levels, with BID remaining 2-fold, and BAX 2.9-fold below the unstimulated level. Apoptosis is not inevitable via the UPR, and TLR signalling is suggested to modify the UPR, initiating a partial response to ER stress (Smith, 2018). This conforms to observations made throughout the experimental process regarding levels of cell death, remaining unaffected by stimulation. It should be noted however, that apoptosis generally results from prolonged ER stress and the increase in terms associated with the

mitochondria combined with increases in mitochondrial/ER interface proteins such as VDAC1 (1.9-fold for $M1^{ST\uparrow}$ and $M1^{TL\uparrow}$), VDAC2 (2.6-fold for $M1^{ST\uparrow}$ and 2.2-fold for $M1^{TL\uparrow}$) and PDIA3 (2.2-fold for $M1^{ST\uparrow}$ and 2-fold for $M1^{TL\uparrow}$), may indicate preparation for apoptotic processes, which are at least in part, still progressing in a tolerised state (Malhotra and Kaufman, 2011). It may of course be that these mitochondrial functions correspond with the generation of ROS as part of the response to stimulation, however, terms associated directly with ROS/RNS are associated with $M1^{ST\downarrow}$. Additionally, as these terms are returned under cellular component, and refer to mitochondrial structure, this may simply be an increase in mitochondrial capacity to increase respiration and maintain cellular responses to stimulation.

PERK phosphorylates EIF2α, inhibiting the action of EIF2β, also known as EIF2S2, which is identified and unchanged in M1 MΦs but increased in M2 MΦs in response to both stimulation and tolerisation (Claudio et al., 2013). This results in a reduction in ribosome function, reducing load requirements of the ER. This can be observed in the terms returned for cellular component which highlight several terms associated with the ribosome in the $M1^{ST\downarrow}$ group. EIF2α phosphorylation, interestingly, can lead to the production of the C/EBP homologous protein (CHOP), a key transcription factor for IL-23 (Marquez et al., 2017). TLR4 signalling however has been shown to suppress ER stress associated CHOP activity and therefore may explain the lack of IL-23 production observed in M1 MΦs (Woo et al., 2009). Of further interest is the ability of PERK to be phosphorylated, independently of ER stress. EIF2AK1 has the ability to do this and is induced by low levels of haem and increased oxidative stress, as does EIF2AK2 in response to double stranded RNA (Smith, 2018). Additionally, as a

function of the UPR, heatshock 70 family protein (BIP), preferentially binds misfolded proteins and releases ATF6, which interacts with a number of transcription factors, including XBP1 and cyclic AMP-response-element-binding protein (CREB) (Asada et al, 2011). Further to these observations, PERK can initiate autophagy (requiring the utilisation of a variety of cellular bodies) and phosphorylate NRF2 (TF that is identified associated with the $M1^{ST\uparrow}$ profile) resulting in antioxidant protein production, which may serve to regulate ROS production (Cullinan et al., 2003). The tolerised state of M2 MΦs appears to demonstrate a level of similarity with those associated with the UPR in M1 MΦs. The UPR response is almost ablated in $M2^{TL\uparrow}$ with just a single term returned. As has been previously demonstrated, stimulation and tolerisation may alter susceptibility of M2 MΦs to cellular internalisation by periopathogenic bacteria, but it is likely that the terms associated with cellular entry observed from both the $M2^{ST\downarrow}$ and $M2^{TL\uparrow}$ profile is due to the hijacking of MHC receptors as routes of internalisation (Blum, Wearsch and Cresswell, 2013).

Antigen processing and presentation are prominent terms returned under molecular function and biological process. Previous studies have shown differential antigen processing and presentation responses following stimulation with PG LPS, suggesting a reduced capability within the M2 subset to perform clearing of phagocytosed bacteria (Lam et al., 2016). Within this study, peptides were identified within the proteome which were identified as HLA-A and HLA-B, members of the MHCI antigen processing and presentation mechanism. MHCI molecules, reside in the ER and receive antigens translocated from the cytosol. There is also a mechanism whereby MHCI can receive proteins normally associated with MHCII presentation via cross-presentation (Blum, Wearsch and Cresswell, 2013). Translocation to the ER occurs via a group of Transporter

Associated with Antigen Processing proteins, TAP1, TAP2 and TAP binding protein (TAPBP). All three are identified within the proteomic data and all follow a similar trend in the M2 subset, being supressed in response to stimulation, TAP-1, 2.2-fold, TAP2, 1.9-fold and TAPBP 2-fold and subsequently restored 3.2-fold, 2.2-fold and 2.5-fold respectively, on tolerisation. Again, these processes require the utilisation of numerous cellular bodies and may have severe implications for the initiation of periodontal disease and survival of internalised pathogens.

The profile of terms associated with the $M2^{ST\uparrow}$ profile raises a number of questions, moreover, the resemblance to the terms returned for the $M1^{ST\downarrow}$ and $M1^{TL\uparrow}$ profiles is remarkable. These terms can be viewed as three separate groups; modifications which affect transcriptional and translational events, responses to stimulation and the likely associated, cellular bodies an adhesion group. That these groups are identified from the $M2^{ST\uparrow}$ profile is not particularly noteworthy, a response to stimulus is expected which would require an increase in translation and transcription and in addition, responses to stimulus would necessitate the upregulation of lysosomal and phagocytic activity and adhesion molecules. Furthermore, the suppression of these in a tolerised state would seem a logical reversal. What might be unexpected is the initiation of the type-I interferon response. However, type-I interferons have recently connected with both periodontal disease and PG, whereby mice infected via oral gavage with PG, demonstrated a prolonged and unrestrained type-I interferon response (Mizraji et al., 2017). Earlier studies identified the role that PG LPS plays in the instigation of type-I interferon responses and its potential role in periodontal disease (Zhou and Amar, 2007). This group propose that not only does PG LPS instigate interferons-α/β in human PBMCs, but that it contributes to optimal

responses to low doses of LPS, which may correspond with low endotoxin activity.

In this study, type-I interferon responses are also upregulated but only in M2 MΦs following stimulation and also maintained following tolerisation. The downregulation of these mechanisms in M1 MΦs following stimulation indicate that exposure to this specific formation of PG LPS modulates overall immune response. This suggests that the reduction in inflammatory responses observed which show a reduced inflammatory potential compared with canonical *E. coli* derived LPS may not be simply a binding event but may result from a number of down-regulated inflammatory mechanisms in pro-inflammatory MΦs.

Initial examination of these results suggest that PG LPS may be able to prepare MΦs for cellular invasion, particularly M2 MΦs which may be infiltrated prior to disease initiation. Furthermore, internalised bacteria in M2 MΦs may be protected due to the prior down-regulation of MHCI associated processes initiated by LPS stimulation. Tolerisation therefore, may not just limit tissue destruction but may also restore recognition and killing of intracellular pathogens.

The induction of inflammatory cytokines by M1 MΦs may in part result from the UPR in conjunction with LPS mediated signalling events, the reduction of which during tolerisation may in part, be responsible for the reduction in inflammatory cytokine secretion. Whilst other inflammatory mechanisms and transcription factors remain in place.

The analysis of these mechanisms and potential role in periodontal disease, combined with results from previous chapters will be studied in depth in chapter 5.

Chapter 5
General Discussion

5.1 General discussion

Chronic periodontitis is an inflammatory disease which arises from an inappropriate host immune response to a dysbiotic microbiome. This study has analysed the pro- and anti-inflammatory associated MΦ subsets (M1 and M2), as key orchestrators of immune response and lipopolysaccharide, the archetypal MAMP, obtained from both the subgingival margins of healthy and diseased patients, as well as that derived from the keystone pathogen *Porphyromonas gingivalis* (PG). This periodontal opportunist is known to modify the immune-stimulatory lipid-A region of LPS which is exhibited on its outer leaflet. Modification of Lipid-A is known to influence disease progression and immune response in a number of pathologies including cystic fibrosis and meningitis (John et al., 2016; SenGupta et al., 2016). It has also been demonstrated that this mechanism is critical for establishment of the dysbiotic subgingival biofilm, yet the molecular mechanisms which facilitate this are not yet understood (Zenobia et al., 2014). The importance of lipid-A structure in periodontal disease is further demonstrated by the contrasting ability of LPS isolated from patients with CP to induce TNF-α and IL-8 expression in M1 and M2 MΦs. TNF-α is considered a principal inflammatory agent, to the extent that it has been successfully proven to be a therapeutic target for inflammatory diseases (Shealy and Visvanathan, 2008). TNF-α can induce several reactionary signalling pathways, leading to neutrophil adhesion, chemotaxis and apoptosis, MΦ proliferation and osteoclast differentiation (Parameswaran and Patial, 2010; Salamone et al., 2001, Wright et al., 2010). IL-8 however, is primarily recognised as a neutrophil chemoattractant, yet it is known to perform a number of additional functions including angiogenesis and T-helper cell recruitment (Gesser et al., 1996; Shi and Wei, 2016). As such both TNF-α and IL-8 are recognised as critical pro-inflammatory mediators

associated with CP. With relevance to CP, this study shows that these inflammatory cytokines demonstrate differential levels of secretion, dependent upon both MΦ subset and structure of LPS. TNF-α secretion being induced significantly higher in M1 MΦs compared to M2 MΦs when stimulated with *E. coli* LPS, whilst PG LPS induced a higher level in M2 MΦs. When IL-8 production was analysed, PG LPS induction followed the same trend as *E. coli* LPS induction, being higher in M1 MΦs than M2 MΦs, but with PG LPS inducing a higher level of IL-8 production in M2 MΦs than *E. coli* LPS (Fig. 3.2).

The addition of IL-23 provides a link between adaptive and innate immunity, integral to chronic disease. The absence of IL-23 measured in response to *E. coli* LPS stimulation in either MΦ subset compared to that secreted by M2 MΦs in response to PG LPS and LPS obtained from both healthy and CP patients, implicates the lipid-A modification identified by mass spectrometry in chapter 2, figures 2.6 and 2.7, in initiating this Th_{17} associated response. This suggests that this response is also dependent upon MΦ subset and LPS structure, taken in conjunction with the inability to detect any IL-12 secretion suggests a role for the M2 MΦ subset in propagating Th_{17} responses associated with CP. A study by Allam et al, supports this observation whereby $CD68^+$ and $CD163^+$ (generally considered markers for M2,) MΦs were shown to predominate in periodontal lesions as well as peripheral Th_{17} infiltration. It should be noted however, that this study, as did the study which forms the basis of chapter 2, recruits patients on the basis of existing disease and does not identify the disease activity at the point of sampling. The secretion of IL-23 by $CD163^+$ MΦs is however, also recognised as a key mechanism in the pathology of psoriasis (Eberle et al., 2016). This is a significant observation in a dynamic pathology with a non-linear route of

progression, in that M2 MΦs may instigate adaptive immune responses rather than pro-inflammatory M1 MΦs. Furthermore M2 MΦs retain the ability to produce significant quantities of IL-8, retaining the ability to recruit neutrophils and T-helper cells as well as secreting TNF-α at a level ≥ M1 MΦs, observations that are replicated when MΦs are stimulated with LPS isolated from patient samples.

This suggestion, that M2 MΦs may act as pro-inflammatory mediators in response to LPS with lower levels of acylation and phosphorylation is further supported by the analysis of cytokine production in response to specific LPS isoforms (Fig 3.3), where it is shown that M2 MΦs are, for the majority, more responsive to PG LPS_{1435} over a period of 24 hours, compared to PG LPS_{1690}. In the context of CP, this may have particular relevance to the inappropriate response to the existing biofilm, if MΦs, traditionally regarded as homeostatic are acting in a moderately pro-inflammatory manner. A switch by PG, possibly due to availability of environmental haem, of lipid-A structure may induce differentiation of M1 MΦs, responsive to higher levels of acylation and phosphorylation of lipid-A building on existing inflammation and infiltration with IL-23 production potentially maintained by dendritic/oral langerhan cells (DCs/OLCs) (Gelderblom et al., 2018; Hovav, 2014). Furthermore, the expression of Annexin 5, an anticoagulant, was shown to be increased in M1 MΦs following stimulation and therefore may factor in the availability of environmental haem. This coincides with a 5.3-fold decrease in HMOX1, a critical component in the catabolism of haem following stimulation, this not only serves to elevate environmental availability but also has protective functions, as excessive haem acts as a stressor leading to the UPR. This study has however shown that bleeding is not a good indicator of disease state, but from the clinical parameters measured, bleeding index gave

the best correlation when compared to endotoxin activity as measured by the rFC assay. This further supports the suggestion that haem availability may be critical in modifying disease state due to the presence of haem auxotrophic bacteria such as PG and the response that it has to these environmental cues.

An additional important observation is the similarity between LPS from PG and that isolated from patients recruited to the study in chapter 2. Whilst amplitude changes dependent upon disease state, the overall pattern of cytokine responses are similar to that of PG LPS rather than *E. coli* LPS. As such the ability to detect subtle changes in lipid-A profile utilising the rFC LAL assay may serve as an aid to diagnosis and prognosis.

The consideration of lipid-A modification and its effect on the induction on ET, presents further implications for the progression of CP. Again, subset dependency is shown to affect responses to repeated stimulation with *E. coli* or PG LPS. Given in context of the variation of TNF-α secretion in both subsets in response to these structurally different LPSs, ET has the potential to significantly modify the local microenvironment. IL-8 tolerisation, or the lack there of, serves to demonstrate that ET is not a total suppression of inflammatory responses and brings in to question the proposed hypothesis that ET is a protective mechanism to prevent prolonged inflammation leading to tissue damage. Repetitive stimulation modified IL-8 responses to induce responses of a similar amplitude between subsets, thus demonstrating a commonality (or plasticity) between subsets following tolerisation. These results seem to suggest a persistence in the attraction of PMNs and to a lesser extent $CD4^+$ T-cells, to the extent where the higher acylated and phosphorylated *E. coli* LPS, upregulates this recruitment mechanism on repeated exposure. The suppression of IL-23 however is less

complex, as the secretion of IL-23, only observed in M2 MΦs following single stimulation, is ablated below the level of detection. Recent studies have presented the Th_{17} subset as an opposing subset to regulatory T cells and may therefore indicate the return to a T-reg population, aiding quiescence and tolerance in those recruited by IL-8 (Lee, 2018). This will however, depend upon the local environment and in particular DCs/OLCs, although numbers of OLCs are suggested to be reduced in the oral epithelia as the disease progresses (Hovav, 2014).

Whole cell proteomic analysis allowed for the examination of cellular mechanisms on a number of levels. Gene ontology allows for the inference of mechanisms through enrichment of groups of proteins, allowing for a number of cellular processes to be identified. Similar analysis which utilises databases which infer associations with transcription factors and signalling molecules allow for the analysis of mechanisms which instigate these cellular responses. Finally, analysis of individual proteins identified through mass spectrometry and their relevant levels of expression allow for direct analysis of signalling mechanisms as well as plasticity on a single protein level.

Endotoxin tolerance and plasticity raise a number of questions, particularly what constitutes ET and plasticity?

The description given on page 4 of chapter 1, could be deemed as somewhat of a vague description as a “reduced capacity” is far from a quantitative term. This is likely due to the inability to pin down specific responses. As this study has demonstrated, ET is not a total suppression and some pro-inflammatory responses remain fully functional if not upregulated. This is further complicated by the varying nature of ET (as demonstrated in chapter 3) dependent upon

stimulus and cell type. ET may better be described in observatory terms as a sub-optimal, primary inflammatory response due to repeated exposure to LPS, or indeed a multitude of PAMPS. This is particularly relevant to a chronic pathology such as periodontitis. This study has demonstrated that the profile of lipid-A can significantly influence immune responses, in MΦs but also in PMNs and adaptive immune responses and should be considered in future studies.

Plasticity is a subject of interest, particularly in MΦ immuno-biology (refer to section 1.6.1). In MΦ biology, plasticity generally refers to similarity in behaviour by different MΦ subsets although as highlighted in chapter 1, the validity of MΦ subsets is the subject of debate. Proteomic analysis allows for the determination of these behavioural mechanisms, both functionally and on an individual protein level. If plasticity is measured as the ability of one subset to perform the function of another, or at least shift towards that functional profile, gene ontology results illustrated in figures 4.4 and 4.5, seem to demonstrate a striking resemblance between M1 MΦs which are tolerised and M2 MΦs which are stimulated. To a degree the same could be said tolerised M2 MΦs and stimulated M1 MΦs which are stimulated. This is not however entirely borne out by the cytokine data. A significant disparity remains between M1 and M2 MΦs when IL-8 is measured, regardless of stimulatory status. TNF-α conforms to a degree, whereby, the level secreted by stimulated M1 MΦs is within 12% of stimulated M2 MΦs. Stimulated M2 MΦs however, secreted more than twice that of tolerised M1 MΦs. A tenuous observation could also be made that tolerised M2 MΦs behave like M1 MΦs regardless of stimulation state as they do not produce IL-23. On a singular protein level, it is statistically evident that a significant number of proteins are expressed

at similar levels (within 95%) when stimulatory status is changed between subset, therefore directly displaying plasticity between subsets (Fig. 4.14).

Gene ontology, as well as indicating plasticity, revealed inextricably linked groups of terms which implicates antigen processing and presentation, the UPR, type-I interferon responses as well as antigen processing and presentation in response to this particular profile of PG LPS. The manipulation of these responses due to stimulation and tolerisation may have profound implications for disease pathogenesis.

As discussed in chapter 4, the UPR, combined with terms associated with the ER, cellular bodies and transporter mechanisms form the majority of those observed from proteins which increase in expression following stimulation of M1 MΦs. Misfolded protein activation of IRE1α leads to the splicing of XBP1, resulting in XBP1s, a TF for which TNF-α exhibits a binding site (Smith, 2018). Activated IRE1α also displays the ability to activate AP-1 via a TRAF2/JNK dependent mechanism and furthermore, IRE1α/TRAF2 can phosphorylate IκBK, thus releasing and activating NFκB. PERK via phosphorylation of EIF2α, can also lead to increased NFκB activity via an imbalance in IκB and NFκB production (Smith, 2018). The identification of the positive regulator of IRE1 mediated PERK activation, TMEM33 and IRE1 independent PERK binding TBL2, which both increase in M1 MΦs following stimulation and notably decrease following tolerisation support the implication of PERK mediated signalling (Muaddi et al., 2010; Tsukumo et al., 2014). Not only can these mechanisms drive TNF-α and IL-8 production, but TLR4 mediated IRE1α can lead to splicing of XBP1 which requires TRAF6 (possibly competing with MyD88-dependant and –independent signalling) and ROS production by the NADPH oxidase NOX2, also known as

CYBB, which is shown to be reduced in M1 MΦs following stimulation in the proteomic data, again suggesting that this mechanism is not operative. TLR4 activation does however halt UPR associated ATF4 production, limiting CHOP, a critical transcription factor for IL-23 transcription (Grootjans et al., 2016, Jansens, Pulendran and Lambrecht, 2014, Smith, 2018). It is therefore likely that whilst not all mechanisms are utilised, AP-1, NFκB and XBP1 all promote the inflammatory response whilst suppressing IL-23 production. It is also suggested that specific to MΦs, a reduction in XBP1, limits TNF-α production and particularly affects TLR2 mediated inflammatory responses (Grootjans et al., 2016; Martinon et al., 2010).

The UPR was traditionally associated with viral sensing and is suggested to be an ancient mechanism predating TLRs (Jansens, Pulendran and Lambrecht, 2014). As such PKR (EIF2AK2) phosphorylates EIF2α in response to dsRNA and is regarded as an interferon inducible gene (Claudio et al., 2013). It is rapidly becoming apparent that bacteria known to undergo cellular internalisation can initiate the UPR, albeit in a modified manner, such as the lack of IL-23 production observed in M1 MΦs (Janssens, Pulendran and Lambrecht, 2014; Smith, 2018). The proteomic data supports this notion as PKR as well as the type-I interferon associated proteins are all reduced in expression in M1 MΦs following stimulation. These proteins are however, restored following tolerisation. What is remarkable is the ability of LPS alone to induce this microbial form of the UPR and presents the question as to what is the benefit for PG? This is an area that warrants further investigation, two factors that should be considered are the overall suppression of cellular protein production as a major function of the UPR and the ability of EIF2AK1 (also known as haem regulatory inhibitor) to

phosphorylate EIF2α in response to low haem availability. The processing of misfolded proteins is a homeostatic process which involves proteasomal and lysosomal degradation through mechanisms of autophagy. Overburdening of this system may prove beneficial for internalised bacteria, simply through overwhelming cellular machinery but also through the occupation of the MHCI processing and presentation mechanisms (Blum, Wearsch and Cresswell, 2013). Should this be the case, it does not affect protein expression as proteins which form the TAP complex (unlike M2 MΦs) remain unaffected by stimulation or tolerisation. The instigation of the UPR within M1 MΦs represents an alternative method of instigating an inflammatory response in M1 MΦs by PG and therefore may represent a target for future therapies, as has been suggested in other pathologies (Hsu et al., 2019; Martinez et al., 2019; Walczak et al., 2019).

In M2 MΦs, terms associated with the UPR predominantly arise in terms which are derived from proteins which decrease following stimulation, this is likely due to a cross over in proteins which are associated with both the UPR and antigen processing and presentation. Both MHCI and MHCII pathways appear to be affected by stimulation of M2 MΦs with PG LPS. A greater number of proteins are identified in the proteomic data which are associated with MHCI signalling. As discussed in chapter 4, reduced expression of the MHCI mechanism may favour survival of internalised pathogens such as PG. TAP1 (↓ 2.2-fold), TAP2 (↓ 1.9-fold) and TAPBP (↓ 2.0-fold), all reduce in expression and therefore reduce the potential for peptide transport from the proteasome to the MHCI molecule. Two peptides were identified for both HLA-A and HLA-B and this is probably due to allelic variation. In M2 MΦs HLA-B is also significantly affected by stimulation, with the peptides identified to be HLA-B reduced in expression (↓ 3.6 and 6.1-

fold) compared to the homeostatic (unstimulated) level of expression. All of these MHCI and associated molecules are restored by inducing tolerisation. Furthermore HLA-B and the TAP complex associated proteins are restored to a level above that of the unstimulated expression. MHCII is more conspicuous in identified associated proteins, those that are however show some of the largest variations in expression. Interferon Gamma-Inducible Protein 30 Preproprotein (IFI30), also known as GILT, following stimulation is reduced in expression 27-fold in comparison to the unstimulated level in stimulated M2 MΦs. This protein is critical in endosomal processing of peptides prior to MHCII presentation along with the cathepsins, of which cathepsins B (↓ 6.9-fold), and D (↓ 4.7-fold), are also significantly reduced in expression. Gene enrichment returned a number of general terms associated with cellular bodies and these also were identified as terms which arose from proteins which reduced in expression following stimulation. Late endosomal adaptor 1 (LAMTOR1) is however, unaffected in M2 MΦs by stimulation or tolerisation. As with MHCI associated proteins, expression of these proteins is restored above the unstimulated level; IFI30 is expressed some 39.6-fold higher in tolerised M2 MΦs compared to stimulated M2 MΦs, thus presenting an additional mechanism of T-cell activation and regulation.

This response is contradictory to what is understood regarding cytokine initiation of MHC expression. Both TNF-α and type-I interferons are known to induce MHC upregulation (Gessani et al., 2014; Hallermalm et al., 2001). As such an alternative method of transcriptional regulation is likely to be supressing MHC expression following stimulation, possibly due to SP1 and ATF2, transcription factors which are identified associated with genes that decrease in expression in M2 MΦs following stimulation (Fig. 4.5) and for which the GeneHancer database

indicates HLA-B has binding sites. Alternatively, another protein that demonstrated a substantial amount of variation in expression is prostaglandin synthase 1 (PTGS1), also reduced 18-fold in comparison to unstimulated levels is stimulated M2 MΦs. This response is restored to basal levels following stimulation and inhibitors of PTGS1 are known to reduce MHC presentation in DCs (Kim et al., 2010). Modification of antigen processing and presentation represents a significant finding which may not only affect the survival of internalised bacteria but may also significantly modify T-cell responses. This adds to the importance of understanding MΦ subsets and further implicates M2 MΦs in the disruption of an appropriate immune response, critical to the onset of CP.

Type-I interferons however, appear to be expressed independently of PTGS1 and it is likely that IFN-β is induced via TLR4 mediated IRF3 activation through the endosomal TRIF/TRAM pathway (Fig. 1.7) (Honda, Takaoka and Taniguchi, 2006). The regulation of type-I interferons is observed through multiple proteins and which act in a similar manner, reduced following stimulation of M1 MΦs and restored following tolerisation. In M2 MΦs, stimulation upregulates these proteins, which remain increased following tolerisation. In M2 MΦs the effects of this can be observed in STAT1 expression. STAT1 expression is decreased in M1 MΦs following stimulation and subsequently restored following tolerisation. In M2 MΦs, stimulation increases expression, with tolerisation failing to restore STAT1 expression to the unstimulated level. Whilst the level of phosphoSTAT1 is unknown, the expression profile of PTK2 is similar to STAT1, of which PTK2 promotes its phosphorylation. Mice deficient in STAT1 are shown to be susceptible to intracellular pathogens and so may represent an immune response to attempt to combat the reduction in MHC activity (Majoros et al., 2017).

Furthermore, STAT1 is often referred to as an M1 MΦ marker and therefore also indicates a level of MΦ subset plasticity (Wang, Liang and Zen, 2014). Type-I interferons signal through receptors which, as does IL-10, IL12 and IL-23 (amongst others), recruit the receptor associated proteins of the JAK/STAT pathway (Bousoik and Aliabadi, 2018). The instigation of type-I interferon responses in M2 MΦs may therefore have significant implications for disease progression. The proteomic data to support the activation of this critical pathway is extensive, not just its activation in M2 MΦs but its suppression in M1 MΦs. Ezrin, part of the 4.1 JAK homology domain, is reduced following stimulation and restored following tolerisation. Whilst proteins that are directly associated with type-I interferons via gene ontology analysis adheres to this pattern of expression between subsets, accessory proteins do exhibit some form of tolerisation.

Importin subunit α (KPNA2) is expressed 3.6-fold lower than the stimulated state which was 2.2 -fold higher than the unstimulated state. KPNA2 binds the nuclear localisation sequence (NLS) on the protein to be transported to the nucleus. It is debated as to whether STATs present a functional NLS but this is something that is found on both the Interferon-induced dynamin-like GTPase' MX1 and MX2, induced and identified as type-I interferon associated proteins. Energy to perform this translocation is generated via the GTPase RAN, RAN binding protein (RANBP) expression interestingly, is only significantly modified in M1 MΦs, in parity with the type-I response observed earlier, in M2 MΦs it remains unchanged (Bousoik and Aliabadi, 2018). KPNA2 and RAN (liberated from inhibition by RANBP) forms a complex with exportin 2 (CSE1L). This transportation associated protein is dramatically supressed in M1 MΦs (↓ 18.2-fold) following stimulation and is only partially restored following tolerisation, being 6.9-fold higher than the

stimulated state but still 2.7-fold lower than the unstimulated state. In M2 MΦs, KPNA2 is one of the few proteins which behaves in a similar manner, being reduced following stimulation, tolerisation however, increases the level of suppression 2.2-fold. As such KPNA2 is expressed 5.7-fold higher in M2 MΦs following stimulation compared to M1 MΦs but this switches to being expressed 2.6-fold higher in M1 MΦs following tolerisation, another example of MΦ plasticity on a protein level. Although not detected, suppression of type-I interferons combined with a lack of IL-12 or IL-23 secretion suggests a potential role for SOCS mediated regulation (Liau et al., 2018). SOCS regulation would also implicate IL-10 activation which was also not detectable, previous studies by this laboratory, have however demonstrated that IL-10 is secreted at low levels and is often retained endogenously or membrane bound (Al-shaghdali et al., 2019; Foey et al., 2017). Furthermore, it is also shown by this group that IL-10 secretion is predominantly produced by M1 MΦs, dependent upon stimulus (Al-shaghdali et al., 2019). IL-10 and IFN signalling both utilise the JAK/STAT pathway and as such an amount or cross-regulation occurs between these signalling mechanisms. IL-10 is associated with STAT3, whereas type-I interferons are associated with STAT1 (Regis et al., 2008). Priming with type-I interferons can however reprogram IL-10 mediated signalling to promote STAT1 activation, to compound this further, accumulation of STAT1 negates STAT3/IL-10 driven suppressive mechanisms (Hu, Chakravarty and Ivashkiv, 2008). Priming also sensitises MΦs to stimulation with LPS, yet this includes priming of TLR4 induced IL-10 production which should induce suppressive mechanisms; subversion of STAT signalling, as is shown above can negate this regulatory effect. It is likely therefore that interferons play a significant role in IL-10 mediated suppressive mechanisms and MΦ responsiveness to them (Hu, Chakravarty and Ivashkiv,

2008; Park et al., 2017). This mechanism is potentially also susceptible to further manipulation and modification, as TNF-α is shown to, in combination with type-I interferons, modify chromatin accessibility to allow gene transcription (Park et al., 2017). This is of particular interest given the substantial amount of terms which arose associated with epigenetics and transcriptional mechanisms, and their opposing behaviour between subsets. It is likely that initial TLR stimulation with PG LPS induces traditional pro-inflammatory MyD88-dependant mechanisms and that the induction of the UPR confers a beneficial extracellular environment due to a general down-regulation of protein synthesis, whilst the observed maintenance of IL-8 secretion, increase in PMN recruitment leading to tissue damage and therefore additional levels of haem availability. Furthermore the downregulation of interferons and epigenetic associated proteins following stimulation of M1 MΦs, may avoid this reprogramming whilst limiting the deleterious effects of type-I interferons on PG. Reduction in epigenetic associated terms may also elucidate a restrictive mechanism which limits TNF-α production compared to that induced by *E. coli.* Restoration of these mechanisms is therefore likely to control the suppressive mechanisms associated with ET in M1 MΦs. M2 MΦs however, appear to favour internalisation and confer a benefit to PG by reducing antigen processing and presentation. The mechanisms associated with reprogramming, i.e. type-I interferons, TNF-α and epigenetics are all upregulated following stimulation of M2 MΦs and therefore are already in place. It is distinctly plausible that the reprogramming mechanisms are induced by PG but at different stages in M1 and M2 MΦs, during stimulation of M2 MΦs, modifying response to both stimulation and tolerisation but only following tolerisation of M1 MΦs. This therefore would account for the striking resemblance

mentioned earlier in figures 4.4 and 4.5 between tolerised M1 MΦs and stimulated M2 MΦs, demonstrating a level of reprogramming and plasticity.

These findings have significant implications for the pathogenesis of disease, incorporating adaptive as well as innate immunity. Whilst this study has demonstrated the ability of PG LPS to induce IL-23 production in M2 MΦs, favouring Th_{17} differentiation, additional cytokine responses may also influence Th mediated immunity. It is also known that IL-12b p40 requires increased chromatin accessibility and therefore the induction and suppression of IL-23 (IL12b p40 and IL23a p19) may be regulated by this mechanism as terms associated with chromatin and epigenetic modification were increased following stimulation in M2 MΦs but decreased following stimulation. The production of IL-10 in the absence of IL-23 therefore may play a critical role in maintaining T-reg populations along with TGF-β. Of particular relevance to TGF-β is the expression of CD109, a negative regulator of TGF-β signalling, thus disrupting the positive feedback loop which may attenuate production (Yan, Xiong and Chen, 2017). Interestingly CD109 remained mostly unaffected in M2 MΦs with a slight upregulation following tolerisation. In M1 MΦs CD109 was significantly induced by stimulation (3.2-fold) and substantially reduced following tolerisation, 8.3-fold vs the stimulated level and 2.6-fold lower than the unstimulated level. This suggests that the suppressive effects associated with TGF-β may be associated with M1 tolerisation but also that tolerisation of M1 MΦs restores Treg populations.

The reprogramming mechanisms highlighted above potentially modify transcription factor and signalling molecule activity. As such transcription factors and signalling molecules indicate a number of TFs recognised as significant

inducers of TNF-α, IL-8 and IL-23. Signalling molecules which are associated with proteins which increase following stimulation in M1 MΦs, indicate roles for the AP-1 family of TFs (JUN and ATF2) as well as NFκB (IκBKE and NFκB1). This is somewhat contradicted as IκBKE, NFκB1 and JUN are also identified in those proteins which decrease following stimulation and might demonstrate an element of fine tuning. Whilst not indicated by cross referencing with the GeneHancer database, NFκB signalling is known to promote the transcription of all three cytokines (Falvo, Tsytsykoa and Goldfeld, 2010; Jundi and Greene, 2015; Liu et al., 2000; Mise-Omata et al., 2007). Many of those which form these down-regulated profiles are however, proteins which affect DNA access and transcription, including MMCs 2-7, the histone binding nuclear autoantigenic sperm protein (NASP) and histone deacetylase HDAC2 and may suggest an aspect of epigenetic regulation. TFs identified using the USCS_TFBS database are wide ranging and implicate a number of TFS including the ATF family, but also CREB, NRF2, RFX1, SP1, and XBP1. From proteins which decrease in M1 MΦs, only Nuclear transcription factor Y (NFY) arises, a transcription factor which, Immunologically is associated with transcription of MHC class II related genes and the TGF-β II receptor (Ly, Yoshida and Yamaguguci, 2013). There are therefore a number of transcription factors which are able to induce transcription of the cytokines of interest in M1 MΦs. This may though, be moderated by epigenetic factors, some of which such as, MCM2 and MCM7 for which the TNF-α promoter possesses TF binding sites and HDAC2 which acts a s a promotor or enhancer for TNF-α, IL-8 and IL-23 p19 on their own. Furthermore the synergistic relationship between AP-1 and NFκB, as well as CREB, which leads to optimal

IL-8 production may serve to upregulate IL-8 production in M1 MΦs compared to the M2 subset (Jundi and Greene, 2015; Bezzerri et al., 2011).

Signalling molecules associated with proteins which increase following stimulation of M2 MΦs centre around NFκB signalling, featuring IκBKE, NFκB1, NFκB2, NFκBIα and RELB as well as MAP3K14, accumulation of which increases NFκB activity (Oeckinghaus, Hayden and Ghosh, 2011; Yang and Sun, 2015). That said, the inhibitory NFκBIα (also known as IκBα), which interacts with the REL family dimers to inhibit NFκB activity, is again primarily due to epigenetic modifying factors (Verma, 2004). The largest protein profile associated with a signalling molecule in this group is that of JUN, which consists of 37 proteins, (the NFκBIα profile is made up of 5). In M2 MΦs, after stimulation, ATF2 only arises from proteins which decrease, although with a relatively small protein profile. As such primary candidates for the signalling mechanisms utilised by M2 MΦs seem also to be the AP-1 and NFκB pathways, albeit associated to an alternative set of proteins. For M2 MΦs however epigenetic modifying proteins such as the MCM family are upregulated and may account for the increased production of TNF-α observed in M2 MΦs compared to M1 MΦs which may be subject to epigenetic regulation.

The visible divergence in cytokine expression occurs following secondary stimulation, whereby IL-8 observes a slight increase in both subsets, TNF-α is suppressed to a greater extent in M2 MΦs compared to M1 MΦs and IL-23 secretion is no longer measurable from M2 MΦs. TFs analysed following tolerisation indicates the restoration of NFY in M1 MΦs and therefore may contribute to the suppressive nature of ET via TGF-β signalling. Proteins which decrease from the stimulated state following tolerisation are associated with a

total of thirteen TFs. CEBPβ, SP1 and YY1 all have corresponding binding sites on the TNF-α gene and were upregulated following stimulation and therefore may account for some of the partial reduction observed following tolerisation.

Of significant importance is the association of proteins which decrease with NFκB and so it is likely that this pathway is integral to the suppression of TNF-α. This is the only time that NFκB was referred to directly, rather than an integral part of the signalling pathway, i.e. NFKB1, IκBKE. Signalling molecules are for the majority the reverse of those observed following stimulation whereby AP-1 and NFκB dominates but the epigenetic associated proteins are now in the group of proteins which have increased following tolerisation. This may indicate that whilst access to transcription has increased, the mechanisms requiring it have reduced.

Tolerisation of M2 MΦs introduces a number of TFs which were not identified following a single stimulation. ELK1 and SRP are both shown to correspond to promoter regions on the IL-23 p19 gene as does TRIM28, and therefore may propose the mechanism for IL-23 suppression. TFs which bind the TNF-α promoter/enhancer, only identify YY1, a TF also associated with down-regulated poteins in M1 MΦs following tolerisation. Signalling molecules however implicate the NFκB pathway in a direct reversal of those observed following stimulation.

There is no standout candidate to explain the lack of IL-8 suppression following tolerisation. There is however a number of aspects which point to the AP-1 family in maintaining IL-8 production. JUN and ATF2 occur throughout when signalling molecules are analysed. Following stimulation, JUN is associated with proteins which increase in M1 and M2 MΦs as well as those that decrease in M1Φs. After tolerisation JUN is associated with both those that increase and decrease in both

subsets. ATF2 is associated with those that increase in M1 MΦs and decrease in M2 MΦs following stimulation, whereas this is reversed after tolerisation. ATF2 is also identified in proteins which increase following stimulation in M1 MΦs, but a key observation is the association of 73 proteins which increase following tolerisation of M2 MΦs, with AP-1. Whilst this is by no means conclusive, the other candidate TFs, CEBPβ and NFκB or its subunits, whether as a TF or signalling molecule appear as a term associated solely with proteins which decrease in expression. NFκB, as previously mentioned is identified as a TF associated with proteins that decrease in M1 MΦs following tolerisation, NFKB1 is identified in those that decrease following stimulation or tolerisation of M1 MΦs, whilst NFκB1, NFκB2 and RELB are all identified inform proteins which decrease following tolerisation of M2 MΦs.

Another possibility is that opposing mechanisms are operating between M1 and M2 MΦs and that CREB, identified in M1 MΦs following stimulation is responsible for IL-8 production in the M1 subsets as this TF does not occur in those that are associated with proteins that decrease in following tolerisation. CREB binding protein also has a function in counteracting the suppressive effects of histone deacetylases such as HDAC1, of which HDAC2 is a paralog. The proteomic data indicates that HDAC2 is reduced in relative expression following initial stimulation, thus removing one of the brakes halting IL-8 transcription. Tolerisation however restores expression to a near identical level and so this cannot be considered the mechanism for continuous expression of IL-8 in M1 MΦs. The transcription factor and signalling molecule data remains inconclusive, but points towards AP-1 playing a significant role in the induction of IL-8 in both subsets. It is likely that this is synergistic with aspects of NFκB signalling,

determined critical to IL-8 transcription in the literature, as well as CREB in M1 MΦs (Hoffman et al., 2002; Mukaida et al., 1994).

5.2 Conclusions

This study has demonstrated a clear link between lipid-A structure and periodontal disease and puts forward the suggestion that the rFC assay may potentially act as a diagnostic tool to aid clinicians. In addition, PG LPS has been demonstrated to initiate diverse and opposing reactions in MΦ subsets, at times, which defer from the accepted subset categorisation. M2 MΦs stimulated with PG LPS may act as a potentially more detrimental subset in periodontal disease, producing higher levels of pro-inflammatory TNF-α and inducing Th_{17} differentiation via IL-23 production. The weak response observed in M1 MΦs may be due to the induction of ER stress and the UPR causing a decrease in overall protein production, whereas tolerisation of M1 and the stimulation and tolerisation of M2 MΦs is proposed to be due to reprogramming event conferred by a combination of TNF-α, type-I interferons and epigenetic regulation, modifying primary transcription factors such as NFκB, AP-1 and CREB. It is therefore proposed that a level of plasticity does occur between subsets, but this does not include the stimulated M1 MΦs. The question of plasticity as discussed previously, is open to interpretation and whilst subsets may not always display markers (supposedly) associated with the opposing MΦ, if plasticity is measured as the ability to perform similar functions, there would appear to be an element of plasticity evident even down to an individual protein level.

Key Findings:

1. **Lipid-A isolated from patients with chronic periodontitis demonstrates a higher level of acylation and phosphorylation than healthy patients.**
2. **Lipid-A from patients with periodontal disease demonstrates a higher level of endotoxin activity, which directly correlates with inflammatory potential.**
3. **The sensitivity and specificity of the rFC LAL assay to lipid-A modification indicates its potential to be used as a diagnostic aid for clinicians.**
4. **M1 and M2 MΦs respond differentially to lipid-A modification, PG LPS stimulates a higher level of TNF-α and IL-23 production in M2 MΦs compared to M1 MΦs and compared to *E. coli* K12 LPS stimulation.**
5. **IL-8 secretion is resistant to tolerisation initiated using PG LPS in both subsets, yet is significantly reduced following tolerisation with *E. coli* K12 LPS in the M1 subset.**
6. **IL-23, induced by PG LPS stimulation of M2 MΦs is ablated following tolerisation.**
7. **Proteomic analysis indicates the ability of PG LPS to induce the unfolded protein response in M1 MΦs leading to a general downregulation of protein production.**
8. **In M2 MΦs, proteomic analysis revealed a potential evasion mechanism due to the manipulation of antigen processing and presentation mechanisms.**

9. **Tolerised M1 MΦs largely resemble stimulated M2 MΦs and plasticity is demonstrated on both a protein and gene ontology term level between M1 and M2 MΦs depending upon stimulatory stimulus.**
10. **This study proposes 2 mechanisms which are driving the observed stimulated and tolerised responses:**
    a. **In stimulated M1 MΦs, the UPR response combined with traditional M1 MΦ inflammatory mechanisms leading to NFκB and AP-1 transcription factor activation drive inflammation.**
    b. **In tolerised M1 MΦs, and both stimulated and tolerised M2 MΦs, the combination of TNF-α, type-I interferons and epigenetic modifications modify MΦ phenotype.**

5.2 Future studies

This study has brought a number of novel findings which may both increase our understanding of MΦ biology as well as the progression of periodontal disease. To build on these findings and further develop our understanding, future studies should be based on 5 key areas, highlighted by the data in this study:

1. **Development of the rFC assay into a chairside test to aid clinicians in diagnosing and planning for dental treatment plans.** The rFC assay itself is a relatively simple colourimetric assay, which does not require substantial methods of preparation, as neither does the plaque sample collection method. The isolation of LPS from subgingival plaque samples is however somewhat time consuming and complex and it is this protocol which may either need refining or the optimisation of an alternative, simpler method.

2. **Susceptibility of MΦ subsets to PG internalisation.** Proteomic analysis has indicated a propensity for differential mediation of bacterial internalisation in response to stimulation with PG LPS. Further studies would incorporate pre-treatment of M1 and M2 MΦs with PG LPS followed by cultured PG to assess the effect of prior stimulation with LPS on the internalisation of PG. this could be assessed via transmission electron microscopy (TEM) in conjunction with immunostaining for the Mac-1 complex, either as part of the TEM protocol of via flow cytometry. TEM and/or a 3D imaging technique such as focussed ion beam scanning electron microscopy (FIB-SEM) or serial block face imaging would also help to identify the intracellular space that is occupied by the internalised bacterium.

3. **Characterisation of the type-I interferon responses.** Studies are currently ongoing to assess the type-I interferon response suggested to initiated by the proteomic data. Experiments are being repeated and ELISAs are being optimised to detect for secreted type-I interferons. In addition, attempts are being made to find a reliable method to label PG LPS to allow for the visualisation of LPS internalisation via TEM. Confirmation of preferential internalisation of PG LPS (and TLR4), compared to *E. coli* LPS, would suggest the utilisation of the Myd-88 independent pathway. Future studies would follow to quantify the activation of this pathway, potentially via a cell reporter/SEAP assay followed by PCR and Western blot to better quantify interferon transcription and translation.

4. **Antigen processing and presentation.** Future studies would analyse two aspects of antigen processing and presentation: the ability to activate T cells and the ability to phagocytose and clear the internalised bacteria. This could be done in a number of ways but co-culture of MΦs which have been either stimulated or tolerised with PG LPS in addition to whole bacteria, with T-cells followed by analysis of T-cell activation markers would potentially indicate the functionality of antigen processing and presentation markers. Further analysis of the proteins identified within the proteomic data such as the tap binding complex via PCR and western blot would further indicate the effects of PG LPS stimulation and tolerisation on these mechanisms. Preliminary studies are planned to assess the degradation of internalised bacteria following stimulation and tolerisation. This is to be carried out by introducing PG to unstimulated, stimulated and tolerised

MΦs, with cells being washed and fixed over a period of time to allow for analysis via TEM of internalised bacterial integrity.

5. **Confirmation of the UPR in M1 MΦs in response to stimulation with PG LPS.** Multiple approaches are possible for the determination of the activatory mechanisms of the UPR. Again, TEM analysis is being optimised to best stain samples to image ER structure. This will need to be combined with other analytical techniques such as PCR to analyse the expression of UPR associated genes such as IRE1-alpha, XBP1, PERK, ATF6, and CHOP. Ultimately it is intended that immunofluorescent labelling of UPR associated proteins such as those above will determine the level and localisation of expression via confocal microscopy. This can then be combined with FIB-SEM analysis to analyse ER size and structure on the nanoscale.

As a result of this study, all future work where LPS is required, prior analysis to quantify the lipid-A composition should be performed and stated.

References

AAS, J. A., PASTER, B. J., STOKES, L. N., OLSEN, I. & DEWHIRST, F. E. 2005. Defining the normal bacterial flora of the oral cavity. *Journal of clinical microbiology,* 43**,** 5721-32.

ABRAHAM, C. & CHO, J. H. 2009. Inflammatory Bowel Disease. *N Engl J Med,* 361**,** 2066-78.

ABUSLEME, L., DUPUY, A. K., DUTZAN, N., SILVA, N., BURLESON, J. A., STRAUSBAUGH, L. D., GAMONAL, J. & DIAZ, P. I. 2013. The subgingival microbiome in health and periodontitis and its relationship with community biomass and inflammation. *Isme j,* 7**,** 1016-25.

ADKINS, J. N., VARNUM, S. M., AUBERRY, K. J., MOORE, R. J., ANGELL, N. H., SMITH, R. D., SPRINGER, D. L. & POUNDS, J. G. 2002. Toward a human blood serum proteome: analysis by multidimensional separation coupled with mass spectrometry. *Mol Cell Proteomics,* 1**,** 947-55.

AGGARWAL, S., GHILARDI, N., XIE, M. H., DE SAUVAGE, F. J. & GURNEY, A. L. 2003. Interleukin-23 promotes a distinct CD4 T cell activation state characterized by the production of interleukin-17. *J Biol Chem,* 278**,** 1910-4.

AL-QUTUB, M. N., BRAHAM, P. H., KARIMI-NASER, L. M., LIU, X., GENCO, C. A. & DARVEAU, R. P. 2006. Hemin-dependent modulation of the lipid A structure of *Porphyromonas gingivalis* lipopolysaccharide. *Infection and immunity,* 74**,** 4474-85.

AL-SHAGHDALI, K., DURANTE, B., HAYWARD, C., BEAL, J. & FOEY, A. 2019. Macrophage subsets exhibit distinct *E. coli*-LPS tolerisable cytokines associated with the negative regulators, IRAK-M and Tollip. *PLoS One,* 14**,** e0214681.

ALEXANDER, C. & RIETSCHEL, E. T. 2001. Bacterial lipopolysaccharides and innate immunity. *J Endotoxin Res,* 7**,** 167-202.

ALEXOPOULOU, L., HOLT, A. C., MEDZHITOV, R. & FLAVELL, R. A. 2001. Recognition of double-stranded RNA and activation of NF-κB by Toll-like receptor 3. *Nature,* 413**,** 732.

ALHAWI, M., STEWART, J., ERRIDGE, C., PATRICK, S. & POXTON, I. R. 2009. *Bacteroides fragilis s*ignals through Toll-like receptor (TLR) 2 and not through TLR4. *Journal of medical microbiology,* 58**,** 1015-22.

ALJEHANI, Y. A. 2014. Risk factors of periodontal disease: review of the literature. *International journal of dentistry,* 2014**,** 182513-182513.

ALLAM, J. P., DUAN, Y., HEINEMANN, F., WINTER, J., GOTZ, W., DESCHNER, J., WENGHOEFER, M., BIEBER, T., JEPSEN, S. & NOVAK, N. 2011. IL-23-producing CD68(+) macrophage-like cells predominate within an IL-17-polarized infiltrate in chronic periodontitis lesions. *J Clin Periodontol,* 38**,** 879-86.

ANANTHAKRISHNAN, A. N. 2015. Epidemiology and risk factors for IBD. *Nature Reviews Gastroenterology & Hepatology,* 12**,** 205-217.

ANDERSON, K. V., BOKLA, L. & NUSSLEIN-VOLHARD, C. 1985. Establishment of dorsal-ventral polarity in the Drosophila embryo: the induction of polarity by the Toll gene product. *Cell,* 42**,** 791-8.

ANDO, T., KOMATSU, T., NAIKI, Y., YOKOCHI, T., WATANABE, D. & KOIDE, N. 2015. Pretreatment of LPS inhibits IFN-beta-induced STAT1 phosphorylation through SOCS3 induced by LPS. *Biomed Pharmacother,* 76**,** 1-5.

ANDROULIDAKI, A., ILIOPOULOS, D., ARRANZ, A., DOXAKI, C., SCHWORER, S., ZACHARIOUDAKI, V., MARGIORIS, A. N., TSICHLIS, P. N. & TSATSANIS, C. 2009. Akt1 controls macrophage response to LPS by regulating microRNAs. *Immunity,* 31**,** 220-31.

ARBELOA, A., GARNETT, J., LILLINGTON, J., BULGIN, R. R., BERGER, C. N., LEA, S. M., MATTHEWS, S. & FRANKEL, G. 2010. EspM2 is a RhoA guanine nucleotide exchange factor. *Cell Microbiol,* 12**,** 654-64.

ARNOLD, I. C., MATHISEN, S., SCHULTHESS, J., DANNE, C., HEGAZY, A. N. & POWRIE, F. 2016. CD11c(+) monocyte/macrophages promote chronic Helicobacter hepaticus-induced intestinal inflammation through the production of IL-23. *Mucosal immunology,* 9**,** 352-63.

ARONOFF, D. M., CARSTENS, J. K., CHEN, G. H., TOEWS, G. B. & PETERS-GOLDEN, M. 2006. Short communication: differences between macrophages and dendritic cells in the cyclic AMP-dependent regulation of lipopolysaccharide-induced cytokine and chemokine synthesis. *J Interferon Cytokine Res,* 26**,** 827-33.

ARIAS-BUJANDA, N., REGUEIRA-IGLESIAS, A., BALSA-CASTRO, C., NIBALI, L., DONOS, N. & TOMÁS, I. 2020. Accuracy of Single Molecular Biomarkers in Saliva for the Diagnosis of Periodontitis: A Systematic Review and Meta-Analysis. *Journal of clinical periodontology,* 47.

ARRANZ, A., DOXAKI, C., VERGADI, E., MARTINEZ DE LA TORRE, Y., VAPORIDI, K., LAGOUDAKI, E. D., IERONYMAKI, E., ANDROULIDAKI, A., VENIHAKI, M., MARGIORIS, A. N., STATHOPOULOS, E. N., TSICHLIS, P. N. & TSATSANIS, C. 2012. Akt1 and Akt2 protein kinases differentially contribute to macrophage polarization. *Proc Natl Acad Sci U S A,* 109**,** 9517-22.

ASADA, R., KANEMOTO, S., KONDO, S., SAITO, A. & IMAIZUMI, K. 2011. The signalling from endoplasmic reticulum-resident bZIP transcription factors involved in diverse cellular physiology. *Journal of biochemistry,* 149.

ASAI, Y., MAKIMURA, Y., KAWABATA, A. & OGAWA, T. 2007. Soluble CD14 discriminates slight structural differences between lipid as that lead to distinct host cell activation. *J Immunol,* 179**,** 7674-83.

BÅGE, T., KATS, A., LOPEZ, B. S., MORGAN, G., NILSSON, G., BURT, I., KOROTKOVA, M., CORBETT, L., KNOX, A. J., PINO, L., JAKOBSSON, P. J., MODÉER, T. & YUCEL-LINDBERG, T. 2011. Expression of Prostaglandin E Synthases in Periodontitis: Immunolocalization and Cellular Regulation. *Am J Pathol,* 178**,** 1676-88.

BAI, Y., WEI, Y., WU, L., WEI, J., WANG, X. & BAI, Y. 2016. C/EBP β Mediates Endoplasmic Reticulum Stress Regulated Inflammatory Response and Extracellular Matrix Degradation in LPS-Stimulated Human Periodontal Ligament Cells. International journal of molecular sciences, 17.

BAJRAMI, B., ZHU, H., KWAK, H. J., MONDAL, S., HOU, Q., GENG, G., KARATEPE, K., ZHANG, Y. C., NOMBELA-ARRIETA, C., PARK, S. Y., LOISON, F., SAKAI, J., XU, Y., SILBERSTEIN, L. E. & LUO, H. R. 2016. G-CSF maintains controlled neutrophil mobilization during acute inflammation by negatively regulating CXCR2 signaling. *J Exp Med,* 213**,** 1999-2018.

BAO, K., BELIBASAKIS, G., SELEVSEK, N., GROSSMANN, J. & BOSTANCI, N. 2015. Proteomic profiling of host-biofilm interactions in an oral infection model resembling the periodontal pocket. *Scientific reports,* 5.

BAQUI, A. A. M. A., MEILLER, T. F. & FALKLER, W. A. 1999. Enhanced interleukin-8 production in THP-1 human monocytic cells by lipopolysaccharide from oral microorganisms and granulocyte-macrophage colony-stimulating factor. *Oral Microbiology and Immunology,* 14**,** 275-280.

BAQUI, A. A., MEILLER, T. F., TURNG, B. F., KELLEY, J. I. & FALKLER, W. A. 1998. Functional changes in THP-1 human monocytic cells after stimulation with lipopolysaccharide of oral microorganisms and granulocyte macrophage colony stimulating factor. *Immunopharmacology and immunotoxicology,* 20**,** 493-518.

BARKSBY, H. E., LEA, S. R., PRESHAW, P. M. & TAYLOR, J. J. 2007. The expanding family of interleukin-1 cytokines and their role in destructive inflammatory disorders. *Clin Exp Immunol,* 149**,** 217-25.

BASHIR, A., MISKEEN, A. Y., HAZARI, Y. M., ASRAFUZZAMAN, S. & FAZILI, K. M. 2016. *Fusobacterium nucleatum*, inflammation, and immunity: the fire within human gut. *Tumour Biol,* 37**,** 2805-10.

BEESON, P. B. 1946. Development of tolerance to typhoid bacterial pyrogen and its abolition by reticulo-endothelial blockade. *Proc Soc Exp Biol Med,* 61**,** 248-50.

BELFIELD, L. A. 2013. *Interactions between porphyromonas gingivalis and macrophages in oral pathology.* Doctorate, University of Plymouth.

BEREZOW, A. B., ERNST, R. K., COATS, S. R., BRAHAM, P. H., KARIMI-NASER, L. M. & DARVEAU, R. P. 2009. The structurally similar, penta-acylated lipopolysaccharides of *Porphyromonas gingivalis* and *Bacteroides* elicit strikingly different innate immune responses. *Microb Pathog,* 47**,** 68-77.

BERGQVIST, F., CARR, A. J., WHEWAY, K., WATKINS, B., OPPERMANN, U., JAKOBSSON, P.-J. & DAKIN, S. G. 2019. Divergent roles of prostacyclin and PGE 2 in human tendinopathy. *Arthritis Research & Therapy,* 21**,** 1-12.

BEUTLER, B. 2004. SHIP, TGF-beta, and endotoxin tolerance. *Immunity,* 21**,** 134-5.

BEUTLER, B. & REHLI, M. 2002. Evolution of the TIR, Tolls and TLRs: Functional Inferences From Computational Biology. *Current topics in microbiology and immunology,* 270.

BEZZERRI, V., BORGATTI, M., FINOTTI, A., TAMANINI, A., GAMBARI, R. & CABRINI, G. 2011. Mapping the transcriptional machinery of the IL-8 gene in human bronchial epithelial cells. *J Immunol,* 187**,** 6069-81.

BIOMARKERS DEFINITION WORKING GROUP. 2001. Biomarkers and Surrogate Endpoints: Preferred Definitions and Conceptual Framework. *Clinical pharmacology and therapeutics,* 69.

BISCHOFF, S. C., BARBARA, G., BUURMAN, W., OCKHUIZEN, T., SCHULZKE, J. D., SERINO, M., TILG, H., WATSON, A. & WELLS, J. M. 2014. Intestinal permeability – a new target for disease prevention and therapy. *BMC Gastroenterol,* 14.

BISWAS, S. K., BIST, P., DHILLON, M. K., KAJIJI, T., DEL FRESNO, C., YAMAMOTO, M., LOPEZ-COLLAZO, E., AKIRA, S. & TERGAONKAR, V. 2007. Role for MyD88-independent, TRIF pathway in lipid A/TLR4-induced endotoxin tolerance. *Journal of immunology,* 179**,** 4083-92.

BISWAS, S. K. & LOPEZ-COLLAZO, E. 2009. Endotoxin tolerance: new mechanisms, molecules and clinical significance. *Trends in immunology,* 30**,** 475-87.

BLUM, J. S., WEARSCH, P. A. & CRESSWELL, P. 2013. Pathways of antigen processing. *Annu Rev Immunol,* 31**,** 443-73.

BOEHME, K. W., GUERRERO, M. & COMPTON, T. 2006. Human cytomegalovirus envelope glycoproteins B and H are necessary for TLR2 activation in permissive cells. *J Immunol,* 177**,** 7094-102.

BOLDEN, J. & SMITH, K. 2017. Application of Recombinant Factor C Reagent for the Detection of Bacterial Endotoxins in Pharmaceutical Products. *PDA journal of pharmaceutical science and technology,* 71.

BOSTANCI, N., HEYWOOD, W., MILLS, K., PARKAR, M., NIBALI, L. & DONOS, N. 2010. Application of label-free absolute quantitative proteomics in human gingival crevicular fluid by LC/MS E (gingival exudatome). *Journal of proteome research,* 9.

BOTTA, G. A., RADIN, L., COSTA, A., SCHITO, G. & BLASI, G. 1985. Gas-liquid chromatography of the gingival fluid as an aid in periodontal diagnosis. *J Periodontal Res,* 20**,** 450-7.

BOUSOIK, E. & MONTAZERI ALIABADI, H. 2018. "Do We Know Jack" About JAK? A Closer Look at JAK/STAT Signaling Pathway. *Front Oncol,* 8**,** 287.

BRANDTZAEG, P. 2013. Secretory immunity with special reference to the oral cavity. *J Oral Microbiol,* 5.

BRENNER, S., PROSCH, S., SCHENKE-LAYLAND, K., RIESE, U., GAUSMANN, U. & PLATZER, C. 2003. cAMP-induced Interleukin-10 promoter activation depends on CCAAT/enhancer-binding protein expression and monocytic differentiation. *J Biol Chem,* 278**,** 5597-604.

BUDUNELI, N. & KINANE, D. F. 2011. Host-derived Diagnostic Markers Related to Soft Tissue Destruction and Bone Degradation in Periodontitis. *Journal of clinical periodontology,* 38 Suppl 11.

BULUT, Y., FAURE, E., THOMAS, L., EQUILS, O. & ARDITI, M. 2001. Cooperation of Toll-like receptor 2 and 6 for cellular activation by soluble tuberculosis factor and *Borrelia burgdorferi* outer surface protein A lipoprotein: role of Toll-interacting protein and IL-1 receptor signaling molecules in Toll-like receptor 2 signaling. *J Immunol,* 167**,** 987-94.

BURNS, E., BACHRACH, G., SHAPIRA, L. & NUSSBAUM, G. 2006. Cutting Edge: TLR2 is required for the innate response to *Porphyromonas gingivalis*: activation

leads to bacterial persistence and TLR2 deficiency attenuates induced alveolar bone resorption. *Journal of immunology (Baltimore, Md. : 1950),* 177**,** 8296-300.

BUTCHER, S. K., O'CARROLL, C. E., WELLS, C. A. & CARMODY, R. J. 2018. Toll-Like Receptors Drive Specific Patterns of Tolerance and Training on Restimulation of Macrophages. *Front Immunol,* 9.

CAMELO-CASTILLO, A. J., MIRA, A., PICO, A., NIBALI, L., HENDERSON, B., DONOS, N. & TOMÁS, I. 2015. Subgingival microbiota in health compared to periodontitis and the influence of smoking. *Front Microbiol,* 6.

CAMPOS, M. A., ALMEIDA, I. C., TAKEUCHI, O., AKIRA, S., VALENTE, E. P., PROCOPIO, D. O., TRAVASSOS, L. R., SMITH, J. A., GOLENBOCK, D. T. & GAZZINELLI, R. T. 2001. Activation of Toll-like receptor-2 by glycosylphosphatidylinositol anchors from a protozoan parasite. *J Immunol,* 167**,** 416-23.

CARLSSON, E., DING, J. L. & BYRNE, B. 2016. SARM modulates MyD88-mediated TLR activation through BB-loop dependent TIR-TIR interactions. *Biochim Biophys Acta,* 1863**,** 244-53.

CASTAGNA, M., TAKAI, Y., KAIBUCHI, K., SANO, K., KIKKAWA, U. & NISHIZUKA, Y. 1982. Direct activation of calcium-activated, phospholipid-dependent protein kinase by tumor-promoting phorbol esters. *J Biol Chem,* 257**,** 7847-51.

CHANPUT, W., MES, J. J., SAVELKOUL, H. F. J. & WICHERS, H. J. 2013. Characterization of polarized THP-1 macrophages and polarizing ability of LPS and food compounds. *Food & function,* 4**,** 266-76.

CHANPUT, W., MES, J., VREEBURG, R. A. M., SAVELKOUL, H. F. J. & WICHERS, H. J. 2010. Transcription profiles of LPS-stimulated THP-1 monocytes and

macrophages: a tool to study inflammation modulating effects of food-derived compounds. *Food & function,* 1**,** 254-61.

CHARON, J., TOTO, P. D. & GARGIULO, A. W. 1981. Activated macrophages in human periodontitis. *Journal of periodontology,* 52**,** 328-35.

CHASSIN, C., KOCUR, M., POTT, J., DUERR, C. U., GÜTLE, D., LOTZ, M., HORNEF, M. W., 2010. miR-146a Mediates Protective Innate Immune Tolerance in the Neonate Intestine. *Cell Host & Microbe,* 8**,** 358-368.

CHEN, X. T., CHEN, L. L., TAN, J. Y., SHI, D. H., KE, T. & LEI, L. H. 2016. Th17 and Th1 Lymphocytes Are Correlated with Chronic Periodontitis. *Immunol Invest,* 45**,** 243-54.

CHEN, L., DENG, H., CUI, H., FANG, J., ZUO, Z., DENG, J., LI, Y., WANG, X. & ZHAO, L. 2018. Inflammatory responses and inflammation-associated diseases in organs. *Oncotarget,* 9**,** 7204-18.

CHIRANJEEVI, T., PRASAD, O. H., PRASAD, U. V., KUMAR, A. K., CHAKRAVARTHI, V. P., RAO, P. B., SARMA, P., REDDY NR, R. & BHASKAR, M. 2014. Identification of Microbial Pathogens in Periodontal disease and Diabetic patients of South Indian Population. *Bioinformation,* 10**,** 241-5.

CHOW, J., TANG, H. & MAZMANIAN, S. K. 2011. Pathobionts of the gastrointestinal microbiota and inflammatory disease. *Curr Opin Immunol,* 23**,** 473-80.

CIRELLI, T., FINOTI, L. S., CORBI, S. C. T., ANOVAZZI, G., NEPOMUCENO, R., CIRELLI, J. A., MAYER, M. SCAREL-CAMINAGA, R. M. 2018. Absolute quantification of *Aggregatibacter actinomycetemcomitans* in patients carrying haplotypes associated with susceptibility to chronic periodontitis: multifaceted evaluation with periodontitis covariants. *Pathogens and Disease,* 75.

CLAUDIO, N., DALET, A., GATTI, E. & PIERRE, P. 2013. Mapping the crossroads of immune activation and cellular stress response pathways. *Embo j,* 32**,** 1214-24.

COATS, S. R., BEREZOW, A. B., TO, T. T., JAIN, S., BAINBRIDGE, B. W., BANANI, K. P. & DARVEAU, R. P. 2011. The lipid A phosphate position determines differential host Toll-like receptor 4 responses to phylogenetically related symbiotic and pathogenic bacteria. *Infection and immunity,* 79**,** 203-10.

COATS, S. R., JONES, J. W., DO, C. T., BRAHAM, P. H., BAINBRIDGE, B. W., TO, T. T., GOODLETT, D. R., ERNST, R. K. & DARVEAU, R. P. 2009. Human Toll-like receptor 4 responses to *P. gingivalis* are regulated by lipid A 1- and 4'- phosphatase activities. *Cell Microbiol,* 11**,** 1587-99.

COATS, S. R., REIFE, R. A., BAINBRIDGE, B. W., PHAM, T. T. T. & DARVEAU, R. P. 2003. *Porphyromonas gingivalis* Lipopolysaccharide Antagonizes Escherichia coli Lipopolysaccharide at Toll-Like Receptor 4 in Human Endothelial Cells. *Infection and Immunity,* 71**,** 6799-6807.

COMER, B. S., CAMORETTI-MERCADO, B., KOGUT, P. C., HALAYKO, A. J., SOLWAY, J. & GERTHOFFER, W. T. 2015. Cyclooxygenase-2 and microRNA-155 expression are elevated in asthmatic airway smooth muscle cells. *Am J Respir Cell Mol Biol,* 52**,** 438-47.

CORNETT, A. L. & LUTZ, C. S. 2014. Regulation of COX-2 expression by miR-146a in lung cancer cells. *Rna,* 20**,** 1419-30.

CORTÉS-VIEYRA, R., ROSALES, C. & URIBE-QUEROL, E. 2016. Neutrophil Functions in Periodontal Homeostasis. *J Immunol Res,* 2016.

COSTALONGA, M. & HERZBERG, M. C. 2014. The oral microbiome and the immunobiology of periodontal disease and caries. *Immunol Lett,* 162**,** 22-38.

COURT, M., PETRE, G., ATIFI, M. & MILLET, A. 2017. Proteomic Signature Reveals Modulation of Human Macrophage Polarization and Functions Under Differing Environmental Oxygen Conditions. *Molecular & cellular proteomics : MCP,* 16.

COUSSENS, A., TIMMS, P. M., BOUCHER, B. J., VENTON, T. R., ASHCROFT, A. T., SKOLIMOWSKA, K. H., NEWTON, S. M., WILKINSON, K. A., DAVIDSON, R. N., GRIFFITHS, C. J., WILKINSON, R. J. & MARTINEAU, A. R. 2009. 1alpha,25-dihydroxyvitamin D3 inhibits matrix metalloproteinases induced by *Mycobacterium tuberculosis* infection. *Immunology,* 127**,** 539-48.

CUENO, M. E., IMAI, K., MATSUKAWA, N., TSUKAHARA, T., KURITA-OCHIAI, T. & OCHIAI, K. 2013. Butyric acid retention in gingival tissue induces oxidative stress in jugular blood mitochondria. *Cell Stress Chaperones,* 18**,** 661-5.

CUENO, M. E. & OCHIAI, K. 2018. Gingival Periodontal Disease (PD) Level-Butyric Acid Affects the Systemic Blood and Brain Organ: Insights Into the Systemic Inflammation of Periodontal Disease. *Front Immunol,* 9.

CUENO, M. E., SAITO, Y. & OCHIAI, K. 2016. Periodontal disease level-butyric acid amounts locally administered in the rat gingival mucosa induce ER stress in the systemic blood. *Microb Pathog,* 94**,** 70-5.

CULLEN, T. W., GILES, D. K., WOLF, L. N., ECOBICHON, C., BONECA, I. G. & TRENT, M. S. 2011. *Helicobacter pylori* versus the host: remodeling of the bacterial outer membrane is required for survival in the gastric mucosa. *PLoS Pathog,* 7**,** e1002454.

CULLINAN, S. B., ZHANG, D., HANNINK, M., ARVISAIS, E., KAUFMAN, R. J. & DIEHL, J. A. 2003. Nrf2 is a direct PERK substrate and effector of PERK-dependent cell survival. *Mol Cell Biol,* 23**,** 7198-209.

CURTIS, M. A., PERCIVAL, R. S., DEVINE, D., DARVEAU, R. P., COATS, S. R., RANGARAJAN, M., TARELLI, E. & MARSH, P. D. 2011. Temperature-dependent modulation of *Porphyromonas gingivalis* lipid A structure and interaction with the innate host defenses. *Infect Immun,* 79**,** 1187-93.

DA SILVA-BOGHOSSIAN, C. M., DO SOUTO, R. M., LUIZ, R. R. & COLOMBO, A. P. V. 2011. Association of red complex, *A. actinomycetemcomitans* and non-oral bacteria with periodontal diseases. *Archives of oral biology,* 56**,** 899-906.

DABRA, S. & SINGH, P. 2012. Evaluating the levels of salivary alkaline and acid phosphatase activities as biochemical markers for periodontal disease: A case series. Dent Res J (Isfahan), 9, 41-5.

DAIGNEAULT, M., PRESTON, J. A., MARRIOTT, H. M., WHYTE, M. K. B. & DOCKRELL, D. H. 2010. The identification of markers of macrophage differentiation in PMA-stimulated THP-1 cells and monocyte-derived macrophages. *PloS one,* 5**,** e8668-e8668.

DARVEAU, R. P., PHAM, T. T., LEMLEY, K., REIFE, R. A., BAINBRIDGE, B. W., COATS, S. R., HOWALD, W. N., WAY, S. S. & HAJJAR, A. M. 2004. *Porphyromonas gingivalis* lipopolysaccharide contains multiple lipid A species that functionally interact with both toll-like receptors 2 and 4. *Infect Immun,* 72**,** 5041-51.

DE, A., DAINICHI, T., RATHINAM, C. V. & GHOSH, S. 2014. The deubiquitinase activity of A20 is dispensable for NF-κB signaling. *EMBO Rep,* 15**,** 775-83.

DE PUNDER, K. 2015. Stress Induces Endotoxemia and Low-Grade Inflammation by Increasing Barrier Permeability. *Frontiers in Immunology,* 6.

DEL CAMPO, R., MARTÍNEZ, E., DEL FRESNO, C., ALENDA, R., GÓMEZ-PIÑA, V., FERNÁNDEZ-RUÍZ, I., SILICEO, M., JURADO, T., TOLEDANO, V., ARNALICH, F., GARCÍA-RÍO, F. & LÓPEZ-COLLAZO, E. 2011. Translocated LPS Might Cause

Endotoxin Tolerance in Circulating Monocytes of Cystic Fibrosis Patients. *PLoS ONE,* 6**,** e29577-e29577.

DEL FRESNO, C., GARCÍA-RIO, F., GÓMEZ-PIÑA, V., SOARES-SCHANOSKI, A., FERNÁNDEZ-RUÍZ, I., JURADO, T., KAJIJI, T., SHU, C., MARÍN, E., GUTIERREZ DEL ARROYO, A., PRADOS, C., ARNALICH, F., FUENTES-PRIOR, P., BISWAS, S. K., BISWAS, S. K. & LÓPEZ-COLLAZO, E. 2009. Potent phagocytic activity with impaired antigen presentation identifying lipopolysaccharide-tolerant human monocytes: demonstration in isolated monocytes from cystic fibrosis patients. *Journal of immunology (Baltimore, Md. : 1950),* 182**,** 6494-507.

DEL FRESNO, C., GOMEZ-PINA, V., LORES, V., SOARES-SCHANOSKI, A., FERNANDEZ-RUIZ, I., ROJO, B., ALVAREZ-SALA, R., CABALLERO-GARRIDO, E., GARCIA, F., VELIZ, T., ARNALICH, F., FUENTES-PRIOR, P., GARCIA-RIO, F. & LOPEZ-COLLAZO, E. 2008. Monocytes from cystic fibrosis patients are locked in an LPS tolerance state: down-regulation of TREM-1 as putative underlying mechanism. *PLoS One,* 3**,** e2667.

DEDE, F. Ö., OZDEN, F. O. & AVCI, B. 2013. 8-hydroxy-deoxyguanosine Levels in Gingival Crevicular Fluid and Saliva in Patients With Chronic Periodontitis After Initial Periodontal Treatment. *Journal of periodontology,* 84.

DENG, Z.-L., SZAFRAŃSKI, S. P., JAREK, M., BHUJU, S. & WAGNER-DÖBLER, I. 2017. Dysbiosis in chronic periodontitis: Key microbial players and interactions with the human host. *Scientific Reports,* 7**,** 3703.

DEWHIRST, F. E., CHEN, T., IZARD, J., PASTER, B. J., TANNER, A. C. R., YU, W.-H., LAKSHMANAN, A. & WADE, W. G. 2010. The human oral microbiome. *Journal of bacteriology,* 192**,** 5002-17.

DHARMANI, P., STRAUSS, J., AMBROSE, C., ALLEN-VERCOE, E. & CHADEE, K. 2011. *Fusobacterium nucleatum* Infection of Colonic Cells Stimulates MUC2 Mucin and Tumor Necrosis Factor Alpha ▿ . *Infect Immun,* 79**,** 2597-607.

DING, J. L. & HO, B. 2010. Endotoxin detection--from limulus amebocyte lysate to recombinant factor C. *Subcell Biochem,* 53**,** 187-208.

DIVARIS, K., MONDA, K. L., NORTH, K. E., OLSHAN, A. F., REYNOLDS, L. M., HSUEH, W. C., LANGE, E. M., MOSS, K., BARROS, S. P., WEYANT, R. J., LIU, Y., NEWMAN, A. B., BECK, J. D. & OFFENBACHER, S. 2013. Exploring the genetic basis of chronic periodontitis: a genome-wide association study. *Hum Mol Genet,* 22**,** 2312-24.

DIYA, Z., LILI, C., SHENGLAI, L., ZHIYUAN, G. & JIE, Y. 2008. Lipopolysaccharide (LPS) of *Porphyromonas gingivalis* induces IL-1beta, TNF-alpha and IL-6 production by THP-1 cells in a way different from that of Escherichia coli LPS. *Innate Immun,* 14**,** 99-107.

DOMON, H., TAKAHASHI, N., HONDA, T., NAKAJIMA, T., TABETA, K., ABIKO, Y. & YAMAZAKI, K. 2009. Up-regulation of the endoplasmic reticulum stress-response in periodontal disease. *Clinica chimica acta; international journal of clinical chemistry,* 401.

DOSSEVA-PANOVA, V., MLACHKOVA, A. & POPOVA, C. 2015. Gene polymorphisms in periodontitis. Overview. *Biotechnology & Biotechnological Equipment,* 29**,** 834-839.

DULUC, D., DELNESTE, Y., TAN, F., MOLES, M. P., GRIMAUD, L., LENOIR, J., PREISSER, L., ANEGON, I., CATALA, L., IFRAH, N., DESCAMPS, P., GAMELIN, E., GASCAN, H., HEBBAR, M. & JEANNIN, P. 2007. Tumor-associated leukemia

inhibitory factor and IL-6 skew monocyte differentiation into tumor-associated macrophage-like cells. *Blood,* 110**,** 4319-30.

EBERLE, F. C., BRUCK, J., HOLSTEIN, J., HIRAHARA, K. & GHORESCHI, K. 2016. Recent advances in understanding psoriasis. *F1000Res,* 5.

EBERSOLE, J. L., DAWSON, D. R., MORFORD, L. A., PEYYALA, R., MILLER, C. S. & GONZALÉZ, O. A. 2013. Periodontal disease immunology: 'double indemnity' in protecting the host. *Periodontol 2000,* 62**,** 163-202.

EBERSOLE, J. L., NAGARAJAN, R., AKERS, D. & MILLER, C. S. 2015. Targeted salivary biomarkers for discrimination of periodontal health and disease(s). *Front Cell Infect Microbiol,* 5.

FALVO, J. V., TSYTSYKOVA, A. V. & GOLDFELD, A. E. 2010. Transcriptional control of the TNF gene. *Curr Dir Autoimmun,* 11**,** 27-60.

FARDINI, Y., WANG, X., TEMOIN, S., NITHIANANTHAM, S., LEE, D., SHOHAM, M. & HAN, Y. W. 2011. *Fusobacterium nucleatum* adhesin FadA binds vascular endothelial cadherin and alters endothelial integrity. *Mol Microbiol,* 82**,** 1468-80.

FASANO, A. 2012. Leaky gut and autoimmune diseases. *Clin Rev Allergy Immunol,* 42**,** 71-8.

FAVERI, M., FIGUEIREDO, L. C., DUARTE, P. M., MESTNIK, M. J., MAYER, M. P. & FERES, M. 2009. Microbiological profile of untreated subjects with localized aggressive periodontitis. *J Clin Periodontol,* 36**,** 739-49.

FERES, M., TELES, F., TELES, R., FIGUEIREDO, L. C. & FAVERI, M. 2016. The subgingival periodontal microbiota of the aging mouth. *Periodontol 2000,* 72**,** 30-53.

FINE, D. H., MARKOWITZ, K., FURGANG, D., FAIRLIE, K., FERRANDIZ, J., NASRI, C., MCKIERNAN, M. & GUNSOLLEY, J. 2007. *Aggregatibacter actinomycetemcomitans* and Its Relationship to Initiation of Localized Aggressive

Periodontitis: Longitudinal Cohort Study of Initially Healthy Adolescents ▿ . *J Clin Microbiol,* 45**,** 3859-69.

FLEIT, H. B. & KOBASIUK, C. D. 1991. The human monocyte-like cell line THP-1 expresses Fc gamma RI and Fc gamma RII. *J Leukoc Biol,* 49**,** 556-65.

FOEY, A. D. 2011. Butyrate regulation of distinct macrophage subsets: opposing effects on m1 and m2 macrophages. *International Journal of Probiotics and Prebiotics,* 6**,** 147-158.

FOEY, A. 2015a. Macrophage Polarisation: A collaboration of Differentiation, Activation and Pre-Programming? *Journal of Clinical & Cellular Immunology,* 06.

FOEY, A. D. 2015b. Macrophages: Tissue-Resident Determinants of Immunomodulation. *Immunotherapy: Open Access,* 2015.

FOEY, A. D. & BRENNAN, F. M. 2004. Conventional protein kinase C and atypical protein kinase Czeta differentially regulate macrophage production of tumour necrosis factor-alpha and interleukin-10. *Immunology,* 112**,** 44-53.

FOEY, A. D. & CREAN, S. 2013. Macrophage subset sensitivity to endotoxin tolerisation by *Porphyromonas gingivalis*. *PloS one,* 8**,** e67955-e67955.

FOEY, A. D., HABIL, N., AL-SHAGHDALI, K. & CREAN, S. 2017. *Porphyromonas gingivalis*-stimulated macrophage subsets exhibit differential induction and responsiveness to interleukin-10. *Arch Oral Biol,* 73**,** 282-288.

FUJISE, O., CHEN, W., RICH, S. & CHEN, C. 2004. Clonal diversity and stability of subgingival eikenella corrodens. *J Clin Microbiol,* 42**,** 2036-42.

FUKUOKA, S., BRANDENBURG, K., MÜLLER, M., LINDNER, B., KOCH, M. H. & SEYDEL, U. 2001. Physico-chemical analysis of lipid A fractions of lipopolysaccharide from *Erwinia carotovora* in relation to bioactivity. *Biochimica et biophysica acta,* 1510**,** 185-97.

FUNG, T. C., ARTIS, D. & SONNENBERG, G. F. 2014. Anatomical localization of commensal bacteria in immune cell homeostasis and disease. *Immunol Rev,* 260**,** 35-49.

GARSIDE, P., MOWAT, A. M. & KHORUTS, A. 1999. Oral tolerance in disease. *BMJ Journals,* 44.

GASPERINI, S., CREPALDI, L., CALZETTI, F., GATTO, L., BERLATO, C., BAZZONI, F., YOSHIMURA, A. & CASSATELLA, M. A. 2002. Interleukin-10 and cAMP-elevating agents cooperate to induce suppressor of cytokine signaling-3 via a protein kinase A-independent signal. *Eur Cytokine Netw,* 13**,** 47-53.

GELDERBLOM, M., GALLIZIOLI, M., LUDEWIG, P., THOM, V., ARUNACHALAM, P., RISSIEK, B., BERNREUTHER, C., GLATZEL, M., KORN, T., ARUMUGAM, T. V., SEDLACIK, J., GERLOFF, C., TOLOSA, E., PLANAS, A. M. & MAGNUS, T. 2018. IL-23 (Interleukin-23)-Producing Conventional Dendritic Cells Control the Detrimental IL-17 (Interleukin-17) Response in Stroke. *Stroke,* 49**,** 155-164.

GESSER, B., LUND, M., LOHSE, N., VESTERGAAD, C., MATSUSHIMA, K., SINDET-PEDERSEN, S., JENSEN, S. L., THESTRUP-PEDERSEN, K. & LARSEN, C. G. 1996. IL-8 induces T cell chemotaxis, suppresses IL-4, and up-regulates IL-8 production by CD4+ T cells. *J Leukoc Biol,* 59**,** 407-11.

GEVERS, D., KUGATHASAN, S., DENSON, L. A., VAZQUEZ-BAEZA, Y., VAN TREUREN, W., REN, B., SCHWAGER, E., KNIGHTS, D., SONG, S. J., YASSOUR, M., MORGAN, X. C., KOSTIC, A. D., LUO, C., GONZALEZ, A., MCDONALD, D., HABERMAN, Y., WALTERS, T., BAKER, S., ROSH, J., STEPHENS, M., HEYMAN, M., MARKOWITZ, J., BALDASSANO, R., GRIFFITHS, A., SYLVESTER, F., MACK, D., KIM, S., CRANDALL, W., HYAMS, J., HUTTENHOWER, C., KNIGHT, R. &

XAVIER, R. J. 2014. The treatment-naive microbiome in new-onset Crohn's disease. *Cell Host Microbe,* 15**,** 382-92.

GIROLOMONI, G., STROHAL, R., PUIG, L., BACHELEZ, H., BARKER, J., BOEHNCKE, W. H. & PRINZ, J. C. 2017. The role of IL-23 and the IL-23/TH 17 immune axis in the pathogenesis and treatment of psoriasis. *J Eur Acad Dermatol Venereol,* 31**,** 1616-1626.

GÖLZ, L., BUERFENT, B. C., HOFMANN, A., HÜBNER, M. P., RÜHL, H., FRICKER, N., SCHMIDT, D., JOHANNES, O., JEPSEN, S., DESCHNER, J., HOERAUF, A., NÖTHEN, M. M., SCHUMACHER, J. & JÄGER, A. 2016. Genome-wide transcriptome induced by *Porphyromonas gingivalis* LPS supports the notion of host-derived periodontal destruction and its association with systemic diseases. *Innate immunity,* 22**,** 72-84.

GONZÁLEZ-RAMÍREZ, J. S.-H., N. CONCEPCIÓN SILVA MANCILLA, M. MARTÍNEZ-CORONILLA, G. FAMANÍA-BUSTAMANTE,J. LÓPEZ LÓPEZ, A.L. 2019. Periodontal Disease - Diagnostic and Adjunctive Non-surgical Considerations. *In:* YUSSIF, N. (ed.) *Periodontal Disease Diagnostic and Adjunctive Non-surgical Considerations.* IntechOpen.

GORDON, S. & MARTINEZ, F. O. 2010. Alternative activation of macrophages: mechanism and functions. *Immunity,* 32**,** 593-604.

GORDON, S. & PLUDDEMANN, A. 2017. Tissue macrophages: heterogeneity and functions. *BMC Biol,* 15**,** 53.

GORDON, S. & TAYLOR, P. R. 2005. Monocyte and macrophage heterogeneity. *Nature reviews. Immunology,* 5**,** 953-64.

GRIFFEN, A. L., BEALL, C. J., CAMPBELL, J. H., FIRESTONE, N. D., KUMAR, P. S., YANG, Z. K., PODAR, M. & LEYS, E. J. 2012. Distinct and complex bacterial

profiles in human periodontitis and health revealed by 16S pyrosequencing. *Isme j,* 6**,** 1176-85.

GRIFFEN, A. L., BECKER, M. R., LYONS, S. R., MOESCHBERGER, M. L. & LEYS, E. J. 1998. Prevalence of *Porphyromonas gingivalis* and periodontal health status. *J Clin Microbiol,* 36**,** 3239-42.

GRINER, P. F., MAYEWSKI, R. J., MUSHLIN, A. I. & GREENLAND, P. 1981. Selection and interpretation of diagnostic tests and procedures. Principles and applications. *Ann Intern Med,* 94**,** 557-92.

GRONBACH, K., FLADE, I., HOLST, O., LINDNER, B., RUSCHEWEYH, H. J., WITTMANN, A., MENZ, S., SCHWIERTZ, A., ADAM, P., STECHER, B., JOSENHANS, C., SUERBAUM, S., GRUBER, A. D., KULIK, A., HUSON, D., AUTENRIETH, I. B. & FRICK, J. S. 2014. Endotoxicity of lipopolysaccharide as a determinant of T-cell-mediated colitis induction in mice. *Gastroenterology,* 146**,** 765-75.

GROOTJANS, J., KASER, A., KAUFMAN, R. J. & BLUMBERG, R. S. 2016. The unfolded protein response in immunity and inflammation. *Nat Rev Immunol,* 16**,** 469-84.

GROVER & GROVER HS, S. R., BHARDWAJ P, BHARDWAJ A 2014. A new dawn in modern perio-diagnostics: Saliva and gingival crevicular fluid. *Journal of Dental and Allied Sciences,* 2, 89-92.

GUNEPIN, M., DERACHE, F., TROUSSELARD, M., SALSOU, B & RISSO, J.-J. 2019. Impact of chronic stress on periodontal health. *Journal of Oral Medicine and Oral Surgery,* 24**,** 44-50.

GUPTA, M., CHATURVEDI, R. & JAIN, A. 2013. Role of Monocyte Chemoattractant protein-1 (MCP-1) as an Immune-Diagnostic Biomarker in the Pathogenesis of Chronic Periodontal Disease. *Cytokine,* 61.

GURSOY, U. K., KÖNÖNEN, E., HUUMONEN, S., TERVAHARTIALA, T., PUSSINEN, P. J., SUOMINEN, A. L. & SORSA, T. 2013. Salivary Type I Collagen Degradation End-Products and Related Matrix Metalloproteinases in Periodontitis. *Journal of clinical periodontology,* 40.

GUTSMANN, T., HOWE, J., ZAHRINGER, U., GARIDEL, P., SCHROMM, A. B., KOCH, M. H., FUJIMOTO, Y., FUKASE, K., MORIYON, I., MARTINEZ-DE-TEJADA, G. & BRANDENBURG, K. 2010. Structural prerequisites for endotoxic activity in the Limulus test as compared to cytokine production in mononuclear cells. *Innate Immun,* 16**,** 39-47.

GYNTHER, P., TOROPAINEN, S., MATILAINEN, J. M., SEUTER, S., CARLBERG, C. & VÄISÄNEN, S. 2011. Mechanism of 1α,25-dihydroxyvitamin D(3)-dependent repression of interleukin-12B. *Biochimica et biophysica acta,* 1813**,** 810-8.

HABIL, N. 2013. *Probiotic Modulation of Mucosal Immune Responses in an In Vitro Co-Culture Model.* Doctorate, Plymouth University.

HABIL, N., AL-MURRANI, W., BEAL, J. & FOEY, A. D. 2011. Probiotic bacterial strains differentially modulate macrophage cytokine production in a strain-dependent and cell subset-specific manner. *Benef Microbes,* 2**,** 283-93.

HABIL, N., BEAL, J. & FOEY, A. 2012. *Lactobacillus casei* strain Shirota selectively modulates macrophage subset cytokine production. *International Journal of Probiotics and Prebiotics,* 7**,** 1 - 12.

HAFFAJEE, A. D., TELES, R. P. & SOCRANSKY, S. S. 2006. Association of *Eubacterium nodatum* and *Treponema denticola* with human periodontitis lesions. *Oral Microbiol Immunol,* 21**,** 269-82.

HAJISHENGALLIS, G. 2009. *Porphyromonas gingivalis*-Host Interactions: Open War or Intelligent Guerilla Tactics? *Microbes Infect,* 11**,** 637-45.

HAJISHENGALLIS, G. 2014a. The inflammophilic character of the periodontitis-associated microbiota. *Mol Oral Microbiol,* 29**,** 248-57.

HAJISHENGALLIS, G. 2014b. Periodontitis: from microbial immune subversion to systemic inflammation. *Nature Reviews Immunology,* 15**,** 30-44.

HAJISHENGALLIS, G., DARVEAU, R. P. & CURTIS, M. A. 2012. The keystone-pathogen hypothesis. *Nature reviews. Microbiology,* 10**,** 717-25.

HAJISHENGALLIS, G. & LAMONT, R. J. 2012. Beyond the red complex and into more complexity: the polymicrobial synergy and dysbiosis (PSD) model of periodontal disease etiology. *Mol Oral Microbiol,* 27**,** 409-19.

HAJISHENGALLIS, G., WANG, M., LIANG, S., SHAKHATREH, M. A. K., JAMES, D., NISHIYAMA, S., YOSHIMURA, F. & DEMUTH, D. R. 2008. Subversion of Innate Immunity by Periodontopathic Bacteria via Exploitation of Complement Receptor-3. *Adv Exp Med Biol,* 632**,** 203-19.

HARBOUR, S. N., MAYNARD, C. L., ZINDL, C. L., SCHOEB, T. R. & WEAVER, C. T. 2015. Th17 cells give rise to Th1 cells that are required for the pathogenesis of colitis. *PNAS,* 112**,** 7061-7066.

HAYASHI, F., SMITH, K. D., OZINSKY, A., HAWN, T. R., YI, E. C., GOODLETT, D. R., ENG, J. K., AKIRA, S., UNDERHILL, D. M. & ADEREM, A. 2001. The innate immune response to bacterial flagellin is mediated by Toll-like receptor 5. *Nature,* 410**,** 1099-103.

HEIL, F., HEMMI, H., HOCHREIN, H., AMPENBERGER, F., KIRSCHNING, C., AKIRA, S., LIPFORD, G., WAGNER, H. & BAUER, S. 2004. Species-specific recognition of single-stranded RNA via toll-like receptor 7 and 8. *Science,* 303**,** 1526-9.

HELLER, D., SILVA-BOGHOSSIAN, C. M., DO SOUTO, R. M. & COLOMBO, A. P. 2012. Subgingival microbial profiles of generalized aggressive and chronic periodontal diseases. *Arch Oral Biol,* 57**,** 973-80.

HEMMI, H., TAKEUCHI, O., KAWAI, T., KAISHO, T., SATO, S., SANJO, H., MATSUMOTO, M., HOSHINO, K., WAGNER, H., TAKEDA, K. & AKIRA, S. 2000. A Toll-like receptor recognizes bacterial DNA. *Nature,* 408**,** 740-5.

HENDERSON, B., WILSON, M., SHARP, L. & WARD, J. M. 2002. *Actinobacillus actinomycetemcomitans*. *J Med Microbiol,* 51**,** 1013-20.

HETZ, C., BERNASCONI, P., FISHER, J., LEE, A. H., BASSIK, M. C., ANTONSSON, B., BRANDT, G. S., IWAKOSHI, N. N., SCHINZEL, A., GLIMCHER, L. H. & KORSMEYER, S. J. 2006. Proapoptotic BAX and BAK modulate the unfolded protein response by a direct interaction with IRE1alpha. *Science,* 312**,** 572-6.

HIENZ, S. A., PALIWAL, S. & IVANOVSKI, S. 2015. Mechanisms of Bone Resorption in Periodontitis. *J Immunol Res,* 2015.

HILTON, D. J., RICHARDSON, R. T., ALEXANDER, W. S., VINEY, E. M., WILLSON, T. A., SPRIGG, N. S., STARR, R., NICHOLSON, S. E., METCALF, D. & NICOLA, N. A. 1998. Twenty proteins containing a C-terminal SOCS box form five structural classes. *PNAS***,** 114-119.

HOEFFLER, J. P. & HABENER, J. F. 1990. Characterization of a cyclic AMP regulatory element DNA-binding protein. *Trends Endocrinol Metab,* 1**,** 155-8.

HOFFMANN, E., DITTRICH-BREIHOLZ, O., HOLTMANN, H. & KRACHT, M. 2002. Multiple control of interleukin-8 gene expression. *J Leukoc Biol,* 72**,** 847-55.

HOL, J., WILHELMSEN, L. & HARALDSEN, G. 2010. The murine IL-8 homologues KC, MIP-2, and LIX are found in endothelial cytoplasmic granules but not in Weibel-Palade bodies. *J Leukoc Biol,* 87**,** 501-8.

HOLDEN, J. A., ATTARD, T. J., LAUGHTON, K. M., MANSELL, A., O'BRIEN-SIMPSON, N. M. & REYNOLDS, E. C. 2014. *Porphyromonas gingivalis* lipopolysaccharide weakly activates M1 and M2 polarized mouse macrophages but induces inflammatory cytokines. *Infection and immunity,* 82**,** 4190-203.

HOLT, S. C. & EBERSOLE, J. L. 2005. *Porphyromonas gingivalis, Treponema denticola*, and *Tannerella forsythia*: the "red complex", a prototype polybacterial pathogenic consortium in periodontitis. *Periodontol 2000,* 38**,** 72-122.

HONDA, K., TAKAOKA, A. & TANIGUCHI, T. 2006. Type I Inteferon Gene Induction by the Interferon Regulatory Factor Family of Transcription Factors. *Immunity,* 25**,** 349-360.

HOSHINO, K., TAKEUCHI, O., KAWAI, T., SANJO, H., OGAWA, T., TAKEDA, Y., TAKEDA, K. & AKIRA, S. 1999. Cutting edge: Toll-like receptor 4 (TLR4)-deficient mice are hyporesponsive to lipopolysaccharide: evidence for TLR4 as the Lps gene product. *J Immunol,* 162**,** 3749-52.

HOUSLAY, M. D. & KOLCH, W. 2000. Cell-Type Specific Integration of Cross-Talk between Extracellular Signal-Regulated Kinase and cAMP Signaling. *Molecular Pharmacology,* 58, 659-668.

HOVAV, A.-H. 2013. Dendritic cells of the oral mucosa. *Mucosal Immunology,* 7**,** 27-37.

HSU, S., CHIU, C., DAHMS, H., CHOU, C., CHENG, C., CHANG, W., CHENG, K., WANG, H. & LIN, I. 2019. Unfolded Protein Response (UPR) in Survival, Dormancy, Immunosuppression, Metastasis, and Treatments of Cancer Cells. *International journal of molecular sciences,* 20.

HU, X., CHAKRAVARTY, S. D. & IVASHKIV, L. B. 2008. Regulation of IFN and TLR Signaling During Macrophage Activation by Opposing Feedforward and Feedback Inhibition Mechanisms. *Immunol Rev,* 226**,** 41-56.

HUANG, R., LI, M. & GREGORY, R. L. 2011. Bacterial interactions in dental biofilm. *Virulence,* 2**,** 435-44.

IOANNIDOU, E. 2017. The Sex and Gender Intersection in Chronic Periodontitis. *Front Public Health,* 5.

ISHISAKA, A., ANSAI, T., SOH, I., INENAGA, K., AWANO, S., YOSHIDA, A., HAMASAKI, T., SONOKI, K., TAKATA, Y., NISHIHARA, T. & TAKEHARA, T. 2008. Association of Cortisol and Dehydroepiandrosterone Sulphate Levels in Serum With Periodontal Status in Older Japanese Adults. *Journal of clinical periodontology,* 35.

ITO, S., ANSARI, P., SAKATSUME, M., DICKENSHEETS, H., VAZQUEZ, N., DONNELLY, R. P., LARNER, A. C. & FINBLOOM, D. S. 1999. Interleukin-10 inhibits expression of both interferon alpha- and interferon gamma- induced genes by suppressing tyrosine phosphorylation of STAT1. *Blood,* 93**,** 1456-63.

IWANAGA, S. 2007. Biochemical principle of Limulus test for detecting bacterial endotoxins. *Proc Jpn Acad Ser B Phys Biol Sci,* 83**,** 110-9.

JAIN, S., COATS, S. R., CHANG, A. M. & DARVEAU, R. P. 2013. A novel class of lipoprotein lipase-sensitive molecules mediates Toll-like receptor 2 activation by *Porphyromonas gingivalis*. *Infect Immun,* 81**,** 1277-86.

JAIN, S. & DARVEAU, R. P. 2010. Contribution of *Porphyromonas gingivalis* lipopolysaccharide to periodontitis. *Periodontology 2000,* 54**,** 53-70.

JANELSINS, B. M., LU, M. & DATTA, S. K. 2014. Altered inactivation of commensal LPS due to acyloxyacyl hydrolase deficiency in colonic dendritic cells impairs mucosal Th17 immunity. *Proc Natl Acad Sci U S A,* 111**,** 373-8.

JANSSENS, S., PULENDRAN, B. & LAMBRECHT, B. N. 2014. Emerging functions of the unfolded protein response in immunity. *Nat Immunol,* 15**,** 910-9.

JI, S., CHOI, Y. S. & CHOI, Y. 2015. Bacterial invasion and persistence: critical events in the pathogenesis of periodontitis? *J Periodontal Res,* 50**,** 570-85.

JIN, S. L. & CONTI, M. 2002. Induction of the cyclic nucleotide phosphodiesterase PDE4B is essential for LPS-activated TNF-alpha responses. *Proc Natl Acad Sci U S A,* 99**,** 7628-33.

JOHN, C. M., PHILLIPS, N. J., DIN, R., LIU, M., ROSENQVIST, E., HOIBY, E. A., STEIN, D. C. & JARVIS, G. A. 2016. Lipooligosaccharide Structures of Invasive and Carrier Isolates of *Neisseria meningitidis* Are Correlated with Pathogenicity and Carriage. *J Biol Chem,* 291**,** 3224-38.

JUNDI, K. & GREENE, C. M. 2015. Transcription of Interleukin-8: How Altered Regulation Can Affect Cystic Fibrosis Lung Disease. *Biomolecules,* 5**,** 1386-98.

KAGAN, J. C., SU, T., HORNG, T., CHOW, A., AKIRA, S. & MEDZHITOV, R. 2008. TRAM couples endocytosis of Toll-like receptor 4 to the induction of interferon-β. *Nat Immunol,* 9**,** 361-8.

KAKUTA, E., NOMURA, Y., MOROZUMI, T., NAKAGAWA, T., NAKAMURA, T., NOGUCHI, K., YOSHIMURA, A., HARA, Y., FUJISE, O., NISHIMURA, F., KONO, T., UMEDA, M., FUKUDA, M., NOGUCHI, T., YOSHINARI, N., FUKAYA, C., SEKINO, S., NUMABE, Y., SUGANO, N., ITO, K., KOBAYASHI, H., IZUMI, Y.,

TAKAI, H., OGATA, Y., TAKANO, S., MINABE, M., MAKINO-OI, A., SAITO, A., ABE, Y., SATO, S., SUZUKI, F., TAKAHASHI, K., SUGAYA, T., KAWANAMI, M., HANADA, N., TAKASHIBA, S. & YOSHIE, H. 2017. Assessing the progression of chronic periodontitis using subgingival pathogen levels: a 24-month prospective multicenter cohort study. *BMC Oral Health,* 17.

KALIM, K. W. & GROETTRUP, M. 2013. Prostaglandin E2 inhibits IL-23 and IL-12 production by human monocytes through down-regulation of their common p40 subunit. *Mol Immunol,* 53**,** 274-82.

KALINSKI, P., VIEIRA, P. L., SCHUITEMAKER, J. H., DE JONG, E. C. & KAPSENBERG, M. L. 2001. Prostaglandin E(2) is a selective inducer of interleukin-12 p40 (IL-12p40) production and an inhibitor of bioactive IL-12p70 heterodimer. *Blood,* 97**,** 3466-9.

KAMADA, N., CHEN, G. Y., INOHARA, N. & NÚÑEZ, G. 2013. Control of Pathogens and Pathobionts by the Gut Microbiota. *Nat Immunol,* 14**,** 685-90.

KAMIZONO, S., HANADA, T., YASUKAWA, H., MINOGUCHI, S., KATO, R., MINOGUCHI, M., HATTORI, K., HATAKEYAMA, S., YADA, M., MORITA, S., KITAMURA, T., KATO, H., NAKAYAMA, K. & YOSHIMURA, A. 2001. The SOCS box of SOCS-1 accelerates ubiquitin-dependent proteolysis of TEL-JAK2. *J Biol Chem,* 276**,** 12530-8.

KAWAHARA, K., TSUKANO, H., WATANABE, H., LINDNER, B. & MATSUURA, M. 2002. Modification of the structure and activity of lipid A in *Yersinia pestis* lipopolysaccharide by growth temperature. *Infect Immun,* 70**,** 4092-8.

KAZI, M. & BHARADWAJ, R. 2017. Role of herpesviruses in chronic periodontitis and their association with clinical parameters and in increasing severity of the disease. *Eur J Dent,* 11**,** 299-304.

KENNY, E. F. & O'NEILL, L. A. 2008. Signalling adaptors used by Toll-like receptors: an update. *Cytokine,* 43**,** 342-9.

KHATIB-SHAHIDI, S., ANDERSSON, M., HERMAN, J. L., GILLESPIE, T. A. & CAPRIOLI, R. M. 2006. Direct molecular analysis of whole-body animal tissue sections by imaging MALDI mass spectrometry. *Anal Chem,* 78**,** 6448-56.

KHAYRULLINA, T., YEN, J. H., JING, H. & GANEA, D. 2008. In Vitro Differentiation of Dendritic Cells in the Presence of Prostaglandin E2 Alters the IL-12/IL-23 Balance and Promotes Differentiation of Th17 Cells1. *J Immunol,* 181**,** 721-35.

KHONGKHUNTHIAN, S., KONGTAWELERT, P., ONGCHAI, S., POTHACHAROEN, P., SASTRARUJI, T., JOTIKASTHIRA, D. & KRISANAPRAKORNKIT, S. 2014. Comparisons between two biochemical markers in evaluating periodontal disease severity: a cross-sectional study. *BMC Oral Health,* 14**,** 107.

KHOR, B., GARDET, A. & XAVIER, R. J. 2011. Genetics and pathogenesis of inflammatory bowel disease. *Nature,* 474**,** 307-17.

KIM, H. J., LEE, Y. H., IM, S. A., KIM, K. & LEE, C. K. 2010. Cyclooxygenase Inhibitors, Aspirin and Ibuprofen, Inhibit MHC-restricted Antigen Presentation in Dendritic Cells. *Immune Netw,* 10**,** 92-8.

KIM, P. D., XIA-JUAN, X., CRUMP, K. E., ABE, T., HAJISHENGALLIS, G. & SAHINGUR, S. E. 2015. Toll-Like Receptor 9-Mediated Inflammation Triggers Alveolar Bone Loss in Experimental Murine Periodontitis. *Infection and immunity,* 83**,** 2992-3002.

KINNEY, J. S., MORELLI, T., OH, M., BRAUN, T. M., RAMSEIER, C. A., SUGAI, J. V. & GIANNOBILE, W. V. 2014. Crevicular Fluid Biomarkers and Periodontal Disease Progression. *J Clin Periodontol,* 41**,** 113-20.

KOBAYASHI, K., HERNANDEZ, L. D., GALÁN, J. E., JANEWAY, C. A., MEDZHITOV, R & FLAVELL, R. A., 2002. IRAK-M Is a Negative Regulator of Toll-like Receptor Signaling. *Cell,* 110**,** 191-202.

KOCIEDA, V. P., ADHIKARY, S., EMIG, F., YEN, J.-H., TOSCANO, M. G. & GANEA, D. 2012. Prostaglandin E2-induced IL-23p19 Subunit Is Regulated by cAMP-responsive Element-binding Protein and C/AATT Enhancer-binding Protein β in Bone Marrow-derived Dendritic Cells. *Jounal of Biological Chemistry,* 287, 36922-36935.

KOMATSU, K., LEE, J. Y., MIYATA, M., HYANG LIM, J., JONO, H., KOGA, T., XU, H., YAN, C., KAI, H. & LI, J. D. 2013. Inhibition of PDE4B suppresses inflammation by increasing expression of the deubiquitinase CYLD. *Nat Commun,* 4**,** 1684.

KONDO, T., KAWAI, T. & AKIRA, S. 2012. Dissecting negative regulation of Toll-like receptor signaling. *Trends in immunology,* 33**,** 449-58.

KONIG, M. F., ABUSLEME, L., REINHOLDT, J., PALMER, R. J., TELES, R. P., SAMPSON, K., ROSEN, A., NIGROVIC, P. A., SOKOLOVE, J., GILES, J. T., MOUTSOPOULOS, N. M. & ANDRADE, F. 2016. *Aggregatibacter actinomycetemcomitans*–induced hypercitrullination links periodontal infection to autoimmunity in rheumatoid arthritis. *Science Translational Medicine,* 8.

KOWALSKI, E. J. A. & LI, L. 2017. Toll-Interacting Protein in Resolving and Non-Resolving Inflammation. *Front Immunol,* 8.

LAINE, M. L., CRIELAARD, W. & LOOS, B. G. 2012. Genetic susceptibility to periodontitis. *Periodontol 2000,* 58**,** 37-68.

KUMAWAT, R. M., GANVIR, S. M., HAZAREY, V. K., QURESHI, A. & PUROHIT, H. J. 2016. Detection of Porphyromonas gingivalis and Treponema denticola in chronic

and aggressive periodontitis patients: A comparative polymerase chain reaction study. *Contemp Clin Dent,* 7**,** 481-6.

LAM, R., O'BRIEN-SIMPSON, N., HOLDEN, J., LENZO, J., FONG, S. & REYNOLDS, E. 2016. Unprimed, M1 and M2 Macrophages Differentially Interact with Porphyromonas gingivalis. *PloS one,* 11.

LAMARCHE, M. G., KIM, S. H., CREPIN, S., MOUREZ, M., BERTRAND, N., BISHOP, R. E., DUBREUIL, J. D. & HAREL, J. 2008. Modulation of hexa-acyl pyrophosphate lipid A population under *Escherichia coli* phosphate (Pho) regulon activation. *J Bacteriol,* 190**,** 5256-64.

LAMONT, R. J. & JENKINSON, H. F. 1998. Life below the gum line: pathogenic mechanisms of *Porphyromonas gingivalis*. *Microbiol Mol Biol Rev,* 62**,** 1244-63.

LARROUY-MAUMUS, G., CLEMENTS, A., FILLOUX, A., MCCARTHY, R. R. & MOSTOWY, S. 2016. Direct detection of lipid A on intact Gram-negative bacteria by MALDI-TOF mass spectrometry. *J Microbiol Methods,* 120**,** 68-71.

LEE, G. R. 2018. The Balance of Th17 versus Treg Cells in Autoimmunity. *Int J Mol Sci,* 19.

LEE, K., ROBERTS, J. S., CHOI, C. H., ATANASOVA, K. R. & YILMAZ, Ö. 2018. *Porphyromonas gingivalis* traffics into endoplasmic reticulum-rich-autophagosomes for successful survival in human gingival epithelial cells. *Virulence,* 9**,** 845-59.

LERTPIMONCHAI, A., RATTANASIRI, S., ARJ-ONG VALLIBHAKARA, S., ATTIA, J. & THAKKINSTIAN, A. 2017. The association between oral hygiene and periodontitis: a systematic review and meta-analysis. *Int Dent J,* 67**,** 332-43.

LEY, R. E., PETERSON, D. A. & GORDON, J. I. 2006. Ecological and evolutionary forces shaping microbial diversity in the human intestine. *Cell,* 124**,** 837-48.

LI, M., CHEN, Q., SHEN, Y. & LIU, W. 2009. *Candida albicans* phospholipomannan triggers inflammatory responses of human keratinocytes through Toll-like receptor 2. *Exp Dermatol,* 18**,** 603-10.

LI, P., LIU, H., ZHANG, Y., LIAO, R., HE, K., RUAN, X. & GONG, J. 2016. Endotoxin Tolerance Inhibits Degradation of Tumor Necrosis Factor Receptor-Associated Factor 3 by Suppressing Pellino 1 Expression and the K48 Ubiquitin Ligase Activity of Cellular Inhibitor of Apoptosis Protein 2. *The Journal of infectious diseases,* 214**,** 906-15.

LI, Y., WANG, Z., CHEN, J., ERNST, R. K. & WANG, X. 2013. Influence of lipid A acylation pattern on membrane permeability and innate immune stimulation. *Marine drugs,* 11**,** 3197-208.

LIAU, N. P. D., LAKTYUSHIN, A., LUCET, I. S., MURPHY, J. M., YAO, S., WHITLOCK, E., CALLAGHAN, K., NICOLA, N. A., KERSHAW, N. J. & BABON, J. J. 2018. The molecular basis of JAK/STAT inhibition by SOCS1. *Nature Communications,* 9**,** 1558.

LIE, M. A., VAN DER WEIJDEN, G. A., TIMMERMAN, M. F., LOOS, B. G., VAN STEENBERGEN, T. J. & VAN DER VELDEN, U. 2001. Occurrence of *Prevotella intermedia* and *Prevotella nigrescens* in relation to gingivitis and gingival health. *J Clin Periodontol,* 28**,** 189-93.

LIU, D., CAO, S., ZHOU, Y. & XIONG, Y. 2019. Recent advances in endotoxin tolerance. *J Cell Biochem,* 120**,** 56-70.

LIU, M., JOHN, C. M. & JARVIS, G. A. 2014. Induction of Endotoxin Tolerance by Pathogenic Neisseria Is Correlated with the Inflammatory Potential of Lipooligosaccharides and Regulated by MicroRNA-146a. *The Journal of Immunology,* 192**,** 1768-1777.

LIU, H., SIDIROPOULOS, P., SONG, G., PAGLIARI, L. J., BIRRER, M. J., STEIN, B., ANRATHER, J. & POPE, R. M. 2000. TNF-alpha gene expression in macrophages: regulation by NF-kappa B is independent of c-Jun or C/EBP beta. *J Immunol,* 164**,** 4277-85.

LIUKKONEN, J., GÜRSOY, U. K., PUSSINEN, P., SUOMINEN, A. L. & KÖNÖNEN, E. 2016. Salivary Concentrations of Interleukin (IL)-1β, IL-17A, and IL-23 Vary in Relation to Periodontal Status. *Journal of periodontology,* 87.

LOBÃO, W. J. M., CARVALHO, R. C. C., LEITE, S. A. M., RODRIGUES, V. P., BATISTA, J. E., GOMES-FILHO, I. S. & PEREIRA, A. L. A. 2019. Relationship Between Periodontal Outcomes and Serum Biomarkers Changes After Non-Surgical Periodontal Therapy. *Anais da Academia Brasileira de Ciencias,* 91.

LONZA, 2020. *Recombinant factor C assay*, viewed 20/04/2020, https://bioscience.lonza.com/lonza_bs/CH/en/recombinant-factor-c-assay

LOPEZ-COLLAZO, E. & DEL FRESNO, C. 2013. Pathophysiology of endotoxin tolerance: mechanisms and clinical consequences. *Crit Care,* 17**,** 242.

LORENZI, T., NIȚULESCU, E. A., ZIZZI, A., LORENZI, M., PAOLINELLI, F., ASPRIELLO, S. D., BANIȚĂ, M., CRĂIȚOIU, Ş., GOTERI, G., BARBATELLI, G., LOMBARDI, T., DI FELICE, R., MARZIONI, D., RUBINI, C. & CASTELLUCCI, M. 2014. The Novel Role of HtrA1 in Gingivitis, Chronic and Aggressive Periodontitis. *PLoS One,* 9.

LU, Q., DARVEAU, R. P., SAMARANAYAKE, L. P., WANG, C. Y. & JIN, L. 2009. Differential modulation of human {beta}-defensins expression in human gingival epithelia by *Porphyromonas gingivalis* lipopolysaccharide with tetra- and penta-acylated lipid A structures. *Innate Immun,* 15**,** 325-35.

LU, M., VARLEY, A. W. & MUNFORD, R. S. 2013. Persistently Active Microbial Molecules Prolong Innate Immune Tolerance In Vivo. *PLoS Pathog,* 9.

LU, M., VARLEY, A. W., OHTA, S., HARDWICK, J. & MUNFORD, R. S. 2008. Host Inactivation of Bacterial Lipopolysaccharide Prevents Prolonged Tolerance Following Gram-Negative Bacterial Infection. *Cell Host & Microbe,* 4**,** 293-302.

LUNDMARK, A., HU, Y. O. O., HUSS, M., JOHANNSEN, G., ANDERSSON, A. F. & YUCEL-LINDBERG, T. 2019. Identification of Salivary Microbiota and Its Association With Host Inflammatory Mediators in Periodontitis. *Front Cell Infect Microbiol,* 9.

LUNDBERG, K., WEGNER, N., YUCEL-LINDBERG, T. & VENABLES, P. J. 2010. Periodontitis in RA-the citrullinated enolase connection. *Nature reviews. Rheumatology,* 6**,** 727-30.

LUPARDUS, P. J. & GARCIA, K. C. 2008. The structure of interleukin-23 reveals the molecular basis of p40 subunit sharing with interleukin-12. *J Mol Biol,* 382**,** 931-41.

LY, L. L., YOSHIDA, H. & YAMAGUCHI, M. 2013. Nuclear transcription factor Y and its roles in cellular processes related to human disease. *Am J Cancer Res,* 3**,** 339-46.

MACFARLANE, G. T. & MACFARLANE, S. 2012. Bacteria, colonic fermentation, and gastrointestinal health. *J AOAC Int,* 95**,** 50-60.

MACKENZIE, K. F., CLARK, K., NAQVI, S., MCGUIRE, V. A., NÖEHREN, G., KRISTARIYANTO, Y., VAN DEN BOSCH, M., MUDALIAR, M., MCCARTHY, P. C., PATTISON, M. J., PEDRIOLI, P. G. A., BARTON, G. J., TOTH, R., PRESCOTT, A. & ARTHUR, J. S. C. 2013. PGE2 Induces Macrophage IL-10 Production and a Regulatory-like Phenotype via a Protein Kinase A–SIK–CRTC3 Pathway. *J Immunol,* 190**,** 565-77.

MACUCH, P. J. & TANNER, A. C. 2000. *Campylobacter* species in health, gingivitis, and periodontitis. *J Dent Res,* 79**,** 785-92.

MADEIRA, A., BURGELIN, I., PERRON, H., CURTIN, F., LANG, A. B. & FAUCARD, R. 2016. MSRV envelope protein is a potent, endogenous and pathogenic agonist of human toll-like receptor 4: Relevance of GNbAC1 in multiple sclerosis treatment. *Journal of Neuroimmunology,* 291**,** 29-38.

MAESHIMA, N. & FERNANDEZ, R. C. 2013. Recognition of lipid A variants by the TLR4-MD-2 receptor complex. *Front Cell Infect Microbiol,* 3**,** 3.

MAJOROS, A., PLATANITIS, E., KERNBAUER-HÖLZL, E., ROSEBROCK, F., MÜLLER, M. & DECKER, T. 2017. Canonical and Non-Canonical Aspects of JAK–STAT Signaling: Lessons from Interferons for Cytokine Responses. *Front Immunol,* 8.

MALHOTRA, J. D. & KAUFMAN, R. J. 2011. ER Stress and Its Functional Link to Mitochondria: Role in Cell Survival and Death. *Cold Spring Harb Perspect Biol.*

MALIK R, C. R., KRISHAN P, GUGNANI S, BALI D 2015. Virulence factors of *Aggregatibacter actinomycetemcomitans* - A status update. *Journal of ICDRO,* 7**,** 137-145.

MANN, M., MEHTA, A., ZHAO, J. L., LEE, K., MARINOV, G. K., GARCIA-FLORES, Y. & BALTIMORE, D. 2017. An NF-κB-microRNA regulatory network tunes macrophage inflammatory responses. *Nature Communications,* 8**,** 851.

MANNEM, S. & CHAVA, V. K. 2012. The effect of stress on periodontitis: A clinicobiochemical study. *J Indian Soc Periodontol.*

MANTOVANI, A., SICA, A., SOZZANI, S., ALLAVENA, P., VECCHI, A. & LOCATI, M. 2004. The chemokine system in diverse forms of macrophage activation and polarization. *Trends Immunol,* 25**,** 677-86.

MÁRQUEZ, S., FERNÁNDEZ, J. J., TERÁN-CABANILLAS, E., HERRERO, C., ALONSO, S., AZOGIL, A., MONTERO, O., IWAWAKI, T., CUBILLOS-RUIZ, J. R., FERNÁNDEZ, N. & CRESPO, M. S. 2017. Endoplasmic Reticulum Stress Sensor IRE1α Enhances IL-23 Expression by Human Dendritic Cells. *Front Immunol,* 8.

MARTIN, M., KATZ, J., VOGEL, S. N. & MICHALEK, S. M. 2001. Differential induction of endotoxin tolerance by lipopolysaccharides derived from *Porphyromonas gingivalis* and *Escherichia coli. Journal of immunology (Baltimore, Md. : 1950),* 167**,** 5278-85.

MARTINEZ, F. O. & GORDON, S. 2014. The M1 and M2 paradigm of macrophage activation: time for reassessment. *F1000Prime Rep,* 6**,** 13.

MARTINEZ, A., LOPEZ, N., GONZALEZ, C. & HETZ, C. 2019. Targeting of the unfolded protein response (UPR) as therapy for Parkinson's disease. *Biology of the cell,* 111.

MARTINON, F., CHEN, X., LEE, A. H. & GLIMCHER, L. H. 2010. TLR activation of the transcription factor XBP1 regulates innate immune responses in macrophages. *Nat Immunol,* 11**,** 411-8.

MASOUD, H., WEINTRAUB, S. T., WANG, R., COTTER, R. & HOLT, S. C. 1991. Investigation of the structure of lipid A from *Actinobacillus actinomycetemcomitans* strain Y4 and human clinical isolate PO 1021-7. *Eur J Biochem,* 200**,** 775-81.

MATHIS, B. J., LAI, Y., QU, C., JANICKI, J. S. & CUI, T. 2015. CYLD-Mediated Signaling and Diseases. *Curr Drug Targets,* 16**,** 284-94.

MATILAINEN, J. M., HUSSO, T., TOROPAINEN, S., SEUTER, S., TURUNEN, M. P., GYNTHER, P., YLÄ-HERTTUALA, S., CARLBERG, C. & VÄISÄNEN, S. 2010. Primary effect of 1α,25$(OH)_2D_3$ on IL-10 expression in monocytes is short-term down-regulation. *Biochimica et biophysica acta,* 1803**,** 1276-86.

MATRICON, J., BARNICH, N. & ARDID, D. 2010. Immunopathogenesis of inflammatory bowel disease. *Self Nonself,* 1**,** 299-309.

MAURAMO, M., RAMSEIER, A. M., MAURAMO, E., BUSER, A., TERVAHARTIALA, T., SORSA, T. & WALTIMO, T. 2018. Associations of Oral Fluid MMP-8 With Periodontitis in Swiss Adult Subjects. Oral diseases, 24.

MAYR, B. & MONTMINY, M. 2001. Transcriptional regulation by the phosphorylation-dependent factor CREB. *Nature Reviews Molecular Cell Biology,* 2**,** 599-609.

MEDEIROS, M. M., PEIXOTO, J. R., OLIVEIRA, A. C., CARDILO-REIS, L., KOATZ, V. L., VAN KAER, L., PREVIATO, J. O., MENDONCA-PREVIATO, L., NOBREGA, A. & BELLIO, M. 2007. Toll-like receptor 4 (TLR4)-dependent proinflammatory and immunomodulatory properties of the glycoinositolphospholipid (GIPL) from *Trypanosoma cruzi*. *J Leukoc Biol,* 82**,** 488-96.

MESCHIARI, C. A., MARCACCINI, A. M., SANTOS MOURA, B. C., ZUARDI, L. R., TANUS-SANTOS, J. E. & GERLACH, R. F. 2013. Salivary MMPs, TIMPs, and MPO levels in periodontal disease patients and controls. *Clin Chim Acta,* 421**,** 140-6.

MEURIC, V., GALL-DAVID, S. L., BOYER, E., ACUÑA-AMADOR, L., MARTIN, B., FONG, S. B., BARLOY-HUBLER, F., BONNAURE-MALLET, M. & MCBAIN, A. J. 2017. Signature of Microbial Dysbiosis in Periodontitis. *Applied Environmental Microbiology, DOI: 10.1128/AEM.00462-17.*

MIRICESCU, D., TOTAN, A., CALENIC, B., MOCANU, B., DIDILESCU, A., MOHORA, M., SPINU, T. & GREABU, M. 2014. Salivary Biomarkers: Relationship Between Oxidative Stress and Alveolar Bone Loss in Chronic Periodontitis. *Acta odontologica Scandinavica,* 72.

MISAKI, T., NAKA, S., HATAKEYAMA, R., FUKUNAGA, A., NOMURA, R., ISOZAKI, T. & NAKANO, K. 2016. Presence of *Streptococcus mutans* strains harbouring the cnm gene correlates with dental caries status and IgA nephropathy conditions. *Scientific Reports, Published online: 4 November 2016; | doi:10.1038/srep36455*.

MISE-OMATA, S., KURODA, E., NIIKURA, J., YAMASHITA, U., OBATA, Y. & DOI, T. S. 2007. A proximal kappaB site in the IL-23 p19 promoter is responsible for RelA- and c-Rel-dependent transcription. *J Immunol,* 179**,** 6596-603.

MIZRAJI, G., NASSAR, M., SEGEV, H., SHARAWI, H., ELI-BERCHOER, L., CAPUCHA, T., NIR, T., TABIB, Y., MAIMON, A., DISHON, S., SHAPIRA, L., NUSSBAUM, G., WILENSKY, A. & HOVAV, A. H. 2017. *Porphyromonas gingivalis* Promotes Unrestrained Type I Interferon Production by Dysregulating TAM Signaling via MYD88 Degradation. *Cell Rep,* 18**,** 419-431.

MOGENSEN, T. H. 2009. Pathogen recognition and inflammatory signaling in innate immune defenses. *Clin Microbiol Rev,* 22**,** 240-73.

MOLINARO, A., HOLST, O., DI LORENZO, F., CALLAGHAN, M., NURISSO, A., D'ERRICO, G., ZAMYATINA, A., PERI, F., BERISIO, R., JERALA, R., JIMENEZ-BARBERO, J., SILIPO, A. & MARTIN-SANTAMARIA, S. 2015. Chemistry of lipid A: at the heart of innate immunity. *Chemistry,* 21**,** 500-19.

MORELLI, T., STELLA, M., BARROS, S. P., MARCHESAN, J. T., MOSS, K. L., KIM, S. J., YU, N., ASPIRAS, M. B., WARD, M. & OFFENBACHER, S. 2014. Salivary Biomarkers in a Biofilm Overgrowth Model. *J Periodontol,* 85**,** 1770-8.

MORINUSHI, T., LOPATIN, D. E., VAN POPERIN, N. & UEDA, Y. 2000. The relationship between gingivitis and colonization by *Porphyromonas gingivalis* and *Actinobacillus actinomycetemcomitans* in children. *J Periodontol,* 71**,** 403-9.

MOUTSOPOULOS, N. M. & KONKEL, J. E. 2018. Tissue-Specific Immunity at the Oral Mucosal Barrier. *Trends Immunol,* 39**,** 276-287.

MOUTSOPOULOS, N. M., KLING, H. M., ANGELOV, N., JIN, W., PALMER, R. J., NARES, S., OSORIO, M. & WAHL, S. M. 2012. *P. gingivalis* promotes Th17 inducing pathways in chronic periodontitis. *J Autoimmun,* 39**,** 294-303.

MUADDI, H., MAJUMDER, M., PEIDIS, P., PAPADAKIS, A. I., HOLCIK, M., SCHEUNER, D., KAUFMAN, R. J., HATZOGLOU, M. & KOROMILAS, A. E. 2010. Phosphorylation of eIF2α at Serine 51 Is an Important Determinant of Cell Survival and Adaptation to Glucose Deficiency. *Mol Biol Cell,* 21**,** 3220-31.

MUKAIDA, N., OKAMOTO, S., ISHIKAWA, Y. & MATSUSHIMA, K. 1994. Molecular mechanism of interleukin-8 gene expression. *J Leukoc Biol,* 56**,** 554-8.

MUKAKA, M. 2012. A guide to appropriate use of Correlation coefficient in medical research. *Malawi Med J,* 24**,** 69-71.

MURDOCK, J. L. & NUNEZ, G. 2016. TLR4: The Winding Road to the Discovery of the LPS Receptor. *J Immunol,* 197**,** 2561-2.

MURPHY, M., XIONG, Y., PATTABIRAMAN, G., QIU, F. & MEDVEDEV, A. E. 2015. Pellino-1 Positively Regulates Toll-like Receptor (TLR) 2 and TLR4 Signaling and Is Suppressed upon Induction of Endotoxin Tolerance. *The Journal of biological chemistry,* 290**,** 19218-32.

MURRAY, P. J., ALLEN, J. E., BISWAS, S. K., FISHER, E. A., GILROY, D. W., GOERDT, S., GORDON, S., HAMILTON, J. A., IVASHKIV, L. B., LAWRENCE, T., LOCATI, M., MANTOVANI, A., MARTINEZ, F. O., MEGE, J. L., MOSSER, D. M., NATOLI, G., SAEIJ, J. P., SCHULTZE, J. L., SHIREY, K. A., SICA, A., SUTTLES, J., UDALOVA, I., VAN GINDERACHTER, J. A., VOGEL, S. N. & WYNN, T. A. 2014.

Macrophage activation and polarization: nomenclature and experimental guidelines. *Immunity,* 41**,** 14-20.

MUTHUKURU, M. & CUTLER, C. W. 2015. Resistance of MMP9 and TIMP1 to endotoxin tolerance. *Pathogens and disease,* 73.

MUTHUKURU, M. & DARVEAU, R. P. 2014. TLR signaling that induces weak inflammatory response and SHIP1 enhances osteogenic functions. *Bone Research,* 2**,** 14031.

NAHID, M. A., PAULEY, K. M., SATOH, M. & CHAN, E. K. L. 2009. MICRORNA-146A is critical for endotoxin-induced tolerance. Implication on innate immunity. *Journal of Biological Chemistry*.

NAKAJIMA, T., HONDA, T., DOMON, H., OKUI, T., KAJITA, K., ITO, H., TAKAHASHI, N., MAEKAWA, T., TABETA, K. & YAMAZAKI, K. 2010. Periodontitis-associated Up-Regulation of Systemic Inflammatory Mediator Level May Increase the Risk of Coronary Heart Disease. *Journal of periodontal research,* 45.

NAN, Y., WU, C. & ZHANG, Y. J. 2017. Interplay between Janus Kinase/Signal Transducer and Activator of Transcription Signaling Activated by Type I Interferons and Viral Antagonism. *Front Immunol,* 8.

NASH, J. A., BALLARD, T. N. S., WEAVER, T. E. & AKINBI, H. T. 2006. The Peptidoglycan-Degrading Property of Lysozyme Is Not Required for Bactericidal Activity In Vivo. *The Journal of Immunology,* 177**,** 519-526.

NATIVEL, B., COURET, D., GIRAUD, P., MEILHAC, O., D'HELLENCOURT, C. L., VIRANAÏCKEN, W. & DA SILVA, C. R. 2017. *Porphyromonas gingivalis* lipopolysaccharides act exclusively through TLR4 with a resilience between mouse and human. *Sci Rep,* 7.

NEWTON, K. & DIXIT, V. M. 2012. Signaling in innate immunity and inflammation. *Cold Spring Harb Perspect Biol,* 4.

NGUYEN, T., SEDGHI, L., GANTHER, S., MALONE, E., KAMARAJAN, P. & KAPILA, Y. 2020. Host-microbe interactions: Profiles in the transcriptome, the proteome, and the metabolome. Periodontology 2000, 82.

NIBALI, L., D'AIUTO, F., GRIFFITHS, G., PATEL, K., SUVAN, J. & TONETTI, M. S. 2007. Severe Periodontitis Is Associated With Systemic Inflammation and a Dysmetabolic Status: A Case-Control Study. *Journal of clinical periodontology,* 34.

NILSEN, N. J., VLADIMER, G. I., STENVIK, J., ORNING, M. P., ZEID-KILANI, M. V., BUGGE, M., BERGSTROEM, B., CONLON, J., HUSEBYE, H., HISE, A. G., FITZGERALD, K. A., ESPEVIK, T. & LIEN, E. 2015. A role for the adaptor proteins TRAM and TRIF in toll-like receptor 2 signaling. *J Biol Chem,* 290**,** 3209-22.

NISHA, K., SURESH, A., ANILKUMAR, A. & PADMANABHAN, S. 2018. MIP-1α and MCP-1 as salivary biomarkers in periodontal disease. *Saudi Dent J,* 30**,** 292-8.

NISHITOH, H., MATSUZAWA, A., TOBIUME, K., SAEGUSA, K., TAKEDA, K., INOUE, K., HORI, S., KAKIZUKA, A. & ICHIJO, H. 2002. ASK1 is essential for endoplasmic reticulum stress-induced neuronal cell death triggered by expanded polyglutamine repeats. *Genes Dev,* 16**,** 1345-55.

NOVEM, V., SHUI, G., WANG, D., BENDT, A. K., SIM, S. H., LIU, Y., THONG, T. W., SIVALINGAM, S. P., OOI, E. E., WENK, M. R. & TAN, G. 2009. Structural and biological diversity of lipopolysaccharides from *Burkholderia pseudomallei* and *Burkholderia thailandensis*. *Clinical and vaccine immunology : CVI,* 16**,** 1420-8.

NUSSBAUM, G. & SHAPIRA, L. 2011. How has neutrophil research improved our understanding of periodontal pathogenesis? *J Clin Periodontol,* 38 Suppl 11**,** 49-59.

O'CARROLL, C., FAGAN, A., SHANAHAN, F. & CARMODY, R. J. 2014. Identification of a unique hybrid macrophage-polarization state following recovery from lipopolysaccharide tolerance. *J Immunol,* 192**,** 427-36.

OCHIAI, K., IMAI, K., TAMURA, M. & KURITA-OCHIAI, T. 2011. Butyric Acid Effects in the Development of Periodontitis and Systemic Diseases. *Journal of Oral Biosciences,* 53**,** 213-220.

OECKINGHAUS, A., HAYDEN, M. & GHOSH, S. 2011. Crosstalk in NF-κB signaling pathways. *Nature immunology,* 12.

OJOGUN, N., KUANG, T.-Y., SHAO, B., GREAVES, D. R., MUNFORD, R. S. & VARLEY, A. W. 2009. Overproduction of acyloxyacyl hydrolase by macrophages and dendritic cells prevents prolonged reactions to bacterial lipopolysaccharide in vivo. *The Journal of infectious diseases,* 200**,** 1685-93.

OLCZAK, T., SOSICKA, P. & OLCZAK, M. 2015. HmuY is an important virulence factor for *Porphyromonas gingivalis* growth in the heme-limited host environment and infection of macrophages. *Biochemical and biophysical research communications,* 467**,** 748-53.

OLLIVIER, V., PARRY, G. C., COBB, R. R., DE PROST, D. & MACKMAN, N. 1996. Elevated cyclic AMP inhibits NF-kappaB-mediated transcription in human monocytic cells and endothelial cells. *J Biol Chem,* 271**,** 20828-35.

OPPMANN, B., LESLEY, R., BLOM, B., TIMANS, J. C., XU, Y., HUNTE, B., VEGA, F., YU, N., WANG, J., SINGH, K., ZONIN, F., VAISBERG, E., CHURAKOVA, T., LIU, M., GORMAN, D., WAGNER, J., ZURAWSKI, S., LIU, Y., ABRAMS, J. S., MOORE, K. W., RENNICK, D., DE WAAL-MALEFYT, R., HANNUM, C., BAZAN, J. F. & KASTELEIN, R. A. 2000. Novel p19 protein engages IL-12p40 to form a

cytokine, IL-23, with biological activities similar as well as distinct from IL-12. *Immunity,* 13**,** 715-25.

OVERMAN, E. L., RIVIER, J. E. & MOESER, A. J. 2012. CRF Induces Intestinal Epithelial Barrier Injury via the Release of Mast Cell Proteases and TNF-α. *PLoS One,* 7.

OZINSKY, A., UNDERHILL, D. M., FONTENOT, J. D., HAJJAR, A. M., SMITH, K. D., WILSON, C. B., SCHROEDER, L. & ADEREM, A. 2000. The repertoire for pattern recognition of pathogens by the innate immune system is defined by cooperation between toll-like receptors. *Proc Natl Acad Sci U S A,* 97**,** 13766-71.

PALSSON-MCDERMOTT, E. M., DOYLE, S. L., MCGETTRICK, A. F., HARDY, M., HUSEBYE, H., BANAHAN, K., GONG, M., GOLENBOCK, D., ESPEVIK, T. & O'NEILL, L. A. 2009. TAG, a splice variant of the adaptor TRAM, negatively regulates the adaptor MyD88-independent TLR4 pathway. *Nat Immunol,* 10**,** 579-86.

PAPA, E., DOCKTOR, M., SMILLIE, C., WEBER, S., PREHEIM, S. P., GEVERS, D., GIANNOUKOS, G., CIULLA, D., TABBAA, D., INGRAM, J., SCHAUER, D. B., WARD, D. V., KORZENIK, J. R., XAVIER, R. J., BOUSVAROS, A. & ALM, E. J. 2012. Non-invasive mapping of the gastrointestinal microbiota identifies children with inflammatory bowel disease. *PLoS One,* 7**,** e39242.

PAPADOPOULOS, G., WEINBERG, E. O., MASSARI, P., GIBSON, F. C., WETZLER, L. M., MORGAN, E. F. & GENCO, C. A. 2013. Macrophage-specific TLR2 signaling mediates pathogen-induced TNF-dependent inflammatory oral bone loss. *Journal of immunology (Baltimore, Md. : 1950),* 190**,** 1148-57.

PARAMESWARAN, N. & PATIAL, S. 2010. Tumor Necrosis Factor-α Signaling in Macrophages. *Crit Rev Eukaryot Gene Expr,* 20**,** 87-103.

PARAMONOV, N., BAILEY, D., RANGARAJAN, M., HASHIM, A., KELLY, G., CURTIS, M. A. & HOUNSELL, E. F. 2001. Structural analysis of the polysaccharide from the lipopolysaccharide of Porphyromonas gingivalis strain W50. *Eur J Biochem,* 268**,** 4698-707.

PARK, S. H., KANG, K., GIANNOPOULOU, E., QIAO, Y., KIM, G., PARK-MIN, K. H. & IVASHKIV, L. B. 2017. Type I IFNs and TNF cooperatively reprogram the macrophage epigenome to promote inflammatory activation. *Nat Immunol,* 18**,** 1104-16.

PARK, B. S. & LEE, J. O. 2013. Recognition of lipopolysaccharide pattern by TLR4 complexes. *Exp Mol Med,* 45**,** e66-.

PARK, B. S., SONG, D. H., KIM, H. M., CHOI, B. S., LEE, H. & LEE, J. O. 2009. The structural basis of lipopolysaccharide recognition by the TLR4-MD-2 complex. *Nature,* 458**,** 1191-5.

PATEL, R. M., VARMA, S., SURAGIMATH, G. & ZOPE, S. 2016. Estimation and Comparison of Salivary Calcium, Phosphorous, Alkaline Phosphatase and pH Levels in Periodontal Health and Disease: A Cross-sectional Biochemical Study. *J Clin Diagn Res,* 10**,** ZC58-61.

PENA, O. M., HANCOCK, D. G., LYLE, N. H., LINDER, A., RUSSELL, J. A., XIA, J., FJELL, C. D., BOYD, J. H. & HANCOCK, R. E. W. 2014. An Endotoxin Tolerance Signature Predicts Sepsis and Organ Dysfunction at Initial Clinical Presentation. *EBioMedicine,* 1**,** 64-71.

PENA, O. M., PISTOLIC, J., RAJ, D., FJELL, C. D. & HANCOCK, R. E. W. 2011. Endotoxin tolerance represents a distinctive state of alternative polarization (M2) in human mononuclear cells. *Journal of immunology (Baltimore, Md. : 1950),* 186**,** 7243-54.

PENG, L., HE, Z., CHEN, W., HOLZMAN, I. R. & LIN, J. 2007. Effects of butyrate on intestinal barrier function in a Caco-2 cell monolayer model of intestinal barrier. *Pediatr Res,* 61**,** 37-41.

PENG, J., YUAN, Q., LIN, B., PANNEERSELVAM, P., WANG, X., LUAN, X. L., LIM, S. K., LEUNG, B. P., HO, B. & DING, J. L. 2010. SARM inhibits both TRIF- and MyD88-mediated AP-1 activation. *Eur J Immunol,* 40**,** 1738-47.

PIAO, W., SONG, C., CHEN, H., DIAZ, M. A. Q., WAHL, L. M., FITZGERALD, K. A., LI, L. & MEDVEDEV, A. E. 2009. Endotoxin tolerance dysregulates MyD88- and Toll/IL-1R domain-containing adapter inducing IFN-beta-dependent pathways and increases expression of negative regulators of TLR signaling. *Journal of leukocyte biology,* 86**,** 863-75.

PLATANIAS, L. C. 2005. Mechanisms of type-I- and type-II-interferon-mediated signalling. *Nat Rev Immunol,* 5**,** 375-86.

PLOGER, S., STUMPFF, F., PENNER, G. B., SCHULZKE, J. D., GABEL, G., MARTENS, H., SHEN, Z., GUNZEL, D. & ASCHENBACH, J. R. 2012. Microbial butyrate and its role for barrier function in the gastrointestinal tract. *Ann N Y Acad Sci,* 1258**,** 52-9.

POPOVA, C., DOSSEVA-PANOVA, V. & PANOV, V. 2014. Microbiology of Periodontal Diseases. A Review. *Biotechnology & Biotechnological Equipment,* 27**,** 3754-3759.

POSCH, G., ANDRUKHOV, O., VINOGRADOV, E., LINDNER, B., MESSNER, P., HOLST, O. & SCHAFFER, C. 2013. Structure and immunogenicity of the rough-type lipopolysaccharide from the periodontal pathogen *Tannerella forsythia*. *Clin Vaccine Immunol,* 20**,** 945-53.

PRIETO, J., EKLUND, A. & PATARROYO, M. 1994. Regulated expression of integrins and other adhesion molecules during differentiation of monocytes into macrophages. *Cell Immunol,* 156**,** 191-211.

QASIM, S., AL-OTAIBI, D., AL-JASSER, R., GUL, S. & ZAFAR, M. 2020. An Evidence-Based Update on the Molecular Mechanisms Underlying Periodontal Diseases. *International journal of molecular sciences,* 21.

QIN, Z. 2012. The use of THP-1 cells as a model for mimicking the function and regulation of monocytes and macrophages in the vasculature. *Atherosclerosis,* 221**,** 2-11.

QUESNIAUX, V. J., NICOLLE, D. M., TORRES, D., KREMER, L., GUERARDEL, Y., NIGOU, J., PUZO, G., ERARD, F. & RYFFEL, B. 2004. Toll-like receptor 2 (TLR2)-dependent-positive and TLR2-independent-negative regulation of proinflammatory cytokines by mycobacterial lipomannans. *J Immunol,* 172**,** 4425-34.

QURESHI, N., MASCAGNI, P., RIBI, E. & TAKAYAMA, K. 1985. Monophosphoryl lipid A obtained from lipopolysaccharides of *Salmonella minnesota* R595. Purification of the dimethyl derivative by high performance liquid chromatography and complete structural determination. *J Biol Chem,* 260**,** 5271-8.

RAETZ, C. R., REYNOLDS, C. M., TRENT, M. S. & BISHOP, R. E. 2007. Lipid A modification systems in gram-negative bacteria. *Annu Rev Biochem,* 76**,** 295-329.

RÄISÄNEN, I. T., SORSA, T., VAN DER SCHOOR, G. J., TERVAHARTIALA, T., VAN DER SCHOOR, P., GIESELMANN, D. R. & HEIKKINEN, A. M. 2019. Active Matrix Metalloproteinase-8 Point-of-Care (PoC)/Chairside Mouthrinse Test vs. Bleeding on Probing in Diagnosing Subclinical Periodontitis in Adolescents. Diagnostics (Basel), 9.

RAJAIAH, R., PERKINS, D. J., POLUMURI, S. K., ZHAO, A., KEEGAN, A. D. & VOGEL, S. N. 2013. Dissociation of endotoxin tolerance and differentiation of alternatively activated macrophages. *Journal of immunology (Baltimore, Md. : 1950),* 190**,** 4763-72.

RALLABHANDI, P., PHILLIPS, R. L., BOUKHVALOVA, M. S., PLETNEVA, L. M., SHIREY, K. A., GIOANNINI, T. L., WEISS, J. P., CHOW, J. C., HAWKINS, L. D., VOGEL, S. N. & BLANCO, J. C. 2012. Respiratory syncytial virus fusion protein-induced toll-like receptor 4 (TLR4) signaling is inhibited by the TLR4 antagonists *Rhodobacter sphaeroides* lipopolysaccharide and eritoran (E5564) and requires direct interaction with MD-2. *MBio,* 3.

RAMS, T. E., FEIK, D., MORTENSEN, J. E., DEGENER, J. E. & VAN WINKELHOFF, A. J. 2014. Antibiotic susceptibility of periodontal *Streptococcus constellatus* and *Streptococcus intermedius* clinical isolates. *J Periodontol,* 85**,** 1792-8.

RANGARAJAN, M., ADUSE-OPOKU, J., PARAMONOV, N., HASHIM, A., BOSTANCI, N., FRASER, O. P., TARELLI, E. & CURTIS, M. A. 2008. Identification of a second lipopolysaccharide in Porphyromonas gingivalis W50. *J Bacteriol,* 190**,** 2920-32.

RANGARAJAN, M., ADUSE-OPOKU, J., PARAMONOV, N. A., HASHIM, A. & CURTIS, M. A. 2017. Hemin binding by Porphyromonas gingivalis strains is dependent on the presence of A-LPS. *Mol Oral Microbiol,* 32**,** 365-374.

RAPPSILBER, J., ISHIHAMA, Y. & MANN, M. 2003. Stop and go extraction tips for matrix-assisted laser desorption/ionization, nanoelectrospray, and LC/MS sample pretreatment in proteomics. *Anal Chem,* 75**,** 663-70.

RATH, M., MÜLLER, I., KROPF, P., CLOSS, E. I. & MUNDER, M. 2014. Metabolism via Arginase or Nitric Oxide Synthase: Two Competing Arginine Pathways in Macrophages. *Front Immunol,* 5.

REGIS, G., PENSA, S., BOSELLI, D., NOVELLI, F. & POLI, V. 2008. Ups and downs: the STAT1:STAT3 seesaw of Interferon and gp130 receptor signalling. *Semin Cell Dev Biol,* 19**,** 351-9.

REVU, S., WU, J., HENKEL, M., RITTENHOUSE, N., MENK, A., DELGOFFE, G. M., POHOLEK, A. C. & MCGEACHY, M. J. 2018. IL-23 and IL-1beta Drive Human Th17 Cell Differentiation and Metabolic Reprogramming in Absence of CD28 Costimulation. *Cell Rep,* 22**,** 2642-2653.

RIETSCHEL, E. T., KIRIKAE, T., SCHADE, F. U., MAMAT, U., SCHMIDT, G., LOPPNOW, H., ULMER, A. J., ZÄHRINGER, U., SEYDEL, U. & DI PADOVA, F. 1994. Bacterial endotoxin: molecular relationships of structure to activity and function. *FASEB journal : official publication of the Federation of American Societies for Experimental Biology,* 8**,** 217-25.

RIZAL, M., SOEROSO, Y., SULIJAYA, B., ASSIDDIQ, B., BACHTIAR, E. & BACHTIAR, B. 2020. Proteomics approach for biomarkers and diagnosis of periodontitis: systematic review. *Heliyon,* 6.

ROSSI, O., PESCE, I., GIANNELLI, C., APREA, S., CABONI, M., CITIULO, F., VALENTINI, S., FERLENGHI, I., MACLENNAN, C. A., D'ORO, U., SAUL, A. & GERKE, C. 2014. Modulation of Endotoxicity of Shigella Generalized Modules for Membrane Antigens (GMMA) by Genetic Lipid A Modifications: relative activation of tlr4 and tlr2 pathways in different mutants. *J Biol Chem,* 289**,** 24922-35.

ROSZER, T. 2015. Understanding the Mysterious M2 Macrophage through Activation Markers and Effector Mechanisms. *Mediators Inflamm,* 2015**,** 816460.

RUSSO, I., LUCIANI, A., DE CICCO, P., TRONCONE, E. & CIACCI, C. 2012. Butyrate Attenuates Lipopolysaccharide-Induced Inflammation in Intestinal Cells and Crohn's Mucosa through Modulation of Antioxidant Defense Machinery. *PLoS One.*

SAITO, A., INAGAKI, S., KIMIZUKA, R., OKUDA, K., HOSAKA, Y., NAKAGAWA, T. & ISHIHARA, K. 2008. *Fusobacterium nucleatum* enhances invasion of human gingival epithelial and aortic endothelial cells by *Porphyromonas gingivalis*. *FEMS Immunol Med Microbiol,* 54**,** 349-55.

SAKAGUCHI, S., NEGISHI, H., ASAGIRI, M., NAKAJIMA, C., MIZUTANI, T., TAKAOKA, A., HONDA, K. & TANIGUCHI, T. 2003. Essential role of IRF-3 in lipopolysaccharide-induced interferon-beta gene expression and endotoxin shock. *Biochem Biophys Res Commun,* 306**,** 860-6.

SALAMONE, G., GIORDANO, M., TREVANI, A. S., GAMBERALE, R., VERMEULEN, M., SCHETTINNI, J. & GEFFNER, J. R. 2001. Promotion of Neutrophil Apoptosis by TNF-α. *Journal of Immunology*, 166, 3476-83

SÁNCHEZ, G. A., MIOZZA, V. A., DELGADO, A. & BUSCH, L. 2013. Salivary IL-1β and PGE2 as Biomarkers of Periodontal Status, Before and After Periodontal Treatment. *Journal of clinical periodontology,* 40.

SARTOR, R. B. 2008. Microbial influences in inflammatory bowel diseases. *Gastroenterology,* 134**,** 577-94.

SARTOR, R. B. 2010. Genetics and environmental interactions shape the intestinal microbiome to promote inflammatory bowel disease versus mucosal homeostasis. *Gastroenterology,* 139**,** 1816-9.

SCHAPPI, P. & ZAPPA, U. 1990. The episodic progression of untreated adult periodontitis. *Parodontol,* 1**,** 351-62.

SCHRODER, N. W., MORATH, S., ALEXANDER, C., HAMANN, L., HARTUNG, T., ZAHRINGER, U., GOBEL, U. B., WEBER, J. R. & SCHUMANN, R. R. 2003. Lipoteichoic acid (LTA) of *Streptococcus pneumoniae* and *Staphylococcus aureus* activates immune cells via Toll-like receptor (TLR)-2, lipopolysaccharide-binding protein (LBP), and CD14, whereas TLR-4 and MD-2 are not involved. *J Biol Chem,* 278**,** 15587-94.

SCHUTYSER, E., STRUYF, S., PROOST, P., OPDENAKKER, G., LAUREYS, G., VERHASSELT, B., PEPERSTRAETE, L., VAN DE PUTTE, I., SACCANI, A., ALLAVENA, P., MANTOVANI, A. & VAN DAMME, J. 2002. Identification of biologically active chemokine isoforms from ascitic fluid and elevated levels of CCL18/pulmonary and activation-regulated chemokine in ovarian carcinoma. *J Biol Chem,* 277**,** 24584-93.

SCHWENDE, H., FITZKE, E., AMBS, P. & DIETER, P. 1996. Differences in the state of differentiation of THP-1 cells induced by phorbol ester and 1,25-dihydroxyvitamin D3. *Journal of leukocyte biology,* 59**,** 555-61.

SENGUPTA, S., HITTLE, L. E., ERNST, R. K., URIARTE, S. M. & MITCHELL, T. C. 2016. A Pseudomonas aeruginosa hepta-acylated lipid A variant associated with cystic fibrosis selectively activates human neutrophils. *J Leukoc Biol,* 100**,** 1047-1059.

SHEALY, D. J. & VISVANATHAN, S. 2008. Anti-TNF antibodies: lessons from the past, roadmap for the future. *Handb Exp Pharmacol***,** 101-29.

SHEMBADE, N. & HARHAJ, E. W. 2012. Regulation of NF-kappaB signaling by the A20 deubiquitinase. *Cell Mol Immunol,* 9**,** 123-30.

SHI, J. & WEI, P. K. 2016. Interleukin-8: A potent promoter of angiogenesis in gastric cancer. *Oncol Lett,* 11**,** 1043-50.

SHI, M., WEI, Y., HU, W., NIE, Y., WU, X. & LU, R. 2018. The Subgingival Microbiome of Periodontal Pockets With Different Probing Depths in Chronic and Aggressive Periodontitis: A Pilot Study. *Front Cell Infect Microbiol,* 8.

SHI, Q., YIN, Z., ZHAO, B., SUN, F., YU, H., YIN, X., ZHANG, L. & WANG, S. 2015. PGE2 Elevates IL-23 Production in Human Dendritic Cells via a cAMP Dependent Pathway. *Mediators of Inflammation,* 2015**,** 7.

SHIMAZU, R., AKASHI, S., OGATA, H., NAGAI, Y., FUKUDOME, K., MIYAKE, K. & KIMOTO, M. 1999. MD-2, a Molecule that Confers Lipopolysaccharide Responsiveness on Toll-like Receptor 4. *J Exp Med,* 189**,** 1777-82.

SIGNAT, B., ROQUES, C., POULET, P. & DUFFAUT, D. 2011. *Fusobacterium nucleatum* in periodontal health and disease. *Curr Issues Mol Biol,* 13**,** 25-36.

SILVA, N., ABUSLEME, L., BRAVO, D., DUTZAN, N., GARCIA-SESNICH, J., VERNAL, R., HERNANDEZ, M. & GAMONAL, J. 2015. Host response mechanisms in periodontal diseases. *J Appl Oral Sci,* 23**,** 329-55.

SILVA, N., DUTZAN, N., HERNANDEZ, M., DEZEREGA, A., RIVERA, O., AGUILLON, J. C., ARAVENA, O., LASTRES, P., POZO, P., VERNAL, R. & GAMONAL, J. 2008. Characterization of progressive periodontal lesions in chronic periodontitis patients: levels of chemokines, cytokines, matrix metalloproteinase-13, periodontal pathogens and inflammatory cells. *Journal of clinical periodontology,* 35**,** 206-14.

SIMOVITCH, M., SASON, H., COHEN, S., ZAHAVI, E. E., MELAMED-BOOK, N., WEISS, A., AROETI, B. & ROSENSHINE, I. 2010. EspM inhibits pedestal formation by enterohaemorrhagic *Escherichia coli* and enteropathogenic *E. coli* and disrupts the architecture of a polarized epithelial monolayer. *Cell Microbiol,* 12**,** 489-505.

SINGER, R. E. & BUCKNER, B. A. 1981. Butyrate and propionate: important components of toxic dental plaque extracts. *Infect Immun,* 32**,** 458-63.

SLOCUM, C., COATS, S. R., HUA, N., KRAMER, C., PAPADOPOULOS, G., WEINBERG, E. O., GUDINO, C. V., HAMILTON, J. A., DARVEAU, R. P. & GENCO, C. A. 2014. Distinct lipid a moieties contribute to pathogen-induced site-specific vascular inflammation. *PLoS Pathog,* 10**,** e1004215.

SLOMIANY, B. L. & SLOMIANY, A. 2004. *Porphyromonas gingivalis* lipopolysaccharide-induced up-regulation in endothelin-1 interferes with salivary mucin synthesis via epidermal growth factor receptor transactivation. *IUBMB Life,* 56**,** 601-7.

SLOMIANY, B. L. & SLOMIANY, A. 2018. Proinflammatory Signaling Cascades of Periodontopathic Oral Pathogen *Porphyromonas gingivalis*. *Journal of Biosciences and Medicines,* 06**,** 63.

SLY, L. M., RAUH, M. J., KALESNIKOFF, J., SONG, C. H. & KRYSTAL, G. 2004. LPS-induced upregulation of SHIP is essential for endotoxin tolerance. *Immunity,* 21**,** 227-39.

SMITH, J. A. 2018. Regulation of Cytokine Production by the Unfolded Protein Response; Implications for Infection and Autoimmunity. *Front Immunol,* 9**,** 422.

SOCRANSKY, S. S., HAFFAJEE, A. D., CUGINI, M. A., SMITH, C. & KENT, R. L. 1998. Microbial complexes in subgingival plaque. *Journal of Clinical Periodontology,* 25**,** 134-144.

SOCRANSKY, S. S., HAFFAJEE, A. D., TELES, R., WENNSTROM, J. L., LINDHE, J., BOGREN, A., HASTURK, H., VAN DYKE, T., WANG, X. & GOODSON, J. M. 2013. Effect of periodontal therapy on the subgingival microbiota over a 2-year

monitoring period. I. Overall effect and kinetics of change. *J Clin Periodontol,* 40**,** 771-80.

SOUZA, D. G., CASSALI, G. D., POOLE, S. & TEIXEIRA, M. M. 2001. Effects of inhibition of PDE4 and TNF-alpha on local and remote injuries following ischaemia and reperfusion injury. *Br J Pharmacol,* 134**,** 985-94.

STATHOPOULOU, P., G, BUDUNELI, N. & KINANE, D. F. 2015. Systemic Biomarkers for Periodontitis. *Current Oral Health Reports,* 2**,** 218-226.

STEIMLE, A. & AUTENRIETH, I. B. 2016. Structure and function: Lipid A modifications in commensals and pathogens. *International Journal of Medical Microbiology,* 306**,** 290-301.

STRAUSS, J., KAPLAN, G. G., BECK, P. L., RIOUX, K., PANACCIONE, R., DEVINNEY, R., LYNCH, T. & ALLEN-VERCOE, E. 2011. Invasive potential of gut mucosa-derived *Fusobacterium nucleatum* positively correlates with IBD status of the host. *Inflamm Bowel Dis,* 17**,** 1971-8.

STRITESKY, G. L., YEH, N. & KAPLAN, M. H. 2008. IL-23 promotes maintenance but not commitment to the Th17 lineage 1. *J Immunol,* 181**,** 5948-55.

SUCH-SANMARTIN, G., BACHE, N., CALLESEN, A. K., ROGOWSKA-WRZESINSKA, A. & JENSEN, O. N. 2015. Targeted mass spectrometry analysis of the proteins IGF1, IGF2, IBP2, IBP3 and A2GL by blood protein precipitation. *J Proteomics,* 113**,** 29-37.

SUCHETT-KAYE, G., DECORET, D. & BARSOTTI, O. 1999. Intra-familial distribution of *Fusobacterium nucleatum* strains in healthy families with optimal plaque control. *J Clin Periodontol,* 26**,** 401-4.

SUZUKI, A., HORIE, T. & NUMABE, Y. 2019. Investigation of molecular biomarker candidates for diagnosis and prognosis of chronic periodontitis by bioinformatics

analysis of pooled microarray gene expression datasets in Gene Expression Omnibus (GEO). *BMC Oral Health,* 19.

TADA, H., NEMOTO, E., SHIMAUCHI, H., WATANABE, T., MIKAMI, T., MATSUMOTO, T., OHNO, N., TAMURA, H., SHIBATA, K., AKASHI, S., MIYAKE, K., SUGAWARA, S. & TAKADA, H. 2002. *Saccharomyces cerevisiae*- and *Candida albicans*-derived mannan induced production of tumor necrosis factor alpha by human monocytes in a CD14- and Toll-like receptor 4-dependent manner. *Microbiol Immunol,* 46**,** 503-12.

TAKEUCHI, O & AKIRA, S. 2010. Pattern Recognition Receptors and Inflammation. *Cell,* 140**,** 805-820.

TAKEUCHI, O., HOSHINO, K., KAWAI, T., SANJO, H., TAKADA, H., OGAWA, T., TAKEDA, K. & AKIRA, S. 1999. Differential roles of TLR2 and TLR4 in recognition of gram-negative and gram-positive bacterial cell wall components. *Immunity,* 11**,** 443-51.

TAKEUCHI, O., KAWAI, T., MÜHLRADT, P. F., MORR, M., RADOLF, J. D., ZYCHLINSKY, A., TAKEDA, K. & AKIRA, S. 2001. Discrimination of bacterial lipoproteins by Toll-like receptor 6. *International Immunology,* 13**,** 933-940.

TAKEUCHI, O., SATO, S., HORIUCHI, T., HOSHINO, K., TAKEDA, K., DONG, Z., MODLIN, R. L. & AKIRA, S. 2002. Cutting edge: role of Toll-like receptor 1 in mediating immune response to microbial lipoproteins. *J Immunol,* 169**,** 10-4.

TAXMAN, D. J., SWANSON, K. V., BROGLIE, P. M., WEN, H., HOLLEY-GUTHRIE, E., HUANG, M. T., CALLAWAY, J. B., EITAS, T. K., DUNCAN, J. A. & TING, J. P. 2012. *Porphyromonas gingivalis* mediates inflammasome repression in polymicrobial cultures through a novel mechanism involving reduced endocytosis. *J Biol Chem,* 287**,** 32791-9.

TAYLOR, J. J. 2014. Protein Biomarkers of Periodontitis in Saliva. *ISRN Inflammation,* 2014**,** 18.

TAYLOR, J. J., JAEDICKE, K. M., MERWE, R. C. V. D., BISSETT, S. M., LANDSDOWNE, N., WHALL, K. M., PICKERING, K., THORNTON, V., LAWSON, V., YATSUDA, H., KOGAI, T., SHAH, D., ATHEY, D. & PRESHAW, P. M. 2019. A Prototype Antibody-based Biosensor for Measurement of Salivary MMP-8 in Periodontitis using Surface Acoustic Wave Technology. *Scientific Reports,* 9**,** 1-9.

TEDELIND, S., WESTBERG, F., KJERRULF, M. & VIDAL, A. 2007. Anti-inflammatory properties of the short-chain fatty acids acetate and propionate: a study with relevance to inflammatory bowel disease. *World J Gastroenterol,* 13**,** 2826-32.

THANABALASURIAR, A., KOUTSOURIS, A., WEFLEN, A., MIMEE, M., HECHT, G. & GRUENHEID, S. 2010. The bacterial virulence factor NleA is required for the disruption of intestinal tight junctions by enteropathogenic Escherichia coli. *Cell Microbiol,* 12**,** 31-41.

THOMPSON-CHAGOYAN, O. C., MALDONADO, J. & GIL, A. 2005. Aetiology of inflammatory bowel disease (IBD): role of intestinal microbiota and gut-associated lymphoid tissue immune response. *Clin Nutr,* 24**,** 339-52.

TO, T. T., GUMUS, P., NIZAM, N., BUDUNELI, N. & DARVEAU, R. P. 2015. Subgingival Plaque in Periodontal Health Antagonizes at Toll-Like Receptor 4 and Inhibits E-Selectin Expression on Endothelial Cells. *Infect Immun,* 84**,** 120-6.

TRAORE, K., TRUSH, M. A., GEORGE, M., JR., SPANNHAKE, E. W., ANDERSON, W. & ASSEFFA, A. 2005. Signal transduction of phorbol 12-myristate 13-acetate (PMA)-induced growth inhibition of human monocytic leukemia THP-1 cells is reactive oxygen dependent. *Leuk Res,* 29**,** 863-79.

TRIMBLE, M. J., MLYNARCIK, P., KOLAR, M. & HANCOCK, R. E. 2016. Polymyxin: Alternative Mechanisms of Action and Resistance. *Cold Spring Harb Perspect Med,* 6.

TRISTAO, F. S. M., ROCHA, F. A., CARLOS, D., KETELUT-CARNEIRO, N., SOUZA, C. O. S., MILANEZI, C. M. & SILVA, J. S. 2017. Th17-Inducing Cytokines IL-6 and IL-23 Are Crucial for Granuloma Formation during Experimental Paracoccidioidomycosis. *Front Immunol,* 8**,** 949.

TSAI, C. C., KAO, C. C & CHEN, C. C. 2017. Gingival crevicular fluid lactoferrin levels in adult per iodontitis patients. *Australian Dental Journal,* 43**,** 40-44.

TSUCHIDA, S., SATOH, M., TAKIWAKI, M. & NOMURA, F. 2019. Current Status of Proteomic Technologies for Discovering and Identifying Gingival Crevicular Fluid Biomarkers for Periodontal Disease. *Int J Mol Sci,* 20.

TSUCHIYA, S., KOBAYASHI, Y., GOTO, Y., OKUMURA, H., NAKAE, S., KONNO, T. & TADA, K. 1982. Induction of maturation in cultured human monocytic leukemia cells by a phorbol diester. *Cancer Res,* 42**,** 1530-6.

TSUKUMO, Y., TSUKAHARA, S., FURUNO, A., IEMURA, S., NATSUME, T. & TOMIDA, A. 2014. TBL2 is a novel PERK-binding protein that modulates stress-signaling and cell survival during endoplasmic reticulum stress. *PLoS One,* 9**,** e112761.

ULEVITCH, R. J. & TOBIAS, P. S. 1995. Receptor-dependent mechanisms of cell stimulation by bacterial endotoxin. *Annu Rev Immunol,* 13**,** 437-57.

VAN DAMME, J., RAMPART, M., CONINGS, R., DECOCK, B., VAN OSSELAER, N., WILLEMS, J. & BILLIAU, A. 1990. The neutrophil-activating proteins interleukin 8 and beta-thromboglobulin: in vitro and in vivo comparison of NH2-terminally processed forms. *Eur J Immunol,* 20**,** 2113-8.

VERGADI, E., IERONYMAKI, E., LYRONI, K., VAPORIDI, K. & TSATSANIS, C. 2017. Akt Signaling Pathway in Macrophage Activation and M1/M2 Polarization. *The Journal of Immunology,* 198**,** 1006 - 1014.

VERGADI, E., VAPORIDI, K. & TSATSANIS, C. 2018. Regulation of Endotoxin Tolerance and Compensatory Anti-inflammatory Response Syndrome by Non-coding RNAs. *Front Immunol,* 9**,** 2705.

VERHULST, M. J. L., TEEUW, W. J., BIZZARRO, S., MURIS, J., SU, N., NICU, E. A., NAZMI, K., BIKKER, F. J. & LOOS, B. G. 2019. A rapid, non-invasive tool for periodontitis screening in a medical care setting. *BMC Oral Health.*

VERMA, I. 2004. Nuclear factor (NF)-κB proteins: therapeutic targets*. *Ann Rheum Dis,* 63**,** ii57-61.

VERMA, R., JUNG, J. H. & KIM, J. Y. 2014. 1,25-Dihydroxyvitamin D3 up-regulates TLR10 while down-regulating TLR2, 4, and 5 in human monocyte THP-1. *The Journal of steroid biochemistry and molecular biology,* 141**,** 1-6.

VRAKAS, S., MOUNTZOURIS, K. C., MICHALOPOULOS, G., KARAMANOLIS, G., PAPATHEODORIDIS, G., TZATHAS, C. & GAZOULI, M. 2017. Intestinal Bacteria Composition and Translocation of Bacteria in Inflammatory Bowel Disease. *PLoS One.*

WADE, W. G. 2013. The oral microbiome in health and disease. *Pharmacol Res,* 69**,** 137-43.

WALCZAK, A., GRADZIK, K., KABZINSKI, J., PRZYBYLOWSKA-SYGUT, K. & MAJSTEREK, I. 2019. The Role of the ER-Induced UPR Pathway and the Efficacy of Its Inhibitors and Inducers in the Inhibition of Tumor Progression. *Oxidative medicine and cellular longevity,* 2019.

WANG, N., LIANG, H. & ZEN, K. 2014. Molecular Mechanisms That Influence the Macrophage M1–M2 Polarization Balance. *Front Immunol,* 5.

WANG, J., QI, J., ZHAO, H., HE, S., ZHANG, Y., WEI, S. & ZHAO, F. 2013. Metagenomic sequencing reveals microbiota and its functional potential associated with periodontal disease. *Sci Rep,* 3**,** 1843.

WEGNER, N., WAIT, R., SROKA, A., EICK, S., NGUYEN, K. A., LUNDBERG, K., KINLOCH, A., CULSHAW, S., POTEMPA, J. & VENABLES, P. J. 2010. Peptidylarginine deiminase from *Porphyromonas gingivalis* citrullinates human fibrinogen and alpha-enolase: implications for autoimmunity in rheumatoid arthritis. *Arthritis Rheum,* 62**,** 2662-72.

WEINTRAUB, A., ZAHRINGER, U., WOLLENWEBER, H. W., SEYDEL, U. & RIETSCHEL, E. T. 1989. Structural characterization of the lipid A component of *Bacteroides fragilis* strain NCTC 9343 lipopolysaccharide. *Eur J Biochem,* 183**,** 425-31.

WEN, A. Y., SAKAMOTO, K. M. & MILLER, L. S. 2010. The role of the transcription factor CREB in immune function. *J Immunol,* 185**,** 6413-9.

WHITE, D. A., TSAKOS, G., PITTS, N. B., FULLER, E., DOUGLAS, G. V., MURRAY, J. J. & STEELE, J. G. 2012. Adult Dental Health Survey 2009: common oral health conditions and their impact on the population. *Br Dent J,* 213**,** 567-72.

WISNIEWSKI, J. R., ZOUGMAN, A., NAGARAJ, N. & MANN, M. 2009. Universal sample preparation method for proteome analysis. *Nat Methods,* 6**,** 359-62.

WOO, C. W., CUI, D., ARELLANO, J., DORWEILER, B., HARDING, H., FITZGERALD, K. A., RON, D. & TABAS, I. 2009. Adaptive suppression of the ATF4-CHOP branch of the unfolded protein response by toll-like receptor signalling. *Nat Cell Biol,* 11**,** 1473-80.

WRIGHT, C. J., BURNS, L. H., JACK, A. A., BACK, C. R., DUTTON, L. C., NOBBS, A. H., LAMONT, R. J. & JENKINSON, H. F. 2013. Microbial interactions in building of communities. *Mol Oral Microbiol,* 28**,** 83-101.

WRIGHT, H. L., MOOTS, R. J., BUCKNALL, R. C. & EDWARDS, S. W. 2010. Neutrophil function in inflammation and inflammatory diseases. *Rheumatology (Oxford),* 49**,** 1618-31.

WU, Y., LAN, C., REN, D. & CHEN, G.-Y. 2016. Induction of Siglec-1 by Endotoxin Tolerance Suppresses the Innate Immune Response by Promoting TGF-β1 Production. *Journal of Biological Chemistry,* 291**,** 12370-12382.

WU, X., ZHANG, G., WANG, X., ZHANG, P. & TAN, Y. 2015. Endotoxin tolerance induction in human periodontal ligament fibroblasts stimulated with different bacterial lipopolysaccharides. *Archives of oral biology,* 60**,** 463-70.

XIMENEZ-FYVIE, L. A., HAFFAJEE, A. D. & SOCRANSKY, S. S. 2000. Comparison of the microbiota of supra- and subgingival plaque in health and periodontitis. *Journal of Clinical Periodontology,* 27**,** 648-657.

XIONG, Y., QIU, F., PIAO, W., SONG, C., WAHL, L. M. & MEDVEDEV, A. E. 2011. Endotoxin tolerance impairs IL-1 receptor-associated kinase (IRAK) 4 and TGF-beta-activated kinase 1 activation, K63-linked polyubiquitination and assembly of IRAK1, TNF receptor-associated factor 6, and IkappaB kinase gamma and increases A20 expression. *The Journal of biological chemistry,* 286**,** 7905-16.

YAJIMA-HIMURO, S., OSHIMA, M., YAMAMOTO, G., OGAWA, M., FURUYA, M., TANAKA, J., NISHII, K., MISHIMA, K., TACHIKAWA, T., TSUJI, T. & YAMAMOTO, M. 2014. The junctional epithelium originates from the odontogenic epithelium of an erupted tooth. *Scientific Reports, Published online: 2 May 2014;* | *doi:10.1038/srep04867*.

YAMADA, H., NAKAJIMA, T., DOMON, H., HONDA, T. & YAMAZAKI, K. 2015. Endoplasmic reticulum stress response and bone loss in experimental periodontitis in mice. *Journal of periodontal research,* 50.

YAMAMOTO, M. & TAKEDA, K. 2010. Current views of toll-like receptor signaling pathways. *Gastroenterol Res Pract,* 2010**,** 240365.

YAN, X., XIONG, X. & CHEN, Y. G. 2018. Feedback regulation of TGF-beta signaling. *Acta Biochim Biophys Sin (Shanghai),* 50**,** 37-50.

YANG, X. D. & SUN, S. C. 2015. Targeting signaling factors for degradation, an emerging mechanism for TRAF functions. *Immunol Rev,* 266**,** 56-71.

YASUKAWA, H., MISAWA, H., SAKAMOTO, H., MASUHARA, M., SASAKI, A., WAKIOKA, T., OHTSUKA, S., IMAIZUMI, T., MATSUDA, T., IHLE, J. N. & YOSHIMURA, A. 1999. The JAK-binding protein JAB inhibits Janus tyrosine kinase activity through binding in the activation loop. *Embo j,* 18**,** 1309-20.

YOSHIDA, H., JONO, H., KAI, H. & LI, J. D. 2005. The tumor suppressor cylindromatosis (CYLD) acts as a negative regulator for toll-like receptor 2 signaling

YU, Y. & CHADEE, K. 1998. Prostaglandin E2 stimulates IL-8 gene expression in human colonic epithelial cells by a posttranscriptional mechanism. *J Immunol,* 161**,** 3746-52.

via negative cross-talk with TRAF6 AND TRAF7. *J Biol Chem,* 280**,** 41111-21.

YU, Y., LIU, Z. Q., LIU, X. Y., YANG, L., GENG, X. R., YANG, G., LIU, Z. G., ZHENG, P. Y. & YANG, P. C. 2013. Stress-Derived Corticotropin Releasing Factor Breaches Epithelial Endotoxin Tolerance. *PLoS One,* 8**,** e65760.

YU, X., SHAHIR, A. M., SHA, J., FENG, Z., EAPEN, B., NITHIANANTHAM, S., DAS, B., KARN, J., WEINBERG, A., BISSADA, N. F. & YE, F. 2014. Short-Chain Fatty Acids from Periodontal Pathogens Suppress Histone Deacetylases, EZH2, and

SUV39H1 To Promote Kaposi's Sarcoma-Associated Herpesvirus Replication. *J Virol.*

YUE, Y., LIU, Q., XU, C., LOO, W. T., WANG, M., WEN, G., CHEUNG, M. N., BAI, L. J., DOU, Y. D., CHOW, L. W., HAO, L., TIAN, Y., LI, J. L., YIP, A. Y. & NG, E. L. 2013. Comparative Evaluation of Cytokines in Gingival Crevicular Fluid and Saliva of Patients With Aggressive Periodontitis. *The International journal of biological markers,* 28.

ZANNETTI, C., PARROCHE, P., PANAYE, M., ROBLOT, G., GRUFFAT, H., MANET, E., DEBAUD, A. L., PLUMAS, J., VEY, N., CAUX, C., BENDRISS-VERMARE, N. & HASAN, U. A. 2014. TLR9 transcriptional regulation in response to double-stranded DNA viruses. *J Immunol,* 193**,** 3398-408.

ZARIC, S. S., COULTER, W. A., SHELBURNE, C. E., FULTON, C. R., ZARIC, M. S., SCOTT, A., LAPPIN, M. J., FITZGERALD, D. C., IRWIN, C. R. & TAGGART, C. C. 2011. Altered Toll-like receptor 2-mediated endotoxin tolerance is related to diminished interferon beta production. *The Journal of biological chemistry,* 286**,** 29492-500.

ZARIC, S., SHELBURNE, C., DARVEAU, R., QUINN, D. J., WELDON, S., TAGGART, C. C. & COULTER, W. A. 2010. Impaired immune tolerance to *Porphyromonas gingivalis* lipopolysaccharide promotes neutrophil migration and decreased apoptosis. *Infection and immunity,* 78**,** 4151-6.

ZENG, K.-W., LIAO, L.-X., LV, H.-N., SONG, F.-J., YU, Q., DONG, X., LI, J., JIANG, Y. & TU, P.-F. 2015. Natural small molecule FMHM inhibits lipopolysaccharide-induced inflammatory response by promoting TRAF6 degradation via K48-linked polyubiquitination. *Scientific Reports,* 5**,** 14715.

ZENOBIA, C., HASTURK, H., NGUYEN, D., VAN DYKE, T. E., KANTARCI, A. & DARVEAU, R. P. 2014. *Porphyromonas gingivalis* lipid A phosphatase activity is critical for colonization and increasing the commensal load in the rabbit ligature model. *Infection and immunity,* 82**,** 650-9.

ZHANG, G. & GHOSH, S. 2002. Negative regulation of toll-like receptor-mediated signaling by Tollip. *J Biol Chem,* 277**,** 7059-65.

ZHANG, Q., HU, Y., ZHANG, J. & DENG, C. 2019. iTRAQ-based proteomic analysis of endotoxin tolerance induced by lipopolysaccharide. *Mol Med Rep.*

ZHANG, X., KIMURA, Y., FANG, C., ZHOU, L., SFYROERA, G., LAMBRIS, J. D., WETSEL, R. A., MIWA, T. & SONG, W. C. 2007. Regulation of Toll-like receptor-mediated inflammatory response by complement in vivo. *Blood,* 110**,** 228-36.

ZHANG, J. & SHEN, B. 2011. SHP limits TLR signaling, an inducible transcriptional corepressor. *Cell Mol Immunol,* 8**,** 445-6.

ZHANG, X., ZHOU, M., GUO, Y., SONG, Z. & LIU, B. 2015. 1,25-Dihydroxyvitamin D3 Promotes High Glucose-Induced M1 Macrophage Switching to M2 via the VDR-PPARγ Signaling Pathway. *Biomed Res Int,* 2015.

ZHOU, Q. & AMAR, S. 2007. Identification of Signaling Pathways in Macrophage Exposed to *Porphyromonas gingivalis* or to Its Purified Cell Wall Components. *The Journal of Immunology,* 179**,** 7777-7790.

ZHOU, L. N., BI, C. S., GAO, L. N., AN, Y., CHEN, F. & CHEN, F. M. 2019. Macrophage polarization in human gingival tissue in response to periodontal disease. *Oral Dis,* 25**,** 265-273.

ZIJNGE, V., VAN LEEUWEN, M. B. M., DEGENER, J. E., ABBAS, F., THURNHEER, T., GMÜR, R. & HARMSEN, H. J. M. 2010. Oral biofilm architecture on natural teeth. *PloS one,* 5**,** e9321-e9321.

Appendix A

Reagents and buffers

Relevant sections	Reagent	Supplier
Enzyme-linked immunosorbent assay (ELISA)		
2.3.10	3,3,5,5-tetramethyl benzidine (TMB) Peroxidase	KPL (Seracare), Massachusetts, US
3.2.5	Biotynilated Mouse Anti-Human IL-8 G265-8 IgG_{2b}	BD Pharmingen, Oxford, UK
4.2.3	Biotynilated Rat Anti-Human IL-10 JES-12G8 IgG_{2a}	BD Pharmingen, Oxford, UK
	Biotynilated Mouse Anti-Human IL-12/IL-23 p40 C8.6 IgG_1	Fisher (eBioscience), Loughborough
	Biotinylated Mouse Anti-Human TNF MAb11 IgG_1	BD Pharmingen, Oxford, UK
	Bovine Serum Albumin (BSA)	Sigma Aldrich, Poole, UK
	Ethanol (laboratory grade)	Fisher, Loughborough, UK
	Phosphate Buffered Saline (PBS)	Melford Laboratories Ltd., Ipswich,U.K.
	Purified Mouse Anti-Human IL-8 G265-5 IgG_{2b}	BD Pharmingen, Oxford, UK
	Purified Rat Anti-Human IL-10 JES3-9D7 IgG_1	BD Pharmingen, Oxford, UK
	Purified Mouse Anti-Human IL-12 p35 BT-21 IgG_1	Fisher (eBioscience), Loughborough
	Purified Mouse Anti-Human IL-23 p19 473P19 IgG1	Fisher (eBioscience), Loughborough
	Purified Mouse Anti-Human TNF MAb1 IgG_1	BD Pharmingen, Oxford, UK
	Recombinant Human IL-8	BD Pharmingen, Oxford, UK
	Recombinant Human IL-10	BD Pharmingen, Oxford, UK
	Recombinant IL-12 p70	Fisher (eBioscience), Loughborough
	Recombinant IL-23	Fisher (eBioscience), Loughborough
	Recombinant Human TNFα	BD Pharmingen, Oxford, UK
	Streptavidin Horse-radish Peroxidase (HRP)	R&D Systems, Abingdon, UK
	Sulphuric Acid (H_2SO_4)	Sigma Aldrich, Poole, UK
	Tween20	Sigma Aldrich, Poole, UK

Lipid-A Isolation		
2.3.5	Chloroform	Sigma Aldrich, Poole, UK
	Ethanol (molecular grade)	Sigma Aldrich, Poole, UK
	Sodium Acetate	Sigma Aldrich, Poole, UK
	Sodium Dodecyl Sulphate (SDS)	Fisher, Loughborough, UK
LPS Extraction		
2.3.4	Chloroform	Sigma Aldrich, Poole, UK
	Ethanol (molecular grade)	Sigma Aldrich, Poole, UK
	LPS Extraction kit	iNtRON Biotechnology, Seongnam, Korea
MTT Assay		
2.3.9.1.1	Dimethyl sulfoxide (DMSO)	Fisher, Loughborough, UK
	Hyrochlocic Acid	Fisher, Loughborough, UK
	Methylthiazolyldiphenyl-tetrazolium bromide	Sigma Aldrich, Poole, UK
Protein Isolation and Quantification		
4.2.4	BCA Protein Assay Kit	Fisher (Pierce), Loughborough, UK
4.2.5	Protease Cocktail Inhibitor	Sigma Aldrich (Roche), Poole, UK
	RIPA Buffer	Fisher, Loughborough, UK
rFC LAL Assay		
2.3.7	EndoZyme rFC LAL Assay	Hyglos, Bernried am Starnberger See, Germany
Scanning Electron Microscopy		
2.3.3	Aclar film	Agar Scientific, Essex, UK
3.2.3	Cacodylate Buffer	Agar Scientific, Essex, UK
	Ethanol (Absolute)	VWR, Lutterworth, UK
	Glutaraldehyde	Agar Scientific, Essex, UK
SDS PAGE		
4.2.6	30% Acrylamide/Bis-Acrylamide	Fisher, Loughborough, UK
	10% Ammonium Persulfate (APS)	Sigma Aldrich, Poole, UK
	Bromophenol blue	Fisher, Loughborough, UK
	Coomassie Blue R-250	Fisher, Loughborough, UK
	Glacial Acetic Acid	Fisher, Loughborough, UK
	Glycerol	Sigma Aldrich, Poole, UK
	Glycine	Fisher, Loughborough, UK
	Hyrochlocic Acid	Fisher, Loughborough, UK
	Mercaptoenthanol	Sigma Aldrich, Poole, UK
	Methanol	Fisher, Loughborough, UK
	Sodium Dodecyl Sulfate	Fisher, Loughborough, UK
	Tetramethylethylenediamine (TEMED)	Sigma Aldrich, Poole, UK
	Tris pH 8.0	Fisher, Loughborough, UK

Silver staining		
2,.35	Ammonium Persulfate (APS)	Sigma Aldrich, Poole, UK
	Bromophenol blue	Fisher, Loughborough, UK
	Ethanol (molecular grade)	Sigma Aldrich, Poole, UK
	Glacial Acetic Acid	Fisher, Loughborough, UK
	Glycerol	Sigma Aldrich, Poole, UK
	Glycine	Fisher, Loughborough, UK
	Mercaptoenthanol	Sigma Aldrich, Poole, UK
	Protean TGX precast gels	Bio-Rad, Watford, UK
	Sodium Dodecyl Sulfate	Fisher, Loughborough, UK
	Silver stain kit	Fisher, Loughborough, UK
	Tris pH 8.0	Fisher, Loughborough, UK
Stage Tip Filtration and Digestion		
4.2.7	2-chloroacetamide	Sigma Aldrich, Poole, UK
	Acetic Acid (molecular grade)	Sigma Aldrich, Poole, UK
	Acetonitrile	Fisher, Loughborough, UK
	Ammonium bicarbonate	Fisher, Loughborough, UK
	C18 membrane	Sigma Aldrich, Poole, UK
	Dithiothreitol (DTT)	Fisher, Loughborough, UK
	Hyrochlocic Acid	Fisher, Loughborough, UK
	Iodoacetamide	Sigma Aldrich, Poole, UK
	LysC	Fisher, Loughborough, UK
	Trifluoroacetic acid (TFA)	Fisher, Loughborough, UK
	Tris pH 8.0	Fisher, Loughborough, UK
	Trypsin	Promega, Southampton, UK
	Urea	Sigma Aldrich, Poole, UK
Stimulation Protocols		
2.3.9.	*E. coli* LPS (Standard)	Invivogen, California, US
3.2.2	PG LPS_{1690} and $_{1449/1435}$	Astarte Biologics, Washington, US
4.2.2	PG LPS (Standard)	Invivogen, California, US
	Polymyxin B Sulphate	Fisher, Loughborough
Tissue Culture		
2.3.8.1	1α,25-Dihydroxyvitamin D3 (VD3)	Sigma Aldrich, Poole, UK
3.2.1	Dimethyl sulfoxide (DMSO)	Fisher, Loughborough, UK
4.2.1	Foetal Bovine Serum	BioSera, Nuaille, France
	L-glutamine	Lonza, Slough, UK
	Phorbol 12-myristate 13-acetate (PMA	Sigma Aldrich, Poole, UK
	RPMI 1640	Lonza, Slough, UK

ELISA Wash buffer

0.05% Tween20 in 1 x PBS

SDS Page gels and buffers:

***x* % Gel composition (per gel)**

Ultrapure water: 1/2(11.03-(0.5 x *x*))

Buffer: 1.87 ml

30% Acrylamide/Bis-acrylamide: ½(0.5 x *x*)

10% APS: 50 µl

TEMED: 50 µl

Stacking Gel (4%)

Ultrapure water 4.5 ml

Stacking buffer 0.75 ml

30% Acrylamide/Bis-acrylamide 1 ml

10% APS 50 µl

TEMED 15 µl

Separating gel buffer:

1.125 M Tris base (68.14 g per 500 ml)

0.3%w/v SDS (1.5 g per 500 ml)

Dissolved in ltrapure water to 450 ml adjusted to pH 8.8 with HCl.

Top up to 500 ml with ultrapure water.

Stacking buffer:

140 mM Tris (8.42 g per 500 ml)

0.11%w/v SDS (0.55 g per 500 ml)

Dissolve in ultrapure water to 450 ml. Adjust to pH 6.8 with concentrated HCl 100%.

Top up to 500 ml with ultrapure water

10% w/v APS (0.1g APS dissolved into 1ml ultrapure water)

Electrophoresis buffer (Running buffer)

Tris 3 g

Glycine 14.4 g

SDS 1 g

Dissolved in 1l ultrapure water, pH 8.3

5X Laemmli loading buffer (Reducing/ Denaturing)

1 M Tris –HCl (pH 6.8) 0.6 ml

50% v/v glycerol 5 ml

10% w/v SDS 2 ml

2-mercaptoethanol 0.5 ml

1% w/v Bromophenol blue 1 ml

0.9 ml DW

Coomassie Gel stains (1l)

Coomassie blue R-250 1.0 g

100% Methanol 450 ml

Ultrapure water 450 ml

100 % glacial acetic acid 100 ml

De-staining Coomassie Gel stain solution (1l)

Methanol 100% 100 ml

Glacial acetic acid 100% 100 ml

Ultrapure water 800 ml

Protein Isolation and purification

Stage tip filtration:

Buffer A

HPLC water 40 ml

Acetic acid 250 µl

TFA. 500 µl

Adjust volume to 50 ml with HPLC water.

Buffer B

Acetonitrile 40 ml

Acetic acid 250 µl

TFA. 500 µl

Adjust volume to 50 ml with HPLC water.

Protein digestion reagents preparation:

1/ Dissolve 200 mg 50 mM Ammonium bicarbonate in 50 ml HPLC water.

2/ Dissolve 7.7 mg 10 mM dithiothreitol in 5 ml HPLC water.

3/ Alkylation buffer: Dissolve 23.35 mg 50 mM 2-chloroacetamide in 5 ml solution 1 (ABC)

(stored in the dark).

4/ Dissolve 605.7 mg 10 mM Tris in 450 mL HPLC water.

Adjust to pH 8.0 with HCL.

Adjust volume to 500 mL with HPLC water.

5/ Dissolve 24.024 g 8M urea in 50 ml solution 4.

Dilute 1 ml TFA with 49 mL HPLC water.

(Stored in glass)

Appendix B

Protein abbreviations

Abbreviation	Aliases	Protein
AARS		Alanine--tRNA ligase, cytoplasmic
ABCF2		ATP-binding cassette, sub-family F (GCN20), member 2
ABHD12	C20orf22	Monoacylglycerol lipase ABHD12
ACADVL	ACAD6	Very long-chain-specific acyl-CoA dehydrogenase, mitochondrial
ACAT1	Testicular tissue protein Li 198	Acetyl-CoA Acetyltransferase 1
ACOT9		Acyl-coenzyme A thioesterase 9, mitochondrial
ACOX1		Acyl-coenzyme A oxidase
ACSL4		Long-chain-fatty-acid--CoA ligase 4
ACTA1	CFTD, SHPM	Actin, alpha skeletal muscle
ACTG1	Actin Gamma 1	Actin, cytoplasmic 2
ADK		Adenosine kinase
ADSL	AMPS	Adenylosuccinate lyase
AHNAK		Neuroblast differentiation-associated protein AHNAK
AIFM1	Programmed Cell Death 8, PDCD8, COXPD6	Apoptosis-inducing factor 1, mitochondrial
AK2		Adenylate kinase 2, mitochondrial
AKR7A2		Aflatoxin B1 aldehyde reductase member 2
ALOX5AP	FLAP	Arachidonate 5-lipoxygenase-activating protein
ALYREF	REF, THO complex subunit 4	Aly/REF Export Factor
AMPD3		AMP deaminase 3
ANP32B		Acidic (Leucine-rich) nuclear phosphoprotein 32 family, member B variant
ANP32E	LANPL	Acidic (Leucine-rich) nuclear phosphoprotein 32 family, member E variant
ANPEP	CD13, GP150	Aminopeptidase
ANXA2	P36, LIP2, LIPOCORTIN II	Annexin 2
ANXA4	Proliferation-Inducing Protein 28, Carbohydrate-Binding Protein P33/P41	Annexin 4
ANXA5	ANXA5, Thromboplastin Inhibitor, Vascular Anticoagulant-Alpha, Calphobindin I, Anchorin CII, Endonexin II, Lipocortin V	Annexin 5
ANXA6	LIPOCORTIN, P68, P70	Annexin 6
ANXA11		Annexin 11
APEH		Acylamino-acid-releasing enzyme
APEX1	REF-1	Apurinic/Apyrimidinic Endodeoxyribonuclease 1
APMAP		Adipocyte plasma membrane-associated protein

APOBR		Apolipoprotein B receptor
ARCN1	COPD	Coatomer subunit delta
ARF4	ARF2	ADP-ribosylation factor 4
ARL6IP5		PRA1 family protein
ASAH1		Acid ceramidase
ASNS	TS11 Cell Cycle Control Protein	o Asparagine synthetase (glutamine-hydrolysing)
ASPH		Aspartyl/asparaginyl beta-hydroxylase
ASS1	CTLN1 3	Argininosuccinate synthase 1 isoform 1
ATL3	HSN1F	Atlastin-3
ATP2A2	Calcium Pump 2	ATPase Ca++ transporting cardiac muscle slow twitch 2 isoform 1
ATP5MF-PTCD1		ATP5MF-PTCD1 readthrough
ATP6		ATP synthase subunit 6
ATP6V0D1	P39	V-type proton ATPase subunit d 1
ATP6V1C1		V-type proton ATPase subunit C
ATP6V1E1	P31, ATP6E	ATPase, H+ transporting, lysosomal 31kDa, V1 subunit E isoform 1
BASP1	NAP22, CAP23	Brain acid soluble protein 1
BAX	Apoptosis Regulator BAX	BCL2-associated X protein
BBF2H7/FUS		BBF2H7/FUS protein
BCAP31		B-cell receptor-associated protein 31 variant
BID		BH3 interacting domain death agonist, isoform CRA_d
BTF3		Transcription factor BTF3
BTF3L4		Transcription factor BTF3
BZW2	HSPC028	Basic leucine zipper and W2 domain-containing protein 2
C1QBP	Hyaluronan-Binding Protein 1, ASF/SF2-Associated Protein P32, P33	Complement component 1 Q subcomponent-binding protein, mitochondrial
C9orf88	MINERVA, MEG-3, NIBAN2, FAM129B	Chromosome 9 open reading frame 88, isoform CRA_a C9orf88
CA2	Carbonic Anhydrase 2, CA2	Epididymis Luminal Protein 76
CALU	Calumenin, crocalbin	CALU protein
CAMK1		Calcium/calmodulin-dependent protein kinase type 1
CAND1	TIP120, KIAA0829	Cullin-associated and neddylation-dissociated 1
CAPG	MCP	Macrophage capping protein
CAPN2		Calpain-2 catalytic subunit
CAPNS1	Calcium-Activated Neutral Proteinase Small Subunit	Calpain small subunit 1
CAPRIN1	Cytoplasmic Activation/Proliferation-Associated Protein-1, Cell Cycle Associated Protein 1	Caprin-1
CAPZA2		Capping protein (Actin filament) muscle Z-line, alpha 2 variant

CAT		Catalase
CD109		CD109 antigen
CD44		CD44 antigen
CDC20	RcCDC20	Cell Division Cycle 20
CDK1	CDC2, CDC28A	Cell division cycle 2, G1 to S and G2 to M, isoform CRA_a
CDK5		Cyclin-dependent kinase 5 isoform 2
CDK6		Cyclin-dependent kinase 6
CERS2	Tumour Metastasis-Suppressor Gene 1 Protein , LAG1 Longevity Assurance 2, TMSG1	Ceramide synthase 2
CES1	Monocyte/Macrophage Serine Esterase, TGH, Methylumbelliferyl-Acetate Deacetylase	Liver carboxylesterase 1
CHI3L1	GP39	Chitinase 3-like 1 (Cartilage glycoprotein-39), isoform CRA_a
CHMP4A	SNF7, C14orf123, HSPC134	Charged multivesicular body protein 4a
cJHBP	GLOD4	Bombyx mori cytosolic juvenile hormone binding protein 36 kDa subunit
CLIC4		Chloride intracellular channel protein
CLNS1A		Chloride Nucleotide-Sensitive Channel 1A
CMAS		Cytidine 5'-monophosphate N-acetylneuraminic acid synthetase variant
CNDP2	PEPTIDASE A, CN2	Cytosolic nonspecific dipeptidase
CORO1A	IMD8, P57	Coronin 1A
CORO1B		Coronin 1B
CORO1C		Coronin 1C
COTL1	CLP	Coactosin-like protein
CPM		Carboxypeptidase M
CPSF5	NUDT21	Cleavage and polyadenylation specific factor 5
CPSF6		Cleavage and polyadenylation specificity factor 6
CPT2		Carnitine O-palmitoyltransferase 2, mitochondrial
CRTAP	Leprecan-Like 3	Cartilage-associated protein
CSE1L	Cellular Apoptosis Susceptibility Protein Exportin-2	Chromosome Segregation 1 Like,
CSF2RB	Beta-GM-CSF Receptor, IL3RB, IL5RB, CD131, Alternative protein CSF2RB	Colony Stimulating Factor 2 Receptor Beta Common Subunit
CSK	CSK, Non-Receptor Tyrosine Kinase	Tyrosine-protein kinase
CTSB		Cathepsin B
CTSD		Cathepsin D
CYB5R3	DIA1	NADH-cytochrome b5 reductase

CYBB	NADPH Oxidase 2, Superoxide-Generating NADPH Oxidase Heavy Chain SUBUNIT, Heme-Binding Membrane Glycoprotein Gp91phox, Neutrophil Cytochrome B 91 KDa Polypeptide, P22 Phagocyte B-Cytochrome, Chronic Granulomatous Disease, NOX2	Cytochrome b-245 heavy chain
CYFIP1	SRA1, KIAA0068	Cytoplasmic FMR1 interacting protein 1
DAD1	Defender Against Cell Death 1, Oligosaccharyltransferase Subunit 2, OST2	Dolichyl-diphosphooligosaccharide--protein glycosyltransferase subunit DAD1
DDX21	GURDB, GUA, Nucleolar RNA helicase 2	DExD-Box Helicase 21,
DDX48	**EIF4A3**, KIAA0111	DEAD (Asp-Glu-Ala-Asp) box polypeptide 48, isoform CRA_a
DERL1		Derlin
DHX15	DBP1	DEAH-Box Helicase 15
DIAPH1		Diaphanous homolog 1
DKFZp586K0821		Uncharacterized protein DKFZp586K0821
DKFZp686L0869		Uncharacterized protein DKFZp686L0869
DKFZp686M0619		Uncharacterized protein DKFZp686M0619
DKFZp761N202		Uncharacterized protein DKFZp761N202
DLST		Dihydrolipoamide S-succinyltransferase (E2 component of 2-oxo-glutarate complex), isoform CRA_a
DNAJC3	Interferon-Induced, Double-Stranded RNA-Activated Protein Kinase Inhibitor	DnaJ (Hsp40) homolog, subfamily C, member 3
DPM1		Dolichyl-phosphate mannosyltransferase polypeptide 1 catalytic subunit isoform 1
DPP7	DPPII	Dipeptidyl-peptidase II variant
EBP		Emopamil binding protein
ECH1		Enoyl-CoA Hydratase 1
EDF1		Endothelial differentiation-related factor 1
EIF1AX		Eukaryotic translation initiation factor 1A, X-chromosomal
EIF2AK2	Protein Kinase, Interferon-Inducible Double Stranded RNA Dependent, **PKR**, PRKR, P68 KINASE	Eukaryotic Translation Initiation Factor 2 Alpha Kinase 2
EIF2S2		Eukaryotic translation initiation factor 2, subunit 2 beta, 38kDa
EIF3A	KIAA00139, TIF32, P180, P167, P185	Eukaryotic translation initiation factor 3 subunit A
EIF3G		Eukaryotic translation initiation factor 3 subunit G

EIF3L	HSPC021, HSPC025	Eukaryotic translation initiation factor 3 subunit L
EIF3M	PCID1, Dendritic Cell Protein	Eukaryotic translation initiation factor 3 subunit M
EIF3S6	EIF3E	Eukaryotic translation initiation factor 3 subunit E
EIF5		Eukaryotic translation initiation factor 5
EIF5A		Eukaryotic translation initiation factor 5A
EIF5B	IF2, KIAA0741	Eukaryotic translation initiation factor 5B
ELAVL1		ELAV-like protein 1
ELOVL1	SSC1	Elongation of very long chain fatty acids protein 1
ELOVL5	HELO1, SCA38	Elongation of very long chain fatty acids protein
EMC2	KIAA0103, TTTC35	ER membrane protein complex subunit 2
EPB41L2		Band 4.1-like protein 2
ERH		Enhancer of rudimentary homolog
ERMP1	KIAA1815	Endoplasmic reticulum metallopeptidase 1
ERP29	C12orf8, PDIA9, ERP29	Endoplasmic reticulum resident protein 29
ESYT2	KIAA1228	Extended synaptotagmin-2
EWSR1		RNA-binding protein EWS
EZR	Cytovillin, P81	Ezrin
FCER1G	Fc Fragment Of IgE Receptor Ig, FcRgamma, IgE Fc Receptor Subunit Gamma	High affinity immunoglobulin epsilon receptor subunit gamma
FEN1	Maturation Factor-1	Flap endonuclease 1
FH		Fumarate hydratase isoform 1
FKBP8		Peptidyl-prolyl cis-trans isomerase FKBP8
FMNL1	FRL1, C17orf1B, C17orf1	Formin-like protein 1
FUCA1		Tissue alpha-L-fucosidase
GBE1		1,4-alpha-glucan-branching enzyme
GCLC	GCS	Glutamate--cysteine ligase catalytic subunit
GCS1	Mannosyl-Oligosaccharide Glucosidase, MOGS	Glucosidase I
GDI1		Rab GDP dissociation inhibitor
GLS		Glutaminase
GLUD1		Glutamate dehydrogenase
GMPS		GMP synthase (glutamine-hydrolysing)
GNB1		Guanine nucleotide binding protein (G protein), beta polypeptide 1
GNG5		Guanine nucleotide-binding protein G(I)/G(S)/G(O) subunit gamma-5
GNS	G6S	N-acetylglucosamine-6-sulphatase
GST01	Glutathione S-Transferase Omega 1, GST01, P28	Epididymis secretory protein Li 21
GSTM3		Glutathione S-transferase
GSTP1	Pi 1, GST3, PI Epididymis secretory protein Li 22	Glutathione S-Transferase
GYS1		Glycogen [starch] synthase

H2AFV		Histone H2A.V
H2AFY		Core histone macro-H2A.1
HACD3	Butyrate-Induced Protein 1, Protein-Tyrosine Phosphatase-Like A Domain-Containing Protein 1, PTPLAD1, BIND1	Very-long-chain (3R)-3-hydroxyacyl-CoA dehydratase 3
HADHB	Acetyl-CoA Acyltransferase, ECHB, MTPB	Trifunctional enzyme subunit beta, mitochondrial
HAT1	KAT1	Histone acetyltransferase type B catalytic subunit
HCC5	Minichromosome Maintenance Complex Component 3, MCM3, DNA Replication Licensing Factor **MCM3**	DNA helicase
hCG_2032701		HCG2032701, isoform CRA_a
HDAC2		Histone deacetylase 2
HIST2H2AB		Histone H2A type 2-B
HIST2H3PS2	histone cluster 2 H3 pseudogene 2	Histone H3
HK1	Glycolytic Enzyme	Hexokinase-1
HLA-A		MHC class I antigen
HLA-B		MHC class I antigen
HM13	Histocompatibility Minor 13, IMP1	Histocompatibility 13 isoform 1
HMGA1	HMG-R, High mobility group AT-hook 1	High mobility group protein HMG-I/HMG-Y
HMGB1	HMG3, SBP-1	High-mobility group box 1, isoform CRA_a
HMGB2		High-mobility group box 2
HMGN1		Non-histone chromosomal protein HMG-14
HMGN2	HMGN17	Non-histone chromosomal protein HMG-17
HMOX1	HSP32	Heme oxygenase
HNMT		Histamine N-methyltransferase
HNRDPL	JKTBP	Heterogeneous nuclear ribonucleoprotein D-like
HNRNPA0		Heterogeneous nuclear ribonucleoprotein A0
HNRNPAB	ABBP1	Heterogeneous nuclear ribonucleoprotein A/B
HNRNPUL2-BSCL2	HCG2044799	HNRNPUL2-BSCL2
HNRPD	AUF, P37	Heterogeneous nuclear ribonucleoprotein D (AU-rich element RNA binding protein 1, 37kDa), isoform CRA_e
HNRPR		HNRPR protein
HPCAL1		Hippocalcin Like 1

HSP70B	HSPA6	Heat shock 70kDa protein 6 (HSP70B') variant
ICAM1	CD54	Intercellular adhesion molecule 1
IDH1	IDH1, PICD, IDP	Isocitrate dehydrogenase [NADP]
IDH2	IDP	Isocitrate dehydrogenase 2 (NADP+), mitochondrial variant
IFI30	IP30	Interferon gamma-inducible protein 30 preproprotein
IFIT1	P56, Interferon, Alpha-Inducible Protein	Interferon-induced protein with tetratricopeptide repeats 1
IGF2R	CD222, MPR1, 300 KDa Mannose 6-Phosphate Receptor	Insulin-like growth factor 2 receptor variant
ILVBL	AHAS	IlvB Acetolactate Synthase Like
IMPA1		Inositol monophosphatase 1
IMPDH2		Inosine-5'-monophosphate dehydrogenase 2
IPO7	IMP7, RANBP7	Importin-7
ISG15	IP17, Ubiquitin Cross-Reactive Protein, Interferon, Alpha-Inducible Protein, ISG15 Ubiquitin-Like Modifier, Interferon-Induced 15 KDa Protein	Ubiquitin-like protein ISG15
IST1	Putative MAPK-Activating Protein PM28, HIST1, OLC1	IST1 Factor Associated With ESCRT-III
ITGAM	Complement Component 3 Receptor 3 Subunit, **CD11B**, CR3A, Macrophage Antigen Alpha Polypeptide, Neutrophil Adherence Receptor 4,	Integrin alpha-M
ITGB1	Glycoprotein Iia, CD29	Integrin beta-1
ITGB2	**CD18**, Complement Receptor C3 Beta-Subunit, LFA-1	Integrin beta-2
ITGB5		Integrin beta 5
ITGB6	AL1H	Integrin beta 6
ITGB7	Gut Homing Receptor Beta Subunit	Integrin beta-7
KCNAB2		Potassium Voltage-Gated Channel Subfamily A Regulatory Beta Subunit 2
KPNA2	SRP1-Alpha, SRP1, Importin Alpha 1	Importin subunit alpha
KYNU		Kynureninase
LACTB		Serine beta-lactamase-like protein LACTB, mitochondrial
LAIR1	CD305, Immunoglobulin Heavy Chain Variable Region	Leukocyte-associated immunoglobulin-like receptor 1

LAMP1	CD107 Antigen-Like Family Member A	Lysosome-associated membrane glycoprotein 1
LAMP2	CD107, Lysosome-Associated Membrane Glycoprotein 2	Lysosome-associated membrane glycoprotein 2
LAMTOR1	Late Endosomal/Lysosomal Adaptor, p18, Ragulator complex protein LAMTOR1	Late Endosomal/Lysosomal Adaptor, MAPK And MTOR Activator 1
LENG4	Membrane Bound O-Acyltransferase Domain Containing 7, MBOAT7, Lysophosphatidylinositol Acyltransferase	Leukocyte receptor cluster (LRC) member 4 (LENG4), Mrna
LETM1		Leucine zipper-EF-hand containing transmembrane protein 1, isoform CRA_a
LGALS1		Galectin-1
LMAN1	GP58	Lectin, mannose-binding, 1 variant
LMNA		Prelamin-A/C
LPXN	LDPL, LDPL	Leupaxin
LRIG1		Leucine-rich repeat protein LRIG1
LSM4	GRP	U6 snRNA-associated Sm-like protein LSm4
LTA4H		Leukotriene A(4) hydrolase
MAGOH		Protein mago nashi homolog
MAN2B1		Alpha-mannosidase
MAP1S	Microtubule Associated Protein 1S, C19orf5, MAP8	BPY2 interacting protein 1, mRNA
MARCKS	Phosphomyristin	Myristoylated alanine-rich C-kinase substrate
MARCKSL1	Macrophage Myristoylated Alanine-Rich C Kinase Substrate, MRP, MLP1, F52	MARCKS-related protein
MCF2		Proto-oncogene DBL
MCM2		Minichromosome Maintenance Complex Component 2
MCM4		Minichromosome Maintenance Complex Component 4
MCM5		Minichromosome Maintenance Complex Component 5
MCM6		Minichromosome Maintenance Complex Component 6
MCM7		Minichromosome Maintenance Complex Component 7
MICAL1	Microtubule Associated Monooxygenase, Calponin And LIM Domain Containing 1	Protein-methionine sulphoxide oxidase
MICALL1	Molecule Interacting with Rab13, KIAA1668	MICAL-like protein 1
MIF		Macrophage migration inhibitory factor

MNDA		Myeloid cell nuclear differentiation antigen, isoform CRA_a
MOB1A	C2orf6	MOB kinase activator 1A
MPC2	SLC54A2	Mitochondrial pyruvate carrier
MPDU1	SL15	Mannose-P-dolichol utilization defect 1, isoform CRA_c
MST065	Translocase of Outer Mitochondrial Membrane 22, TOMM22	Mitochondrial Import Receptor Subunit TOM22 Homolog
MT-CO2	COII	Cytochrome oxidase subunit II
MX1	Interferon-Inducible Protein P78, Myxovirus (Influenza Virus) Resistance 1	Interferon-induced GTP-binding protein Mx1
MX2	Second Interferon-Induced Protein P78, Myxovirus (Influenza Virus) Resistance 2	Interferon-induced GTP-binding protein Mx2
MYL1		Myosin Light Chain 1
MYO1G	HLA-HA2	Myosin IG
MYO5B	KIAA1119	Myosin 5B OS
NACA		Nascent polypeptide-associated complex subunit alpha
NAPA		Alpha-soluble NSF attachment protein
NARS		Asparagine--tRNA ligase, cytoplasmic
NASP	Histone H1-Binding Protein	Nuclear autoantigenic sperm protein
NAXE	AIBP	NAD(P)H-hydrate epimerase
NCSTN		Nicastrin
NDUFA9	CC6	NADH dehydrogenase [ubiquinone] 1 alpha subcomplex subunit 9, mitochondrial
NDUFA13	Cell Death-Regulatory Protein GRIM19, Gene Associated With Retinoic And IFN-Induced Mortality 19 Protein	NADH dehydrogenase [ubiquinone] 1 alpha subcomplex subunit 13
NOMO1	PM5	Nodal modulator 1
NSUN2	Substrate Of AIM1/Aurora Kinase B	NOP2/Sun RNA Methyltransferase 2
NUCB1		Nucleobindin 1 variant
NUCB2		Nucleobindin-2
NUCKS1	P1	Nuclear ubiquitous casein and cyclin-dependent kinase substrate 1
NUDC		Nuclear migration protein nudC
NUP210	GP210	Nuclear pore membrane glycoprotein 210
NUP93	NIC96, KIAA0095	Nuclear pore complex protein Nup93
OAS2		2'-5'-oligoadenylate synthase 2
OAS3	P100	2'-5'-oligoadenylate synthetase 3
OGDH	OGDC, AKGDH	2-oxoglutarate dehydrogenase E1 component
OGFR		Opioid growth factor receptor
OSTC	DC2	Oligosaccharyltransferase complex subunit

OTUB1		Ubiquitin thioesterase
P3H1	Leucine Proline-Enriched Proteoglycan (Leprecan) 1, Leucine- And Proline-Enriched Proteoglycan 1, Procollagen-Proline 3-Dioxygenase, LEPRE1, GROS1	Prolyl 3-hydroxylase 1
PA2G4	EBP2, HG4-1	Proliferation-associated 2G4, 38kDa
PABPN1		Polyadenylate-binding protein 2
PACSIN2	Syndapin-II	Protein Kinase C and Casein Kinase Substrate in Neurons 2
PBEF1	NAMPT	Pre-B-cell colony enhancing factor 1, isoform CRA_a
PC4	Keratin 6B, PC2, CK6B	PC4 protein
PCBP2		Poly(rC)-binding protein 2
PCNA	CYCLIN	Proliferating cell nuclear antigen
PDIA3	P58, ER60, Epididymis Secretory Protein Li 269, Protein Disulphide-Isomerase A3,	Protein disulphide-isomerase A3
PDXK	Vitamin B6 Kinase, PKH, PNK, C21orf97, C21orf124	Pyridoxal kinase
PECAM1	CD31, ENDOCAM	Platelet endothelial cell adhesion molecule 1
PFN1		Profilin-1
PGRMC2		Membrane-associated progesterone receptor component 2
PHB	Epididymis luminal protein 215, PHB/1	Prohibitin
PHGDH		D-3-phosphoglycerate dehydrogenase
PK2	PKM2, P58, TCB, PK2	Pyruvate kinase
PLAUR	CD87	Urokinase plasminogen activator surface receptor
PLD3	AD19, HUK4, Choline Phosphatase, Phosphatase D3	Phospholipase D family, member 3, isoform CRA_b
PLEK	P47	Pleckstrin
PLEKHO2		Pleckstrin homology domain-containing family O member 2
PLIN3	Mannose-6-Phosphate Receptor-Binding Protein 1	Perilipin-3
PLOD1		Procollagen-lysine, 2-oxoglutarate 5-dioxygenase 1
PLOD3	Lysine Hydroxylase 3	Procollagen-lysine,2-oxoglutarate 5-dioxygenase 3
PMPCA	KIAA0123, P-55	Mitochondrial-processing peptidase subunit alpha
PNN	Desmosome Associated Protein, Neutrophil Protein, DRS, SDK3	Pinin
POR	CPR, P450R	NADPH--cytochrome P450 reductase

PPCS	COAB	Phosphopantothenate--cysteine ligase
PPIA	PPIA, Cyclosporin A-Binding Protein, CYPA, CYPH, T Cell Cyclophilin	Peptidyl-prolyl cis-trans isomerase
PPIF		Peptidyl-prolyl cis-trans isomerase
PPM1G		Protein phosphatase 2C isoform gamma
PREP	PEP	Prolyl endopeptidase
PRKCD		Protein kinase C delta
PSAPL1		Proactivator polypeptide
PSAT1	Endometrial Progesterone-Induced Protein	Phosphoserine aminotransferase 1
PSIP1	P75, P52	PC4 and SFRS1-interacting protein 1
PSMA1	Macropain Subunit C2	Proteasome endopeptidase complex 1
PTGS1	Cyclooxygenase-1, COX1, COX3	Prostaglandin G/H synthase 1
PTK2		Tyrosine-protein kinase 2
PTMA		Prothymosin alpha
PUF60	RoBP1	Poly(U)-binding-splicing factor PUF60
PYGB	GPBB	Glycogen phosphorylase, brain form
QARS		Glutaminyl-tRNA synthetase
RAB8B		Ras-related protein Rab-8B
RAB10		Ras-related protein Rab-10
RAB31		Ras-related protein Rab-31
RANBP1		RAN binding protein 1, isoform CRA_g
RAP1A		RAP1A, member of RAS oncogene family
RBBP4		Histone-binding protein RBBP4
RBM3		RNA binding motif (RNP1, RRM) protein 3, isoform CRA_c
RBM39	Coactivator of Activating Protein-1 And Estrogen Receptors, HCC1, CAPER, FSA59	RNA-binding protein 39
RCC1		Regulator of chromosome condensation
RCC2	Regulator of Chromosome Condensation	RCC2 protein
RCN1	Reticulocalbin 1, RCN, RCN1, PIG20, RCAL	Epididymis secretory protein Li 84
REEP5		Receptor expression-enhancing protein
RHOC		Rho-related GTP-binding protein RhoC
RNH1	PRI	Ribonuclease/angiogenin inhibitor 1, isoform CRA_a
RNPEP	Arginine Aminopeptidase, ABP	Aminopeptidase B
RPL19		Ribosomal protein L19
RPL28		60S ribosomal protein L28
RPL31		60S ribosomal protein L31
RPL32		60S ribosomal protein L32
RPL35A	Cell Growth-Inhibiting Gene 33 Protein, L35A	60S ribosomal protein L35a
RPL36A	L36A, L44L	60S ribosomal protein L36a
RPL37A		60S ribosomal protein L37a
RPLP1		RPLP1 protein

RPLP2		Ribosomal protein, large, P2, isoform CRA_a
RPS15	RIG Protein	40S ribosomal protein S15
RPS24		40S ribosomal protein S24
RPS26		40S ribosomal protein S26
RPS27	Metallopanstimulin, MPS1	40S ribosomal protein S27
RPS29		40S ribosomal protein S29
RRM1		Ribonucleoside-diphosphate reductase
RSL1D1	PBK1	Ribosomal L1 domain-containing protein 1
RTN4	ASY, KIAA0886	Reticulon
S100A6	Calcyclin, Growth Factor-Inducible Protein 2A9	Protein S100-A6
S100A8	S100 Calcium Binding Protein A8, Migration Inhibitory Factor-Related Protein 8, Leukocyte L1 Complex Light Chain, Calprotectin L1L Subunit, Calgranulin A, MRP-8	Protein S100-A8
S100A11	S100A11, Calgizzarin,	Protein S100 A11
SARNP	Cytokine Induced Protein 29 Kda, Proliferation-Associated Cytokine-Inducible Protein, HSPC316	SAP domain-containing ribonucleoprotein
SCARB2	Scavenger Receptor Class B Member 2, **CD36** Antigen	Lysosome membrane protein 2
SCCPDH		Saccharopine dehydrogenase-like oxidoreductase
SCPEP1		Carboxypeptidase
SDHB	SDH1, SDH, IP	Succinate dehydrogenase [ubiquinone] iron-sulphur subunit, mitochondrial
SEC22B		SEC22 vesicle trafficking protein B
SEC61A1		Sec61 alpha 1 subunit (S. cerevisiae), isoform CRA_c
SEC61B		Protein translocation complex beta variant
SERPINB1	Monocyte/Neutrophil Elastase Inhibitor, P12	Leukocyte elastase inhibitor
SERPINB8	Cytoplasmic Antiproteinase 2, p18, Peptidase Inhibitor 8, Minor Histocompatibility Protein HMSD Variant Form, C18orf53	Serine (or cysteine) proteinase inhibitor, clade B (ovalbumin), member 8
SERPINH1	Rheumatoid Arthritis Antigen A-47, HSP47, CBP1, CBP2, GP46, Collagen Binding Protein	Serpin peptidase inhibitor, clade H (Heat shock protein 47), member 1, (Collagen binding protein 1), isoform CRA_a
SFRS3	SRSF3	Splicing factor arginine/serine-rich 3

SH3BGRL3	TNF Inhibitory Protein	SH3 domain-binding glutamic acid-rich-like protein 3
SH3BP1		SH3 domain-binding protein 1
SLC25A11	Solute Carrier Family 25 Member 11, SLC20A4, OGCP, OGC	Mitochondrial 2-oxoglutarate/malate carrier protein
SLC25A24	APC1	Solute carrier family 25, member 24, transcript variant 1, Mrna
SLC2A1	GLUT-1	Solute carrier family 2, facilitated glucose transporter member 1
SLIRP	C14orf156, DC50	SRA stem-loop-interacting RNA-binding protein, mitochondrial
SMBP	TM9SF3	Transmembrane 9 superfamily member
SNRP70	SNRNP70	Small nuclear ribonucleoprotein 70kDa polypeptide (RNP antigen)
SNX9		Sorting nexin-9
SOD2		Superoxide dismutase
SQRDL	PRO1975	Sulphide Quinone Oxidoreductase
SRRT	ASR2	Serrate RNA effector molecule homolog
SSB	Autoantigen La, Lupus La Protein, LARP3	Sjogren Syndrome Antigen B
SSBP1		Single-stranded DNA-binding protein, mitochondrial
SSR1	1Translocon-associated protein subunit alpha, TRAP Alpha	Signal Sequence Receptor Subunit
SSRM1		S-adenosylmethionine synthase
SSRP1	Facilitates Chromatin Transcription Complex 80 KDa Subunit	FACT complex subunit SSRP1
STAT1		Signal transducer and activator of transcription 1-alpha/beta
STK10	LOK	Serine/threonine-protein kinase 10
STOM	Erythrocyte band 7 integral membrane protein, EPB7	Stomatin
SUPT16H	HSPT16, SCS68, FACT140	FACT complex subunit SPT16
TAGLN2	KIA0120	Transgelin-2
TAP1	PSF1, APT1, ABC Transporter, MHC 1	Antigen peptide transporter 1
TAP2	PSF2, APT2	Antigen peptide transporter 2
TAPBP		TAP binding protein
TARS		Threonyl-tRNA synthetase
TBCA	Chaperonin Cofactor A, CFA	Tubulin-specific chaperone A
TBL2		Transducin beta-like protein 2
TCIRG1	V-type proton ATPase subunit a, ATPase H+ Transporting V0 Subunit A3	T-Cell Immune Regulator 1
TFRC	P90, CD71	Transferrin receptor protein 1
TLN1	KIAA1027	Talin-1

TMCO1	PCIA3	Calcium load-activated calcium channel
TMED2	P24	Transmembrane emp24 domain-containing protein 2
TMED4	Endoplasmic Reticulum Stress-Response Protein 25, Putative NF-Kappa-B-Activating Protein 156, P24alpha3, GMP25iso, ERS25	Transmembrane emp24 domain-containing protein 4
TMEM33	DB83	Transmembrane protein 33
TMEM43	LUMA, ARVF5, EDMD7, ARVD5	Transmembrane protein 43 isoform 1
TMEM165	TPARL, FT27, CDG2K, GDT1	Transmembrane protein 165
TNFAIP8L2	Inflammation Factor 20	Tumour necrosis factor alpha-induced protein 8-like protein 2
TNRC5	Canopy FGF Signalling Regulator 3, Protein Associated with Toll-Like Receptor 4A, CAG4A, CGT4A	Trinucleotide repeat containing 5, isoform CRA_g
TOP2A	TP2A	DNA topoisomerase 2-alpha
TPP1	Growth-Inhibiting Protein, SCAR7, GIG1, CLN2	Tripeptidyl-peptidase 1
TPP2		Tripeptidyl-peptidase 2
TRIM25		E3 ubiquitin/ISG15 ligase TRIM25
TRIP13	Pachytene checkpoint protein 2 homolog, PCH2	Thyroid Hormone Receptor Interactor 13
TRIM28	Nuclear Corepressor KAP-1, E3 SUMO-Protein Ligase TRIM28, TIF1B, KAP-1, TF1B	Tripartite motif-containing 28
TTLL12	KIAA0153	Tubulin tyrosine ligase-like family, member 12, isoform CRA_a
TUBA4A		Tubulin alpha-4A chain
TUBB4A		Tubulin beta-4A chain
TWF2	Twinfilin Actin Binding Protein 2, Protein Tyrosine Kinase 9-Like (A6-Related Protein), PTK9L	Twinfilin-2
TYMP	ECGF	Thymidine phosphorylase
UBE2N	BLU, UBE2N, Epididymis secretory protein Li 71	Ubiquitin Conjugating Enzyme E2 N
UGGT		UDP-glucose ceramide glucosyltransferase-like 1
UQCRFS1		Ubiquinol-cytochrome c reductase complex ubiquinone-binding protein QP-C
UQCRH		UQCRH protein
USP5		Ubiquitinyl hydrolase 1
UTS2		Urotensin 2
VAMP8		Vesicle-associated membrane protein 8
VASP		Vasodilator-stimulated phosphoprotein isoform 4

VCL		Vinculin, isoform CRA_c
VDAC1	Sperm binding protein 1a	Voltage-dependent anion-selective channel protein 1
VDAC2		Voltage-dependent anion-selective channel protein 2
VIM	Epididymis luminal protein 113	Vimentin
VKORC1		Vitamin K Epoxide Reductase Complex Subunit 1,
XPNPEP1	APP1	Xaa-Pro aminopeptidase 1
YBX1	Major Histocompatibility Complex, Class II, Y Box-Binding Protein	Nuclease-sensitive element-binding protein 1
YWHAG	Protein Kinase C Inhibitor Protein 1, KCIP-1	14-3-3 protein gamma
YWHAH	ETA, AS1	Tyrosine 3-monooxygenase/tryptophan 5-monooxygenase activation protein, eta polypeptide, isoform CRA_b
ZMPSTE24	PRO1	CAAX prenyl protease 1 homolog
ZNF432		Zinc finger protein 432

Appendix C

Publications and presentations

Publications:

Clinical Oral Investigations
https://doi.org/10.1007/s00784-018-2771-9

ORIGINAL ARTICLE

Subgingival lipid A profile and endotoxin activity in periodontal health and disease

Alexander Strachan[1] · Zoe Harrington[1] · Clare McIlwaine[1] · Matthew Jerreat[1] · Louise A. Belfield[1] · Aniko Kilar[2] · Simon K. Jackson[1] · Andrew Foey[1] · Svetislav Zaric[1]

Received: 22 August 2018 / Accepted: 5 December 2018

Abstract

Objectives Regulation of lipopolysaccharide (LPS) chemical composition, particularly its lipid A domain, is an important, naturally occurring mechanism that drives bacteria-host immune system interactions into either a symbiotic or pathogenic relationship. Members of the subgingival oral microbiota can critically modulate host immuno-inflammatory responses by synthesizing different LPS isoforms. The objectives of this study were to analyze subgingival lipid A profiles and endotoxin activities in periodontal health and disease and to evaluate the use of the recombinant factor C assay as a new, lipid A-based biosensor for personalized, point-of-care periodontal therapy.

Materials and methods Subgingival plaque samples were collected from healthy individuals and chronic periodontitis patients before and after periodontal therapy. Chemical composition of subgingival lipid A moieties was determined by ESI-Mass Spectrometry. Endotoxin activity of subgingival LPS extracts was assessed using the recombinant factor C assay, and their inflammatory potential was examined in THP-1-derived macrophages by measuring TNF-α and IL-8 production.

Results Characteristic lipid A molecular signatures, corresponding to over-acylated, bi-phosphorylated lipid A isoforms, were observed in diseased samples. Healthy and post-treatment samples were characterized by lower *m/z* peaks, related to under-acylated, hypo-phosphorylated lipid A structures. Endotoxin activity levels and inflammatory potentials of subgingival LPS extracts from periodontitis patients were significantly higher compared to healthy and post-treatment samples.

Conclusions This is the first study to consider structure-function-clinical implications of different lipid A isoforms present in the subgingival niche and sheds new light on molecular pathogenic mechanisms of subgingival biofilm communities.

Clinical relevance Subgingival endotoxin activity (determined by lipid A chemical composition) could be a reliable, bacterially derived biomarker and a risk assessment tool for personalized periodontal care.

Currently under review:

'Comparative analysis of total salivary lipopolysaccharide chemical and biological properties with periodontal status.'

Authors: Zaric, S., Mcilwaine, C., Strachan, A., Harrington, Z., Jerreat, M., Belfield, L., Sandor, V and Foey, A.

Submission no: AOB_2019_851

Submitted manuscript to: Archives of Oral Biology

Oral Presentations:

September, 2017. Plymouth, UK. British Society for Oral and Dental Research Annual Scientific Meeting:

'Development and Evaluation of a Novel, Lipid-A Based Biosensor for Personalised and Predictive Periodontal Therapy.'

&

'Monitoring Salivary LPS Activity for Preventive, Participatory, Point-of-Care Periodontal Therapy.'

March, 2017. Plymouth, UK. Peninsula Schools of Medicine and Dentistry Annual Research Event.

'Subgingival Endotoxin Activity in Patients with Chronic Periodontitis.'

September, 2016. Jerusalem, Israel. International Association for Dental Research Congress:

'Chronic Periodontitis Patients Exhibit Differential Endotoxin Activity and Inflammatory Potential.'

April, 2016. Plymouth, UK. Peninsula Schools of Medicine and Dentistry Annual Postgraduate Research Event.

'*Porphyromonas gingivalis* Lipopolysaccharide Isoforms Differentially Modulate Cytokine Secretion and Tolerisation Responses in M1 and M2 Macrophages.'

Poster Presentations

July, 2019. Manchester, UK. Microscience Microscopy Congress:

'Scanning Electron Microscopy of Subgingival Biofilm and its Endotoxin Activity in Patients with Chronic Periodontitis.'

March, 2019. Plymouth, UK. South West Electron Microscopy Meeting:

'Subgingival Endotoxin Activity in Patients with Chronic Periodontitis.'

December, 2016. Liverpool, UK. British Society of Immunology Congress:

'*Porphyromonas gingivalis* Lipopolysaccharide Isoforms Differentially Modulate Cytokine Secretion and Tolerisation Responses in M1 and M2 Macrophages.'

September, 2015. Cardiff, UK. British Society for Oral and Dental Research Annual Scientific Meeting:

'*Porphyromonas gingivalis* Lipopolysaccharide Isoforms Initiate Cytokine Tolerisation Responses in M1 and M2 Macrophages.'

September, 2015. Plymouth. UK. Peninsula Schools of Medicine and Dentistry Annual Postgraduate Research Event.

'Porphrymonas gingivalis

Lipopolysaccharide Isoforms Differentially Modulate TNF Secretion and Cytokine Tolerisation Responses in M1 and M2 Macrophages.'

June, 2015, London, UK. PGLondon meeting:

'*Porphyromonas gingivalis*

Lipopolysaccharide Isoforms Modulate Differential Cytokine Responses in M1 and M2 Macrophages.'

October, 2014. Plymouth, UK. Peninsula Schools of Medicine and Dentistry Annual Postgraduate Research Event.

‘Macrophage Response

to Lipopolysaccharide Isoforms Isolated from the

Periodontal Pathogen *Porphyromonas gingivalis*’

Appendix D

Proteomic supplemental figures

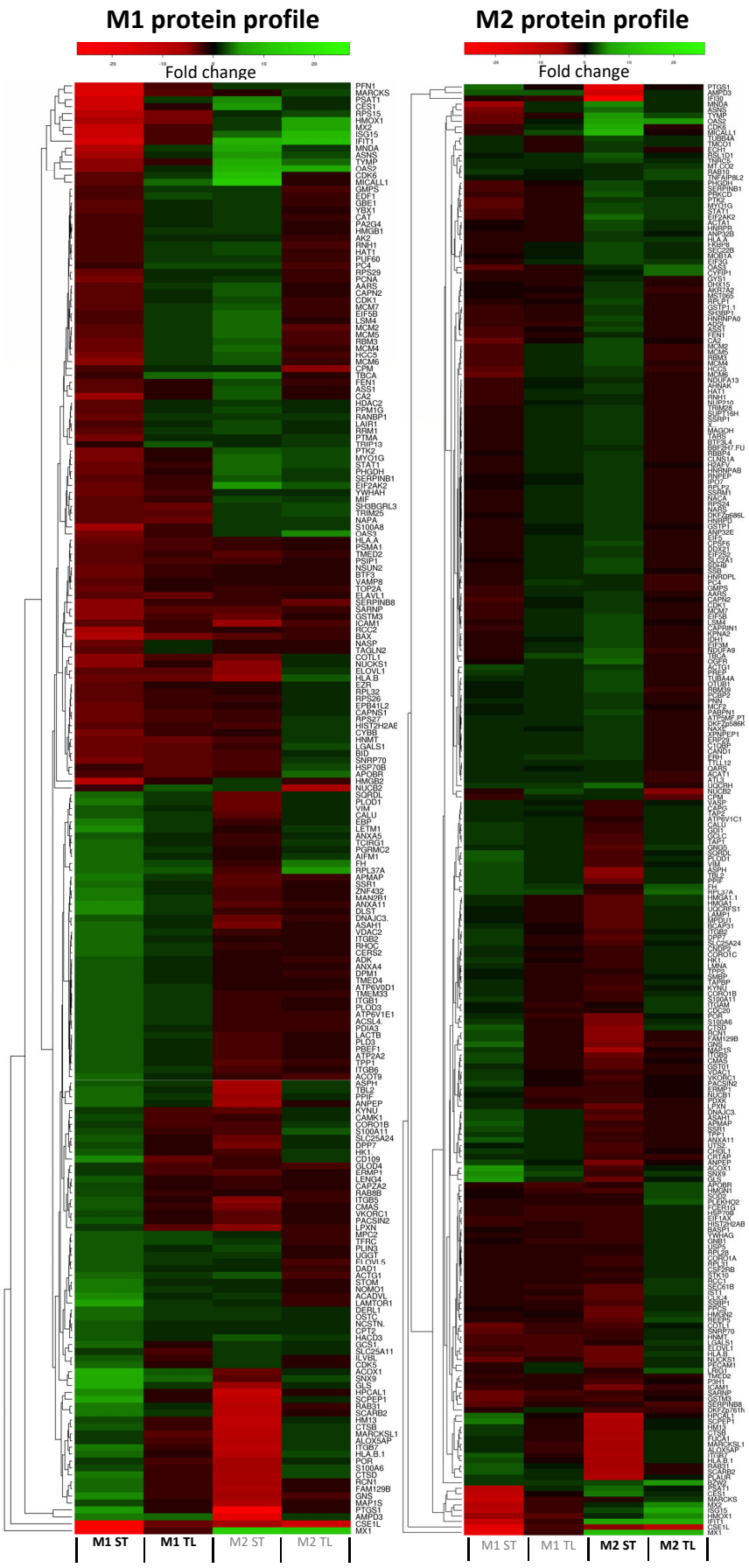

Figure PS 1.1 Heatmap indicating all proteins which demonstrated a 2-fold change in expression. Complete responsive protein profiles are mapped to include all proteins which demonstrated a 2-fold change in state either M1 or M2 MΦs. For illustrative purposes, fold change is indicated compared to basal/unstimulated levels of expression. The opposing subset is included in each map for comparison. The clustering method used was average linkage and applied to rows, the distance measurement method used was Euclidean.

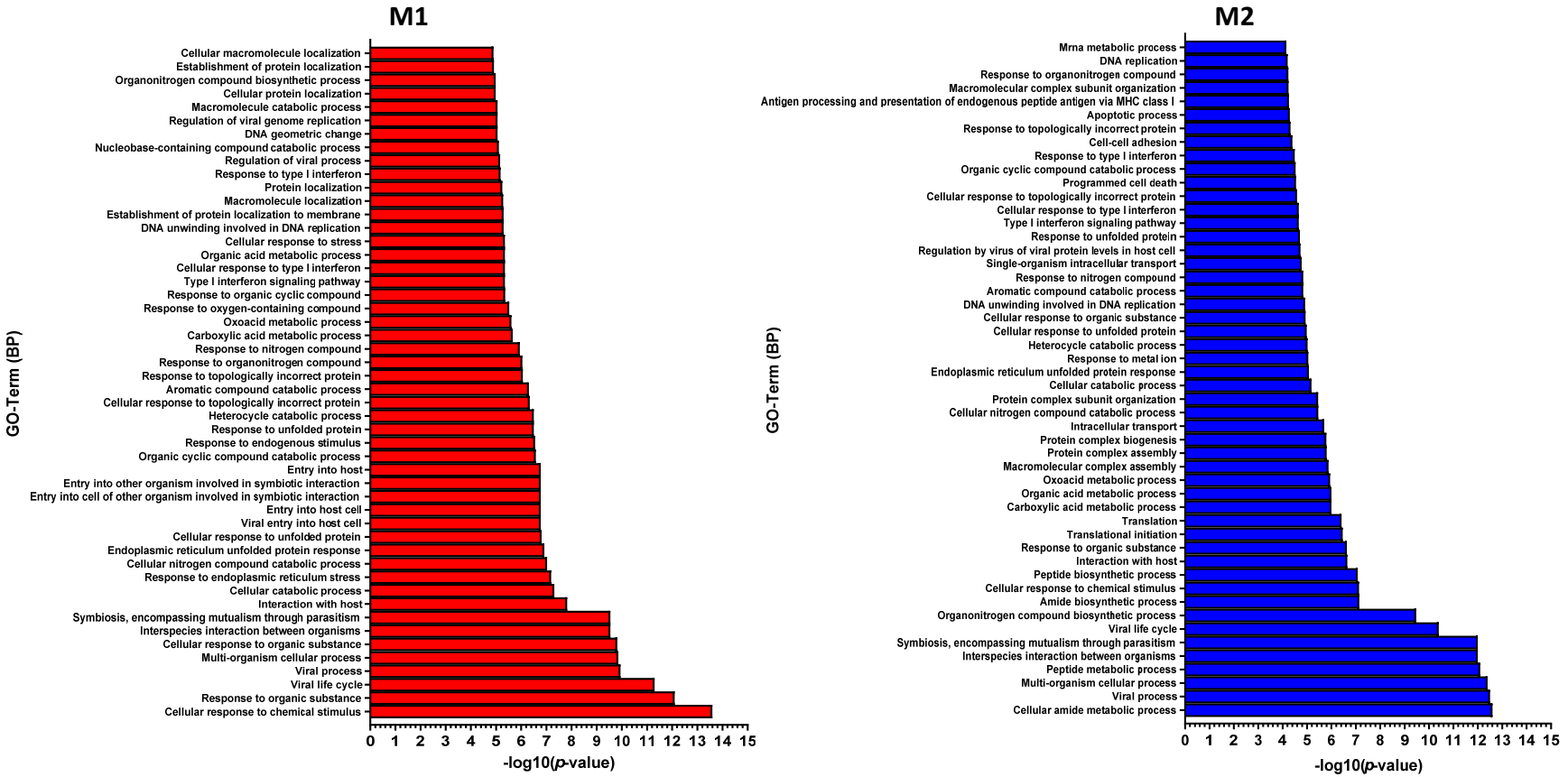

Figure PS1.2a Comparison gene ontology term annotation for BIOLOGICAL PROCESS in the responsive proteome in M1 and M2 MΦs. GO analysis was performed using the David database (GOTERM_BP_FAT) by analysing all proteins in either M1 (red) or M2 (blue) MΦs which demonstrated a minimum 2-fold change in expression when comparing unstimulated, stimulated or tolerised. Data is shown as a –log10 of the *p-value*. GO terms are given to a maximum of 50 ranked by *p-value* and/or to the minimum *p-value* equivalent to 0.05.

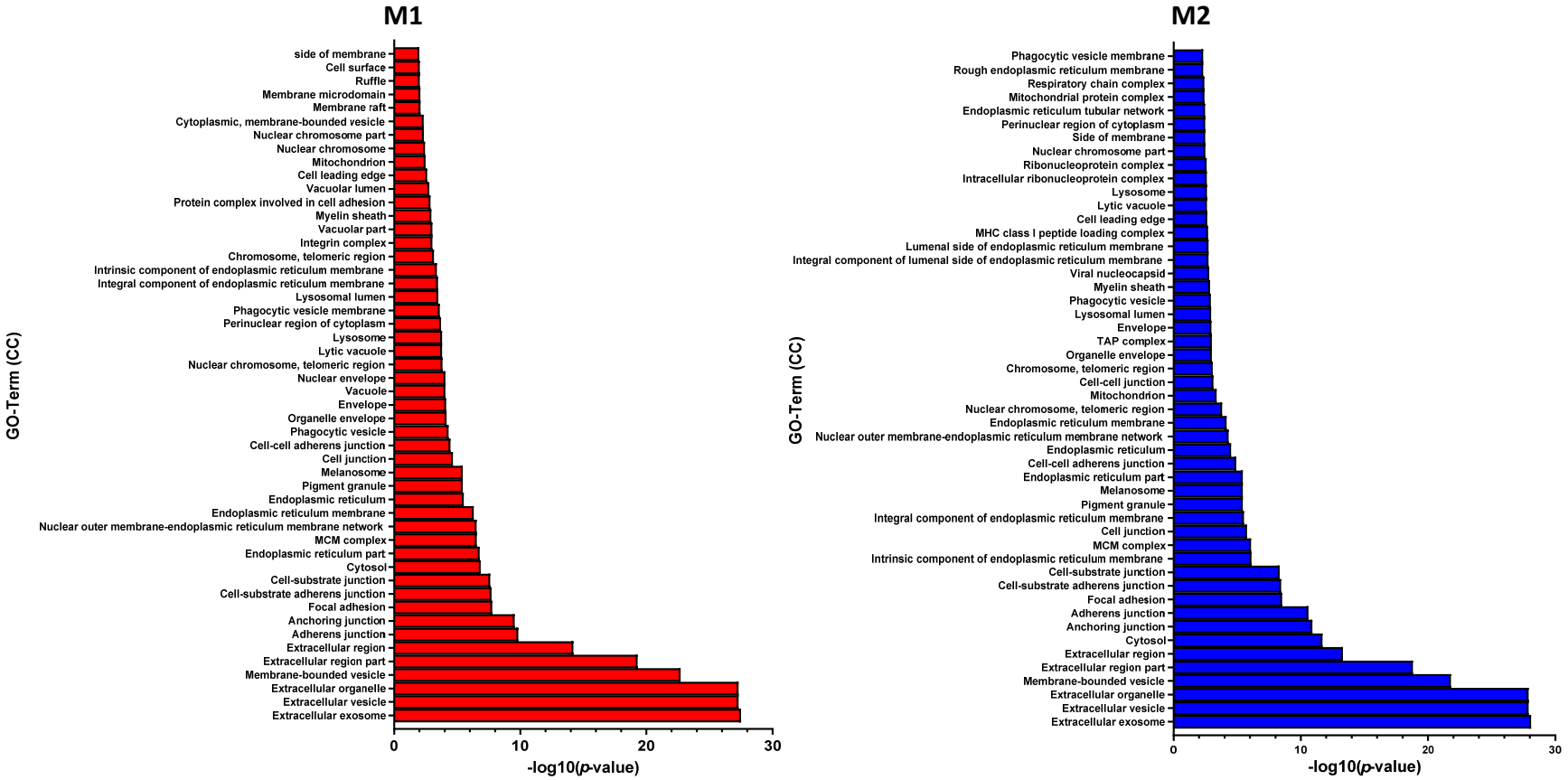

Figure PS1.2b Comparison gene ontology term annotation for CELLULAR COMPONENT in the responsive proteome in M1 and M2 MΦs. GO analysis was performed using the David database (GOTERM_CC_FAT) by analysing all proteins in either M1 (red) or M2 (blue) MΦs which demonstrated a minimum 2-fold change in expression when comparing unstimulated, stimulated or tolerised. Data is shown as a –log10 of the *p-value*. GO terms are given to a maximum of 50 ranked by *p-value* and/or to the minimum *p-value* equivalent to 0.05.

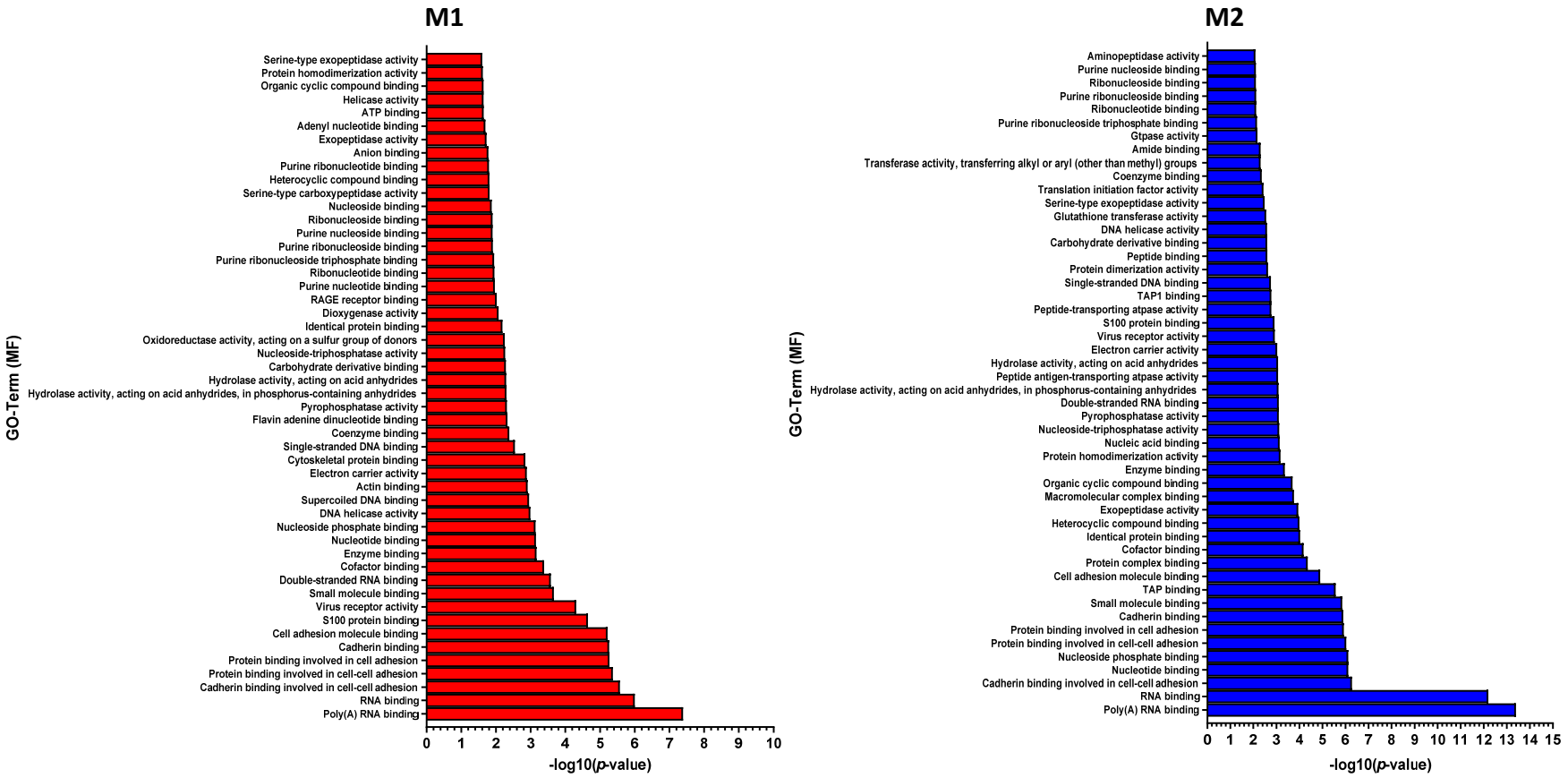

Figure PS1.2c Comparison gene ontology term annotation for MOLECULAR FUNCTION in the responsive proteome in M1 and M2 MΦs. GO analysis was performed using the David database (GOTERM_MF_FAT) by analysing all proteins in either M1 (red) or M2 (blue) MΦs which demonstrated a minimum 2-fold change in expression when comparing unstimulated, stimulated or tolerised. Data is shown as a –log10 of the *p-value*. GO terms are given to a maximum of 50 ranked by *p-value* and/or to the minimum *p-value* equivalent to 0.05.

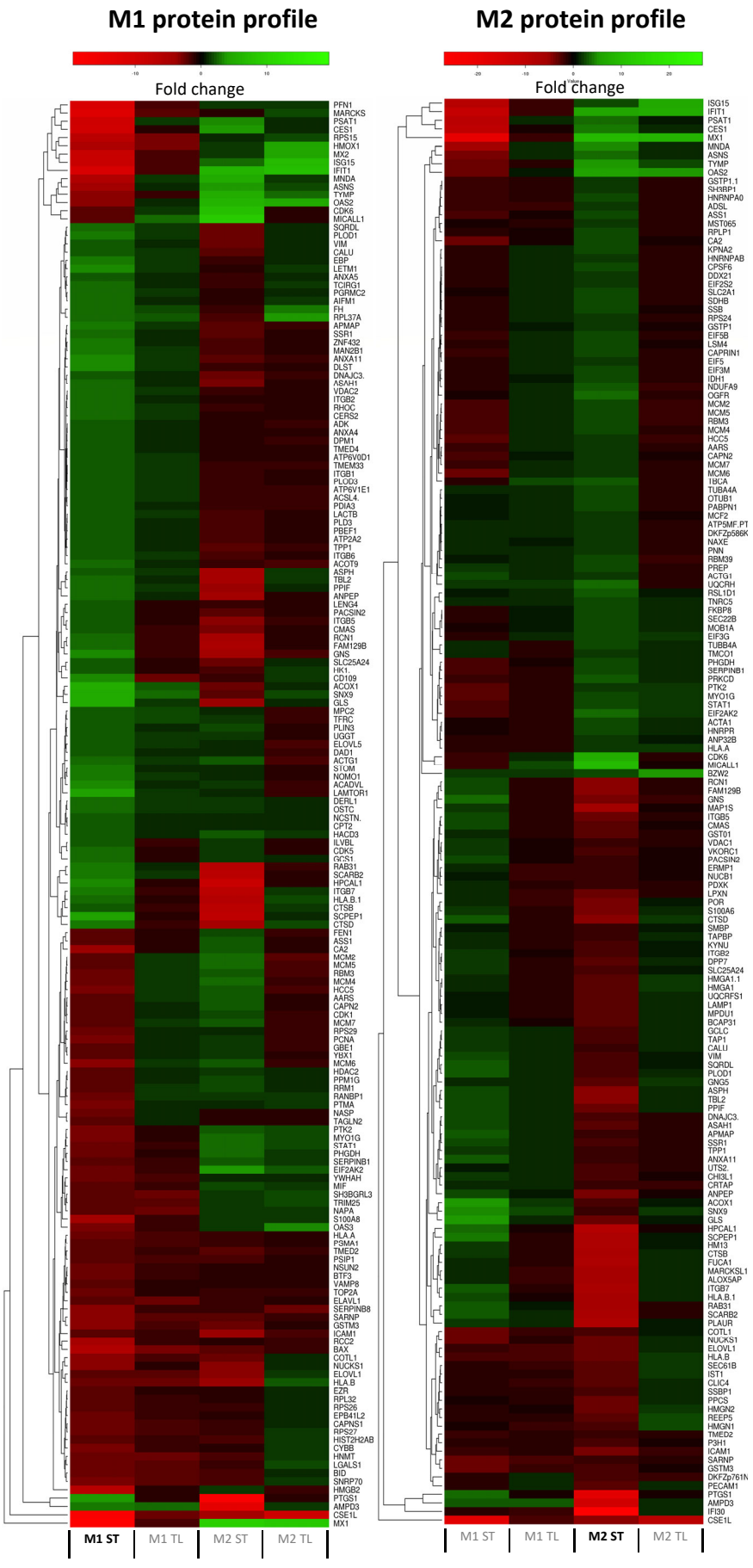

Figure PS1.3 Heatmap indicating proteins which demonstrated a 2-fold change in expression when stimulated (ST) compared to the basal (US) level. Protein profiles for each subset are mapped to include all proteins, within that subset, which demonstrated a 2-fold change compared to basal/unstimulated levels of expression. The opposing subset and TL induced expression is included for comparison. The clustering method used was average linkage and applied to rows, the distance measurement method used was Euclidean.

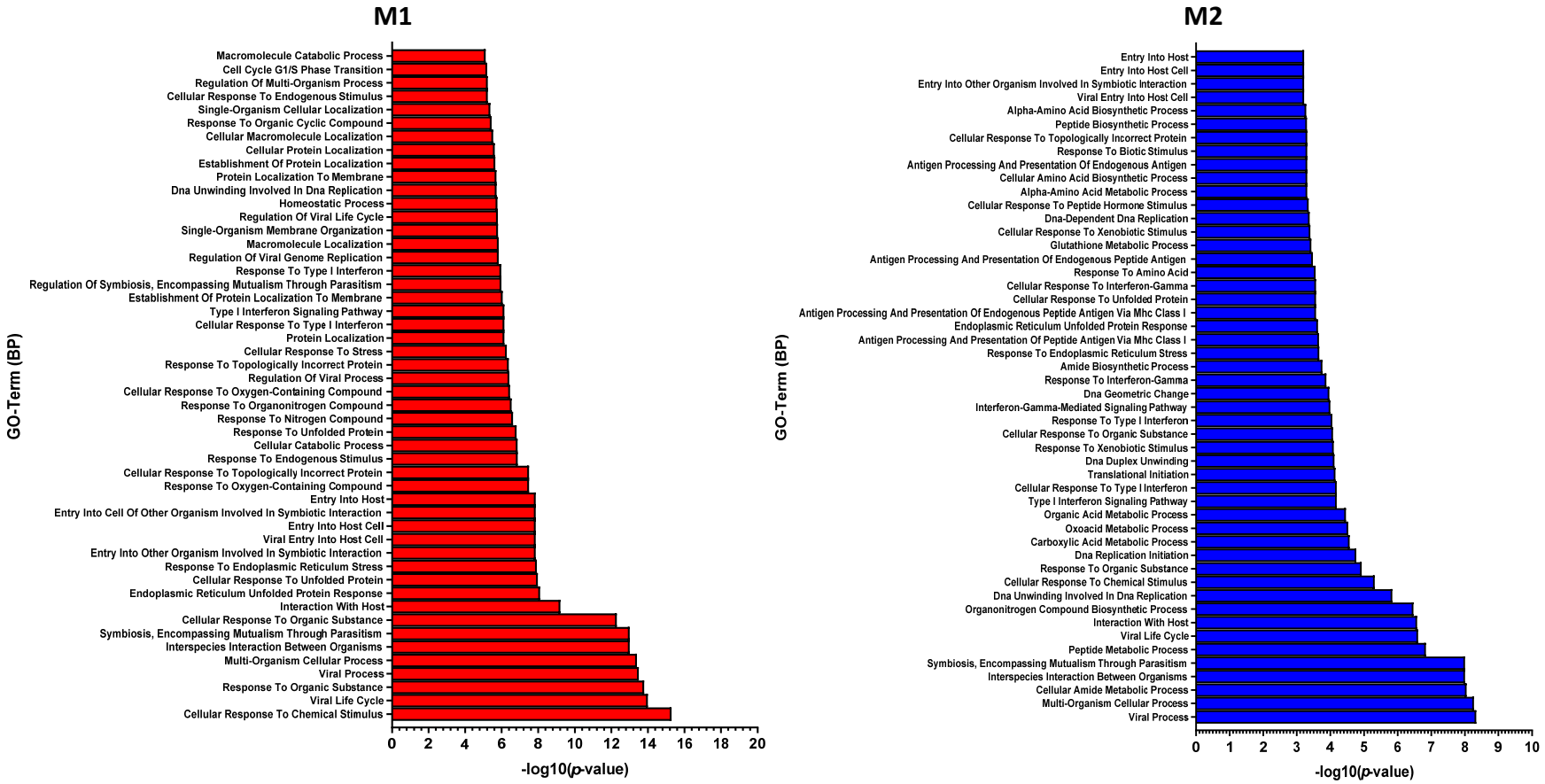

Figure 1.4a Comparison gene ontology term annotation for BIOLOGICAL PROCESS in M1 and M2 MΦs stimulated with PG LPS. GO analysis was performed using the David database (GOTERM_BP_FAT) by analysing all proteins in either M1 (red) or M2 (blue) MΦs which responded to stimulation with PG LPS by instigating a minimum 2-fold change in expression compared to the unstimulated level. Data is shown as a –log10 of the *p-value*. GO terms are given to a maximum of 50 ranked by *p-value* and/or to the minimum *p-value* equivalent to 0.05.

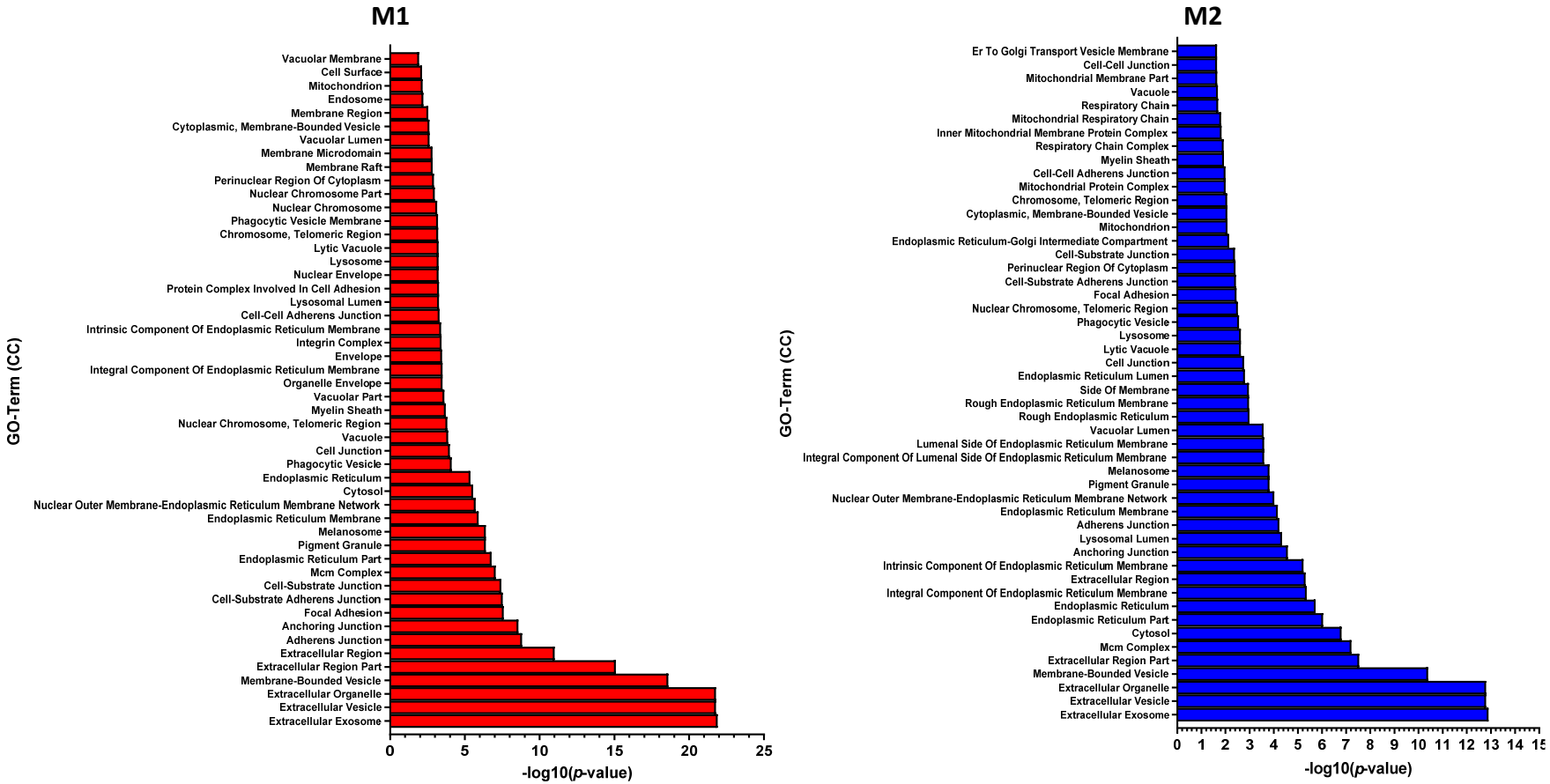

Figure 1.4b Comparison gene ontology term annotation for CELLULAR COMPONENT in M1 and M2 MΦs stimulated with PG LPS. GO analysis was performed using the David database (GOTERM_CC_FAT) by analysing all proteins in either M1 (red) or M2 (blue) MΦs which responded to stimulation with PG LPS by instigating a minimum 2-fold change in expression compared to the unstimulated level. Data is shown as a –log10 of the *p-value*. GO terms are given to a maximum of 50 ranked by *p-value* and/or to the minimum *p-value* equivalent to 0.05.

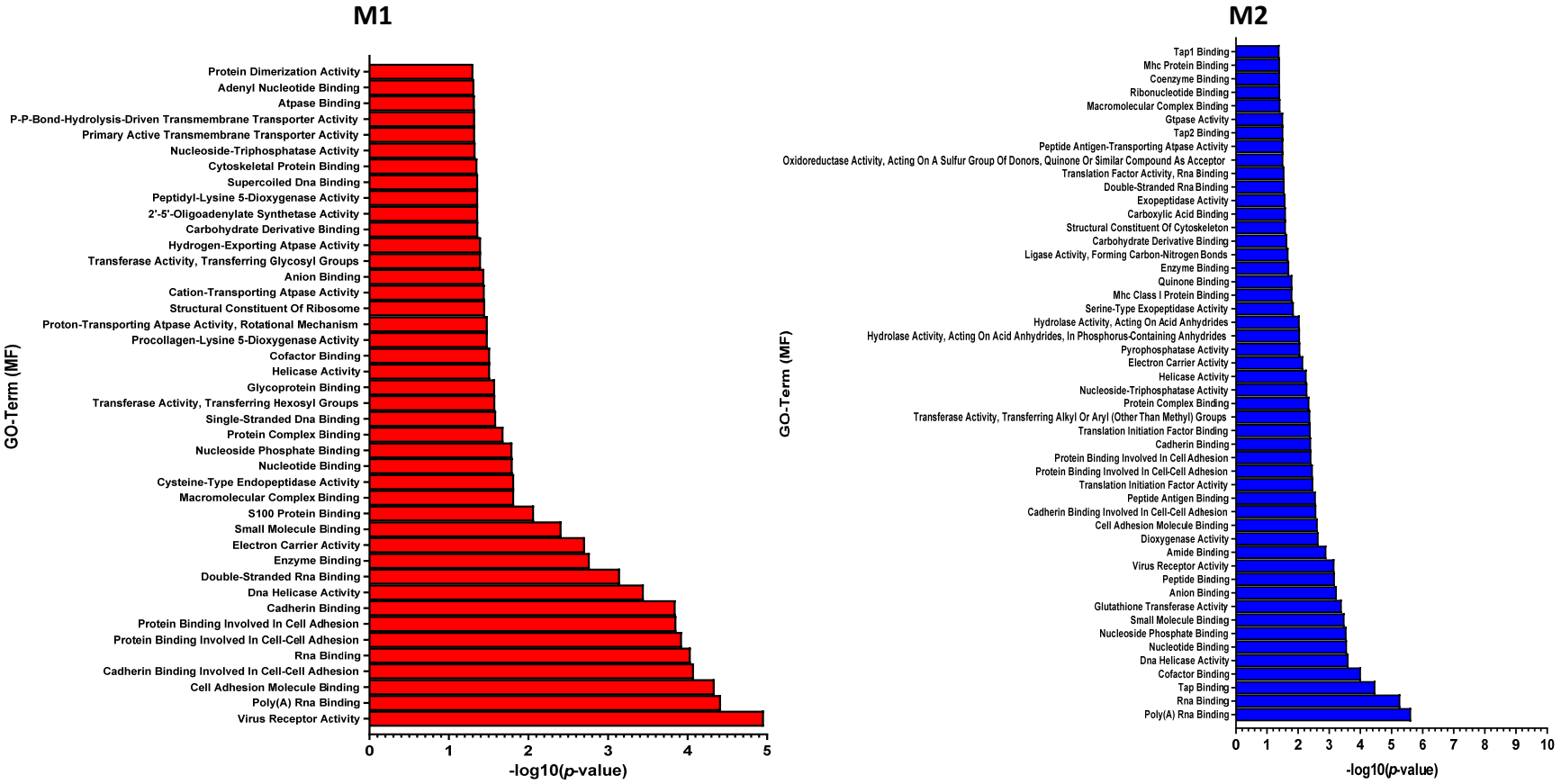

Figure 1.4c Comparison gene ontology term annotation for MOLECULAR FUNCTION in M1 and M2 MΦs stimulated with PG LPS. GO analysis was performed using the David database (GOTERM_MF_FAT) by analysing all proteins in either M1 (red) or M2 (blue) MΦs which responded to stimulation with PG LPS by instigating a minimum 2-fold change in expression compared to the unstimulated level. Data is shown as a –log10 of the *p-value*. GO terms are given to a maximum of 50 ranked by *p-value* and/or to the minimum *p-value* equivalent to 0.05.

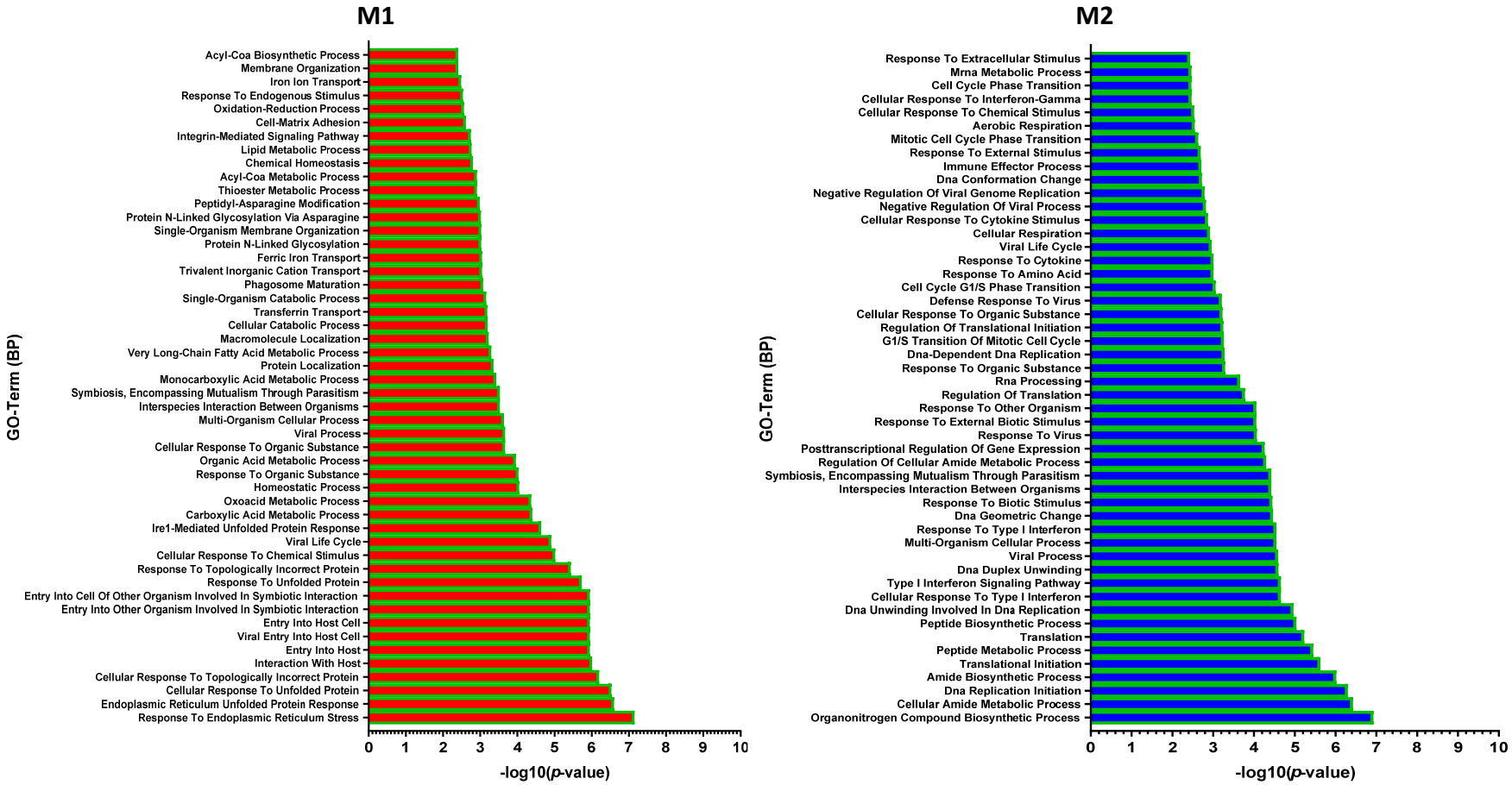

Figure PS1.5a. Comparison gene ontology term annotation for BIOLOGICAL PROCESS in M1 and M2 MΦs, which demonstrated an increase following stimulation with PG LPS. GO analysis was performed using the David database (GOTERM_BP_FAT) by analysing proteins in either M1 (red) or M2 (blue) MΦs which responded to stimulation with PG LPS by instigating a minimum 2-fold **increase (green outline)** in expression compared to the unstimulated level. Data is shown as a –log10 of the *p-value*. GO terms are given to a maximum of 50 ranked by *p-value* and/or to the minimum *p-value* equivalent to 0.05.

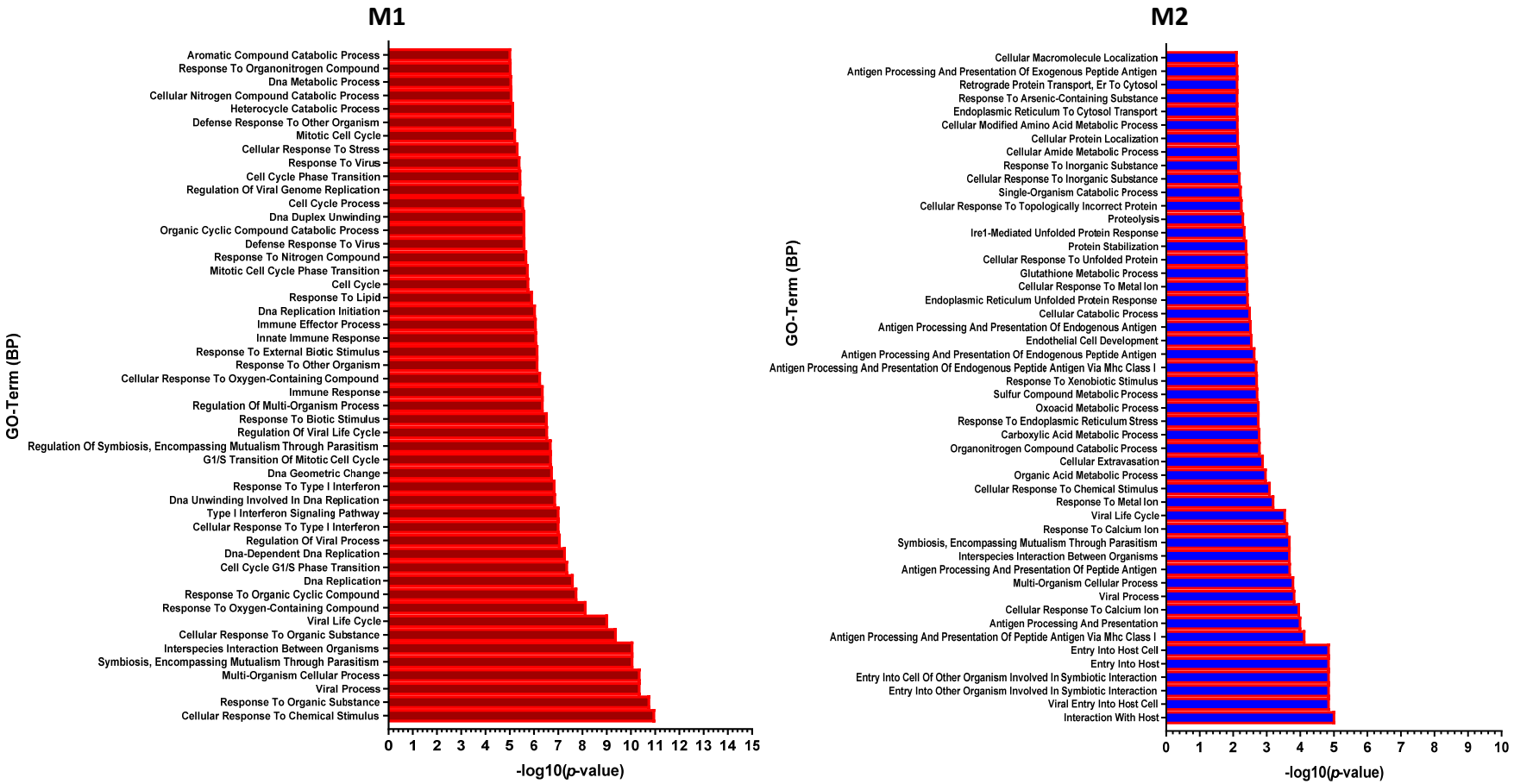

Figure PS1.5b. Comparison gene ontology term annotation for BIOLOGICAL PROCESS in M1 and M2 MΦs, which demonstrated a decrease following stimulation with PG LPS. GO analysis was performed using the David database (GOTERM_BP_FAT) by analysing proteins in either M1 (red) or M2 (blue) MΦs which responded to stimulation with PG LPS by instigating a minimum 2-fold **decrease (red outline)** in expression compared to the unstimulated level. Data is shown as a –log10 of the *p-value*. GO terms are given to a maximum of 50 ranked by *p-value* and/or to the minimum *p-value* equivalent to 0.05.

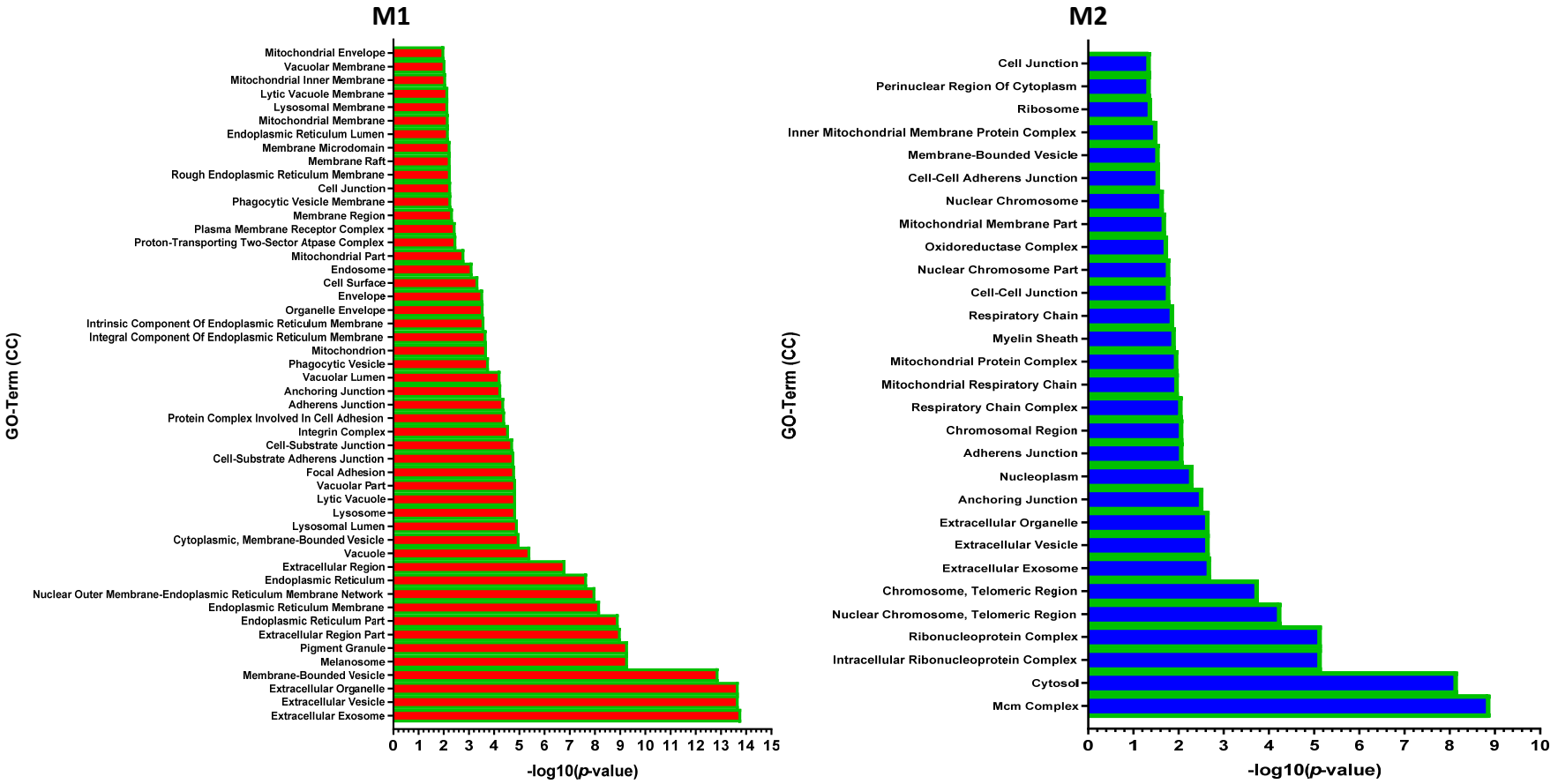

Figure PS1.6a. Comparison gene ontology term annotation for CELLULAR COMPONENT in M1 and M2 MΦs, which demonstrated an increase following stimulation with PG LPS. GO analysis was performed using the David database (GOTERM_CC_FAT) by analysing proteins in either M1 (red) or M2 (blue) MΦs which responded to stimulation with PG LPS by instigating a minimum 2-fold **increase (green outline)** in expression compared to the unstimulated level. Data is shown as a –log10 of the *p-value*. GO terms are given to a maximum of 50 ranked by *p-value* and/or to the minimum *p-value* equivalent to 0.05.

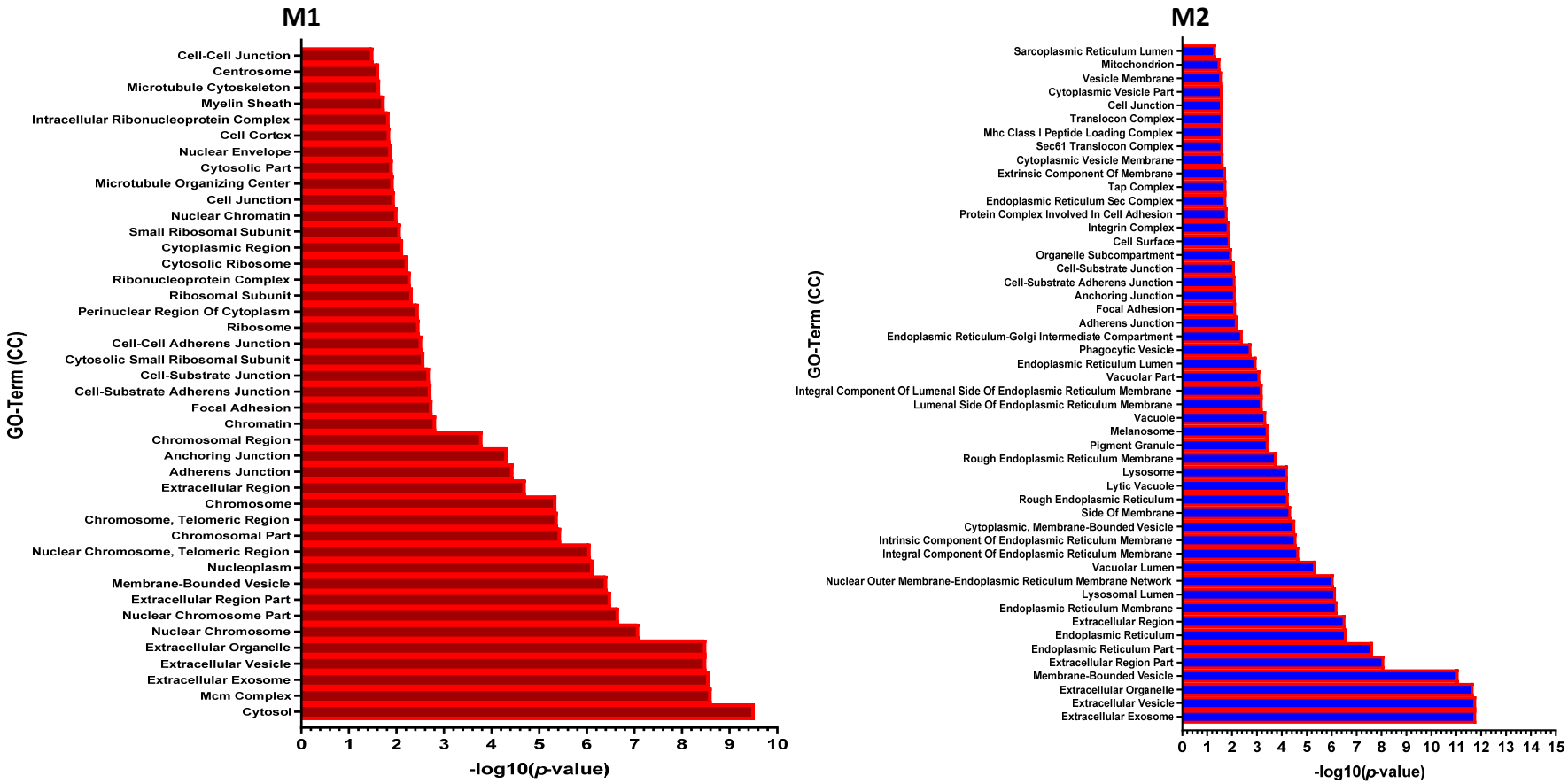

Figure PS1.6b. Comparison gene ontology term annotation for CELLULAR COMPONENT in M1 and M2 MΦs, which demonstrated a decrease following stimulation with PG LPS. GO analysis was performed using the David database (GOTERM_CC_FAT) by analysing proteins in either M1 (red) or M2 (blue) MΦs which responded to stimulation with PG LPS by instigating a minimum 2-fold **decrease (red outline)** in expression compared to the unstimulated level. Data is shown as a –log10 of the *p-value*. GO terms are given to a maximum of 50 ranked by *p-value* and/or to the minimum *p-value* equivalent to 0.05.

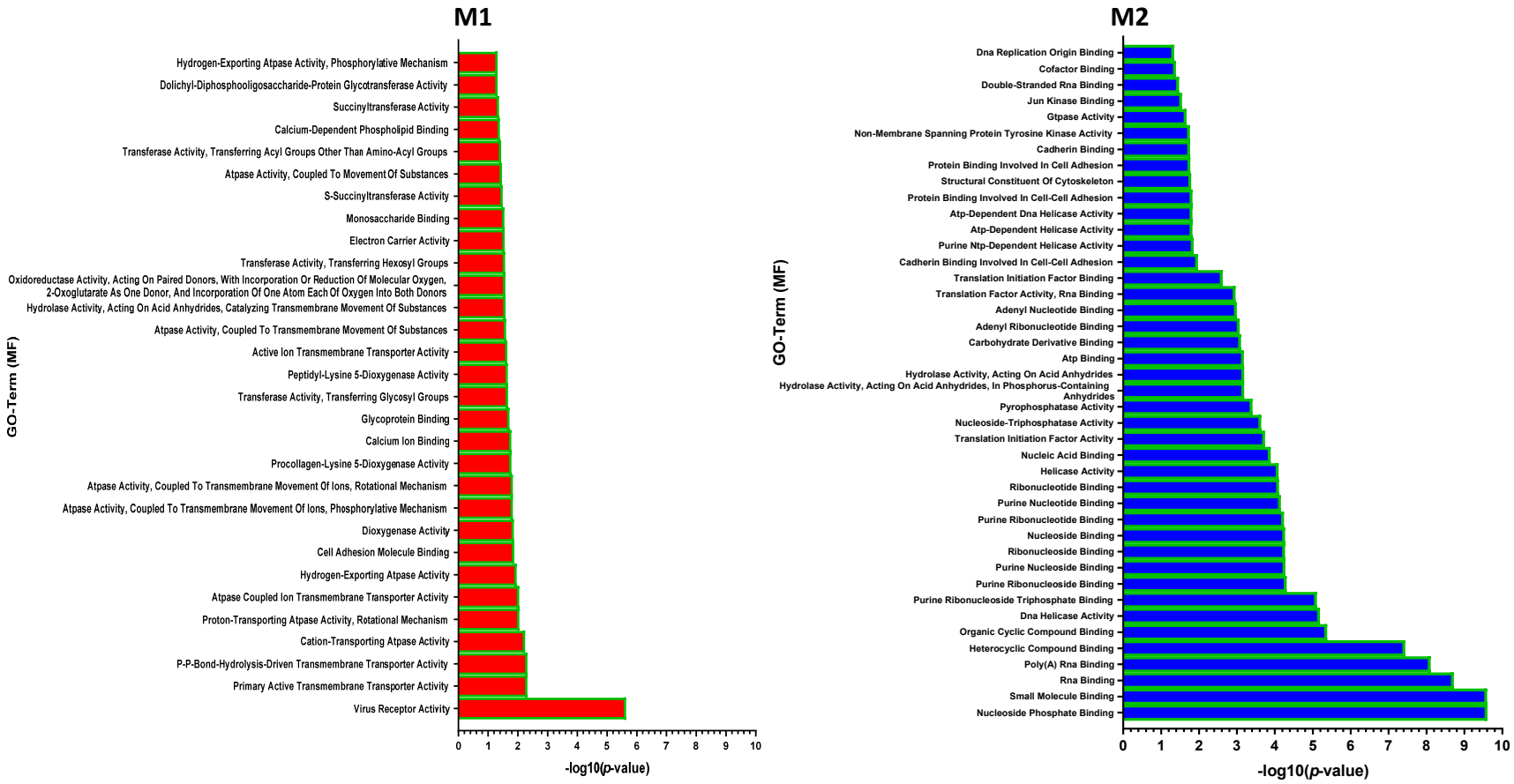

Figure PS1.7a. Comparison gene ontology term annotation for MOLECULAR FUNCTION in M1 and M2 MΦs, which demonstrated an increase following stimulation with PG LPS. GO analysis was performed using the David database (GOTERM_MF_FAT) by analysing proteins in either M1 (red) or M2 (blue) MΦs which responded to stimulation with PG LPS by instigating a minimum 2-fold **increase (green outline)** in expression compared to the unstimulated level. Data is shown as a –log10 of the *p-value*. GO terms are given to a maximum of 50 ranked by *p-value* and/or to the minimum *p-value* equivalent to 0.05.

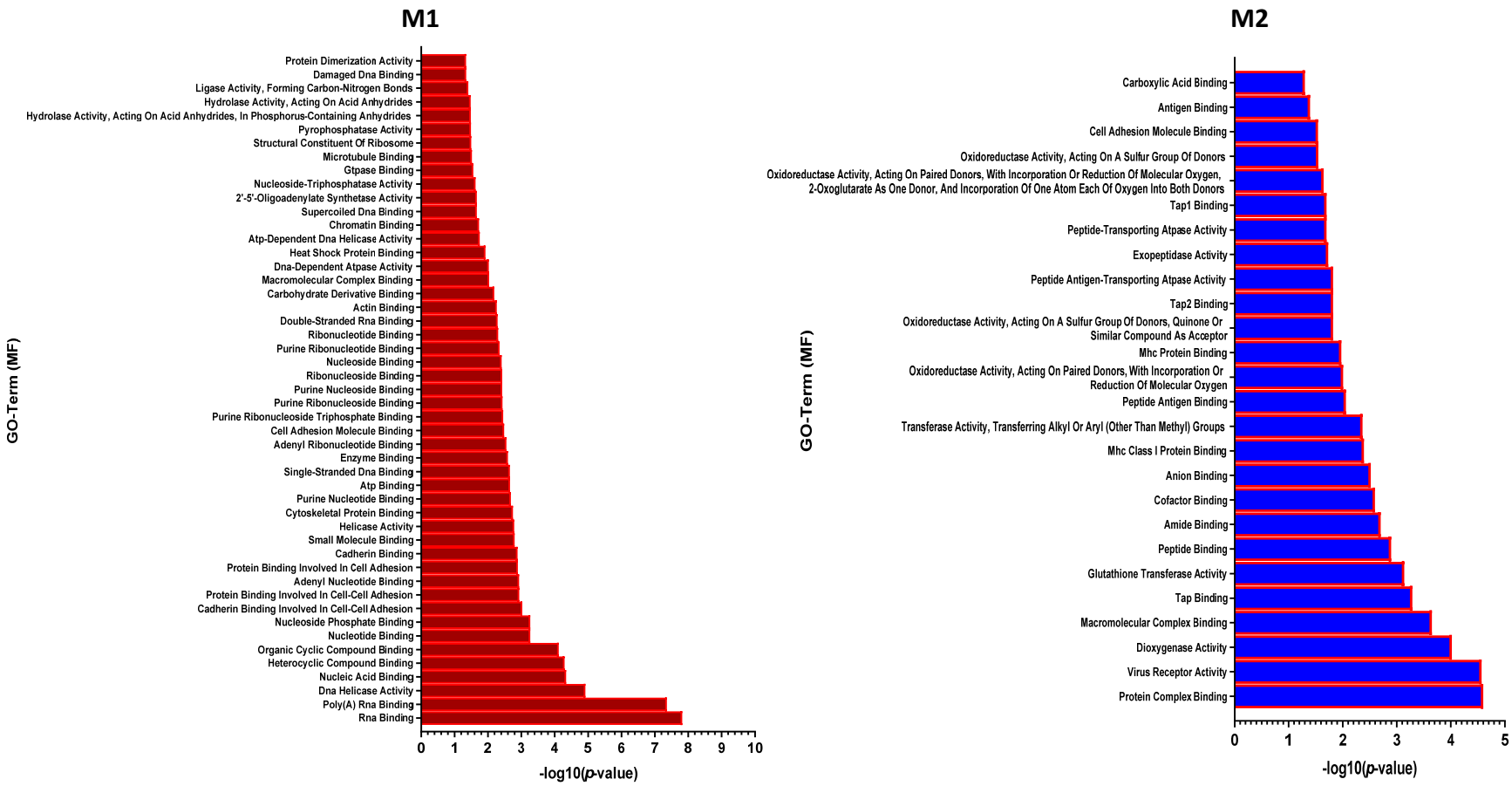

Figure PS1.7b. Comparison gene ontology term annotation for MOLECULAR FUNCTION in M1 and M2 MΦs, which demonstrated a decrease following stimulation with PG LPS. GO analysis was performed using the David database (GOTERM_MF_FAT) by analysing proteins in either M1 (red) or M2 (blue) MΦs which responded to stimulation with PG LPS by instigating a minimum 2-fold **decrease (red outline)** in expression compared to the unstimulated level. Data is shown as a –log10 of the *p-value*. GO terms are given to a maximum of 50 ranked by *p-value* and/or to the minimum *p-value* equivalent to 0.05.

a) antigen processing and presentation

GO-TERM	MΦ Subset	Response (↑↓)	BCAP29	CTSD	HLA-B	ICAM1	IF30	ITGB5	TAP1	TAPBP
Antigen Processing And Presentation (APP)	M2	↓	■	■	■	■	■	■	■	■
APP Of Endogenous Antigen	M2	↓			■				■	■
APP Of Endogenous Peptide Antigen	M2	↓			■				■	■
APP Of Endogenous Peptide Antigen Via Mhc Class I	M2	↓			■				■	■
APP Of Exogenous Peptide Antigen	M2	↓		■	■		■	■	■	
APP Of Peptide Antigen	M2	↓	■	■	■		■	■	■	■
APP Of Peptide Antigen Via Mhc Class I	M2	↓	■		■		■	■	■	■

b) epigenetic modification, transcription and translation

GO-TERM	MΦ Subset	Response (↑↓)	AARS	ANP32B	BAX	CAPRIN1	CDK1	CPSF6	DDX21	EIF2AK2	EIF2S2	EIF3G	EIF3M	EIF5	EIF5B	FEN1	HCC5	HMGB2	HNRNPA0	HNRPR	ISG15	LSM4	MCM2	MCM4	MCM5	MCM6	MCM7	NASP	NUCKS1	PABPN1	PCNA	PFN1	PNN	PRKCD	RBM3	RBM39	RPLP1	RPS24	RRM1	RSL1D1	SSB	TOP2A	TRIM25
Dna Conformation Change	M2	↑		■													■						■	■	■	■	■																
Dna Duplex Unwinding	M1	↓															■						■	■	■	■	■																■
Dna Duplex Unwinding	M2	↑															■						■	■	■	■	■																
Dna Geometric Change	M1	↓															■	■					■	■	■	■	■																■
Dna Geometric Change	M2	↑															■						■	■	■	■	■																
Dna Metabolic Process	M1	↓			■		■									■	■	■			■		■	■	■	■	■	■	■		■								■				■
Dna Replication	M1	↓					■									■	■						■	■	■	■	■	■			■								■				■
Dna Replication Initiation	M1	↓														■	■						■	■	■	■	■																
Dna Replication Initiation	M2	↑														■	■						■	■	■	■	■																
Dna Unwinding Involved In Dna Replication	M1	↓																					■	■	■	■	■																■
Dna Unwinding Involved In Dna Replication	M2	↑																					■	■	■	■	■																
Dna-Dependent Dna Replication	M1	↓														■	■						■	■	■	■	■		■	■													■
Dna-Dependent Dna Replication	M2	↑															■						■	■	■	■	■																
Posttranscriptional Regulation Of Gene Expression	M2	↑	■			■				■		■	■	■	■				■	■													■	■								
Regulation Of Translation	M2	↑	■			■				■		■	■	■	■				■	■													■								
Regulation Of Translational Initiation	M2	↑								■		■	■	■	■																										
Rna Processing	M2	↑	■					■	■										■	■		■							■			■		■	■	■	■					
Translation	M2	↑	■			■				■	■	■	■	■	■				■	■														■	■	■			■	■		
Translational Initiation	M2	↑								■	■	■	■	■	■																									■	■		

c) ER stress and unfolded protein response

GO-TERM	MΦ Subset	Response (↑↓)	ACADVL	AIFM1	ATP2A2	ATP6V0	BCAP31	DERL1	DNAJC3	HM13	PDIA3	SEC61B	SSR1	TBL2	TMEM33	TPP1	UGGT
Cellular Response To Topologically Incorrect Protein	M1	↑	■				■	■	■				■	■			■
Cellular Response To Topologically Incorrect Protein	M2	↓							■				■	■		■	
Cellular Response To Unfolded Protein	M1	↑	■				■	■	■				■	■	■		■
Cellular Response To Unfolded Protein	M2	↓							■				■	■		■	
Endoplasmic Reticulum Unfolded Protein Response	M1	↑	■				■	■	■				■	■	■		■
Endoplasmic Reticulum Unfolded Protein Response	M2	↓							■				■	■			
Ire1-Mediated Unfolded Protein Response	M1	↑	■				■		■				■		■		
Ire1-Mediated Unfolded Protein Response	M2	↓							■				■				
Response To Endoplasmic Reticulum Stress	M1	↑	■	■	■	■	■	■	■	■			■	■	■	■	■
Response To Endoplasmic Reticulum Stress	M2	↓					■	■	■				■	■	■	■	
Response To Unfolded Protein	M1	↑	■				■	■	■				■	■	■		■
Response To Topologically Incorrect Protein	M1	↑	■				■	■	■				■	■	■		■

d) immune responses to stimulus

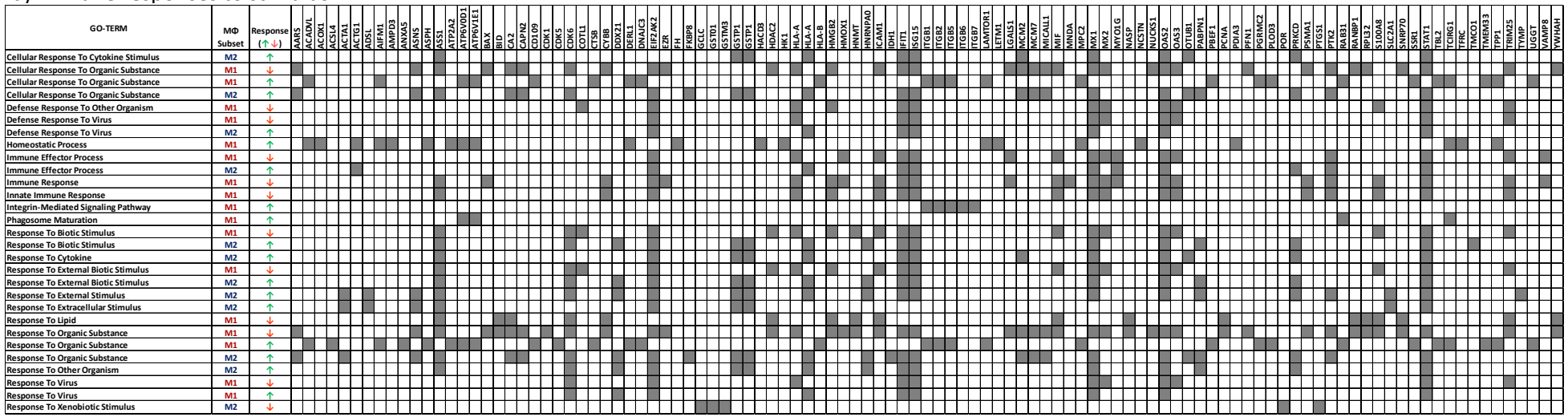

e) type-I interferon associated

GO-TERM	MΦ Subset	Response (↑↓)	HLA-A	HLA-A	IFIT1	ISG15	MX1	MX2	OAS2	OAS3	STAT1
Cellular Response To Type I Interferon	M1	↓		■	■	■	■				■
Cellular Response To Type I Interferon	M2	↑	■		■	■	■		■		■
Response To Type I Interferon	M1	↓		■	■	■	■	■	■	■	■
Response To Type I Interferon	M2	↑	■		■	■	■		■	■	■
Type I Interferon Signaling Pathway	M1	↓		■	■	■	■	■	■	■	■
Type I Interferon Signaling Pathway	M2	↑	■		■	■	■		■	■	■

f) viral/microbial interaction with host

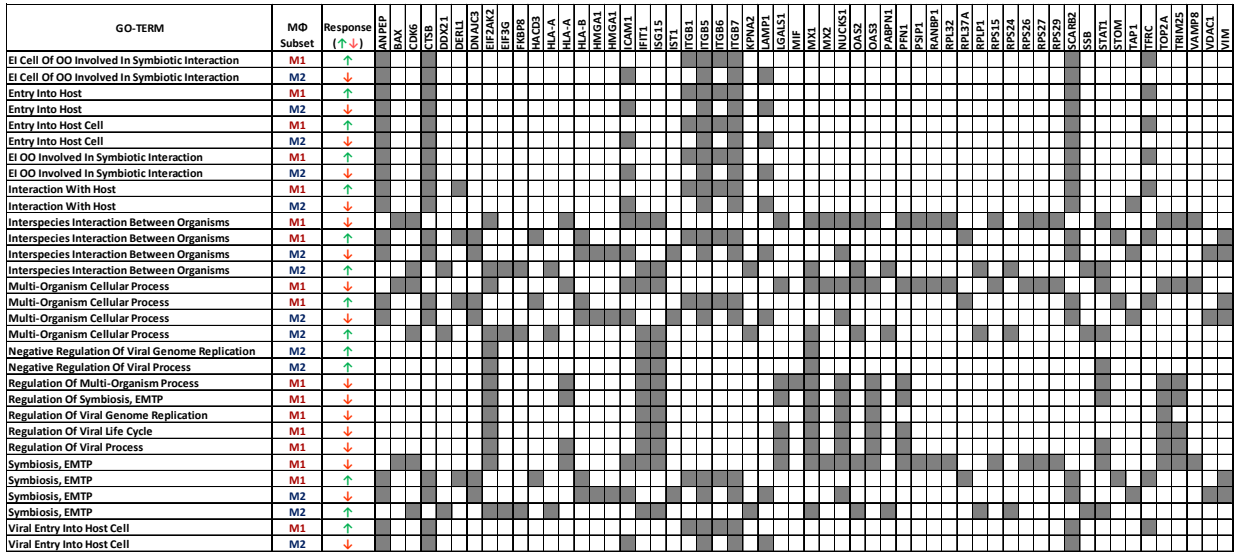

Abbreviations;

EI: Entry into
OO: Other organism
EMTP: Encompassing mutualism through parasitism

Figure PS1.8. GO-Terms grouped by functional association for BIOLOGICAL PROCESS in M1 and M2 MΦs following stimulation. GO-terms were grouped by similarity of function or association to an overall function and plotted to demonstrate individual protein responses in M1 and M2 MΦs stimulated with PG. Terms identified in figure PS1.4 a & b were grouped and incorporated into a matrices; a) antigen processing and presentation, b) epigenetic modification, transcription and translation, c) ER stress and unfolded protein response, d) immune responses to stimulus, e) type-I interferon associated and f) viral/microbial interaction with host. Go-Terms are listed indicating both the subset (**M1** and **M2**) and the direction of response, increase (↑) or decrease (↓) from which the term arose.

a) Adhesion

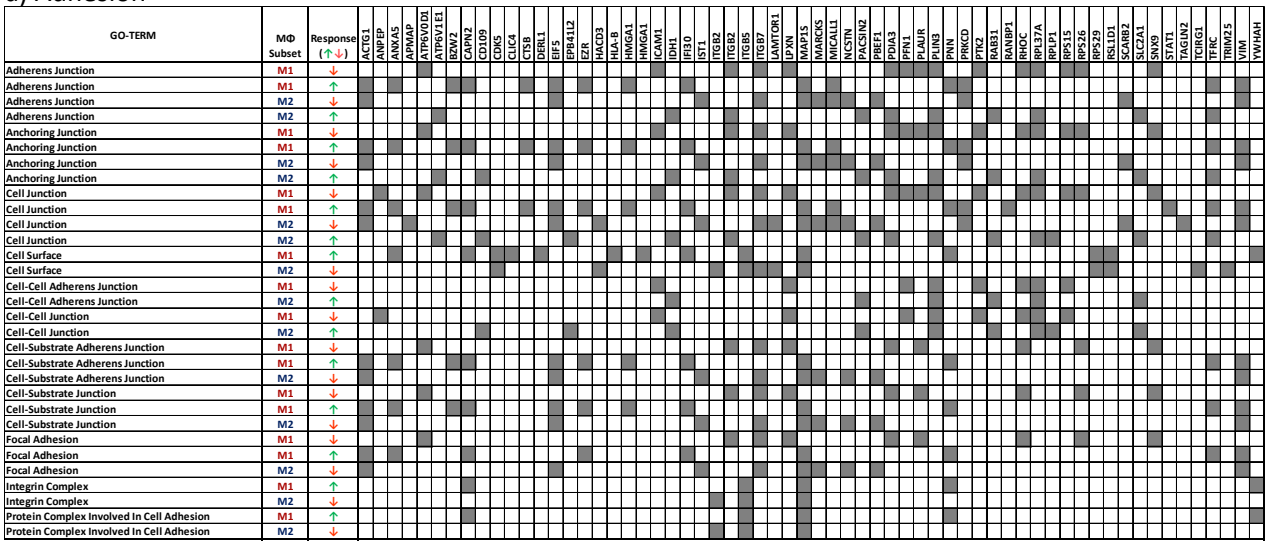
GO-TERM
MΦ Subset
Response (↑↓)
ACTG1
ANPEP
ANXA5
APMAP
ATP6V0D1
ATP6V1E1
BZW2
CAPN2
CD109
CDK5
CLIC4
CTSB
DERL1
EIF5
EPB41L2
EZR
HACD3
HLA-B
HMGA1
HMGA1
ICAM1
IDH1
IFI30
IST1
ITGB2
ITGB2
ITGB5
ITGB7
LAMTOR1
LPXN
MAP1S
MARCKS
MICALL1
NCSTN
PACSIN2
PBEF1
PDIA3
PFN1
PLAUR
PLIN3
PNN
PRKCD
PTK2
RAB31
RANBP1
RHOC
RPL37A
RPLP1
RPS15
RPS26
RPS29
RSL1D1
SCARB2
SLC2A1
SNX9
STAT1
TAGLN2
TCIRG1
TFRC
TRIM25
VIM
YWHAH
Adherens Junction
M1
Adherens Junction
M1
Adherens Junction
M2
Adherens Junction
M2
Anchoring Junction
M1
Anchoring Junction
M1
Anchoring Junction
M2
Anchoring Junction
M2
Cell Junction
M1
Cell Junction
M1
Cell Junction
M2
Cell Junction
M2
Cell Surface
M1
Cell Surface
M2
Cell-Cell Adherens Junction
M1
Cell-Cell Adherens Junction
M2
Cell-Cell Junction
M1
Cell-Cell Junction
M2
Cell-Substrate Adherens Junction
M1
Cell-Substrate Adherens Junction
M1
Cell-Substrate Adherens Junction
M2
Cell-Substrate Junction
M1
Cell-Substrate Junction
M1
Cell-Substrate Junction
M2
Focal Adhesion
M1
Focal Adhesion
M1
Focal Adhesion
M2
Integrin Complex
M1
Integrin Complex
M2
Protein Complex Involved In Cell Adhesion
M1
Protein Complex Involved In Cell Adhesion
M2

b *i*) cellular bodies

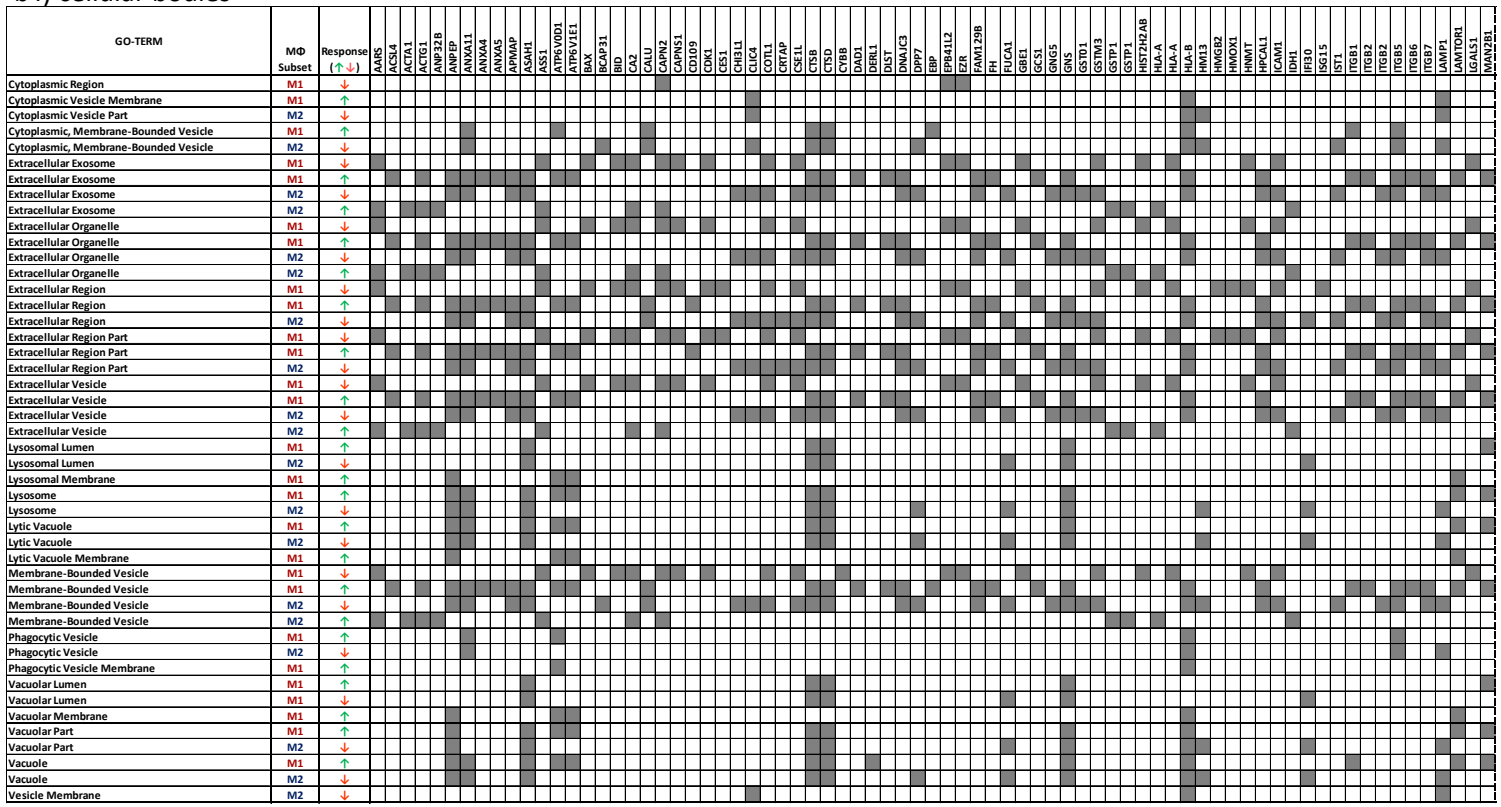

b *ii*) cellular bodies cont'

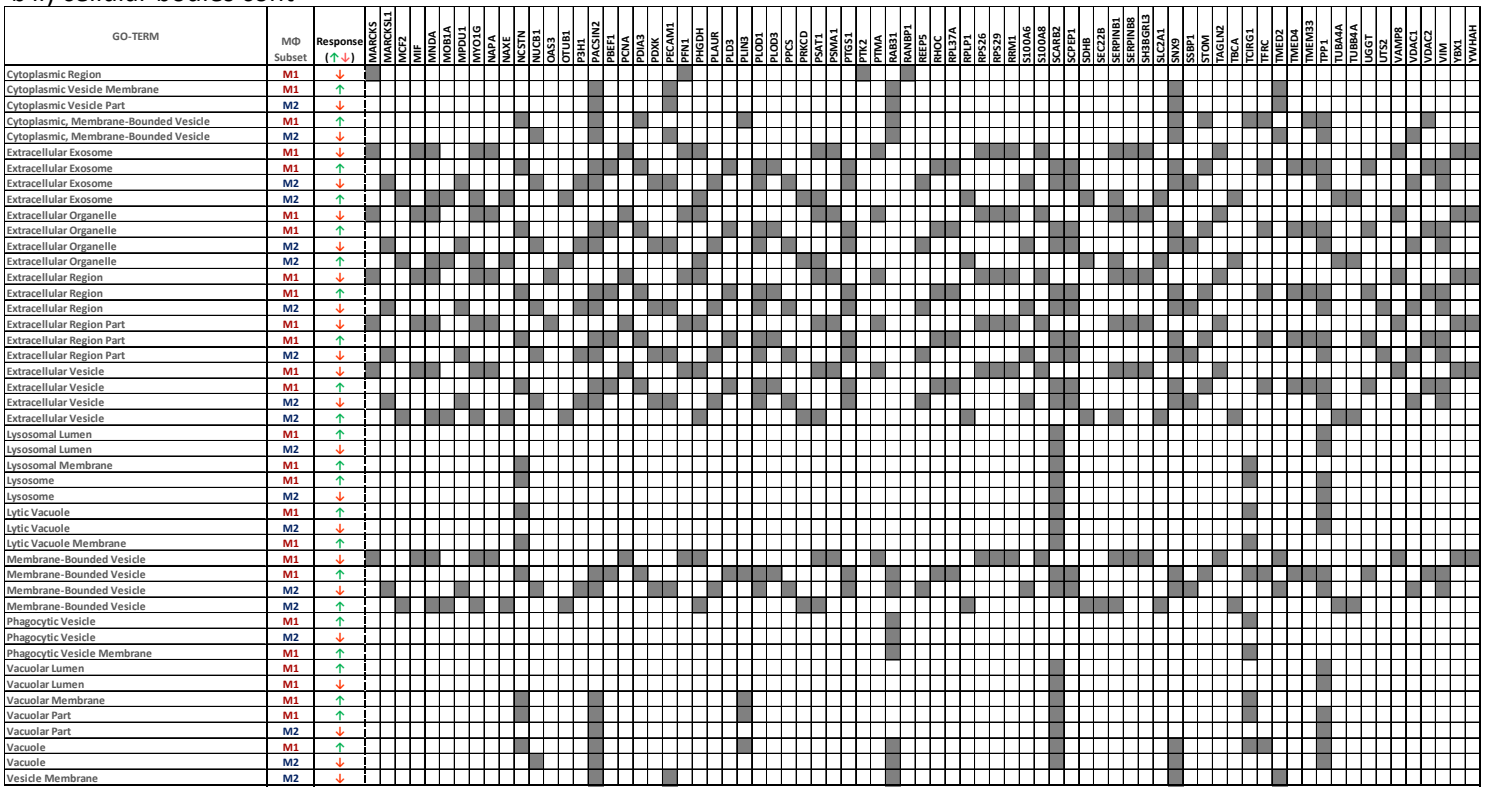

c) DNA, epigenetics and translation

GO-TERM	MΦ Subset	Response (↑↓)	CAPN2	CAPRIN1	CDK1	CPSF6	EIF2AK2	EIF3G	EIF3M	ELAVL1	FEN1	HCC5	HDAC2	HIST2H2AB	HMGB2	HNRNPA0	HNRNPAB	HNRPR	LSM4	MCM2	MCM4	MCM5	MCM6	MCM7	NASP	NSUN2	NUCKS1	PABPN1	PCNA	PNN	PSIP1	PSMA1	RBM3	RCC2	RPL32	RPLP1	RPS15	RPS24	RPS26	RPS27	RPS29	RSL1D1	SNRP70	SSB	STAT1	TOP2A	YBX1
Chromatin	M1	↓	■										■	■	■					■				■	■		■				■														■		
Chromosomal Part	M1	↓	■		■						■	■	■	■	■					■	■	■	■	■	■		■		■		■			■											■		
Chromosomal Region	M1	↓			■						■	■								■	■	■	■	■					■					■													
Chromosomal Region	M2	↑										■								■	■	■	■	■																				■			
Chromosome	M1	↓	■		■						■	■	■	■	■					■	■	■	■	■	■		■		■		■			■											■	■	
Chromosome, Telomeric Region	M1	↓			■						■	■								■	■	■	■	■					■																		
Chromosome, Telomeric Region	M2	↑										■								■	■	■	■	■																				■			
Mcm Complex	M1	↓										■								■	■	■	■	■																							
Mcm Complex	M2	↑										■								■	■	■	■	■																							
Nuclear Chromatin	M1	↓											■	■	■										■		■				■														■		
Nuclear Chromosome	M1	↓			■						■	■	■	■	■					■	■	■	■	■	■		■		■		■														■	■	
Nuclear Chromosome	M2	↑										■								■	■	■	■	■																				■	■		
Nuclear Chromosome Part	M1	↓			■						■	■	■	■	■					■	■	■	■	■	■		■		■		■														■		
Nuclear Chromosome Part	M2	↑										■								■	■	■	■	■																				■	■		
Nuclear Chromosome, Telomeric Region	M1	↓			■						■	■								■	■	■	■	■					■																		
Nuclear Chromosome, Telomeric Region	M2	↑										■								■	■	■	■	■																				■			
Intracellular Ribonucleoprotein Complex	M1	↓					■																			■						■	■		■		■		■	■	■		■				■
Intracellular Ribonucleoprotein Complex	M2	↑		■		■	■	■	■							■	■	■	■									■		■			■			■		■				■		■			
Ribonucleoprotein Complex	M1	↓					■			■																■						■	■		■		■		■	■	■		■				■
Ribonucleoprotein Complex	M2	↑		■		■	■	■	■							■	■	■	■									■		■			■			■		■				■		■			

d) endoplasmic reticulum

GO-TERM	MΦ Subset	Response (↑↓)	ACSL4	ALOX5AP	ANPEP	APMAP	ASPH	ATP2A2	BCAP31	CALU	CERS2	CHI3L1	CRTAP	DAD1	DERL1	DNAJC3	DPM1	EBP	EIF2AK2	ELOVL1	ELOVL5	ERMP1	GCS1	HACD3	HLA-B	HM13	IST1	LENG4	MPDU1	NCSTN	NUCB1	OSTC	P3H1	PDIA3	PLAUR	PLD3	PLOD1	PLOD3	POR	PTGS1	RBM3	RCN1	REEP5	RPL32	RPLP1	RPS15	RPS24	RPS26	RPS27	RPS29	RSL1D1	SEC61B	SSR1	STOM	TAP1	TAPBP	TBL2	TMED2	TMED4	TMEM33	UGGT	VKORC1
Cytosolic Ribosome	M1	↓																																									■		■		■	■	■												
Cytosolic Small Ribosomal Subunit	M1	↓																																											■		■	■	■												
Endoplasmic Reticulum	M1	↑	■			■	■	■		■	■			■	■	■	■	■			■		■	■	■			■		■		■		■		■	■	■		■		■											■	■			■		■	■	■	
Endoplasmic Reticulum	M2	↓		■		■	■		■	■		■	■			■				■		■			■	■			■		■		■		■		■		■	■		■	■										■	■		■	■	■	■				■
Endoplasmic Reticulum Lumen	M1	↑					■			■						■																		■								■																			■	
Endoplasmic Reticulum Lumen	M2	↓					■			■			■			■																	■		■							■																			
Endoplasmic Reticulum Membrane	M1	↑	■				■	■		■	■			■	■	■	■	■			■		■	■	■			■				■				■	■	■		■													■				■		■	■		
Endoplasmic Reticulum Membrane	M2	↓		■			■		■	■						■				■		■			■	■			■						■		■		■	■												■	■		■	■	■	■				■
Endoplasmic Reticulum Part	M1	↑	■				■	■		■	■			■	■	■	■	■			■		■	■	■			■				■		■		■	■	■		■		■											■				■		■	■	■	
Endoplasmic Reticulum Part	M2	↓		■			■		■	■			■			■				■		■			■	■			■				■		■		■		■	■		■	■										■	■		■	■	■	■				■
Endoplasmic Reticulum Sec Complex	M2	↓														■																																			■										
ER-Golgi Intermediate Compartment	M2	↓			■				■																		■				■																											■				
Integral Component Of ER Membrane	M1	↑					■								■						■			■	■																																■			■		
Integral Component Of ER Membrane	M2	↓					■		■											■					■	■																													■	■	■					
Integral Component Of Lumenal Side Of ER Membrane	M2	↓							■																■	■																														■						
Intrinsic Component Of ER Membrane	M1	↑					■								■						■			■	■																																■			■		
Intrinsic Component Of ER Membrane	M2	↓					■		■											■					■	■																													■	■	■					
Lumenal Side Of ER Membrane	M2	↓							■																■	■																														■						
Nuclear Outer Membrane-ER Membrane Network	M1	↑	■				■	■		■	■			■	■	■	■	■			■		■	■	■			■				■				■	■	■		■													■				■		■	■		
Nuclear Outer Membrane-ER Membrane Network	M2	↓		■			■		■	■						■				■		■			■	■			■						■		■		■	■												■	■		■	■	■	■				■
Ribosomal Subunit	M1	↓																																						■			■		■		■	■	■												
Ribosome	M1	↓																	■																						■			■		■		■	■	■												
Ribosome	M2	↑																	■																						■				■		■				■											
Rough Endoplasmic Reticulum	M2	↓							■							■										■					■						■															■										
Rough Endoplasmic Reticulum Membrane	M1	↑														■																					■	■																								
Rough Endoplasmic Reticulum Membrane	M2	↓							■							■																					■															■										
Sec61 Translocon Complex	M2	↓							■																																										■										
Small Ribosomal Subunit	M1	↓																																											■		■	■	■												

e) mitochondria.

GO-TERM	MΦ Subset	Response (↑↓)	ACADVL	ACOT9	ACOX1	ACSL4	AIFM1	ATP6V1E1	BCAP31	CLIC4	CPT2	CYB	DKFZp586K0821	DLST	FH	GLS	GNG5	HACD3	HK1	KYNU	LACTB	LETM1	MPC2	MPDU1	MSTO65	NDUFA9	POR	PPIF	SDHB	SLC25A24	SQRDL	SSBP1	STOM	TAP1	TCIRG1	TPP1	UQCRFS1	UQCRH	VDAC1	VDAC2
Inner Mitochondrial Membrane Protein Complex	M2	↑											■													■			■											
Mitochondrial Envelope	M1	↑	■			■	■				■							■				■	■				■			■	■							■		■
Mitochondrial Inner Membrane	M1	↑	■			■	■				■							■				■	■				■			■	■							■		■
Mitochondrial Membrane	M1	↑	■			■	■				■							■				■	■				■			■	■							■		■
Mitochondrial Membrane Part	M2	↑											■												■	■			■											
Mitochondrial Part	M1	↑	■	■		■	■				■			■	■	■			■			■	■				■			■	■							■		■
Mitochondrial Protein Complex	M2	↑											■												■	■			■											
Mitochondrial Respiratory Chain	M2	↑											■												■	■			■											
Mitochondrion	M1	↑	■	■	■	■	■	■		■	■	■		■	■	■		■	■		■	■	■				■	■		■	■		■		■	■			■
Mitochondrion	M2	↓			■				■	■		■				■	■			■				■			■	■		■	■	■		■		■	■		■	
Respiratory Chain	M2	↑											■													■			■								■			
Respiratory Chain Complex	M2	↑											■													■			■								■			

Figure PS1.9. GO-Terms grouped by functional association for CELLULAR COMPONENT in M1 and M2 MΦs following stimulation. GO-terms were grouped by similarity of function or association to an overall function and plotted to demonstrate individual protein responses in M1 and M2 MΦs stimulated with PG LPS. Terms identified in figure PS1.5a & b were grouped and incorporated into a matrices; a) Adhesion, b) cellular bodies c) DNA, epigenetics and translation, d) endoplasmic reticulum e) mitochondria. Go-Terms are listed indicating both the subset (**M1** and **M2**) and the direction of response, increase (↑) or decrease (↓) from which the term arose.

a) Adhesion

GO-TERM	MΦ Subset	Response (↑↓)	ACTA1	ACTG1	BZW2	EIF3M	EIF5	EZR	FAM129B	ICAM1	IDH1	IST1	ITGB1	ITGB2	ITGB2	ITGB6	ITGB7	MCM4	MCM6	MCM7	MICALL1	PACSIN2	PFN1	PLIN3	RANBP1	RPS24	RPS26	RSL1D1	SNX9	STAT1	TAGLN2	TRIM25	TUBA4A	TUBB4A
Cadherin Binding	M1	↓						■													■		■		■		■			■	■	■		
Cadherin Binding	M1	↑			■		■				■										■							■		■				
Cadherin Binding Involved In Cell-Cell Adhesion	M1	↓						■													■		■		■		■			■	■	■		
Cadherin Binding Involved In Cell-Cell Adhesion	M2	↑				■	■																			■								
Cell Adhesion Molecule Binding	M1	↓						■		■											■		■		■		■			■	■	■		
Cell Adhesion Molecule Binding	M1	↑							■				■	■		■	■					■		■					■					
Cell Adhesion Molecule Binding	M2	↓							■	■		■			■		■					■							■					
Protein Binding Involved In Cell Adhesion	M1	↓						■													■		■		■		■			■	■	■		
Protein Binding Involved In Cell Adhesion	M2	↑	■	■																													■	■
Protein Binding Involved In Cell-Cell Adhesion	M1	↓						■													■		■		■		■			■	■	■		
Protein Binding Involved In Cell-Cell Adhesion	M2	↑																■	■	■														

b) Antioxidants

GO-TERM	MΦ Subset	Response (↑↓)	ALOX5AP	ASPH	CLIC4	GSTO1	GSTM3	IFI30	P3H1	PLOD1	PLOD3	POR	PTGS1	SQRDL
Dioxygenase Activity	M1	↑		■						■	■		■	
Dioxygenase Activity	M2	↓	■	■					■	■		■	■	
Glutathione Transferase Activity	M2	↓	■		■	■	■							
Oxidoreductase Activity (ORA), Acting On A SGOD	M2	↓				■		■						■
ORA, Acting On A SGOD, Quinone Or SCAA	M2	↓				■								■
ORA, AOPD, WIoROMO	M2	↓		■					■	■		■	■	
ORA, AOPD, WIoROMO, 2-OG As 1 Donor, And I Of 1 AE Of O IBD	M1	↑		■						■	■			
ORA, AOPD, WIoROMO, 2-OG As 1 Donor, And I Of 1 AE Of O IBD	M2	↓		■					■	■				

c) antigen processing and presentation

GO-TERM	MΦ Subset	Response (↑↓)	ANPEP	ANXA11	BCAP31	CRTAP	CTSB	GSTM3	HLA-B	HMGN1	HMGN2	ICAM1	IST1	ITGB2	MAP1S	P3H1	PPIF	SNX9	TAP1	TAPBP	TPP1	UQCRFS1	VDAC1	VIM
Antigen Binding	M2	↓		■					■										■	■				
Mhc Class I Protein Binding	M2	↓			■														■	■				
Mhc Protein Binding	M2	↓			■														■	■				
Peptide Antigen Binding	M2	↓							■										■	■				
Peptide Antigen-Transporting Atpase Activity	M2	↓																	■	■				
Peptide Binding	M2	↓	■					■	■								■		■	■	■			
Peptide-Transporting Atpase Activity	M2	↓																	■	■				
Protein Complex Binding	M2	↓		■	■	■	■			■	■	■	■	■	■	■		■				■	■	■
Tap Binding	M2	↓							■										■	■				
Tap1 Binding	M2	↓																	■	■				
Tap2 Binding	M2	↓																	■	■				

d) DNA translation and transcription

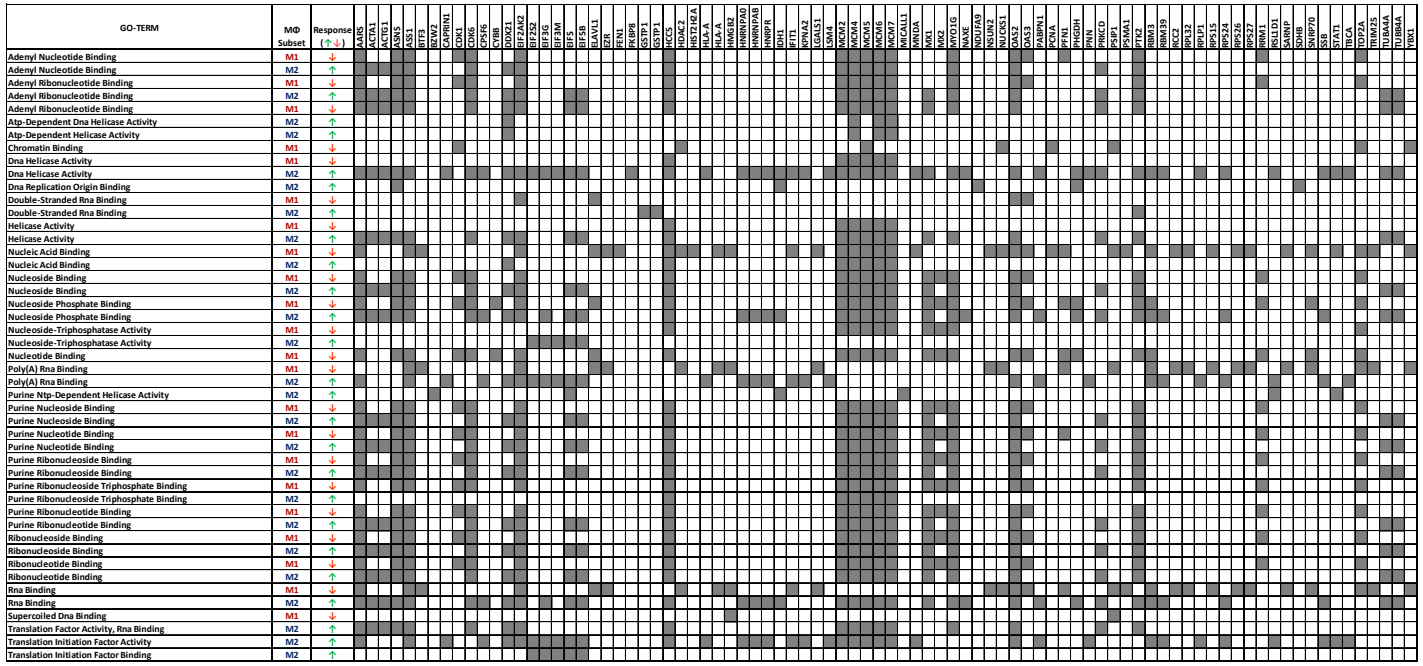

e) Transport and transferases

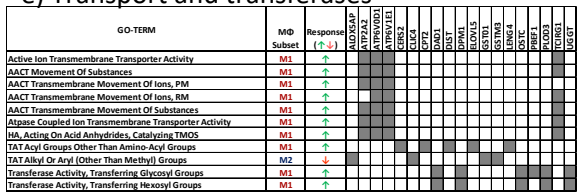

Abbreviations;

AACT: Atpase Activity, Coupled To
PM: Phosphorylative Mechanism
RM: Rotational Mechanism
HA: Hydrolase Activity
TMOS: Transmembrane Movement of Substances
TAT: Transferase Activity, Transferring
SGOD: Sulphur Group of Donors
SCAA: Similar Compound as Receptor
AOPD: Acting on Paired Donors
WIoROMO: With Incorporation or Reduction of Molecular Oxygen
2-OG: 2-Oxyglutarate
I of 1 AE: Incorporation of One Atom Each
O IBD: Oxygen in Both Donors

Figure PS1.10. GO-Terms grouped by functional association for MOLECULAR FUNCTION in M1 and M2 MΦs following stimulation. GO-terms were grouped by similarity of function or association to an overall function and plotted to demonstrate individual protein responses in M1 and M2 MΦs stimulated with PG LPS. Terms identified in figure PS1.6a & b were grouped and incorporated into matrices; a) Adhesion, b) Antioxidants c) antigen processing and presentation, d) DNA translation and transcription e) Transport and transferases. Go-Terms are listed indicating both the subset (**M1** and **M2**) and the direction of response, increase (↑) or decrease (↓) from which the term arose.

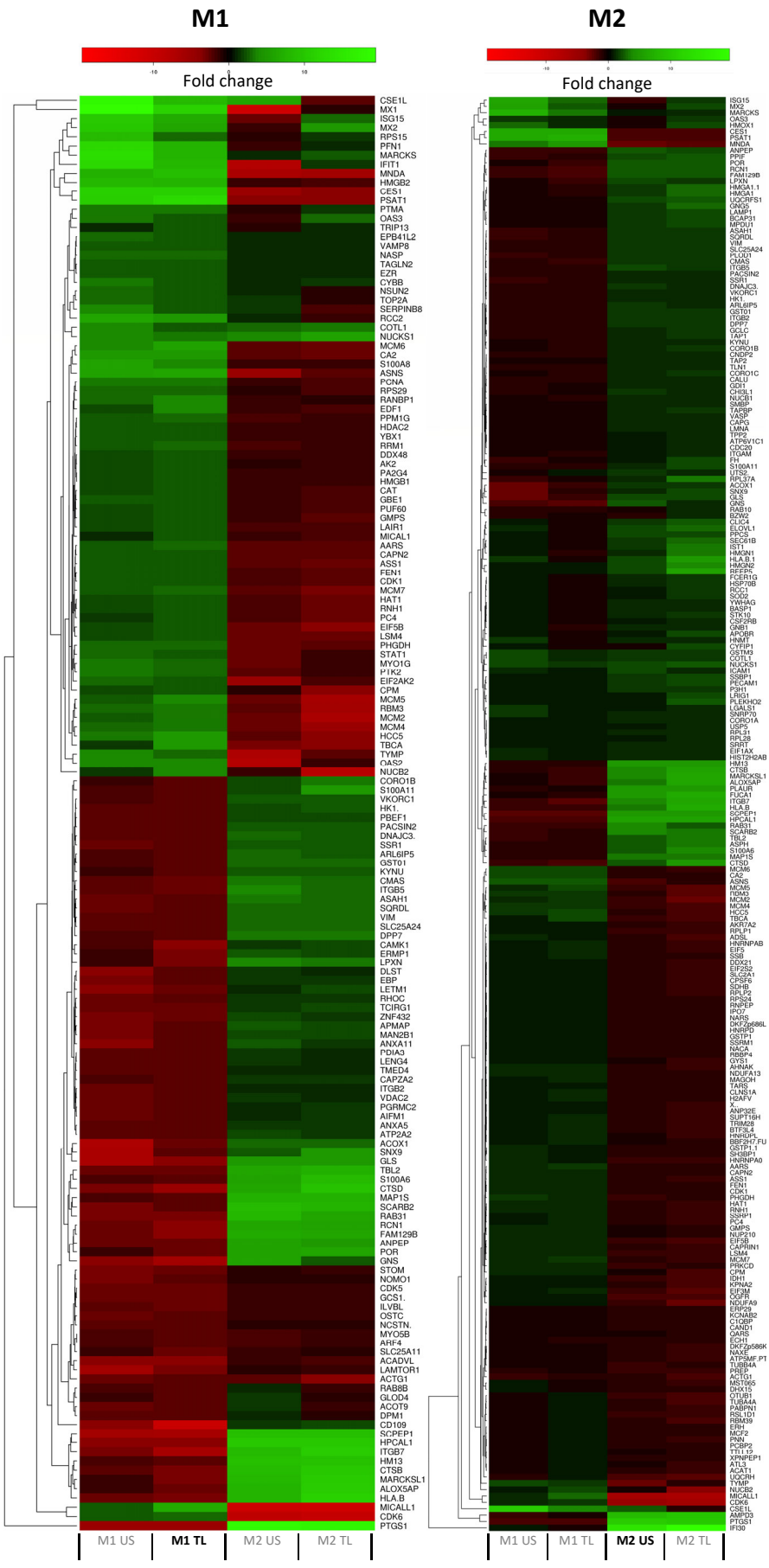

Figure PS1.11 Heatmap indicating proteins which demonstrated a 2-fold change in expression when tolerised (TL) compared to the stimulated (ST) level. Protein profiles for each subset are mapped to include all proteins, within that subset, which demonstrated a 2-fold change compared to stimulated levels of expression. The opposing subset and unstimulated level are included for comparison. The clustering method used was average linkage and applied to rows, the distance measurement method used was Euclidean.

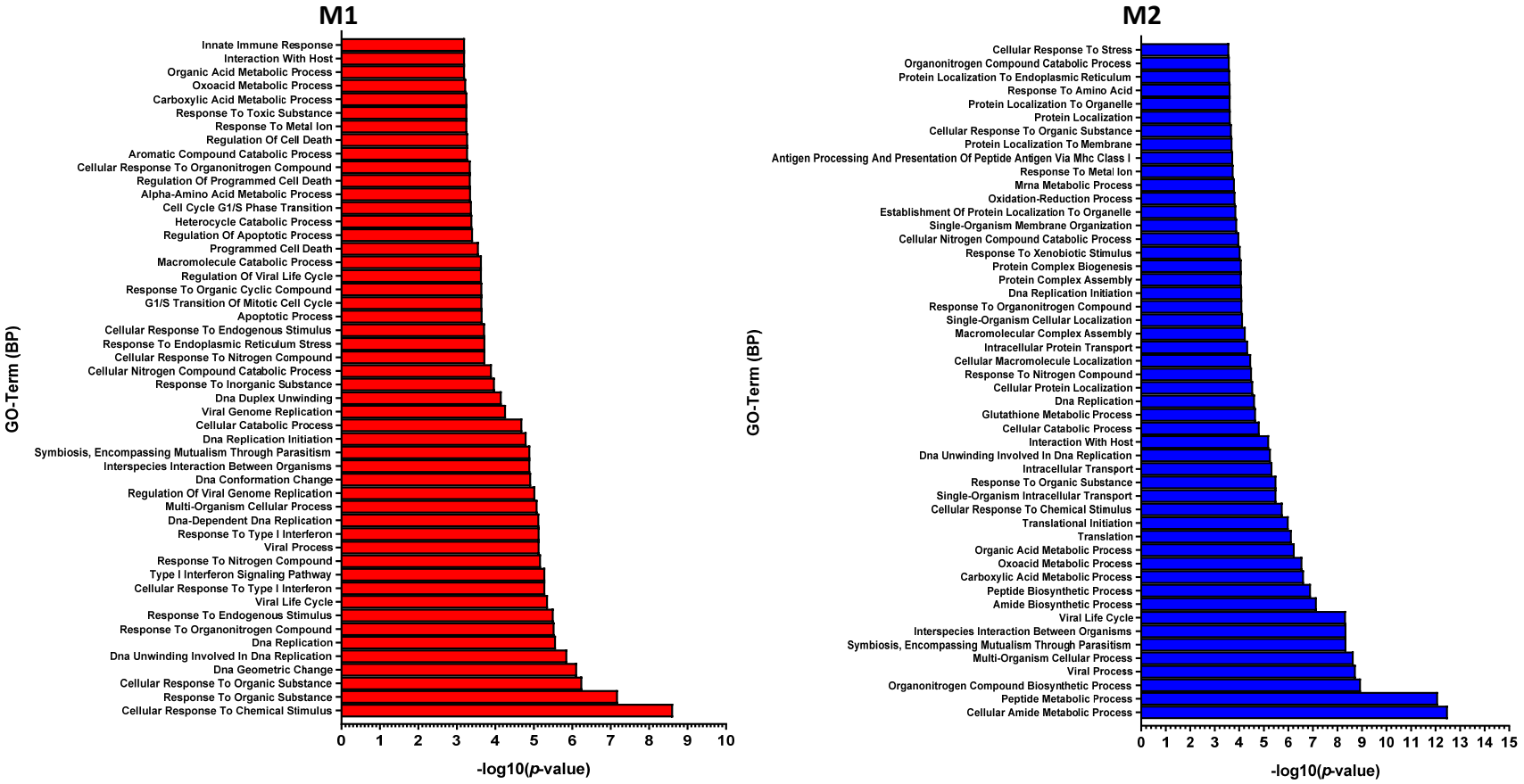

Figure 1.12a Comparison gene ontology term annotation for BIOLOGICAL PROCESS in the proteins responsive to secondary stimulation in M1 and M2 MΦs. GO analysis was performed using the David database (GOTERM_BP_FAT) by analysing all proteins in either M1 (red) or M2 (blue) MΦs which demonstrated a minimum 2-fold change in expression compared to either stimulated or unstimulated levels. Data is shown as a –log10 of the *p-value*. GO terms are given to a maximum of 50 ranked by *p-value* and/or to the minimum *p-value* equivalent to 0.05.

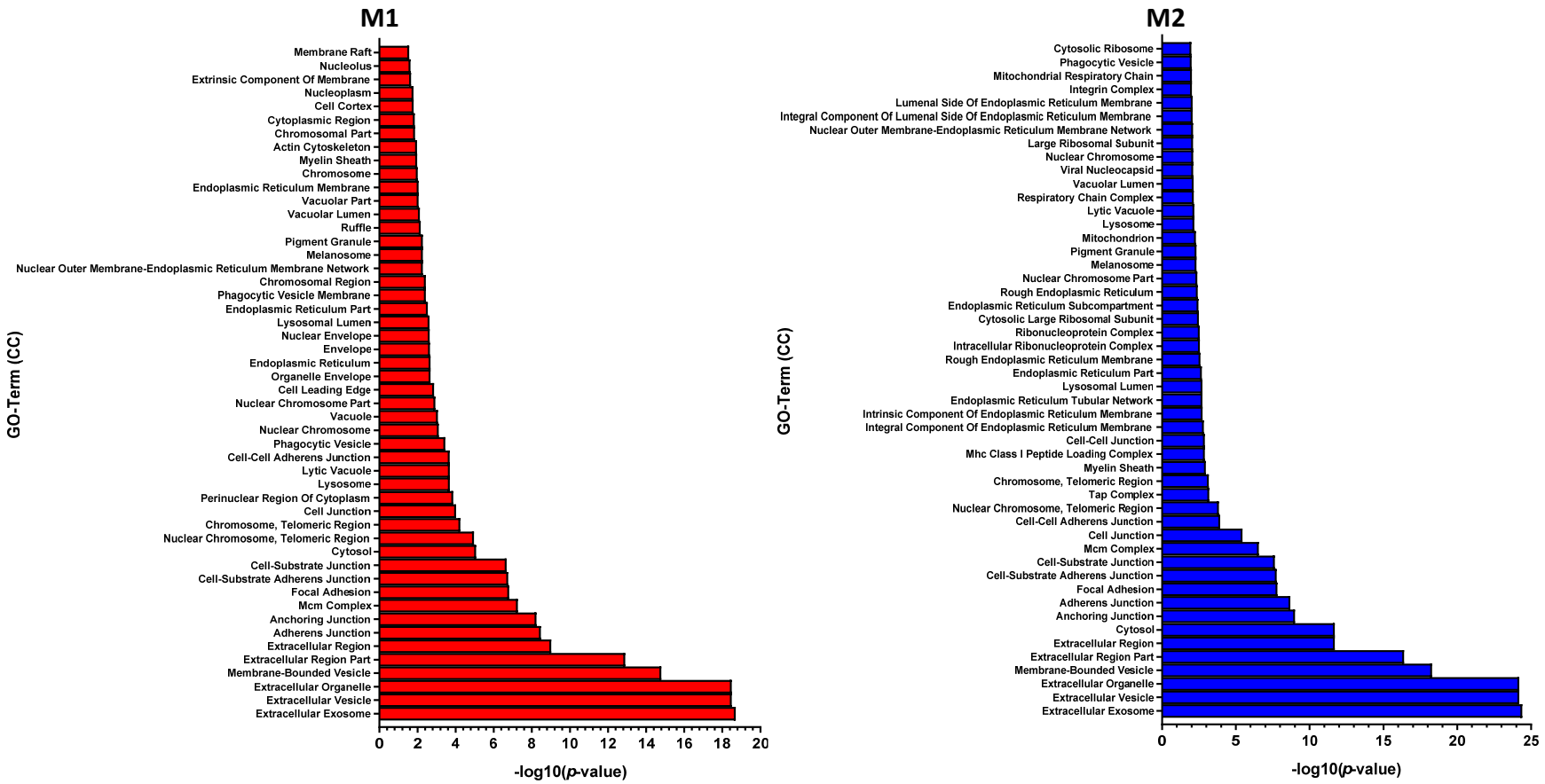

Figure 1.12b Comparison gene ontology term annotation for CELLULAR COMPONENT in the proteins responsive to secondary stimulation in M1 and M2 MΦs. GO analysis was performed using the David database (GOTERM_CC_FAT) by analysing all proteins in either M1 (red) or M2 (blue) MΦs which demonstrated a minimum 2-fold change in expression compared to either stimulated or unstimulated levels. Data is shown as a –log10 of the *p-value*. GO terms are given to a maximum of 50 ranked by *p-value* and/or to the minimum *p-value* equivalent to 0.05.

Figure 1.12c Comparison gene ontology term annotation for MOLECULAR FUNCTION in the proteins responsive to secondary stimulation in M1 and M2 MΦs. GO analysis was performed using the David database (GOTERM_MF_FAT) by analysing all proteins in either M1 (red) or M2 (blue) MΦs which demonstrated a minimum 2-fold change in expression compared to either stimulated or unstimulated levels. Data is shown as a –log10 of the *p-value*. GO terms are given to a maximum of 50 ranked by *p-value* and/or to the minimum *p-value* equivalent to 0.05.

Figure PS1.13a. Comparison gene ontology term annotation for BIOLOGICAL PROCESS in M1 and M2 MΦs, which demonstrated an increase following a secondary stimulation with PG LPS. GO analysis was performed using the David database (GOTERM_BP_FAT) by analysing proteins in either M1 (red) or M2 (blue) MΦs which responded to stimulation with PG LPS by instigating a minimum 2-fold **increase (green outline)** in expression compared to the stimulated level. Data is shown as a –log10 of the *p-value*. GO terms are given to a maximum of 50 ranked by *p-value* and/or to the minimum *p-value* equivalent to 0.05.

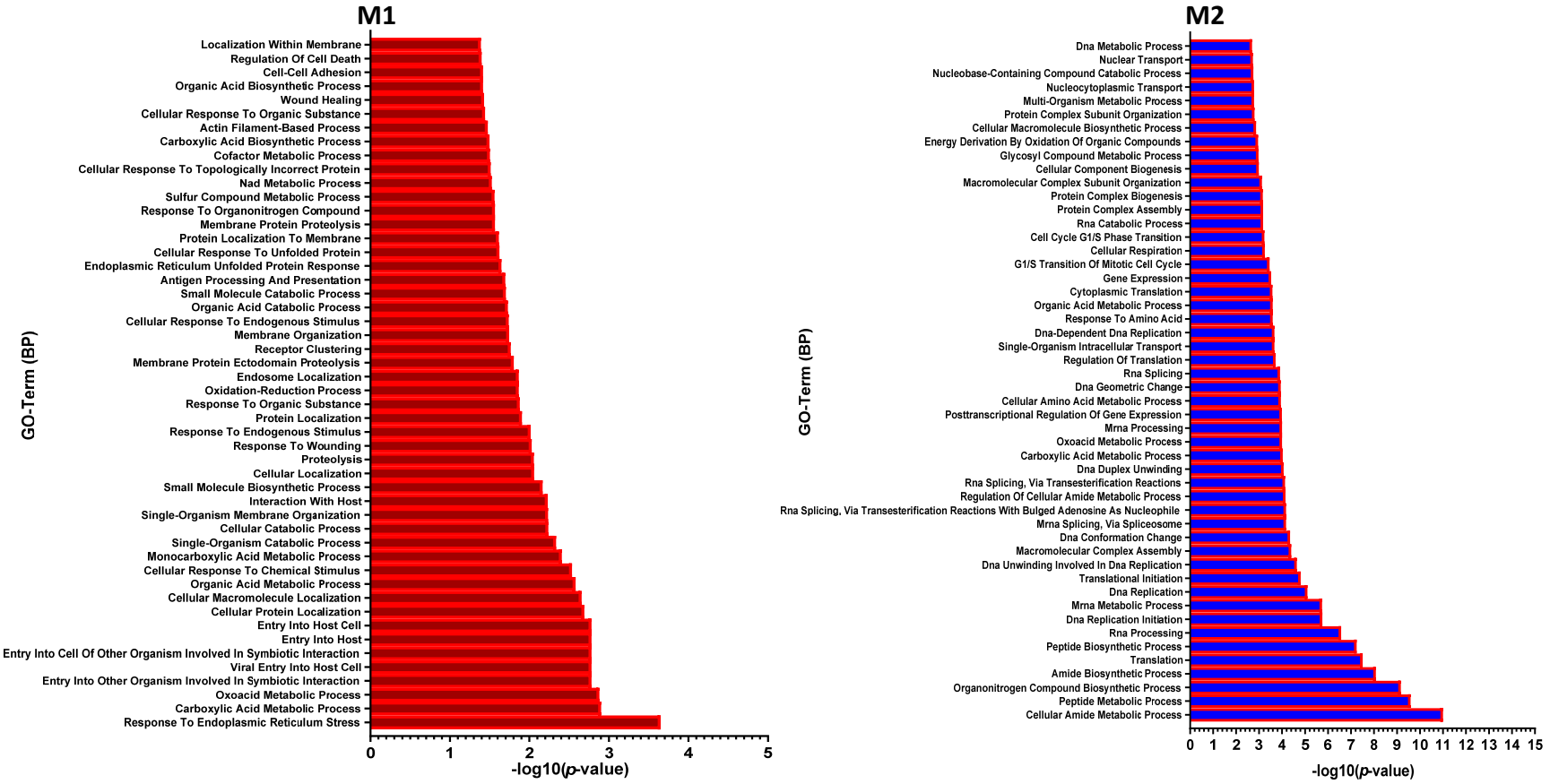

Figure PS1.13b. Comparison gene ontology term annotation for BIOLOGICAL PROCESS in M1 and M2 MΦs, which demonstrated a decrease following a secondary stimulation with PG LPS. GO analysis was performed using the David database (GOTERM_BP_FAT) by analysing proteins in either M1 (red) or M2 (blue) MΦs which responded to stimulation with PG LPS by instigating a minimum 2-fold **decrease (red outline)** in expression compared to the stimulated level. Data is shown as a –log10 of the *p-value*. GO terms are given to a maximum of 50 ranked by *p-value* and/or to the minimum *p-value* equivalent to 0.05.

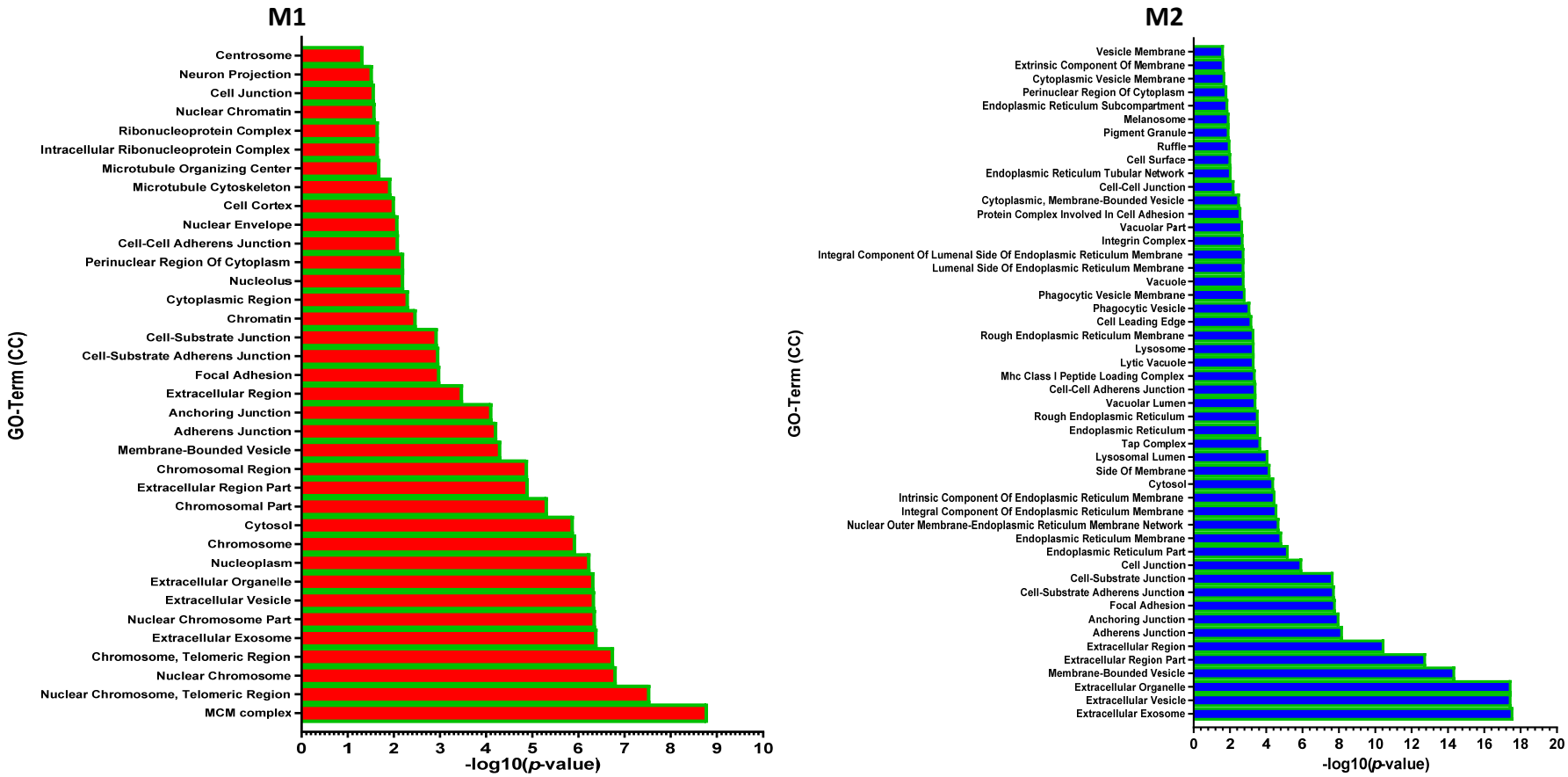

Figure PS1.14a. Comparison gene ontology term annotation for CELLULAR COMPONENT in M1 and M2 MΦs, which demonstrated an increase following a secondary stimulation with PG LPS. GO analysis was performed using the David database (GOTERM_CC_FAT) by analysing proteins in either M1 (red) or M2 (blue) MΦs which responded to stimulation with PG LPS by instigating a minimum 2-fold **increase (green outline)** in expression compared to the stimulated level. Data is shown as a –log10 of the *p-value*. GO terms are given to a maximum of 50 ranked by *p-value* and/or to the minimum *p-value* equivalent to 0.05.

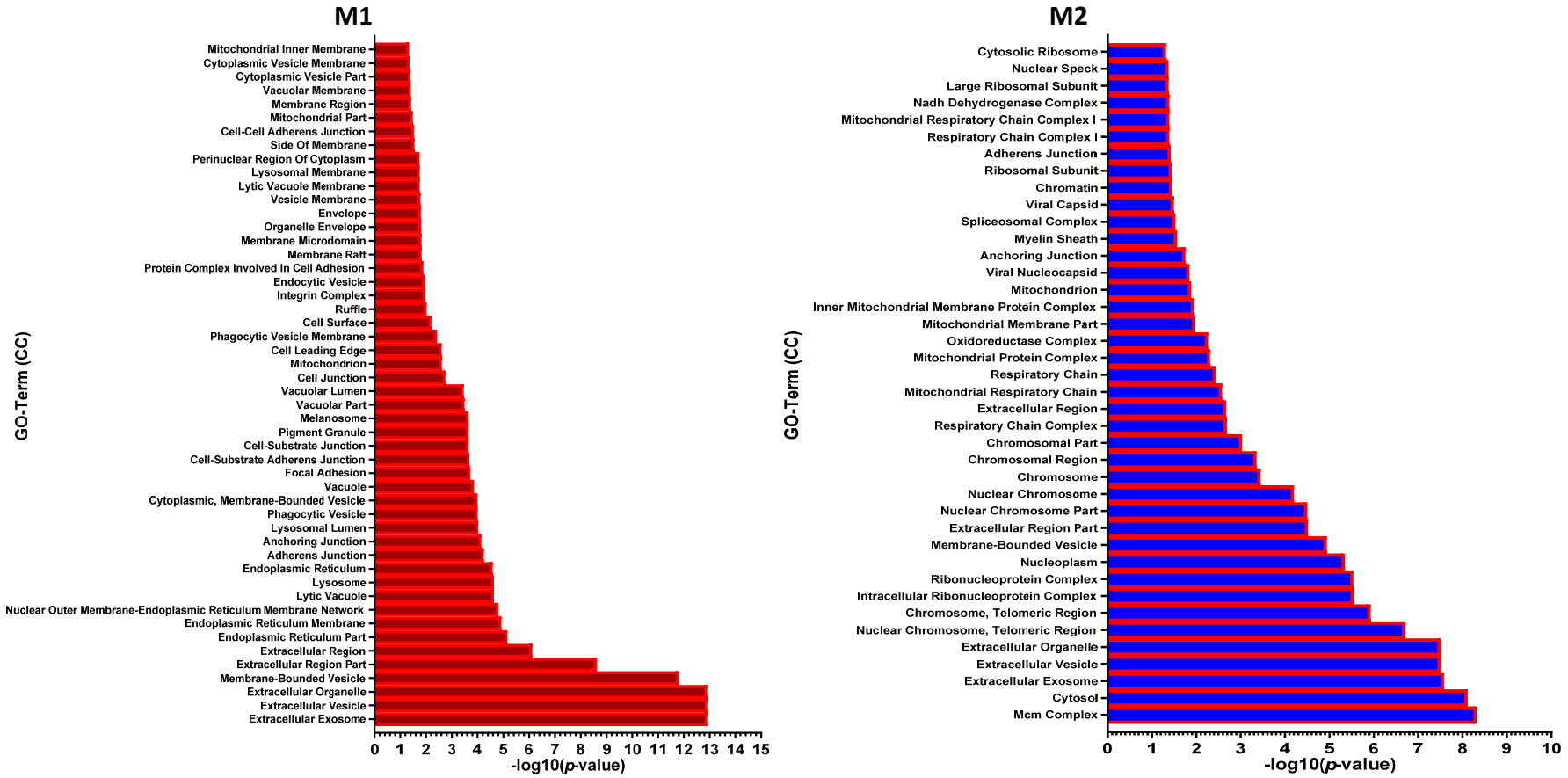

Figure PS1.14b. Comparison gene ontology term annotation for CELLULAR COMPONENT in M1 and M2 MΦs, which demonstrated a decrease following a secondary stimulation with PG LPS. GO analysis was performed using the David database (GOTERM_CC_FAT) by analysing proteins in either M1 (red) or M2 (blue) MΦs which responded to stimulation with PG LPS by instigating a minimum 2-fold **decrease (red outline)** in expression compared to the stimulated level. Data is shown as a –log10 of the *p-value*. GO terms are given to a maximum of 50 ranked by *p-value* and/or to the minimum *p-value* equivalent to 0.05.

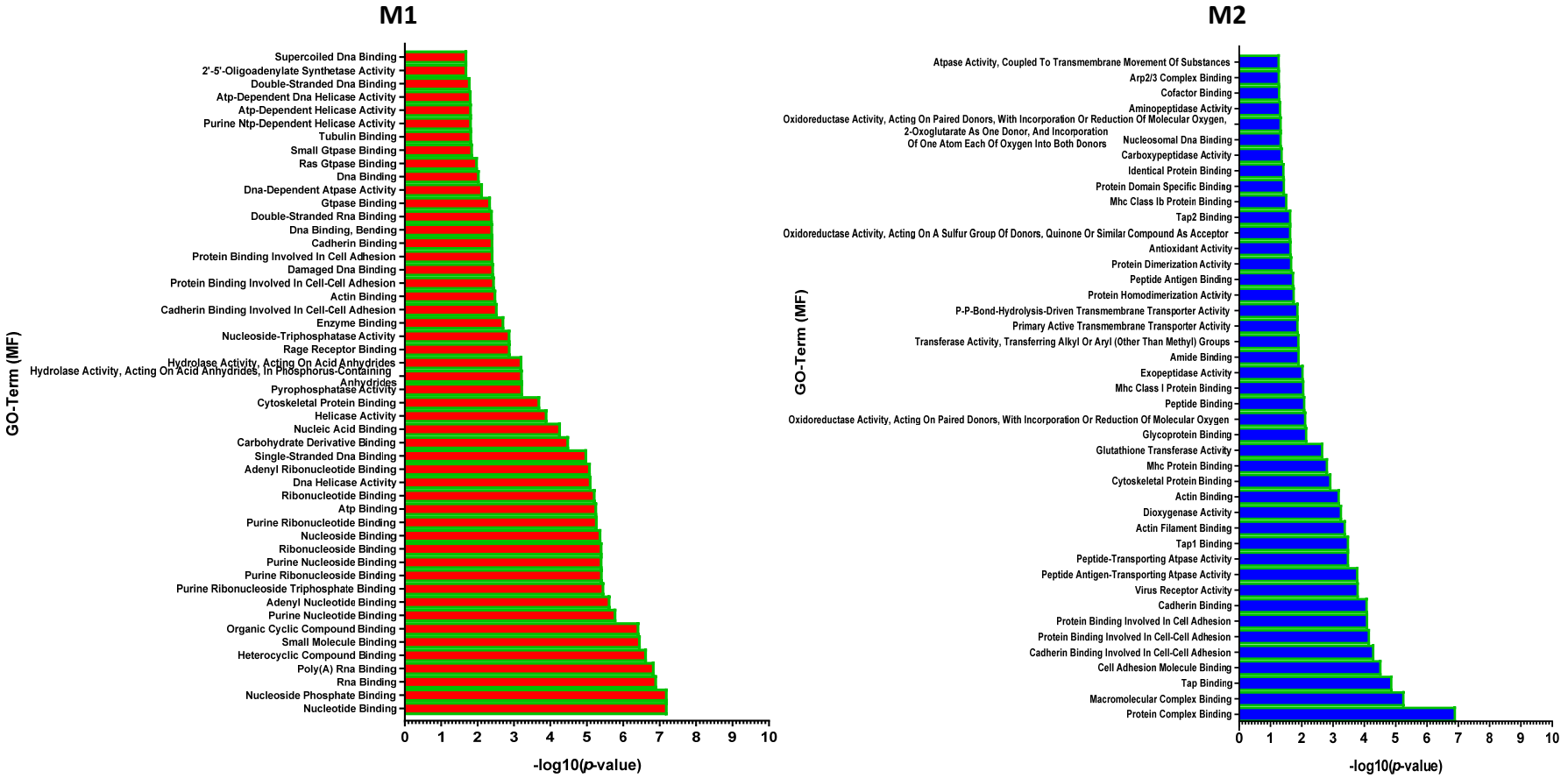

Figure PS1.15a. Comparison gene ontology term annotation for MOLECULAR FUNCTION in M1 and M2 MΦs, which demonstrated an increase following a secondary stimulation with PG LPS. GO analysis was performed using the David database (GOTERM_MF_FAT) by analysing proteins in either M1 (red) or M2 (blue) MΦs which responded to stimulation with PG LPS by instigating a minimum 2-fold **increase (green outline)** in expression compared to the stimulated level. Data is shown as a –log10 of the *p-value*. GO terms are given to a maximum of 50 ranked by *p-value* and/or to the minimum *p-value* equivalent to 0.05.

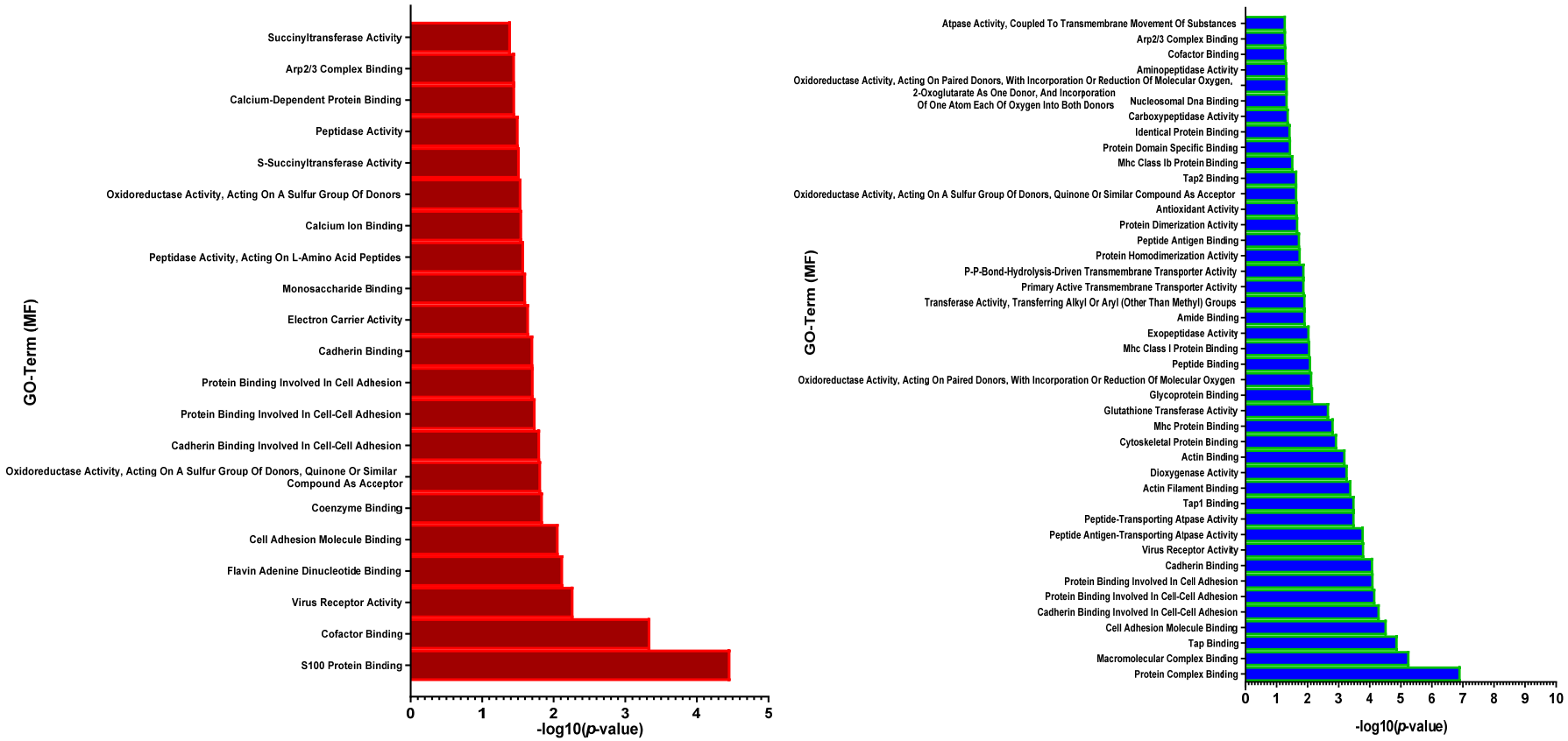

Figure PS1.15b. Comparison gene ontology term annotation for MOLECULAR FUNCTION in M1 and M2 MΦs, which demonstrated a decrease following a secondary stimulation with PG LPS. GO analysis was performed using the David database (GOTERM_MF_FAT) by analysing proteins in either M1 (red) or M2 (blue) MΦs which responded to stimulation with PG LPS by instigating a minimum 2-fold **decrease (red outline)** in expression compared to the stimulated level. Data is shown as a –log10 of the *p-value*. GO terms are given to a maximum of 50 ranked by *p-value* and/or to the minimum *p-value* equivalent to 0.05.

a) antigen processing and presentation

GO-TERM	MΦ Subset	Response (↑↓)	BCAP31	CTSD	FCER1G	HLA-B	ICAM1	IFI30	ITGB5	PDIA3	RAB10	RAB8B	TAP1	TAP2	TAPBP
Antigen Processing And Presentation (APP)	M1	↓		■		■			■	■		■			
Antigen Processing And Presentation	M2	↑	■	■	■	■	■	■	■		■		■	■	■
APP Of Endogenous Antigen	M2	↑				■							■	■	■
APP Of Endogenous Peptide Antigen	M2	↑				■							■	■	■
APP Of Endogenous Peptide Antigen Via Mhc Class I	M2	↑				■							■	■	■
APP Of Exogenous Antigen	M2	↑		■	■	■		■	■				■	■	
APP Of Exogenous Peptide Antigen	M2	↑		■	■	■		■	■				■	■	
APP Of Peptide Antigen	M2	↑	■	■	■	■		■	■				■	■	■
APP Of Peptide Antigen Via Mhc Class I	M2	↑	■		■	■		■	■				■	■	■

b) epigenetic modification, transcription and translation

GO-TERM	MΦ Subset	Response (↑↓)	AARS	AHNAK	ANP32E	C1QBP	CAND1	CAPN2	CAPRIN1	CDK1	CDK6	CLNS1A	CPM	CPSF6	CSE1L	DDX21	DHX15	EIF2S2	EIF3M	EIF5	EIF5B	ERP29	FEN1	H2AFV	HAT1	HCC5	HDAC2	HMGB1	HMGB2	HNRDPL	HNRNPA0	HNRNPAB	HNRPD	IPO7	ISG15	KPNA2	LSM4	MAGOH
Chromosome Organization	M1	↑								■													■		■	■	■	■	■									
Dna Conformation Change	M1	↑								■															■	■		■	■									
Dna Conformation Change	M2	↓			■					■															■	■												
Dna Duplex Unwinding	M1	↑																								■												
Dna Duplex Unwinding	M2	↓																								■												
Dna Geometric Change	M1	↑																								■		■	■									
Dna Geometric Change	M2	↓																								■												
Dna Metabolic Process	M1	↑								■													■			■		■	■						■			
Dna Metabolic Process	M2	↓								■													■			■										■		
Dna Replication	M1	↑								■													■			■												
Dna Replication	M2	↓								■													■			■												
Dna Replication Initiation	M1	↑																								■												
Dna Replication Initiation	M2	↓																								■												
Dna Unwinding Involved In Dna Replication	M1	↑																																				
Dna Unwinding Involved In Dna Replication	M2	↓																																				
Dna-Dependent Dna Replication	M1	↑																					■			■												
Dna-Dependent Dna Replication	M2	↓																					■			■												
Gene Expression	M2	↓	■	■		■	■	■	■	■	■	■	■	■		■	■	■	■	■	■	■		■	■					■	■	■	■				■	■
Mrna Processing	M2	↓				■						■		■			■														■		■				■	■
Nuclear Transport	M2	↓			■					■					■																			■		■		■
Posttranscriptional Regulation Of Gene Expression	M2	↓	■			■			■										■	■	■										■		■					■
Regulation Of Translation	M2	↓	■			■			■										■	■	■												■					■
Rna Processing	M2	↓	■			■						■		■		■	■													■	■		■				■	■
Translation	M2	↓	■			■			■									■	■	■	■												■					
Translational Initiation	M2	↓																■	■	■	■																	

GO-TERM	MΦ Subset	Response (↑↓)	MCM2	MCM4	MCM5	MCM6	MCM7	MNDA	NACA	NARS	NASP	NDUFA13	NUCKS1	NUP210	OTUB1	PABPN1	PC4	PCBP2	PCNA	PFN1	PNN	PRKCD	PTMA	QARS	RBBP4	RBM3	RBM39	RCC2	RPLP1	RPLP2	RPS24	RRM1	RSL1D1	SSB	SSRP1	SUPT16H	TARS	TOP2A	TRIM28	TRIP13
Chromosome Organization	M1	↑	■	■	■	■	■				■		■						■				■					■										■		■
Dna Conformation Change	M1	↑	■	■	■	■	■				■																											■		
Dna Conformation Change	M2	↓	■	■	■	■	■																		■															
Dna Duplex Unwinding	M1	↑	■	■	■	■	■																															■		
Dna Duplex Unwinding	M2	↓	■	■	■	■	■																																	
Dna Geometric Change	M1	↑	■	■	■	■	■																															■		
Dna Geometric Change	M2	↓	■	■	■	■	■																																	
Dna Metabolic Process	M1	↑	■	■	■	■	■				■		■						■	■												■						■		■
Dna Metabolic Process	M2	↓	■	■	■	■	■								■							■			■										■	■			■	
Dna Replication	M1	↑	■	■	■	■	■				■		■						■													■						■		
Dna Replication	M2	↓	■	■	■	■	■																		■										■	■				
Dna Replication Initiation	M1	↑	■	■	■	■	■																																	
Dna Replication Initiation	M2	↓	■	■	■	■	■																																	
Dna Unwinding Involved In Dna Replication	M1	↑	■	■		■	■																															■		
Dna Unwinding Involved In Dna Replication	M2	↓	■	■		■	■																																	
Dna-Dependent Dna Replication	M1	↑	■	■	■	■	■						■						■																			■		
Dna-Dependent Dna Replication	M2	↓	■	■	■	■	■																																	
Gene Expression	M2	↓						■	■	■		■		■		■	■	■			■	■		■	■	■	■		■	■	■		■	■	■	■	■		■	
Mrna Processing	M2	↓														■		■			■						■													
Nuclear Transport	M2	↓												■		■						■																	■	
Posttranscriptional Regulation Of Gene Expression	M2	↓																				■		■		■														
Regulation Of Translation	M2	↓																						■		■														
Rna Processing	M2	↓														■		■			■					■	■		■	■	■		■	■						
Translation	M2	↓							■	■								■						■		■			■	■	■		■	■			■			
Translational Initiation	M2	↓																■											■	■	■			■						

c) ER stress and unfolded protein response

GO-TERM	MΦ Subset	Response (↑↓)	ACADVL	AIFM1	ATP2A2	DNAJC3	HM13	HSP70B	LMNA	PDIA3	SEC61B	SSR1	TBL2	TLN1
Cellular Response To Topologically Incorrect Protein	M1	↓	■			■						■	■	
Cellular Response To Unfolded Protein	M1	↓	■			■						■	■	
Endoplasmic Reticulum Unfolded Protein Response	M1	↓	■			■						■	■	
Response To Endoplasmic Reticulum Stress	M1	↓	■	■	■	■	■			■		■	■	
Response To Unfolded Protein	M2	↑				■		■	■		■	■	■	■

d) immune responses to stimulus

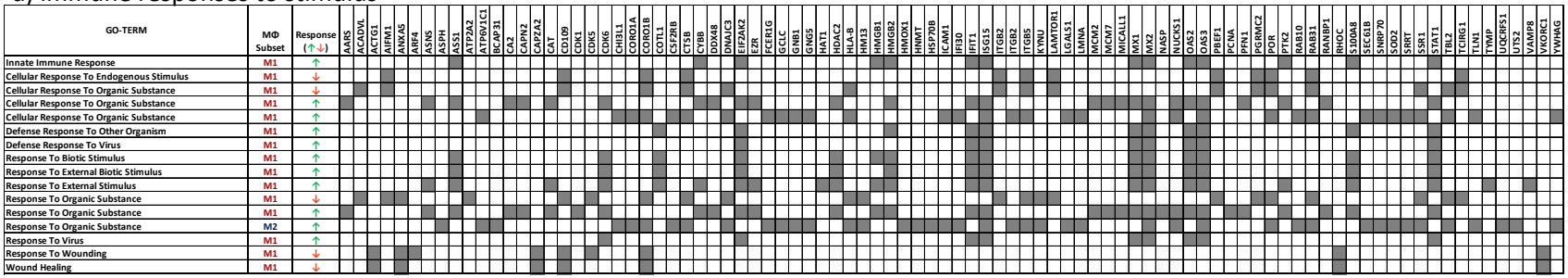

e) type-I interferon associated

GO-TERM	MΦ Subset	Response (↑↓)	IFIT1	ISG15	MX1	MX2	OAS2	OAS3	STAT
Cellular Response To Type I Interferon	M1	↑							
Response To Type I Interferon	M1	↑							
Type I Interferon Signaling Pathway	M1	↑							

f) viral/microbial interaction with host

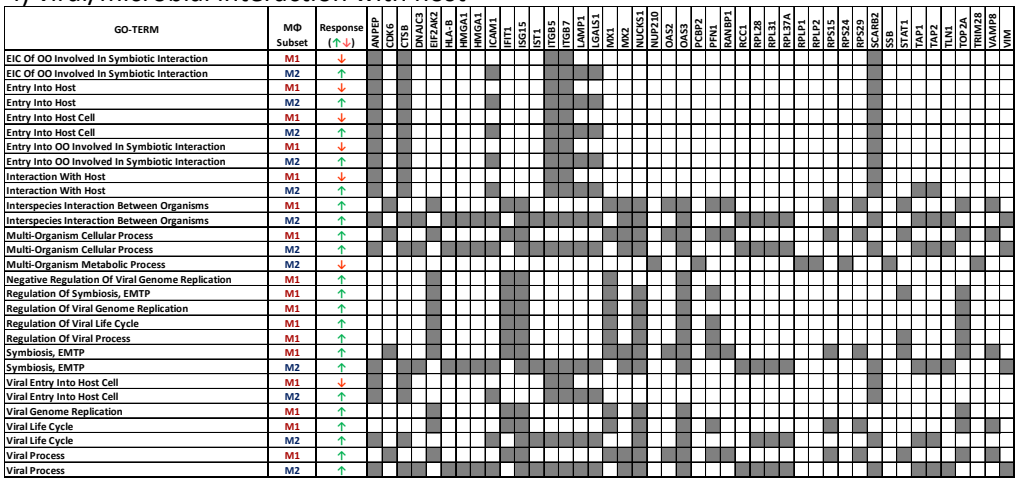

Figure PS1.16. GO-Terms grouped by functional association for biological process in M1 and M2 MΦs following tolerisation. GO-terms were grouped by similarity of function or association to an overall function and plotted to demonstrate individual protein responses in M1 and M2 MΦs repetitively stimulated with PG LPS. Terms identified in figure PS1.11 a & b were grouped and incorporated into matrices; a) antigen processing and presentation, b) epigenetic modification, transcription and translation, c) ER stress and unfolded protein response, d) immune responses to stimulus, e) type-I interferon associated and f) viral/microbial interaction with host. Go-Terms are listed indicating both the subset (**M1** and **M2**) and the direction of response, increase (↑) or decrease (↓) from which the term arose.

a) Adhesion

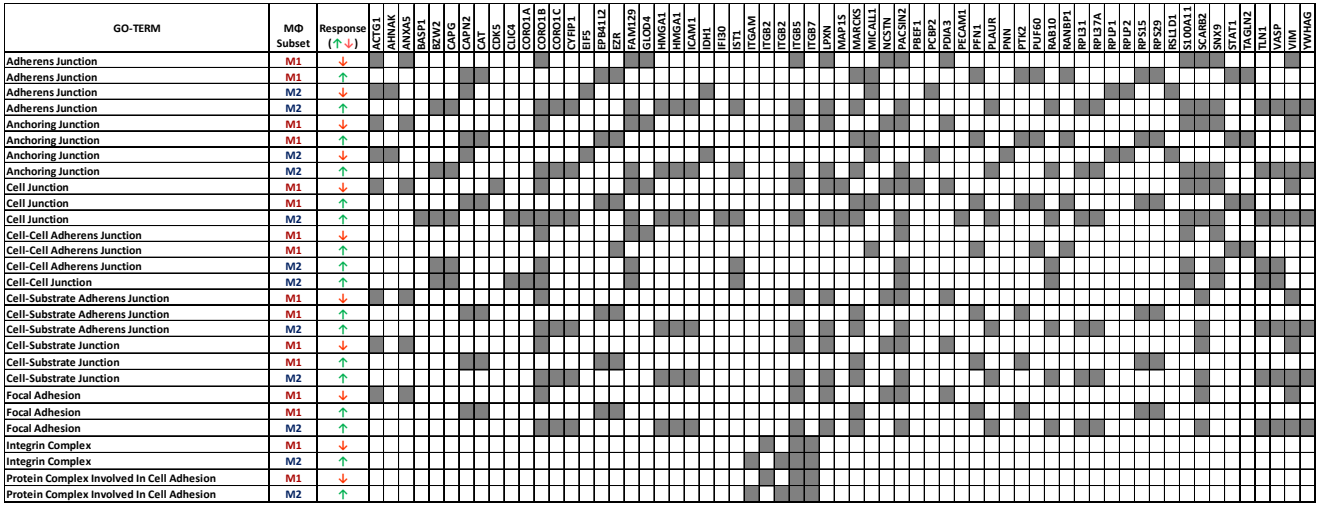
GO-TERM
MΦ Subset
Response (↑↓)
ACTG1
AHNAK
ANXA5
BASP1
BZW2
CAPG
CAPN2
CAT
CDK5
CLIC4
CORO1A
CORO1B
CORO1C
CYFIP1
EIF5
EPB41L2
EZR
FAM129
GLOD4
HMGA1
HMGA1
ICAM1
IDH1
IFI30
IST1
ITGAM
ITGB2
ITGB2
ITGB5
ITGB7
LPXN
MAP1S
MARCKS
MICALL1
NCSTN
PACSIN2
PBEF1
PCBP2
PDIA3
PECAM1
PFN1
PLAUR
PNN
PTK2
PUF60
RAB10
RANBP1
RPL31
RPL37A
RPLP1
RPLP2
RPS15
RPS29
RSL1D1
S100A11
SCARB2
SNX9
STAT1
TAGLN2
TLN1
VASP
VIM
YWHAG
Adherens Junction
M1
Adherens Junction
M1
Adherens Junction
M2
Adherens Junction
M2
Anchoring Junction
M1
Anchoring Junction
M1
Anchoring Junction
M2
Anchoring Junction
M2
Cell Junction
M1
Cell Junction
M1
Cell Junction
M2
Cell-Cell Adherens Junction
M1
Cell-Cell Adherens Junction
M1
Cell-Cell Adherens Junction
M2
Cell-Cell Junction
M2
Cell-Substrate Adherens Junction
M1
Cell-Substrate Adherens Junction
M1
Cell-Substrate Adherens Junction
M2
Cell-Substrate Junction
M1
Cell-Substrate Junction
M1
Cell-Substrate Junction
M2
Focal Adhesion
M1
Focal Adhesion
M1
Focal Adhesion
M2
Integrin Complex
M1
Integrin Complex
M2
Protein Complex Involved In Cell Adhesion
M1
Protein Complex Involved In Cell Adhesion
M2

b *i*) cellular bodies

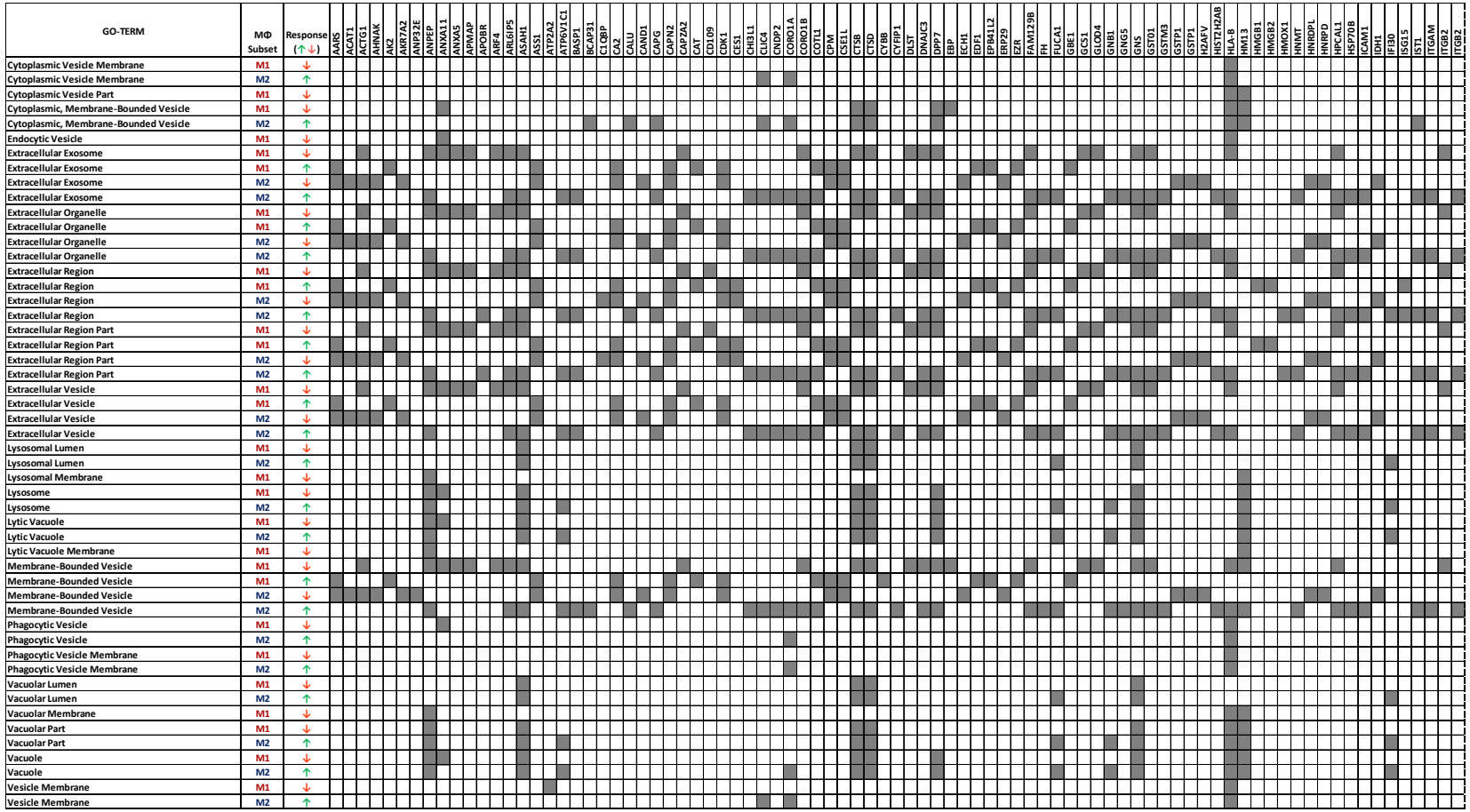

b *ii*) cellular bodies cont’

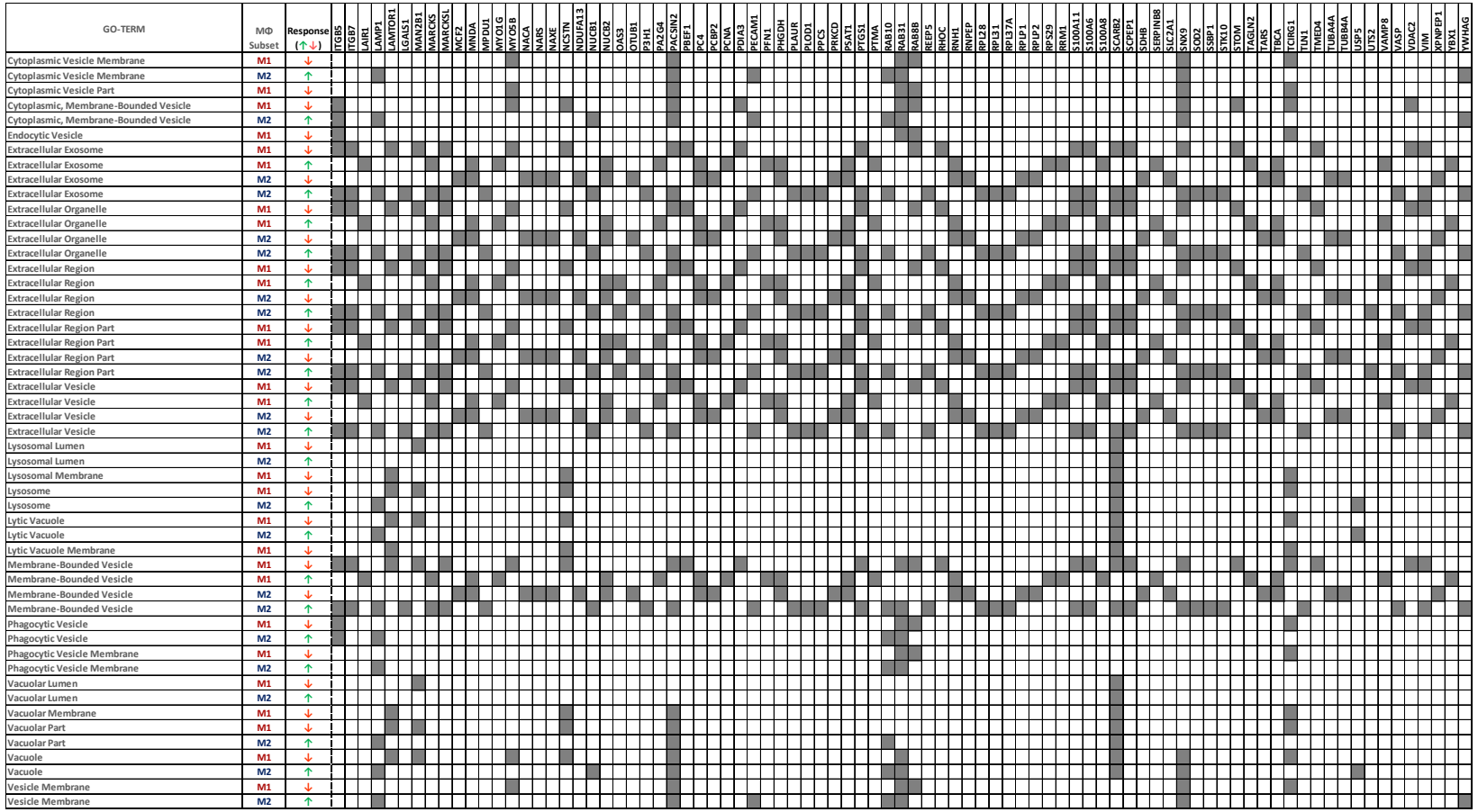

c) DNA, epigenetics and translation

GO-TERM	MΦ Subset	Response (↑↓)	ANP32E	CAPN2	CAPRIN1	CDK1	CPSF6	DDX48	DHX15	EIF2AK2	EIF3M	FEN1	H2AFV	HAT1	HCC5	HDAC2	HMGB1	HMGB2	HNRDPL	HNRNPA0	HNRNPAB	HNRPD	LSM4	MAGOH	MCM2	MCM4	MCM5	MCM6	MCM7	NASP	NSUN2	NUCKS1	PA2G4	PABPN1	PCBP2	PCNA	PNN	PUF60	RBBP4	RBM3	RCC2	RPLP1	RPLP2	RPS15	RPS24	RPS29	RSL1D1	S5B	SSRP1	STAT1	SUPT16H	TCP2A	TRIM28	YBX1
Chromatin	M1	↑		■	■									■	■		■	■							■				■			■																							
Chromatin	M2	↓	■	■									■	■		■									■				■										■															■	
Chromosomal Part	M1	↑		■		■							■	■	■	■		■							■	■	■	■	■	■		■			■				■		■									■				
Chromosomal Part	M2	↓	■	■		■							■	■	■										■	■	■	■	■										■														■	
Chromosomal Region	M1	↑				■							■	■	■										■	■	■	■	■						■				■		■													
Chromosomal Region	M2	↓				■							■	■	■										■	■	■	■	■																					■				
Chromosome	M1	↑		■		■							■	■	■	■	■	■							■	■	■	■	■	■		■			■				■		■									■	■	■		
Chromosome	M2	↓	■	■		■							■	■	■										■	■	■	■	■										■										■	■		■		
Chromosome, Telomeric Region	M1	↑				■							■	■	■										■	■	■	■	■							■																		
Chromosome, Telomeric Region	M2	↓				■							■	■	■										■	■	■	■	■																					■				
Intracellular Ribonucleoprotein Complex	M1	↑			■		■	■		■		■						■						■								■		■		■		■			■			■		■							■
Intracellular Ribonucleoprotein Complex	M2	↓			■		■		■		■								■	■	■	■	■	■											■	■		■		■		■	■		■	■		■	■					
MCM complex	M1	↑													■										■	■	■	■	■																									
Mcm Complex	M2	↓													■										■	■	■	■	■																									
Nuclear Chromatin	M1	↑												■		■		■												■		■																						
Nuclear Chromosome	M1	↑				■							■	■	■	■		■							■	■	■	■	■	■		■			■				■														
Nuclear Chromosome	M2	↓	■			■							■	■	■										■	■	■	■	■										■														■	
Nuclear Chromosome Part	M1	↑				■							■	■	■	■		■							■	■	■	■	■	■		■			■				■													
Nuclear Chromosome Part	M2	↓	■			■							■	■	■										■	■	■	■	■										■														■	
Nuclear Chromosome, Telomeric Region	M1	↑				■							■	■	■										■	■	■	■	■							■																	
Nuclear Chromosome, Telomeric Region	M2	↓				■							■	■	■										■	■	■	■	■																					■				
Ribonucleoprotein Complex	M1	↑			■		■	■		■		■						■						■								■		■		■		■			■			■		■							■
Ribonucleoprotein Complex	M2	↓			■		■		■		■								■	■	■	■	■	■											■	■		■		■		■	■		■	■		■	■					

d) endoplasmic reticulum

GO-TERM	MΦ Subset	Response (↑↓)	ALOX5AP	APMAP	ARL6IP5	ASPH	ATP2A2	BCAP31	C4ALI	CH3L1	DNAJC3	DPM1	EBP	ELOVL1	ERMP1	GCS1	HLA-B	HM13	HMOX1	LENG4	MPDU1	NCSTN	NUCB1	OSTC	P3H1	PDIA3	PLAUR	PLOD1	POR	PTGS1	RAB10	RBM3	RCN1	REEP5	RPLP1	RPLP2	RPS24	RSL1D1	SEC61B	SSR1	STOM	TAP1	TAP2	TAPBP	TBL2	TMED4	VKORC1
Cytosolic Ribosome	M2	↓																																■	■		■												
Endoplasmic Reticulum (ER)	M1	↓	■	■	■		■				■	■	■		■	■	■	■		■		■		■				■	■	■			■						■	■										
Endoplasmic Reticulum	M2	↑	■		■	■	■	■	■	■	■			■		■	■	■	■		■		■		■	■	■	■	■	■		■						■	■		■	■	■	■	■	■	■	■	■
Endoplasmic Reticulum Membrane	M1	↓	■		■	■		■			■	■	■		■	■	■	■		■		■		■				■	■	■			■						■	■										
Endoplasmic Reticulum Membrane	M2	↑	■		■	■	■	■	■	■	■			■		■	■	■	■		■		■		■	■	■	■	■	■		■						■	■		■	■	■	■	■	■	■	■	■
Endoplasmic Reticulum Part	M1	↓	■		■	■		■			■	■	■		■	■	■	■		■		■		■				■	■	■			■						■	■										
Endoplasmic Reticulum Part	M2	↑	■		■	■	■	■	■	■	■			■		■	■	■	■		■		■		■	■	■	■	■	■		■						■	■		■	■	■	■	■	■	■	■	■
Endoplasmic Reticulum Subcompartment	M2	↑				■								■																			■																	
Endoplasmic Reticulum Tubular Network	M2	↑				■								■																			■																	
Integral Component Of ER Membrane	M2	↑				■		■						■			■	■																																	
Integral Component Of Lumenal Side Of ER Membrane	M2	↑						■									■	■																																	
Intrinsic Component Of ER Membrane	M2	↑				■		■						■			■	■																																	
Large Ribosomal Subunit	M2	↓																																■	■		■												
Lumenal Side Of Endoplasmic Reticulum Membrane	M2	↑						■									■	■																																	
Nuclear Outer Membrane-ER Membrane Network	M1	↓	■		■	■		■			■	■	■		■	■	■	■		■		■		■				■	■	■			■						■	■										
Nuclear Outer Membrane-ER Membrane Network	M2	↑	■		■	■	■	■	■	■	■			■		■	■	■	■		■		■		■	■	■	■	■	■		■						■	■		■	■	■	■	■	■	■	■	■
Ribosomal Subunit	M2	↓																																■	■	■	■	■											
Rough Endoplasmic Reticulum	M2	↑						■				■					■						■				■																							
Rough Endoplasmic Reticulum Membrane	M2	↑																																														

e) mitochondria

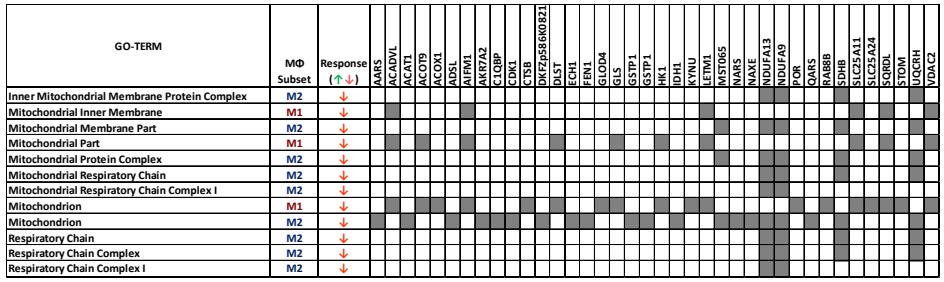

Figure PS1.17. GO-Terms grouped by functional association for CELLULAR COMPONENT in M1 and M2 MΦs following tolerisation. GO-terms were grouped by similarity of function or association to an overall function and plotted to demonstrate individual protein responses in M1 and M2 MΦs repetitively stimulated with PG LPS. Terms identified in figure PS1.12 a & b were grouped and incorporated into matrices; a) Adhesion, b) cellular bodies c) DNA, epigenetics and translation, d) endoplasmic reticulum e) mitochondria. Go-Terms are listed indicating both the subset (**M1** and **M2**) and the direction of response, increase (↑) or decrease (↓) from which the term arose.

a) Adhesion

GO-TERM	MΦ Subset	Response (↑↓)	BZW2	CAPG	CORO1B	EZR	FAM129	GLOD4	ICAM1	IST1	ITGB2	ITGB2	ITGB7	MICALL1	PACSIN2	PFN1	PUF60	RAB10	RANBP1	S100A11	SNX9	STAT1	TAGLN2	TLN1	VASP
Cadherin Binding	M1	↓			■		■	■							■					■	■				
Cadherin Binding	M1	↑				■								■		■	■		■			■	■		
Cadherin Binding	M2	↑	■	■	■		■			■					■			■		■	■			■	■
Cadherin Binding Involved In Cell-Cell Adhesion	M1	↓			■		■	■							■					■	■				
Cadherin Binding Involved In Cell-Cell Adhesion	M1	↑				■								■		■	■		■			■	■		
Cadherin Binding Involved In Cell-Cell Adhesion	M2	↑	■	■	■		■			■					■			■		■	■			■	■
Cell Adhesion Molecule Binding	M1	↓			■		■	■			■		■		■					■	■				
Cell Adhesion Molecule Binding	M2	↑	■	■	■		■		■	■		■	■		■			■		■	■			■	■
Protein Binding Involved In Cell Adhesion	M1	↓			■		■	■							■					■	■				
Protein Binding Involved In Cell Adhesion	M1	↑				■								■		■	■		■			■	■		
Protein Binding Involved In Cell Adhesion	M2	↑	■	■	■		■			■					■			■		■	■			■	■
Protein Binding Involved In Cell-Cell Adhesion	M1	↓			■		■	■							■					■	■				
Protein Binding Involved In Cell-Cell Adhesion	M1	↑				■								■		■	■		■			■	■		
Protein Binding Involved In Cell-Cell Adhesion	M2	↑	■	■	■		■			■					■			■		■	■			■	■

b) Antioxidants

GO-TERM	MΦ Subset	Response (↑↓)	ALOX5AP	ASPH	CLIC4	DKFZp586K0821	GST01	GSTM3	HMOX1	NDUFA13	NDUFA9	P3H1	PDIA3	PLOD1	POR	PTGS1	SOD2	SQRDL
Antioxidant Activity	M2	↑	■				■									■	■	
Dioxygenase Activity	M2	↑	■	■								■		■	■	■		
Glutathione Transferase Activity	M2	↑	■		■		■	■										
Nadh Dehydrogenase (Quinone) Activity	M2	↓				■				■	■							
Nadh Dehydrogenase (Ubiquinone) Activity	M2	↓				■				■	■							
Nadh Dehydrogenase Activity	M2	↓				■				■	■							
Oxidoreductase Activity (ORA), Acting On A SGOD	M1	↓					■						■					■
ORA, Acting On A SGOD, Quinone Or SCAA	M1	↓					■											■
ORA, Acting On A SGOD, Quinone Or SCAA	M2	↑					■											■
ORA, Acting On Paired Donors, WIoROMO	M2	↑		■					■			■		■	■	■		
ORA, AOPD, WIoROMO, 2-OG As 1 Donor, And I Of 1 AE Of O IBD	M2	↑		■								■		■				

c) antigen processing and presentation

GO-TERM	MΦ Subset	Response (↑↓)	ANPEP	BCAP31	GSTM3	HLA-B	PPIF	TAP1	TAP2	TAPBP	TPP2
Mhc Class I Protein Binding	M2	↑		■				■		■	
Mhc Class Ib Protein Binding	M2	↑						■	■		
Mhc Protein Binding	M2	↑		■				■	■	■	
Peptide Antigen Binding	M2	↑				■		■		■	
Peptide Antigen-Transporting Atpase Activity	M2	↑						■	■	■	
Peptide Binding	M2	↑	■		■	■	■	■		■	■
Peptide-Transporting Atpase Activity	M2	↑						■	■	■	
Tap Binding	M2	↑				■		■	■	■	
Tap1 Binding	M2	↑						■	■	■	
Tap2 Binding	M2	↑						■		■	

d) DNA translation and transcription

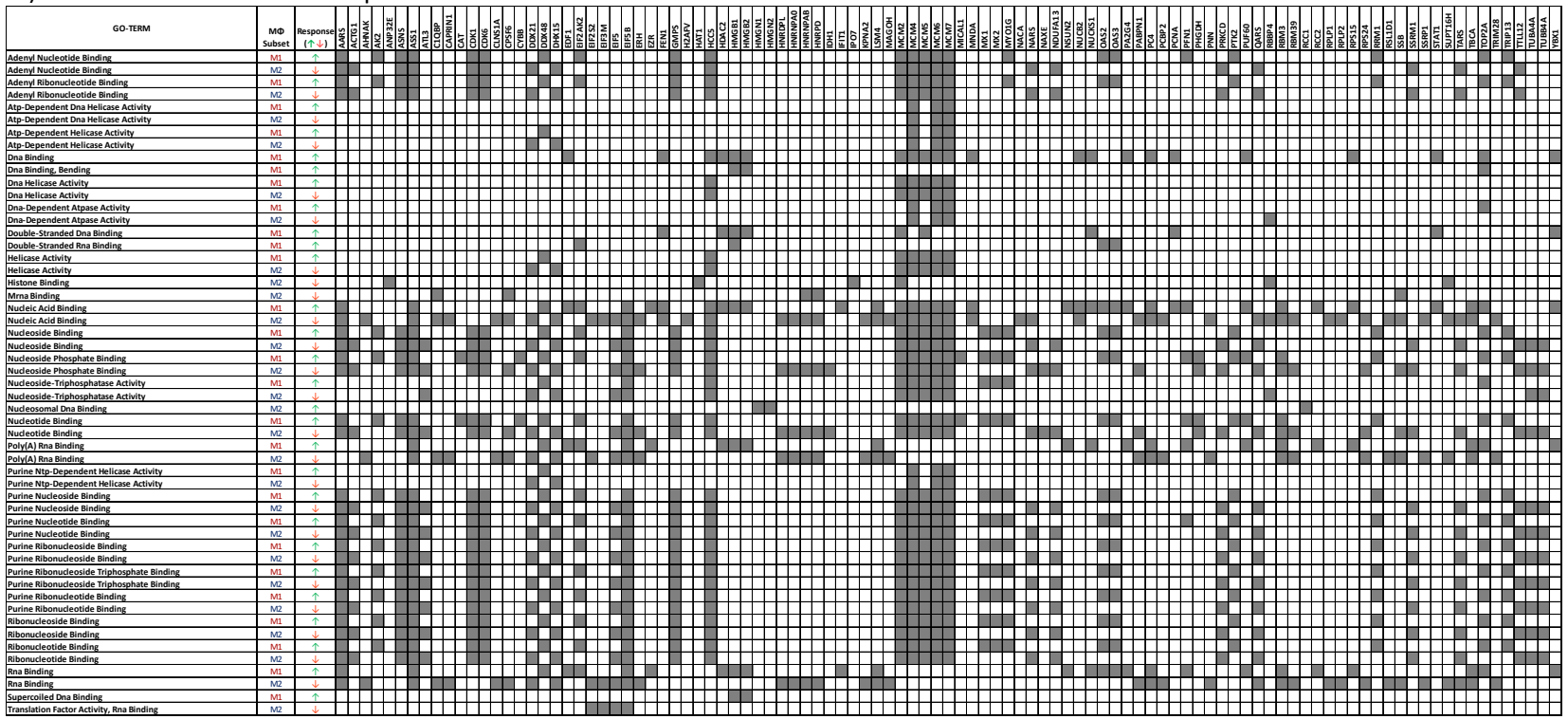

e) Transport and transferases

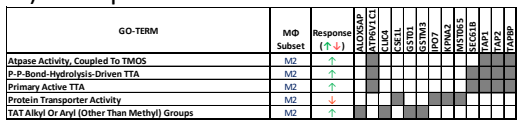

Figure PS1.18. GO-Terms grouped by functional association for MOLECULAR FUNCTION in M1 and M2 MΦs following tolerisation. GO-terms were grouped by similarity of function or association to an overall function and plotted to demonstrate individual protein responses in M1 and M2 MΦs repetitively stimulated with PG LPS. Terms identified in figure PS1.13 a & b were grouped and incorporated into matrices; a) Adhesion, b) Antioxidants c) antigen processing and presentation, d) DNA translation and transcription e) Transport and transferases. Go-Terms are listed indicating both the subset (**M1** and **M2**) and the direction of response, increase (↑) or decrease (↓) from which the term arose.

Abbreviations;

AACT: Atpase Activity, Coupled To
TAT: Transferase Activity, Transferring
SGOD: Sulphur Group of Donors
SCAA: Similar Compound as Receptor
AOPD: Acting on Paired Donors
WIoROMO: With Incorporation or Reduction of Molecular Oxygen
2-OG: 2-Oxyglutarate
I of 1 AE: Incorporation of One Atom Each
O IBD: Oxygen in Both Donors
TMOS: Transmembrane Movement of Substances
TTA: Transmembrane Transferase Activity

Appendix E

Supplemental figures

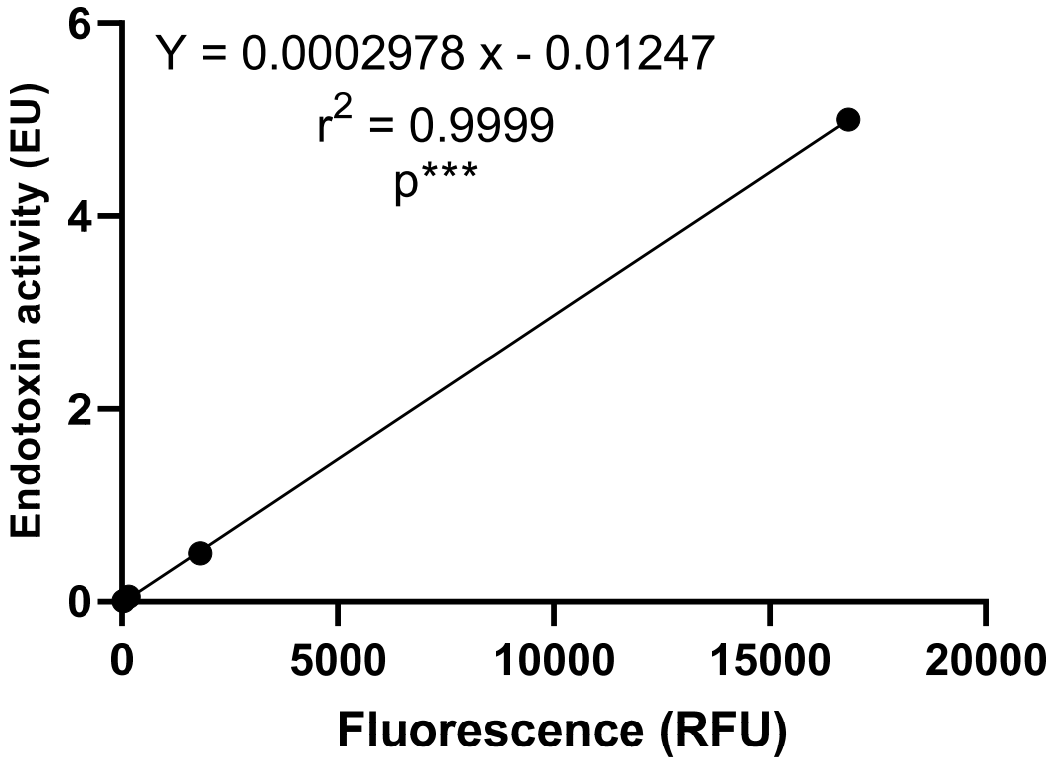

Figure S1 Standard curve for rFC assay. *E. coli* LPS standards of known endotoxin activity between 0.005 and 5 EU was plotted against fluorescence which was read on a fluorescence plate reader with an excitation filter of 380/20 and an emission filter of 440/40. Test samples were then calculated using the linear regression method as recommended by the manufacturer of the assay.

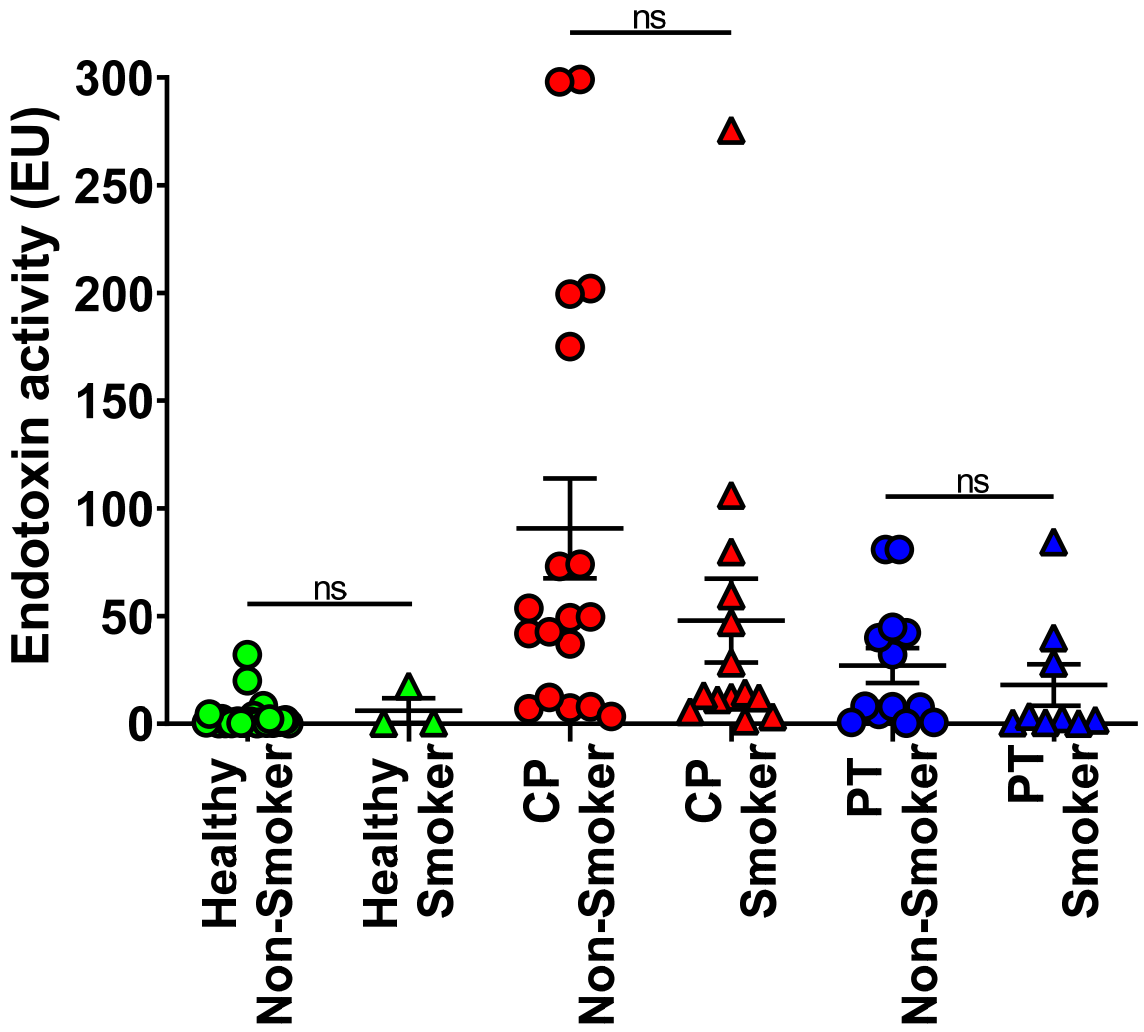

Figure S2 Statistical analysis of the effect of smoking status on each patient group. Smokers and non-smokers were compared within each patient group using a T test (Graphpad prism v8.1, San Diego, CA, USA). Smoking status did not demonstrate any significant difference within each patient group i.e. healthy (green), CP (red) and post treatment (PT) (blue).

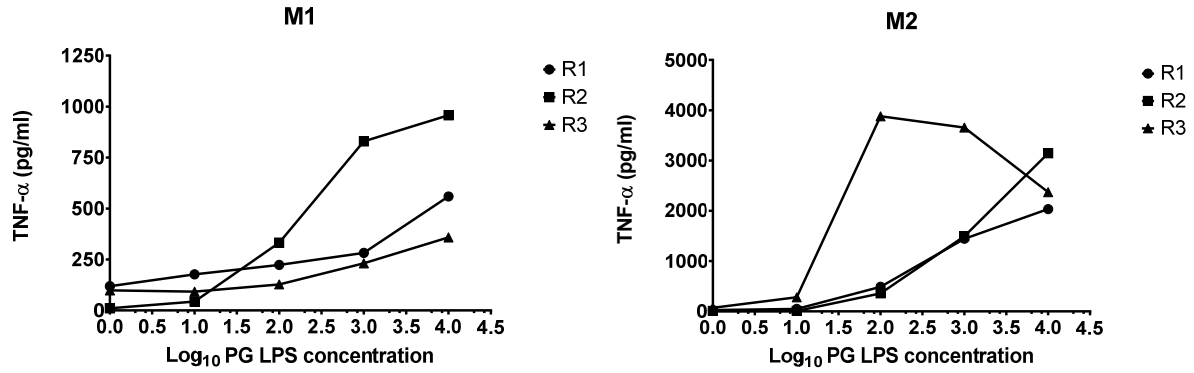

Optimum concentration was determined using the following formula:

$$C = \frac{(A-B)}{2} + B$$

Where A = highest value for replicate

B= lowest significant value above control (0) for replicate

C= optimum value

Value of C was then used to find the correlating log value of concentration. The inverse log was then calculated to give concentration and the mean was calculated for M1 and M2 MΦs across replicates.

M1					
Value			Corresponding Log_{10}	Concentration (µg/ml)	Mean (µg/ml)
A	B	C			
559.25	119	339.1	3.25	1.78	0.99
957.33	10.33	483.8	2.3	0.2	
358.33	97.83	228.1	3.0	1.0	

M2					
Value			Corresponding Log_{10}	Concentration (pg/ml)	Mean (µg/ml)
A	B	C			
2034.8	24.8	1041.2	2.59	0.39	0.40
3144.2	7.25	1575.7	2.9	0.79	
3880.5	71	2079.5	1.45	0.028	

Mean concentration (M1 and M2): 0.7 µg/ml

Figure S3 Calculation of optimal PG LPS concentration. M1 and M2 MΦs were stimulated with PG LPS at the following concentrations: 0.001, 0.01, 0.1, 1.0 and 10 µg/ml. each experiment was performed at a minimum of duplicate technical and triplicate biological experiments (indicated as R1, R2 and R3). Results were plotted and the optimum concentration was calculated as per the formula above.

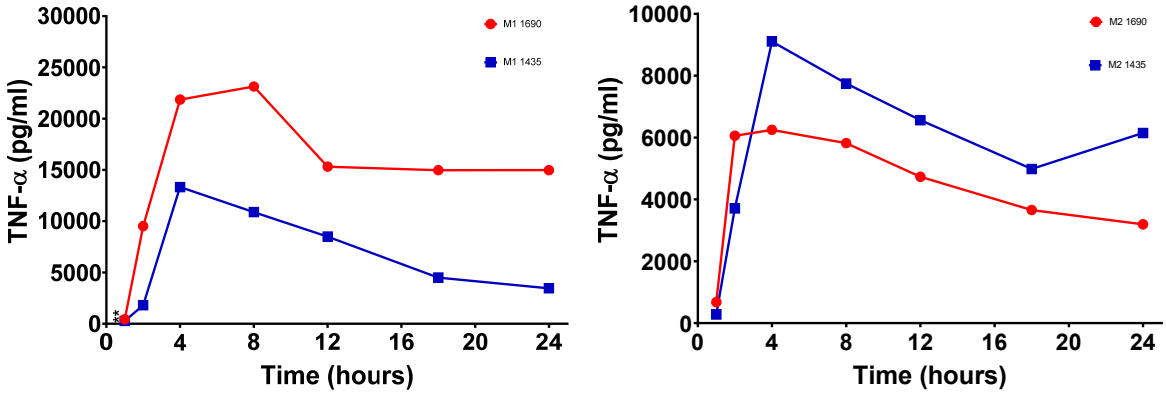

Figure S4 24-hour study of M1 and M2 MΦs stimulated with PG LPS isoforms. M1 and M2 MΦs were stimulated with 700 ng/ml of either PG LPS_{1690} or PG LPS_{1435} for a period of 24 hours to calculate optimal stimulation time point. Experiments were performed in technical duplicates and biological triplicates, figures are results from one biological replicate, indicative of all results.

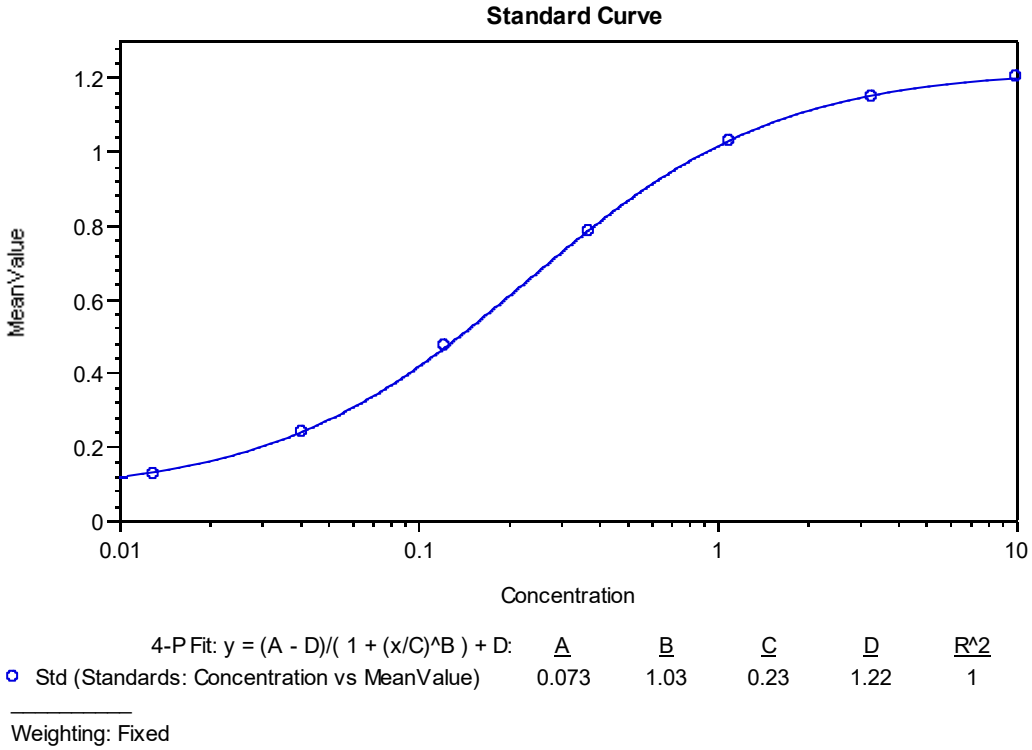

Figure S5 Representative standard curve for IL-8 ELISA. IL-8 protein standards were prepared with a range between 13 – 10,000 pg/ml. Absorbance was read on an absorbance plate reader at a wavelength of 450 nm. Standard curve illustrated is representative of multiple experiments where n>6.

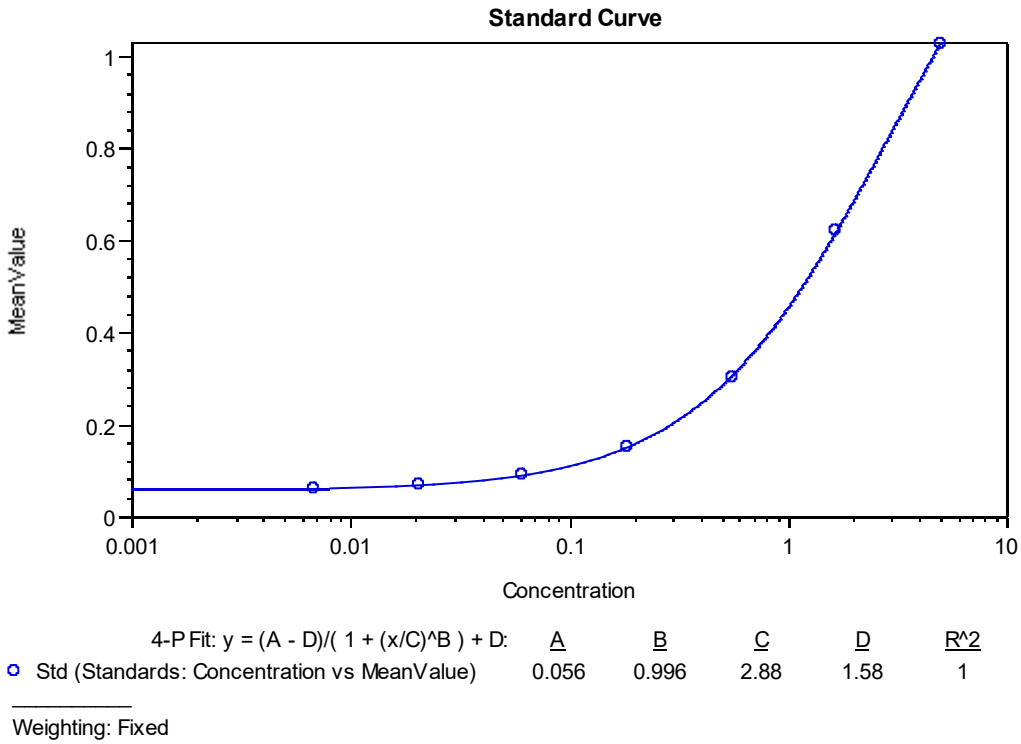

Figure S6 Representative standard curve for TNF-α ELISA. TNF-α protein standards were prepared with a range between 7 – 5,000 pg/ml. Absorbance was read on an absorbance plate reader at a wavelength of 450 nm. Standard curve illustrated is representative of multiple experiments where n>6.

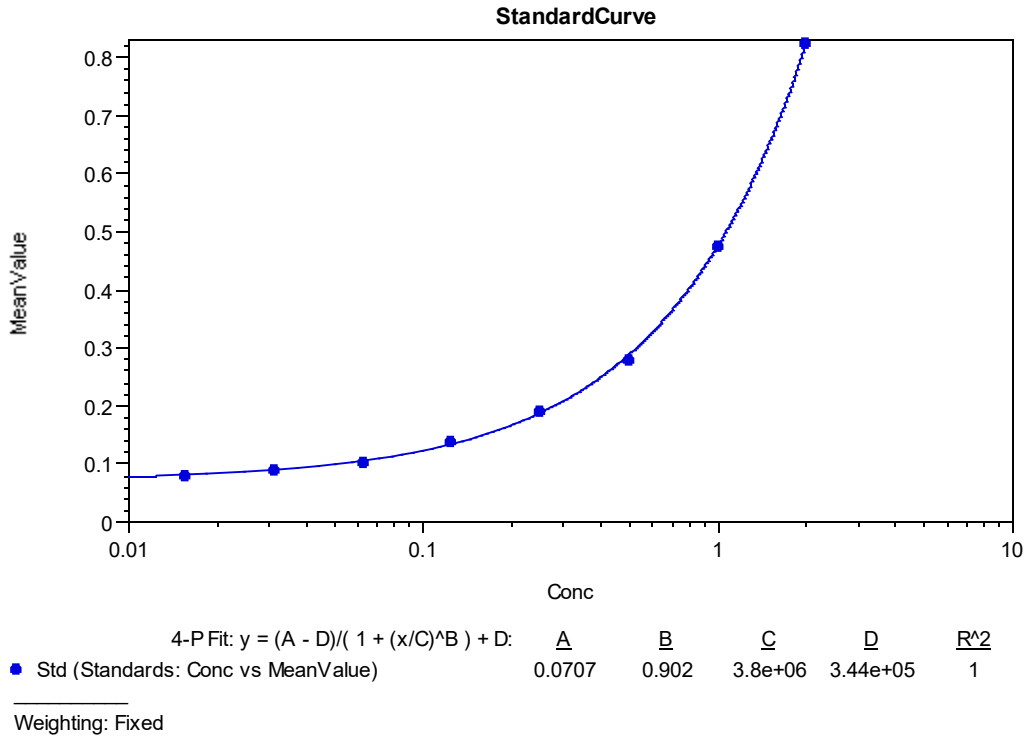

Figure S7 Representative standard curve for IL-23 ELISA. IL-23 protein standards were prepared with a range between 16 – 2,000 pg/ml. Absorbance was read on an absorbance plate reader at a wavelength of 450 nm. Standard curve illustrated is representative of multiple experiments where n>6.

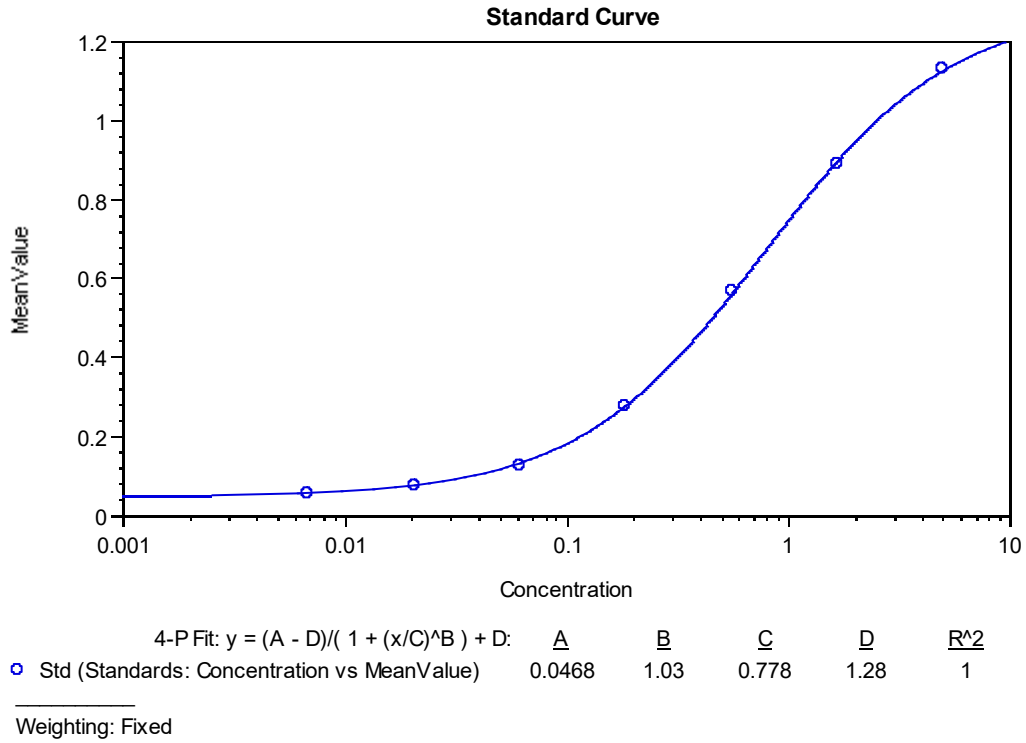

Figure S8 Representative standard curve for IL-10 ELISA. IL-10 protein standards were prepared with a range between 7 – 5,000 pg/ml. Absorbance was read on an absorbance plate reader at a wavelength of 450 nm. Standard curve illustrated is representative of multiple experiments where n>3.

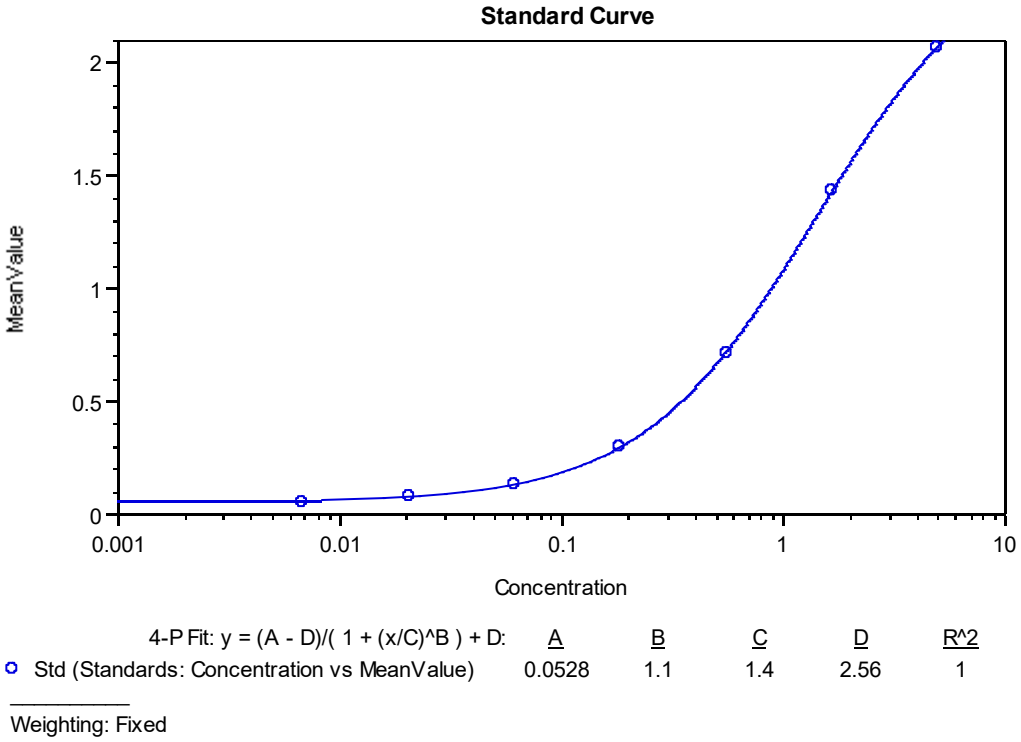

Figure S9 Representative standard curve for IL-12 ELISA. IL-12 protein standards were prepared with a range between 7 – 5,000 pg/ml. Absorbance was read on an absorbance plate reader at a wavelength of 450 nm. Standard curve illustrated is representative of multiple experiments where n>3.

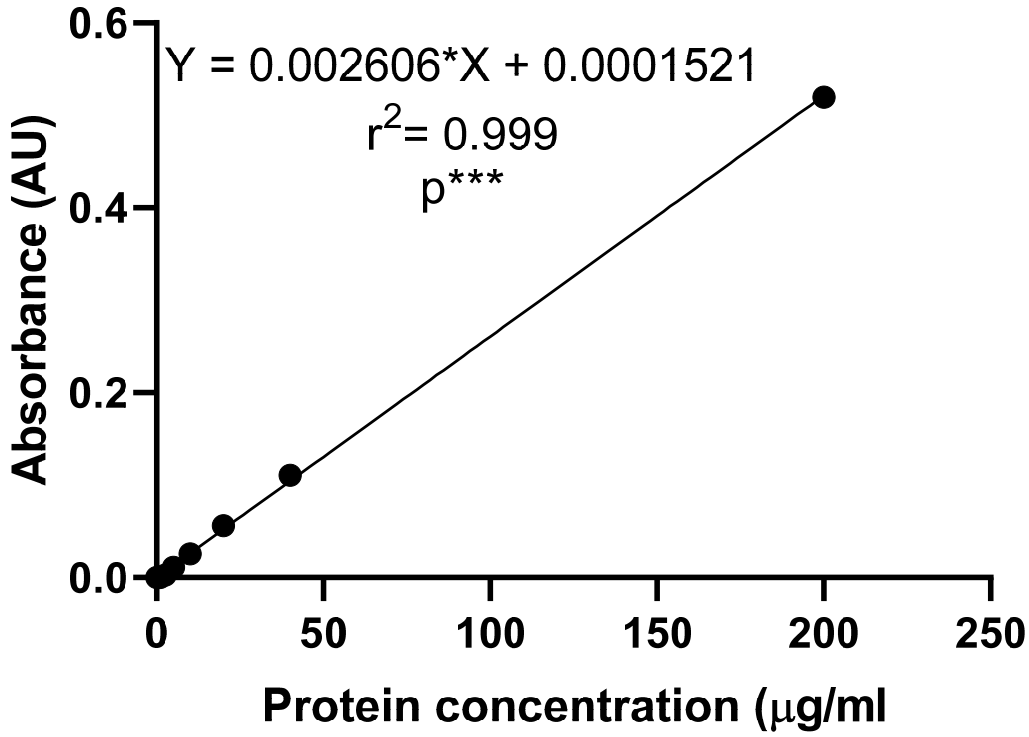

Figure S10 Standard curve for BCA assay. Bovine serum albumin (BSA) protein standards were prepared with a range between 1 – 200 μg/ml. Absorbance was read on an absorbance plate reader at a wavelength of 562 nm. Standard curve illustrated is representative of multiple experiments where n=3.